The effect of hypoxia and reoxygenation on STAT3 regulation in potential cardiomyocyte models

By Emma Louise Evans, MSci (hons)

Thesis submitted to the University of Nottingham for the degree of Doctor of Philosophy

2012

Table of contents

Abstract

Cardiomyocyte apoptosis is an important contributory factor towards the progression of ischaemic heart disease. Signal Transducer and Activator of Transcription 3 (STAT3) is a transcription factor has that been implicated in normal heart development and function. Most interestingly, STAT3 also appears to play a role in cardioprotection, including hypoxic preconditioning. In this thesis the levels and activities of STAT3 were measured in response to hypoxic insult in primary rat cardiomyocytes (RCMs) and two cardiomyocyte cell lines (H9c2 and P19CL6 cells). P19CL6 cells were extremely sensitive to hypoxia-induced apoptosis whereas RCMs and H9c2 cells were highly resistant.

Apoptosis in P19CL6 cells correlated with loss of STAT3 DNA binding, which was preceded by serine phosphorylation and followed by loss of tyrosine phosphorylation. Treatment with LIF partially protected P19CL6 cells from hypoxia-induced apoptosis, as did exogenous expression of STAT3 but not a redox-insensitive STAT3 mutant ($STAT3^{C3S}$). Moreover, STAT3 expression rescued mitochondrial ATP production during hypoxia whereas the redox-insensitive mutant did not. These data indicate that the contribution of STAT3 to cardiomyocyte survival under hypoxic stress involves the maintenance of mitochondrial function by a redox-dependent mechanism.

Understanding how STAT3 is regulated in cardiomyocytes will be important for the development of therapeutic approaches for ischaemic heart disease in the future.

Acknowledgments

After all those years, I've got quite a list of people who contributed in some way to this thesis, for which I would like to express my many thanks. Firstly this thesis would not have been possible without the help, support and patience of my supervisor, Prof Peter Shaw, I am particularly grateful for his encouragement and stimulating discussions throughout this research project and his constructive criticism during the preparation of this thesis. I would like to thank members of the Shaw laboratory, past and present for their help and advise throughout my studies. In particular I would like to thank Janice Saxton, Samuel Shelton and Li Li for their invaluable technical support.

I am also very grateful for the finical support I received from the British Heart Foundation and administrative assistance from Wendy Solis.

Finally, I am forever indebted to Robert and the rest of my family for their understanding, endless patience and encouragement when it was most required.

Publication list

Journal articles

Evans, E.L., Saxton, J., Shelton, S.,, Begitt, A., Holliday, N., Hipskind, R., and Shaw, P.E. (2011) Dimer formation and conformational flexibility ensure cytoplasmic stability and nuclear accumulation of Elk-1. Nucleic Acids Res, 1-13.

Li, L., Cheung, S.H., **Evans, E.,** Shaw, P.E. (2010) Modulation of gene expression and tumor cell growth by redox modification of STAT3. Cancer Res. 70 8222-32.

Zhang, H. M., Li, L., Papadopoulou, N., Hodgson, G., **Evans, E.,** Galbraith, M., Dear, M., Vougier, S., Saxton, J. & Shaw, P. E. (2008) Mitogen-induced recruitment of ERK and MSK to SRE promoter complexes by ternary complex factor Elk-1. Nucleic Acids Res, 36, 2594-607.

Shelton, S.J., **Evans, E.L.,** Saxton, J., Atkins, R., Constantin-Teodosiu D. and Shaw, P.E. Protection against hypoxia-induced apoptosis involves redox regulation of mitochondrial STAT3 (manuscript in preparation; Equal contribution by EE and SS)

Evans, E.L., Shelton, S.J. and Shaw, P.E. Serine phosphorylation of STAT3: is there a downside associated with oxidative stress? (Review in preparation)

Conference abstract

Evans, E.L., Cheung, S.H., Li, L., Shelton, S.J. and Shaw, P.E. The effect of hypoxia and oxidative stress on STAT3 regulation in cardiomyocytes. London 14-15 May 2009. Molecular Regulation of Cardiac Disease Symposium. Poster 6.

Abbreviations

ADP	Adenosine diphosphate
Amp	Ampicillin
AP-1	Activating protein 1
Apaf-1	Apoptotic peptidase activating factor 1
APS	Ammonium persulphate
ATCC	American Type Culture Collection
ATP	Adenosine triphosphate
BSA	Bovine serum albumin
CIAP	Calf intestinal alkaline phosphatase
cDNA	Complementary DNA
DMEM	Dulbecco's Modified Eagle's Medium
DMSO	Dimethyl sulphoxide
DNA	Deoxyribonucleic acid
dNTPs	Deoxyribonucleotide triphosphates
DTT	Dithiothreitol
EDTA	Ethylenediaminetetraacetic acid
EMSA	Electrophoretic mobility shift assay
ERK	Extracellular signal-regulated kinase
ETC	Electron transport chain
FACS	Fluorescence activated cell sorting
FCS	Foetal calf serum

FITC	Fluorescein isothiocyanate
GFP	Green fluorescent protein
GPCR	G protein-coupled receptor
GRIM-19	Genes associated with retinoid-IFN-induced mortality
HBS	HEPES buffered saline
HEK293	Human embryonic kidney 293
HEPES	4-(2-hydroxyethyl)-1-piperazineethanesulphonic acid
HIF1α	Hypoxia inducible factor 1α
IFN	Interferon
IP	Immunoprecipitation
JAK	Janus activated kinase
JNK	c-Jun N-terminal kinase
LB	Luria-Bertani broth
LIF	Leukaemia inhibitory factor
MAC	Mitochondrial apoptosis-induced channel
MAPK	Mitogen-activated protein kinase
MEM	Minimal essential medium
MPTP	Mitochondrial permeability transition pore
NADPH	Nicotinamide adenine dinucleotide phosphate
NF-κB	Nuclear factor-kappa B
NP-40	Nonyl phenoxylpolethoxylethanol-40
nRCM	Neonatal rat cardiomyocytes
PAGE	Polyacrylamide gel electrophoresis

PARP	Poly-ADP ribose polymerase
PBS	Phosphate buffered saline
PCR	Polymerase chain reaction
PI	Propidium iodide
PIAS	Protein inhibitor of activated STATs
PKC	Protein kinase C
PP2A	Protein phosphatase 2A
PS	Phosphatidylserine
PVDF	Polyvinylidene fluoride
ROS	Reactive oxygen species
RT	Room temperature
SDS	Sodium dodecyl sulphate
SH2	Src-homology-2
SIE	Sis-inducible element
SODs	Superoxide dismutase
STAT	Signal transducer and activator of transcription
SUMO	Small ubiquitin like modification
TAD	Transactivation domain
TAE	Tris-acetate EDTA
TBE	Tris-borate EDTA
TBS	Tris-buffered saline
TBST	Tris-buffered saline plus Tween

TE	Tris-EDTA
TEMED	Tetramethylethylenediamine
Tm	Melting temperature
Ubi	Ubiquitin
UPS	Ubiquitin proteasome system
WCE	Whole cell extract
Wt	Wild type
VDAC	Voltage-dependent anionic channel

Chapter 1. Introduction

1.1. Cardiovascular disease

1.1.1. The statistics

Cardiovascular disease (CVD) is responsible for the highest morbidity rates worldwide, accounting for approximately 17 million deaths each year. Ischaemic heart disease (IHD) resulted in 12.2% of total deaths in 2004 (table 1) and this figure is estimated to rise to 14.2% by 2030 (WHO, 2008). In the UK, CVD accounts for almost 191,000 deaths each year – one in three of all deaths (Scarborough, 2010). As well as human losses, CVD places a great financial burden on the UK and is estimated to cost the economy £30.7 billion a year. Of the total costs of CVD to the UK, around 47% is due to direct health care costs, 27% to productivity losses and 26% to the informal care of people with CVD (Scarborough, 2010).

Table 1 Top 5 causes of death worldwide. Data taken from (WHO, 2008)

Disease causing death	Deaths (Millions)	Percent of total deaths
1. Ischaemic heart Disease	7.2	12.2
2. Cerebrovascular disease	5.7	9.7
3. Lower respiratory infections	4.2	7.1
4. Chronic obstructive pulmonary disease	3.0	5.1
5. Diarrhoeal diseases	2.2	3.7

1.1.2 Structure and function of the heart

The heart is a powerful muscle that pumps blood throughout the body through coordinated contraction. The heart is composed of four chambers; two thin-walled atria that receive blood returning to the heart and two thick-walled ventricles consisting of multiple layers of muscle to aid contraction – pumping deoxygenated blood to the lungs and oxygenated blood rest of the body (Selzer, 1992). The heart consists of three layers; an inner lining (endocardium), the heart muscle (myocardium) and the outer layer (pericardium). The endocardium consists of a single layer of endothelial cells which lines the surface of heart valves and the inner lining of the chambers. The subendocardial (layer between the endocardium and myocardial) contains fibroblasts, elastic and collagen fibres, nerves and branches of the conducting system that are required for normal function of the heart (Selzer, 1992).

The myocardium is the thickest layer consisting of highly organised rod-shaped branching striated muscle cells (cardiomyocytes) that are attached to adjacent myocytes (Gregorio and Antin, 2000). Working cardiomyocytes usually contain a single centrally located nucleus and are rich in mitochondria - occupying ~40% of myocyte cell volume (Figure 1.1) (Katz, 2006). A prominent and unique feature of cardiac muscle is the presence of irregularly spaced dark bands between myocytes. These are known as intercalated discs, and are due to areas where the membranes of adjacent myocytes come very close together (figure 1.1). The intercalated discs help to 'glue' the myocytes together

and allow an electrical connection between the cells, which is required for contraction of the heart muscle.

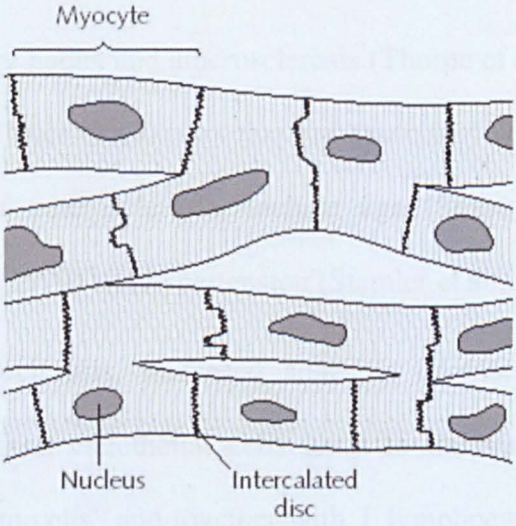

Figure 1.1. Schematic representation of cardiomyocytes. Rod-shaped branching striated muscle cells (cardiomyocytes) that are attached to adjacent myocytes via intercalated discs.

Finally the third layer external to the myocardial layer is composed of connective and adipose tissue through which pass the larger blood vessels and nerve supply to the heart (Selzer, 1992).

1.1.2 What is ischaemic heart disease?

IHD is characterised by ischaemia (reduced blood supply) to the myocardium, usually due to atherosclerosis of the coronary arteries. Endothelial cell injury and inflammation are thought to be the first steps in the development of atherosclerosis, which can lead to the accumulation of lipids in the injured area of the artery (figure 1.2). Atherosclerosis is attributed to a western life style, whereby a high fat

and salt diet are combined with low levels of physical activity, high levels of alcohol consumption and tobacco smoking. Diet is implicated because the deposits on arterial walls contain high levels of fat and cholesterol; studies of both animals and humans have shown links between dietary habits and atherosclerosis (Thorpe et al., 1996, McGill et al., 2002). Other risk factors that are associated with the onset and progression of atherosclerosis, include age (Stout, 1987), diabetes (Grundy et al., 1999) and hypertension (Stamler et al., 1989).

During atherosclerosis, increased adhesion of macrophages to the injured lipid-lined endothelial cells leads to the formation of lipid-engorged "foam cells" and together with T lymphocytes these become "fatty streaks", which ultimately lead to the formation of fibrous plaques. A coronary vessel occlusion can be caused by the formation of arterial thrombi (blood clot), which is induced by atherosclerotic plaques. Thrombi formation is induced by platelet adhesion and platelet aggregation on the collagenous plaque components, followed by the formation of thrombin and fibrin by activated coagulation (Lippi et al., 2011).

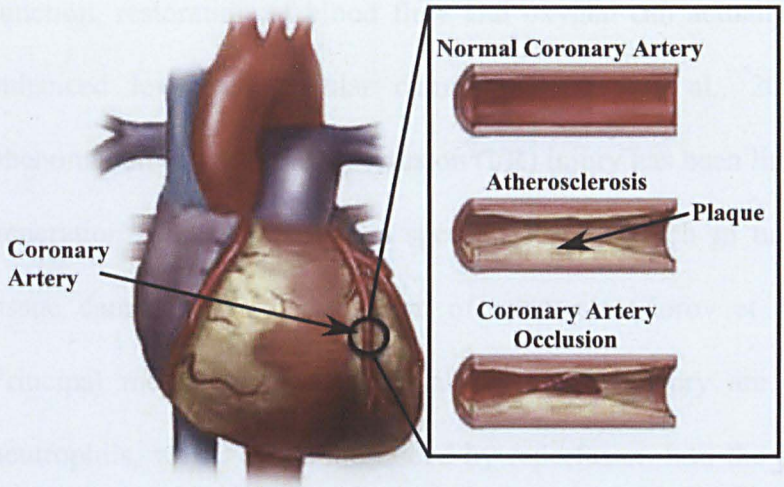

Figure 1.2. The progression of atherosclerosis. Plaque formation during atherosclerosis can lead to occluded arteries. Image modified from (MedicalSymptomsGuide, 2009)

The heart, like any other muscle requires an oxygenated blood supply in order to maintain function. During a coronary vessel occlusion, blood flow is severely restricted to the heart and myocardial tissue becomes deprived of oxygen (hypoxia) and nutrients. Under these conditions, the myocardial tissue is unable to function appropriately and cardiomyocytes cease to beat. When the blood flow is restricted for a significant period of time, the cardiomyocytes become damaged and begin to die leading to a myocardial infarction (MI) or more commonly known as a heart attack (Selzer, 1992). The severity of an MI depends on three factors: the level of the occlusion in the coronary artery, the length of time of the occlusion, and the presence or absence of collateral circulation. The longer the period of vessel occlusion, the greater the chances of irreversible myocardial damage distal to the occlusion (Selzer, 1992). Antithrombotic (anticoagulants and anti-platelet) drugs or surgical intervention can restore blood flow to the ischaemic cardiac tissue. Although critical to re-establish cardiac

function, restoration of blood flow and oxygen can actually result in enhanced levels of cellular damage (Eefting et al., 2004). This phenomenon of Ischemia/reperfusion (I/R) injury has been linked to the generation of reactive oxygen species (ROS), which in turn lead to tissue damage through induction of apoptosis (Zorov et al., 2006). Principal mediators of myocardial reperfusion injury are ROS and neutrophils, which are reintroduced by reperfusion into the previously ischaemic cardiac tissue. Oxygen radicals are very reactive chemical species that are capable of inducing oxidative modification of other molecules and formed by various mechanisms, that can overwhelm cellular defenses and induce tissue damage (discussed in more detail in section 1.3.2) Neutrophils are also important contributors to I/R injury by releasing ROS and proteolytic enzymes, which can directly induce tissue damage (Duilio et al., 2001).

1.1.3 Modes of cell death

The death of a cell can be defined as an irreversible loss of plasma membrane (Kroemer et al., 2005). Cell death is an important aspect of normal organ development and cellular regulation and plays a role in a wide range of physiological and pathological conditions. Three modes of cells death have been identified which include, necrosis and apoptosis.

1.1.3.1 Necrosis

Necrosis derived from the Greek "nekros" for corpse, is a rapid and irreversible process that occurs when cells are severely damaged. Necrosis is characterised by swelling of the cell and its organelles, mitochondrial disruption and breakdown of the plasma membrane. It is a destructive process, as the release of cellular content into the surrounding environment can cause further damage or kill neighbouring cells (Searle et al., 1982). There is accumulating evidence showing that several signal transduction cascades are involved in the propagation of necrotic cell death. In particular, the serine/threonine kinase RIP1 (Receptor-Interacting Protein 1) has been described as one of the key mediators of necrotic cell death (Festjens et al., 2007).

1.1.3.2. Apoptosis

A third mode of cell death is apoptosis, which is an evolutionarily conserved "programmed cell death process" and plays fundamental roles in many biological processes including embryonic development (Brill et al., 1999), inflammation (Haanen and Vermes, 1995) and the development and regulation of the immune system. Kerr and colleagues first described the loss of cells through programmed cell death looking at ischaemic injury of rat liver (Kerr, 1965). This was later termed apoptosis and characterised by cellular shrinkage, blebbing, condensation of nuclear chromatin, DNA fragmentation, protein cleavage and cytoplasmic vacuolisation (Kerr et al., 1972). Dysregulation of apoptosis has been implicated in many diseases (Thompson, 1995). For example, excessive apoptosis is associated with

neurodegenerative diseases such as Parkinson's or Alzheimer's diseases, as apoptosis is thought to account for much of the cell death and the progressive loss of neurons (Mattson, 2000). However insufficient apoptosis may participate in carcinogenesis (Wyllie, 1997) and play a role in the progression of many auto-immune diseases. For example, in the case of rheumatoid arthritis, excessive proliferation of synovial cells is thought to be due to the resistance of these cells to apoptotic stimuli (Perlman et al., 2001).

Apoptosis is mediated by two central pathways: the extrinsic (death receptor) pathway and the intrinsic (mitochondrial) pathway (Danial and Korsmeyer, 2004). Successful apoptotic signaling requires the activation of intracellular pro-caspases and the disabling of mitochondrial function.

Caspases are aspartate-specific cysteine proteases that are highly homologous to the *c.elegans* cell death gene CED-3 (Hengartner and Horvitz, 1994). Fourteen human caspases have been identified to date and are numbered in the order in which they were discovered. Caspases are synthesized as inactive pro-caspases and regulated at a post-translational level, to ensure rapid activation. Caspases are sub-divided into upstream signaling caspases (Caspases 2, 8, 9, 10 and 11) that are activated by dimerisation and downstream executioner caspases (Caspases 3, 6 and 7) that are activated by proteolytic cleavage and responsible for the proteolytic destruction to the cell (Fischer et al., 2003).

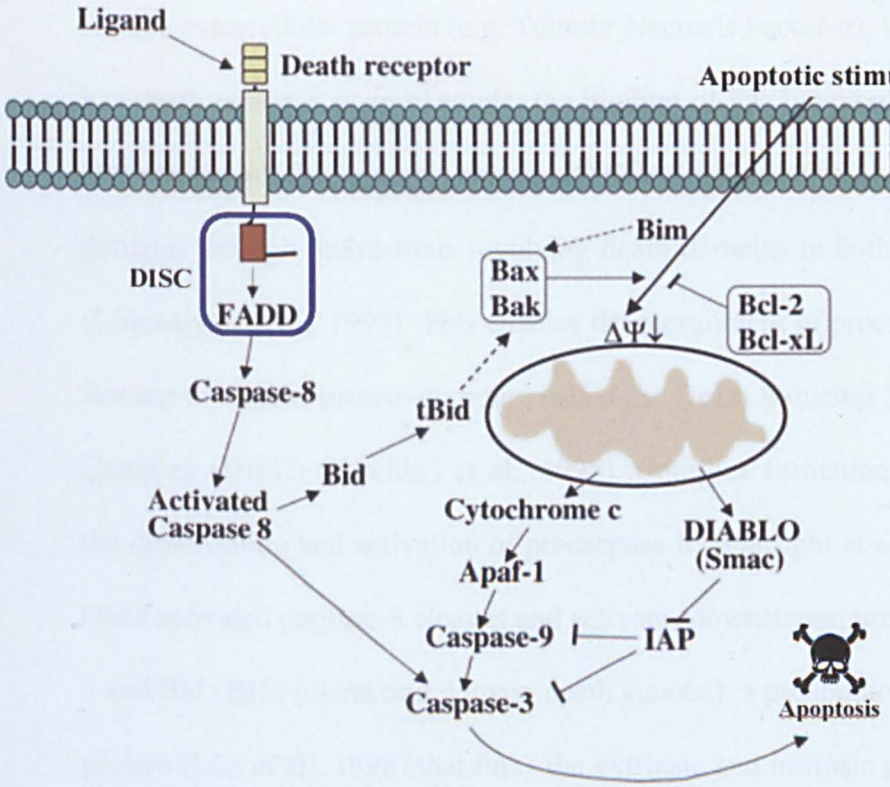

Figure 1.3. Apoptotic signaling pathways. The extrinsic pathway is triggered by death receptor activation and the formation of the death-inducing signaling complex (DISC), which initiates a signaling cascade mediated by caspase-8 activation. Caspase-8 directly activates caspase-3 and indirectly stimulates the release of cytochrome c from the mitochondria. Activated caspase-3 degrades cellular proteins necessary to maintain cell survival and integrity, leading to apoptosis. The intrinsic pathway occurs when apoptotic stimuli triggers the release of cytochrome c from the mitochondria (independently of caspase-8 activation). Cytochrome c interacts with Apaf-1 and caspase-9 to promote the activation of caspase-3. Various intermediary signaling molecules and proteins inhibiting the apoptotic cascade are also shown. Apaf-1 (apoptosis-activating factor 1), Bak (bacille Calmette–Guérin), Bax, (BCL-2-associated x protein), Bid, (proapoptotic Bcl-2 family member), Bim (proapoptotic Bcl-2 family member), DIABLO (direct IAP binding protein with low PI), FADD (Fas-associated death domain protein), IAP (inhibitors of apoptosis), Smac (second mitochondria-derived activator of caspase) tBid (truncated beta interaction). Modified from (Mak and Yeh, 2002).

The extrinsic pathway is initiated by the binding of a death ligand trimer to its specific cell surface receptor (Ashkenazi and Dixit, 1998). A number of death receptors have been identified such as Fas, Tumor Necrosis Factor Receptor 1 (TNFR1) and TNF-Related Apoptosis Inducing Ligand Receptor 1(TRAILR1). The ligand may be an integral membrane protein on the surface of another cell (e.g. Fas ligand) or a

soluble extracellular protein (e.g. Tumour Necrosis Factor-α). Using the Fas death receptor as an example, the binding of Fas ligand allows the recruitment of the adaptor protein FADD (Fas-associated via death domain) through interactions involving death domains in both proteins (Chinnaiyan et al., 1995). This enables the recruitment of procaspase-8, leading to a multi-protein complex called the Death Inducing Signaling Complex (DISC) (Kischkel et al., 1995). Complex formation leads to the dimerisation and activation of procaspase-8 (Boatright et al., 2003). Once activated caspase-8 cleaves and activates downstream procaspase-3 and Bid (BH3 interacting domain death agonist), a proapoptotic Bcl-2 protein (Luo et al., 1998) that links the extrinsic and intrinsic pathways (figure 1.3).

Procaspases are also activated through a mitochondrial-dependent pathway (Intrinsic Pathway) through apoptotic stimuli such as oxidative stress or DNA damage, which regulate the permeability of the mitochondrial membrane. Changes in mitochondrial membrane permeability allow the release of pro-apoptotic effectors such as cytochrome c (Liu et al., 1996). Cytochrome c can directly activate some upstream procaspases (e.g. procaspase-9) or form a multimeric protein complex called the apoptosome by oligomerising with Apaf-1 (Apoptotic Protease Activation Factor-1). The apoptosome facilitates the dimerisation and activation of procaspase-9, which leads to the activation of downstream executioner caspases (Li et al., 1997a) and ultimately the proteolytic destruction to the cell. The control and regulation of these pro-apoptotic mitochondrial events occur through

members of the Bcl-2 family of proteins (Cory and Adams, 2002) (figure 1.3). The Bcl-2 family of proteins governs mitochondrial membrane permeability and can either be pro-apoptotic (Bax, Bid and Bad) or anti-apoptotic (Bcl-2 and Bcl_{XL}). It is thought that the main mechanism of action of Bcl-2 family members is regulation of cytochrome c release from the mitochondrial via alteration of mitochondrial membrane permeability (figure 1.3).

Cardiomyocyte apoptosis has been documented as a significant form of cell death during I/R damage, with reports stating an apoptotic rate of 2-12% in the boarder-zone of the myocardial infarct (Ottaviani et al., 1999, Olivetti et al., 1996). I/R injury have to been shown to activate activates both the extrinsic and intrinsic pathways (Jeremias et al., 2000)

1.1.4 Cardiovascular disease and cell death

Although apoptosis was first documented in 1972 by Kerr and colleagues (Kerr et al., 1972), apoptosis in cardiomyocytes was not reported until 1994 (Gottlieb et al., 1994). In rabbit hearts, I/R injury was induced and apoptosis identified using TUNEL, DNA fragmentation and electron microscopy (Gottlieb et al., 1994).

There is accumulating evidence from both animal and human studies strongly suggesting that apoptosis occurs in various cardiovascular diseases (Gottlieb et al., 1994, Sharov et al., 1998). Animal studies have demonstrated that I/R injury and myocardial infarction both lead to the onset of apoptosis in cardiomyocytes (Gottlieb et al., 1994). Gottlieb

and colleagues identified nucleosomal ladders of DNA fragments (approx. 200 base pairs) from ischaemic reperfused rabbit myocardial tissue – a characteristic indicative of apoptosis (Gottlieb et al., 1994). Also studies performed on left ventricular tissue obtained from dogs with chronic heart failure demonstrated that loss of cardiomyocytes by apoptosis led to the progressive deterioration of heart function. Apoptosis was analysed using transmission electron microscopy (morphological characteristics of apoptosis) and *in situ* immunohistochemical labeling of nuclear DNA fragments (Sharov et al., 1998). Apoptosis has also been identified in human studies; (Itoh et al., 1995, Saraste et al., 1997) DNA fragmentation was described in the infarcted myocardium using DNA electrophoresis (Itoh et al., 1995). Also studies from hearts obtained at autopsy from subjects who suffered from coronary artery thrombosis (in which reperfusion of the occluded artery had been achieved) revealed apoptotic myocytes found in the border zone between viable myocardium and infarcted tissue (Saraste et al., 1997).

It is clear that apoptosis plays a critical role in the pathogenesis of cardiovascular disease and that inhibition promises to be an important target for potential therapies. However, more work is required to understand the molecular mechanisms that govern these processes. For example, although caspase inhibition has been shown to reduce the loss of cardiomyocytes due to I/R injury in various animal models (Yaoita et al., 1998, Laugwitz et al., 2001), it may not be completely effective in

blocking apoptosis, due to a significant contribution of caspase-independent apoptotic cell death (Okamura et al., 2000).

1.1.5 Cellular and molecular adaptations to cardiac cell death

The heart undergoes cellular and molecular adaptations in response to stresses associated with CVD. At the cellular level maladaptation is associated with elevated levels of fibrosis. As cardiomyocytes are terminally differentiated, once lost they are replaced by non-specialised cardiac fibroblasts. In fibrosis, the excessive production of extracellular matrix proteins alters the structure, architecture and shape of the heart. Such changes have marked effect on ventricular contractility, valvular function and electrical conduction (Weber and Brilla, 1991).

Myocyte cell loss also causes regional myocardial wall thinning which impairs cardiac function. Compensatory hypertrophy occurs as an adaptive mechanism whereby cardiomyocytes increase in size (cell enlargement) as a mean of compensating for damaged heart tissue in order to increase cardiac output (Sonnenblick et al., 1983). This cardiac adaptation leads to changes in gene expression - fetal cardiac genes are activated, including the up-regulation of fetal gene isoforms whose products regulate cardiac contractility and calcium handling while a down-regulation of adult isoforms is often observed (i.e., up-regulation of ß-MHC and down-regulation of α-MHC) (Iemitsu et al., 2001). Compensatory hypertrophy has been described in pigs exposed to chronic episodes of reversible ischaemia to induce myocyte cell loss. Myocyte nuclear density decreased to 71%; however, the myocyte

volume was maintained by regional compensatory hypertrophy as manifested by a 65% increase in myocyte size (Lim et al., 1999). Compensatory hypertrophy has also been identified in humans with end-stage congestive heart failure due to ischaemic cardiomyopathy (Beltrami et al., 1994, Olivetti et al., 1997). Although compensatory hypertrophy is an initial adaptive mechanism in response to myocyte cell loss it subsequently leads to myocardial ischaemia, heart failure and even death (Weber, 1991).

Ischaemic preconditioning (IPC) is a phenomenon by which brief exposures to ischaemia protect against subsequent, prolonged ischaemia. The protective effect of IPC in the myocardium was first demonstrated by Murry and colleagues (Murry et al., 1986). Their data shows that brief, intermittent episodes of ischaemia (four 5 minute circumflex coronary occlusion, each separated by 5 minute reperfusion) have a protective effect on the myocardium that is subjected to subsequent more prolonged ischaemic insult (40 minutes sustained occlusion). They reported that IPC resulted in infarct sizes that were approximately 25% of those observed in untreated hearts. The complex signal transduction cascade of IPC has not yet been fully elucidated, but is known to involve activation of receptors in the plasma membrane, which transduces signals via the activation of many kinases. Liu and colleagues were the first to identify a signal transduction element as part of the precondioning mechanism (Liu et al., 1991). They discovered that stimulation of the G_i-coupled adenosine A_1 receptor

was necessary to trigger IPC's protection and an adenosine receptor antagonist could abolish this protection. Other signal transduction pathways implicated in this process include PI3-Kinase/AKT pathway (Tong et al., 2000, Mocanu et al., 2002) and the JAK/STAT pathway (section 1.2.7.1) (Xuan et al., 2001, Smith et al., 2004). Protein kinase C (PKC) isoforms have also been shown to play a pivotal role in mediating both the early and late phases of IPC (Yellon and Dana, 2000, Tong et al., 2000). The evidence supporting PKCδ in the role of IPC is somewhat contradictory. For example, Wang and colleagues demonstrated that mitochondrial translocation of PKCδ is related to cardioprotection induced by IPC (Wang and Ashraf, 1999); whereas Fryer and colleagues reported that PKCδ plays an important role in pharmacological-induced preconditioning but not IPC (Fryer et al., 2001). A later study using PKCδ knockout mice demonstrated that the cardioprotection observed in IPC is abolished in hearts lacking PKCδ (Mayr et al., 2004).

A molecular mechanism in the defence against ischaemic injury utilises an oxygen-sensing pathway that involves the hypoxia-inducible transcription factor 1 (HIF-1). This pathway mediates gene expression to allow adaption to a hypoxic environment. HIF was initially identified as a hypoxia-inducible DNA-binding activity capable of interacting with a hypoxia response element in the 3' region of the erythropoietin gene (Pugh et al., 1991). HIF is a heterodimer consisting of an α-subunit and a β-subunit, which induces a variety of genes in the acute

and chronic adaption to hypoxia. Examples include genes that regulate angiogenesis, survival, and glycolysis (Safran and Kaelin, 2003). Although HIF-β is ubiquitously expressed, HIF-α is tightly regulated by oxygen through post-translational hydroxylation by oxygen-dependant prolyl hydroxylases (PHD) and asparaginyl hydroxylases (Ivan et al., 2001). Under normoxic conditions, HIF-α is hydroxylated at either of two conserved prolyl residues enabling its recognition by the von Hippel-Lindau (VHL) tumour suppressor protein, a component of the E3 ubiquitin ligase complex that leads to the ubiquitination and subsequent proteasome-dependent degradation of the HIF-α subunit. Hydroxylation of an asparaginyl residue in the C-terminal transactivation domain of HIF-α directly prevents its interaction with the co-activator p300 from the transcription complex. Hydroxylation is intrinsically oxygen dependent because the oxygen atom of the hydroxyl group is derived from molecular oxygen (McNeill et al., 2002). Under hypoxic conditions, levels of HIF-α rise, allowing its dimerisation with HIF-β and enabling transcriptional activation.

In swine models of coronary artery occlusion, myocardial ischaemia induces VEGF expression and collateral blood vessel development (White et al., 1992, Banai et al., 1994). More recently, a study has used the adenoviral (Ad) intramyocardial vascular endothelial growth factor (VEGF)-B_{186} gene transfer and shown it is capable of inducing myocardium-specific angiogenesis and arteriogenesis in both pigs and rabbits (Lahteenvuo et al., 2009). After acute myocardial infarction, AdVEGF-B_{186} increased blood vessel area, perfusion, collateral artery

formation which induced changes towards an ischeamic-resistant myocardial phenotype (Lahteenvuo et al., 2009).

Human patients with coronary artery stenosis (abnormal narrowing of the coronary artery) have an impaired development of collateral vessels. Due to the inverse correlation between infarct size and collateral blood flow (Sabia et al., 1992) such adaptations in response to ischaemia could determine the risk and severity of myocardial infarction.

1.2 Signal Transducers and Activators of Transcription

1.2.1 Discovery

In 1992 Darnell and colleagues (Schindler et al., 1992a) identified a 91kDa protein (and an 84kDa form, lacking 39 C-terminal amino acids) and a 113kDa protein through the study of interferon-α (IFN-α) and IFN-γ induction of transcription. The identified proteins became tyrosine phosphorylated upon treatment of cells with IFN-α (Schindler et al., 1992b), whereas only the 91kDa protein was also phosphorylated in response to INF-γ (Shuai et al., 1992). These proteins serve a dual function as signal transducers and activators of transcription and were later named accordingly in the order they were characterised. Thus, the 91kDa and 84kDa proteins were designated Signal Transducers and Activators of Transcription 1-α (STAT1α) and STAT1β respectively and the 113kDa protein named STAT2. Due to the fact that IFN-α and IFN-γ transcriptional responses used different STATs that share ~40%

amino acid identity with each other, it seemed plausible that additional family members might direct the formation of distinct DNA binding in response to other signaling(Saraste et al., 1997) molecules. STAT3 was initially identified as the acute response factor (APRF) activated by interleukin- 6 (IL-6) (Wegenka et al., 1993). STAT3 cDNA was cloned a year later by Akira and colleagues (Akira et al., 1994), which exhibited 53.5% overall homology with STAT1α cDNA. The STAT3 protein was also tyrosine phosphorylated and activated as a DNA-binding protein in response to epidermal growth factor (EGF) or IL-6 but not IFN-γ (Zhong et al., 1994). STAT4 was first cloned and characterised due to its similarity to STAT1 (52% identical) and shown to be predominantly expressed in the spleen, thymus and testis and is differentially regulated during differentiation (Yamamoto et al., 1994). STAT5 was originally identified as a prolactin-response factor termed mammary gland factor (MGF) and confers the prolactin response (Wakao et al., 1994). Later, two STAT5 homologues were identified, named STAT5a and STAT5b that were encoded by two highly related genes and activated by IL-3, granulocyte-macrophage colony-stimulating factor (GM-CSF) and IL-5 (Azam et al., 1995, Mui et al., 1995). The last transcriptional family member to be identified was STAT6, which was initially termed IL-4 STAT due to its activation by IL-4, a cytokine secreted by activated T lymphocytes, basophils, and mast cells (Hou et al., 1994).

1.2.2 Structure of STATs

All STAT proteins consist of approximately 750-850 amino acids and have several conserved domains that are critical for protein function (figure 1.4).

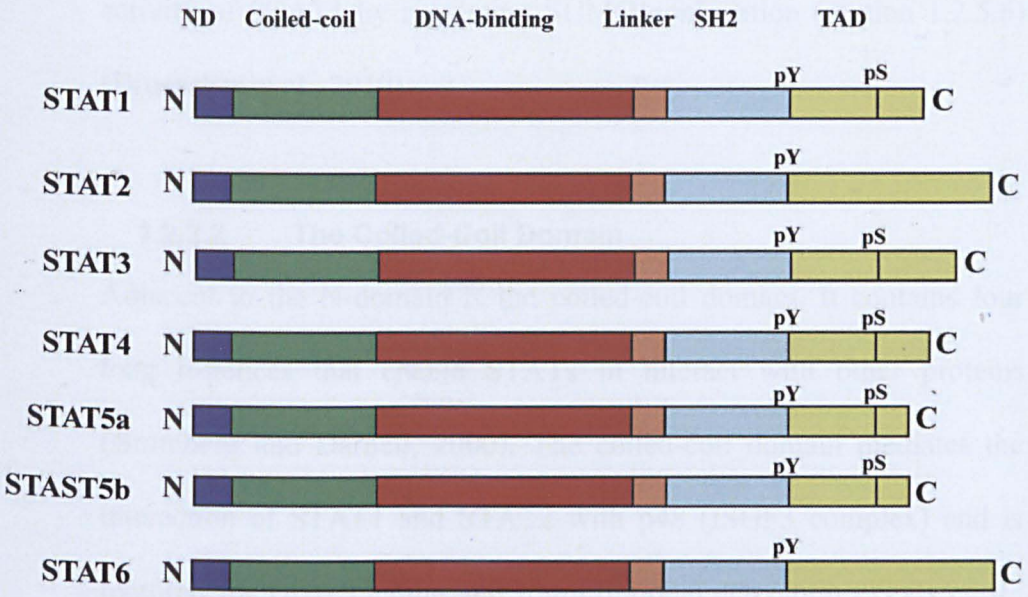

Figure 1.4. STAT protein family members. Schematic diagram representing the conserved domains present in STAT proteins. **N; amino-terminus, C; carboxy-terminus, pY; phospho-tyrosine site, pS; phospho-serine site** Modified from (Yu and Jove, 2004).

1.2.2.1 The N-Domain

The N-domain is located to the amino terminus of STAT proteins and is important for protein-protein and dimer-dimer interactions to form tetrameric STAT molecules. Many promoters contain closely spaced tandem STAT binding sites (~20bp apart). When two such sites are occupied with STATs, dimer-dimer interactions exist that are mediated

through the N-domain (Xu et al., 1996, Vinkemeier et al., 1998). Protein interactions between the N-terminus of STAT1 and histone acetyltransferases CBP/P300 have also been reported which may contribute to transcriptional activation (Paulson et al., 1999). Recently it has been reported that the N-domain of STAT1 is required for the paracrystals formation. Cytokine-induced paracrystals prolong the activity of STAT1 by regulating SUMO conjugation (section 1.2.5.6) (Droescher et al., 2010).

1.2.2.2 The Coiled-Coil Domain

Adjacent to the N-domain is the coiled-coil domain. It contains four long α-helices that enable STATs in interact with other proteins (Bromberg and Darnell, 2000). The coiled-coil domain mediates the interaction of STAT1 and STAT2 with p48 (ISGF3 complex) and is required for DNA binding and transcriptional activation (Veals et al., 1992). STAT3 interacts with c-Jun via the coiled-coil domain to aid co-operative transcriptional activation (Zhang et al., 1999). Also, it has been demonstrated that the coiled-coil domain of STAT3 is also essential for SH2 domain mediated recruitment to its receptor and subsequent tyrosine phosphorylation. Single point mutations of Asp170, or to a lesser extent Lys177, diminish STAT3 receptor binding and tyrosine phosphorylation (Zhang et al., 2000).

1.2.2.3 The DNA-Binding Domain

The DNA binding domain contains several β-sheets and intervening loops that determine DNA specificity (figure 1.5). All STATs can bind to an element similar to GAS (gamma-interferon activated sequence) ($TTN_{5-6}AA$), which is probably due to the highly conserved amino acid composition within this domain. However, DNA binding analysis using activated STATs and synthetic oligonucleotides yielded different DNA binding affinities between STAT members (Lamb et al., 1995). The experiments demonstrated that spacing between the palindromic TT-AA core influences DNA binding affinity. For example, the palindrome TT-AA separated by 6bp resulted in selective binding of STAT6 dimers, whereas a spacing of 4bp preferentially favoured STAT3 dimers. Also DNA binding might depend on the composition of the STAT dimers, since STAT1/STAT3 heterodimers appear to bind to different response elements compared to STAT1 and STAT3 homodimers (Lamb et al., 1995). Several years later, Ehret and colleagues described experiments in which they quantified the relative affinity of a series of weak DNA binding sites for STAT1, STAT5a, STAT5b and STAT6. Clear differences observed in the fine specificity between STAT proteins are reflected amongst the natural target sites of different STAT proteins, indicating they contribute to the selective gene activation by these proteins (Ehret et al., 2001).

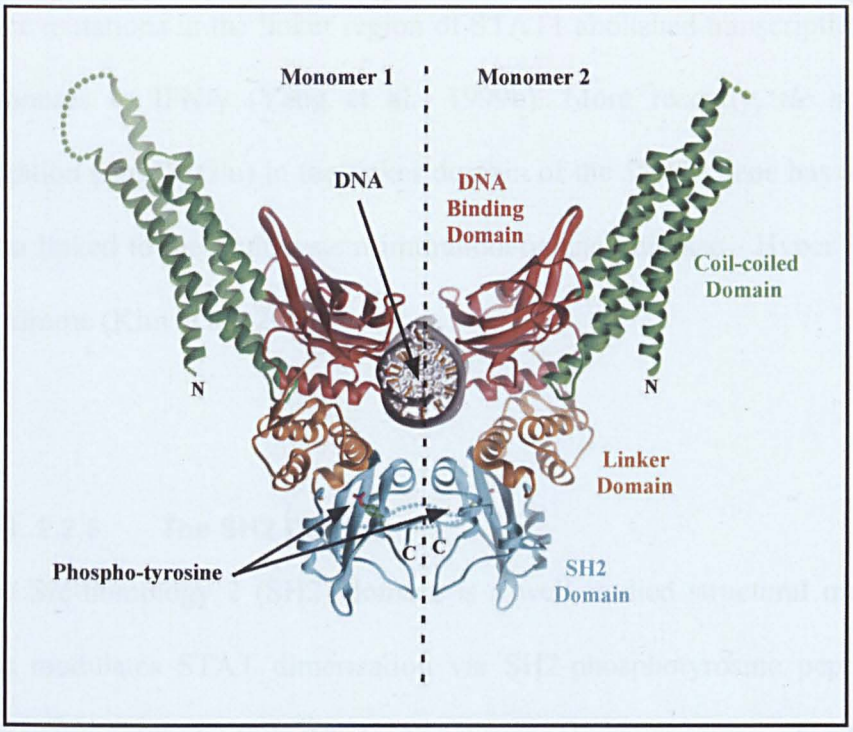

Figure 1.5. Three-dimensional structure of STAT1 protein. The core structure (amino acids 130-712) shows binding of a STAT1 dimer to DNA. Various domains are indicated. Modified from (Levy and Darnell, 2002)

Mutations within the DNA-binding domain of STAT3 are associated with the autosomal-dominant multisystem immuno-deficiency disease known as Hyper IgE syndrome (HIES). HIES presents with elevated serum IgE levels, dermatitis and recurrent skin and lung infections. Minegishi and colleagues identified missence and single codon in-frame deletions of STAT3 located in the STAT3 DNA-binding domain of familial and sporadic cases of HIES (OMIM; 147060) (Minegishi et al., 2007).

1.2.2.4 The Linker Domain

Carboxy-terminal to the DNA binding domain is the highly conserved EF-hand-like linker domain consisting of approximately 100 amino acids. The linker domain may contribute to transcriptional activity,

since mutations in the linker region of STAT1 abolished transcriptional responses to IFN-γ (Yang et al., 1999b). More recently, *de novo* mutation (Lys531Glu) in the linker domain of the *STAT3* gene has also been linked to the multisystem immunodeficiency disease - Hyper IgE syndrome (Kim et al., 2009).

1..2.2.5. The SH2 Domain

The Src-homology 2 (SH2) domain is a well-studied structural motif that modulates STAT dimerisation via SH2-phosphotyrosine peptide interactions (Shuai et al., 1994). The negatively charged phosphate on the tyrosine residue (Y701 for STAT1 and Y705 for STAT3) located at the C-terminal end of the SH2 domain is stablised by a positively charged arginine residue located at the N-terminal region of the SH2 domain STAT partner molecule. Mutations of either the tyrosine or arginine residue completely abolishes STAT dimerisation (Reviewed in (Schindler and Darnell, 1995)).

1.2.2.6 The Transcriptional Activation Domain

The carboxyl-terminal domain of all STAT proteins contains the transcriptional activation domain (TAD), which is the least conserved domain among STAT family members. However, STAT1, STAT3, STAT4 all share a conserved stretch of amino acids in their C-terminal TADs (LPMSP) that includes a phosphorylated serine residue (described in detail in section 1.2.5.1.) that is important to achieve maximal transcriptional activity (Wen et al., 1995, John et al., 1999,

Decker and Kovarik, 2000). The C-terminal region is also important for protein-protein interactions. For example, the C-terminal region of both STAT1 and STAT2 interact with the histone acetyltransferase, CBP/p300 (Paulson et al., 1999) and STAT1 also associates with the mini chromosome maintenance protein (MCM)-5 (Zhang et al., 1998).

1.2.3 STAT isoforms

Naturally occurring splice variants have been identified for all STAT proteins, with the exception of STAT2. These splice variants lack regions of the C-terminal transactivation domain. This leads to a competitive negative effect on gene induction, counteracting the transcriptional activation of full-length STATs. The splice variants are known as STAT1β, STAT3β, STAT4β, STAT5β and STAT6β (Schindler et al., 1992a, Caldenhoven et al., 1996, Hoey et al., 2003, Sherman et al., 1999, Wang et al., 1996) and can be generated by two distinct mechanisms: alternative mRNA splicing and proteolytic processing. STAT3β is generated from alternative splicing, which arises from the alternative-splice acceptor sties in exon 23, which differs from STAT3α by the lack of 50 amino acids from the C-terminal domain (Schaefer et al., 1995). In the case of proteolytic processing, STAT5 is truncated at the transactivation domain (Azam et al., 1995). Cathepsin G has been identified as the protease that cleaves full length STAT5 (STAT5α) to generate a C-terminally truncated form in immature myeloid cells (Lee et al., 1999), however there is some

controversy over whether this cleavage occurs *in vivo* (Garimorth et al., 1999).

1.2.4 Activation of STATs

STATs are activated in response to a variety of cytokines and growth factors, each initiating signal transduction by association with their appropriate receptor (figure 1.6). The various receptor families include transmembrane receptors lacking an intrinsic protein tyrosine kinase domain (non-RTK receptors), single transmembrane receptors with an intrinsic protein tyrosine kinase domain (RTK receptors), and seven transmembrane receptors (G-protein coupled-receptors) (figure 1.5).

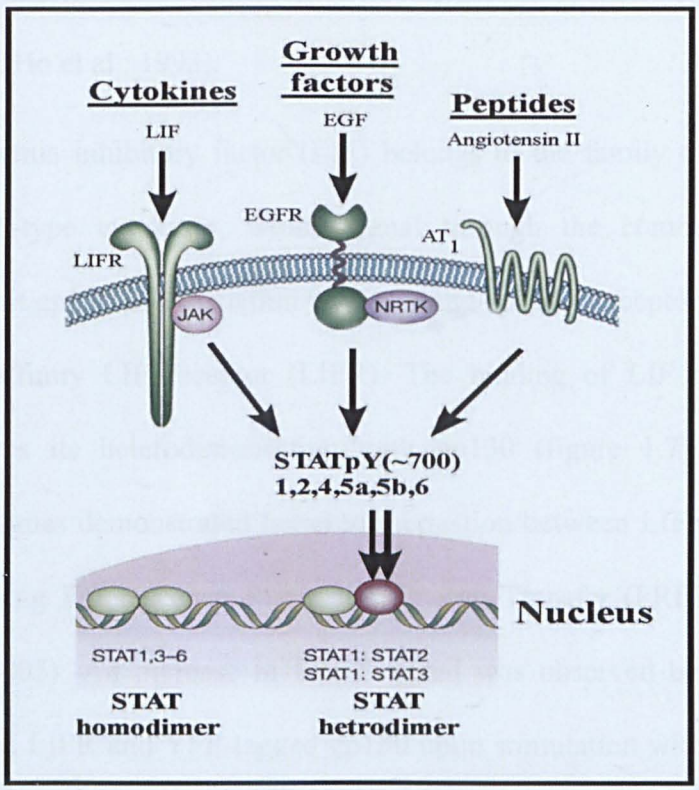

Figure 1.6 Overview of STAT signaling. STAT proteins can be activated by a variety of cytokines, growth factors and peptides. Acivated STAT proteins (STATpY) are able to dimerise and bind to specific DNA sequences to bring about transcription. LIF; Leukemia Inhibitory Factor, LIFR; Leukemia Inhibitory Factor Receptor, EGF; Epidermal Growth Factor, EGFR; Epidermal Growth

Factor Receptor, AT1; Angiotensin II Receptor Type I. Adapted from (Levy and Darnell, 2002).

1.2.4.1 Non-RTK receptors

Non-RTK (cytokine) receptors can be subdivided into two groups on the basis of conserved amino acids in their extracellular domain, termed class I and class II receptors (Schindler and Darnell, 1995). Class I receptors can be further divided into four families (gp130, IL-2, IL-3/IL-5/GM-CSF (gp140) and growth hormone (GH) family), which all share four conserved cysteine residues, an extracellular (WSXWS) motif and a variable intracellular domain. Class II receptors bind interferons including IFN-α, INF-γ and IL-10. These receptors share sequence homology with type I receptors, but have additional cysteine pairs and several conserved proline and tyrosine residues (Novick et al., 1994, Ho et al., 1993).

Leukemia inhibitory factor (LIF) belongs to the family of interleukin (IL)-6-type cytokines, which signal through the common receptor subunit gp130 in association with a ligand-specific receptor subunit, the low-affinity LIF receptor (LIFR). The binding of LIF to the LIFR induces its heterodimerisation with gp130 (figure 1.7). Giese and colleagues demonstrated herterodimeriastion between LIFR and gp130 by using Fluorescence Resonance Energy Transfer (FRET) (Giese et al., 2005). An increase in FRET signal was observed between CFP-tagged LIFR and YFP-tagged gp130 upon stimulation with LIF (Giese et al., 2005). Like all non-RTKs, the LIFR/gp130 receptor complex lacks an intrinsic protein kinase domain, but are able to signal through

the association with Janus Kinase (JAK) family members, a group of receptor associated tyrosine kinases (Darnell, 1997).

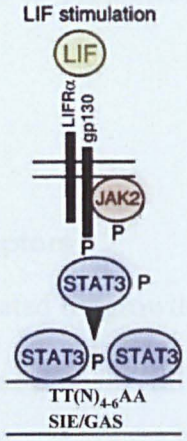

Figure 1.7. JAK/STAT3 pathway via the LIF receptor. LIF binding rapidly induces the LIF receptor (LIFR) and gp130 subunits to form a heterodimer receptor complex. Receptor complex formation leads to autophosphorylation of receptor-associated JAK2, followed by tyrosine phosphorylation of the receptor's cytoplasmic domain and recruitment of STAT proteins to the receptor complex. Subsequent tyrosine phosphorylation of STATs enables homo- or heterodimerisation of STAT proteins. STAT dimers translocate to the nucleus and bind to specific STAT-binding elements in the promoter region of various genes. Modified from (Auernhammer and Melmed, 2001).

In mammalian cells the family consists of four members; Jak1, Jak2, Jak3 and Tyk2, which are phosphorylated via activated non-PTK receptors. JAKs consist of seven JAK homology domains, which share high sequence similarity. At the C-terminus, they contain a tyrosine kinase domain (JH1), which is preceded by a pseudo-kinase domain (JH2). The activated JAKs phosphorylate specific tyrosine residues on the cytoplasmic tails of the cytokine receptors thus, providing docking sites for STAT proteins via their SH2 domains. The recruited STAT monomers are then phosphorylated on their specific tyrosine residues by JAKs, which allows the formation of active STAT dimers through reciprocal phosphotyrosine-SH2 interactions (Darnell, 1997). It has also

been shown that SRC kinases can also facilitate in this process (Reddy et al., 2000). STAT dimers can translocate to the nucleus in a regulated manner where they bind to promoters and enhancer regions of their target genes.

1.2.4.2 RTK-receptors

STATs can also be activated by growth factor receptors, which contain an intrinsic tyrosine kinase domain (Silvennoinen et al., 1993, Zhong et al., 1994, Schaefer et al., 2002). These RTK-receptors include epidermal growth factor receptor (EGFR), platelet derived growth factor receptor (PDGFR) and vascular endothelial growth factor receptor (VEGFR). STAT activation by various RTKs can be JAK-dependant or JAK-independent as both models are present in the literature (Vignais and Gilman, 1999, Paukku et al., 2000, Olayioye et al., 1999, Schaefer et al., 2002). EGFR, VEGFR and PDGFR all possess an intrinsic tyrosine kinase domains and can phosphorylate STATs directly (Vignais and Gilman, 1999, Paukku et al., 2000). However, under some conditions RTKs require the presence of JAK or Src for STAT phosphorylation (Olayioye et al., 1999, Schaefer et al., 2002).

1.2.4.3 G protein-coupled receptors

G protein-coupled receptors have also been reported to activate STAT proteins (figure 1.6). These receptors span the cell membrane seven times and activate GTP-binding proteins. In rat aortic smooth-muscle

cells, angiotensin II induces phosphorylation and activation of JAK2, leading to the rapid tyrosine phosphorylation of STAT1, STAT2, STAT3 and STAT5 (Marrero et al., 1995). In cardiomyocytes, McWhinny and colleagues showed that angiotensin II, acting through the AT_1 receptor could induce STAT1 and STAT3 phosphorylation, translocation to the nucleus and induction of gene transcription (McWhinney et al., 1997). Although it is established that the AT_1 receptor activated the JAK/STAT pathway, the sequence of events leading to the association of AT_1 receptor and STAT proteins has yet to be defined.

1.2.4.4 Non-receptor kinases

In addition, non-receptor cytoplasmic tyrosine kinases such as activated Src and Abelson Leukemia Protein (ABL) (Danial and Rothman, 2000) can directly phosphorylate STAT proteins in the absence of ligand-induced receptor activation. Src-transformed NIH3T3 cells were found to contain a phosphorylated tyrosine form of STAT3 in a constitutive manner (Yu et al., 1995) and studies have shown that v-src is able to bind to and phosphorylate STAT3 *in vitro* (Cao et al., 1996).

These pathways ultimately lead to the tyrosine phosphorylation of STAT proteins that results in homo and heterodimerisation through reciprocal interactions between SH2 domains and phosphotyrosines. STAT1, STAT3, STAT4, STAT5a and STAT5b form homodimers whereas STAT1:STAT2 and STAT1:STAT3 heterodimers are also

capable of forming. STAT dimers translocate to the nucleus where they bind to response elements in the promoters of target genes to initiate transcription. It was initially thought that STAT proteins would only translocate to the nucleus upon activation, however it has been shown that nucleocytoplasmic shuttling of STAT1 and STAT3 is a dynamic process and was first demonstrated using the fluorescence recovery after photobleaching (FRAP) approach. Constitutive shuttling of STAT3 was observed in the absence of cytokine stimulation and IL-6 induction resulted in nuclear accumulation of STAT3 (Pranada et al., 2004).

1.2.5 Regulation of STATs through post-translational modification

Post-translational modification is a common mechanism to regulate protein function, activity and localisation. Post-translational modifications include phosphorylation, acetylation, methylation, glutathionylation, and sumoylation and ubiquitylation.

1.2.5.1 Serine phosphorylation

All STAT proteins contain a tyrosine phosphorylation site that is required for dimerisation and ultimately activation. However, most STAT proteins (STAT1, STAT3, STAT4, STAT5a and STAT5b) can also be phosphorylated at a serine residue present in their C-terminal TAD. Serine phosphorylation was first identified for STAT1 and STAT3 by isolation of proteins from ^{32}P-labelled cells after stimulation

with appropriate cytokines and then subjected to phospho-amino acid analysis (Eilers et al., 1995, Wen et al., 1995). Zhang and colleagues first reported the role of serine phosphorylation for STAT1 and STAT 3 activities, showing its requirement for DNA binding and transcriptional activation (Zhang et al., 1995). These conserved sites consist of a LPMSP motif (Ser^{727} in STAT1, 3 and Ser^{721} in STAT4) (Wen et al., 1995) and LPSP motif (Ser^{725} in STAT5a and Ser^{730} in STAT5b (Yamashita et al., 1998) (figure 1.8).

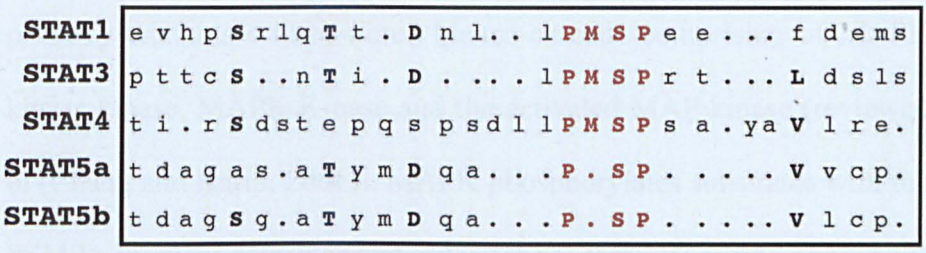

Figure 1.8 Comparison of human STATs containing the P(M)SP phosphorylation site. The P(M)SP motif is highlighted in red. Uppercase letters denotes amino acids conforming consensus sequences. Modified from (Decker and Kovarik, 2000).

The most pronounced effects of serine phosphorylation have been observed in relation to transcriptional activation. Overexpression of STAT3β (lacking the serine 727 phosphorylation site) severely impairs IL-6-induced STAT3 transactivation (Caldenhoven et al., 1996). Also STAT1 and STAT3 Ser-Ala mutations display a reduced transcriptional activity in response to IFNγ or IL-6 type cytokines (Wen et al., 1995), indicating a positive regulatory effect on transcription. However repressive effects on transcription have also been reported with STAT3 serine phosphorylation. A STAT3 (Ser-Ala) mutant increased

transactivation in response to EGF *in vitro* and *in vivo*, suggesting serine phosphorylation either prevents tyrosine phosphorylation or increases tyrosine dephosphorylation (Chung et al., 1997b).

Serine phosphorylation of STAT proteins is mediated by a number of different kinases including; Mitogen-activated protein kinases (MAPK) and Protein kinase C isoforms (PKCδ and PKCε) (Lim and Cao, 1999). The MAPKs are a group of protein serine/threonine kinases that are activated in response to a variety of extracellular stimuli and mediate signal transduction from the cell surface to the nucleus. Each MAPK pathway contains a three-tiered kinase cascade comprising of MAPK kinase kinase, MAPK Kinase and the activated MAP kinase (reviewed in (Chang and Karin, 2001)). MAPK phosphorylates substrates with the PSMP consensus sequence and indeed the C-terminal region of STAT1, STAT3 and STAT4 all resemble the MAPK consensus sequence PxpS/pTP (Gonzalez et al., 1991). Studies have shown that the MAPKs extracellular signal-regulated kinases (ERKs), c-Jun N-terminal kinases (JNKs) and p38MAPK (p38) are involved in serine phosphorylation of STAT proteins (Chung et al., 1997b, Lim and Cao, 1999, Ceresa et al., 1997, Turkson et al., 1999).

Jain and colleagues were in search of an H7-sensitive, IL-6 activated STAT3 serine kinase when they identified PKCδ – a PKC family member of serine-threonine kinases. (Jain et al., 1999). In mammals the PKC family members can be divided into four structurally and functionally distinct subgroups according to their regulatory domains. These are the classical isoforms (α,β,γ), novel isoforms (δ,ε,η,θ),

atypical isoforms (ζ,ι/λ) and the PKC-related kinases (PKN1, PKN2 and PKN3) (Rosse et al., 2010). Activated G-protein coupled seven transmembrane receptors bind and activate phospholipase C (PLC) at the plasma membrane where it hydrolyses phosphatidylinositol 4,5 bisphosphate (PtdIns(4,5)P2) into diacylglycerol (DAG) and inositol 1,4,5-triphosphate (IP3). PKCδ belongs to the novel subfamily and requires diacylglycerol (DAG) for activation (Mellor and Parker, 1998). In addition to DAG, PKCδ is also regulated by phosphorylation (Li et al., 1997b). While most PKC isoforms are phosphorylated at conserved Ser/Thr sites, PKCδ is also phosphorylated at several tyrosine residues by various stimuli including oxidative stress and DNA damaging agents (Steinberg, 2008, Yoshida, 2007).

PKCδ is associated with cardiomyocyte cell death. Murriel and colleagues have shown that PKCδ increases ischaemia and reperfusion-induced apoptosis by affecting the balance between pro- and anti-apoptotic signals (Murriel et al., 2004). By using δVI-1 to specifically inhibit PKCδ translocation at the onset of reperfusion, they observed inhibition of cytochrome c release, caspase-3 activation and PARP cleavage (Murriel et al., 2004). Prolonged exposure to hypoxia has also been associated with the proteolytic and feed-forward activation of PKCδ and caspase-3, resulting in the irreversible commitment to apoptosis (Clavijo et al., 2007).

Studies regarding STAT3 serine phosphorylation by PKCδ are somewhat contradictory. For example, studies by Jain and colleagues revealed that serine phosphorylation by PKCδ has a negative influence

on DNA binding and transcriptional activity (Jain et al., 1999) whereas, activated forms of PKCδ and STAT3 were essential for the insulin-induced PKCδ-STAT3 activation in kerationcyte proliferation (Gartsbein et al., 2006).

Another member of the novel PKC subfamily, PKCε has also been associated with the STAT3 serine phosphorylation. Studies show that PKCε interacts with and serine phosphorylates STAT3, which increases DNA binding and transcriptional activity. PKCε-mediated STAT3 serine phosphorylation seems to be essential for the constitutive activation of STAT3 and prostate cancer invasion (Aziz et al., 2007).

1.2.5.2 Acetylation

The idea that STAT proteins could be acetylated was due to the discovery that various STATs associate with histone acetyltransferase CREB-binding (CBP/p300) and show enhanced transcriptional activity (Zhang et al., 1996, Korzus et al., 1998). The first report described that acetylation of STAT6 by CBP/p300 was required for the transcriptional activation of 15-lipoxygenase (15-lox-1) by IL-4 (McDonald and Reich, 1999, Shankaranarayanan et al., 2001). Treatment of cells with histone deacetylase inhibitors (HDACi) was reported to reveal the acetylation sites in STAT1 at Lys410 and Lys413 (Kramer et al., 2006) and was proposed to regulate apoptosis by facilitating binding of NF-κB and control immune responses by suppressing STAT1 tyrosine phosphorylation (Kramer et al., 2009). However, recently Antunes and colleagues have questioned this work as they demonstrate that

inhibition of deacetylase had no effect on STAT1 acetylation and did not suppress tyrosine phosphorylation. They propose that the defective DNA binding activity and transcriptional activity may be due to inactivation of the DNA binding domain of STAT1 or nuclear import signal rather than due to its acetylation status (Antunes et al., 2011).

It was also reported that STAT3 could be acetylated in the N-terminal region, at positions Lys49 and Lys87 by CBP/p300. Mutational analysis (STAT3 K49R/K87R) had no effect on inducible DNA binding, but blocked CBP/p300-mediated STAT3 acetylation and abrogated IL-6-induced human angiotensinogen (hAGT) gene activation in hepatocytes (Ray et al., 2005).

1.2.5.3 Methylation

Methylation of STAT proteins was first described for STAT1 at residue Arg31 in the N-terminal domain in response to IFN-γ by protein arginine methyl-transferase (PRMT1). Interestingly, methylation led to a weaker interaction between STAT1 and the protein inhibitor of activated STATs (PIAS), resulting in increased DNA binding by STAT1 (Mowen et al., 2001). Recently, it has been reported that STAT3 is methylated at residue Lys140 by the H3K4 methyltransferase, SET9 in response to IL-6. Prevention of methylation by mutation of K140 allowed greater phosphorylation of STAT3 Y705 in response to IL-6, which was associated with enhanced expression of the negative regulator of STAT3 activation (SOCS3) (Yang et al., 2010).

1.2.5.4 Glutathionylation

Glutathione plays a role in reversible post-translational modification called S-glutathionylation, which is a physiological, reversible protein modification of cysteines residues with glutathione that occurs in response to mild oxidative stress (Klatt and Lamas, 2000). Recently a study has shown that STAT3 is novel target for protein S-glutathionylation (Xie et al., 2009). Increased levels of S-glutathionylated STAT3 were observed in cells treated with diamide - a thiol oxidising agent. S-glutathionylation of STAT3 was accompanied with a reduction in IL-6 induced tyrosine phosphorylation of STAT3, subsequent nuclear retention and transcriptional activities of STAT3 target genes (Xie et al., 2009).

1.2.5.5 Ubiquitination

Ubiquitination, the conjugation of proteins with a protein called ubiquitin (Ub) is essential for the degradation of proteins.

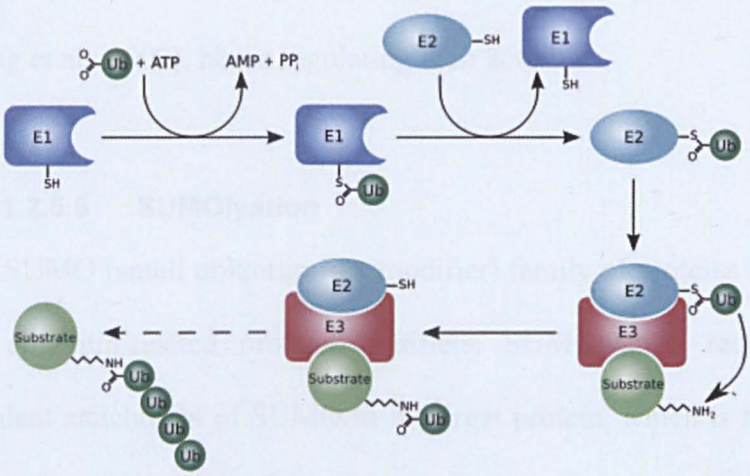

Figure 1.9.The ubiquitylation system. The ubiquitination pathway consists of three sequential steps: 1) An ATP dependent step of loading E1 activating enzyme with ubiquitin (Ub), 2) Transfer of the E1's ubiquitin to an E2 conjugating enzyme and 3) the E3 ligase mediated transfer of ubiquitin from an E2 to the substrate. Taken from (Dodd, 2005)

Free Ub is activated in an ATP-dependent manner, by the activity of an ubiquitin-activation enzyme E1, leading to the formation of a thiol-ester linkage between E1 and the carboxyl terminus of ubiquitin (figure 1.9). The ubiquitin is subsequently transferred to one of many ubiquitin-conjugating enzymes E2. The last step in the process utilises a ubiquitin protein ligase E3 to catalyse the transfer of Ub from the E2 enzyme to the target proteins (Nandi et al., 2006). Degradation of ubiquitinated proteins is performed by the 26S proteasome system, which is composed of the two terminal 19S regulatory subunits bound to the

proteolytic core. The ubiquitin-proteasome degradation has shown to be important for the regulation of the JAK/STAT pathway. Studies show that with the use of proteasome inhibitors, JAK1, JAK2 and JAK3 are all targets for degradation (Ungureanu et al., 2002, Yu and Burakoff, 1997). In addition, tyrosine phosphorylated STAT1, STAT4, STAT5 and STAT6 were also targets for degradation (Kim and Maniatis, 1996, Wang et al., 2000), hence regulating their activities.

1.2.5.6 SUMOlyation

The SUMO (small ubiquitin-like modifier) family of proteins belong to the ubiquitin-related protein modifiers. SUMOlyation requires the covalent attachment of SUMO to its target protein, which is facilitated by a set of enzymes; E1 activating enzyme (Aos1 and Uba2), conjugating E2 enzyme (Ubc9) and ligating E3 enzyme (PIAS, RAN-binding protein 3 (RanBP2) or polycomb protein (PC2)). SUMOlyation was first described for STAT1 at residue Lys703 in the presence of PIASxα – an E3 ligase. A negative regulatory function for SUMOlyation of STAT1 was suggested due to the fact that mutation of Lys703 in STAT1 resulted in increased mediated IFN-γ mediated transcriptional activation (Ungureanu et al., 2003). STAT3 activity is inhibited by SUMO-conjugation. Inhibition occurs directly by decreasing STAT1 tyrosine phosphorylation and indirectly by facilitating STAT1 dephosphorylation, consequential to increase STAT1 solubility due to suppressed paracrystals assembly (Droescher et al., 2010).

1.2.6 Negative regulation of STATs

The rapid and transient nature of STAT activation suggests there are mechanisms in place to switch off this signaling pathway. Studies have show that STAT signaling is negatively regulated at different points within the signaling cascade. Factors involved in negative regulation are members of the SOCS (suppressors of cytokine signaling) family, the PIAS (protein inhibitor of activated STATs) family and PTPs (protein tyrosine phosphatases).

1.2.6.1 Suppressors of cytokine signaling

The suppressors of cytokine signaling (SOCS) family comprise a family of 8 members that includes CIS-1 (cytokine-inducible SH2 containing protein) and SOCS1-7. All family members share a similar structure with a central SH2 domain, a region of homology called the SOCS box at the C-terminus and a kinase inhibitory region located at the N-terminus (Naka et al., 1997, Krebs and Hilton, 2000). SOCS proteins are generally expressed at low levels in unstimulated cells and expression is greatly enhanced upon cytokine, insulin and EGF stimulation (Alexander, 2002). The mechanism of inhibition varies between different SOCS proteins. For example, SOCS1 binds directly to tyrosine-phosphorylated JAKs via its SH2 domain and as a consequence JAK activity is directly inhibited. SOCS3 acts by binding directly to the activated receptors inhibiting IL-6 and LIF signal transduction (Nicholson et al., 1999). SOCS are also direct gene targets

of STATs indicating that SOCS act part of a classical feedback inhibition loop (Matsumoto et al., 1997).

1.2.6.2 Protein inhibitors of activated STATs

Five members belong to the family of proteins that inhibit activated STATs (PIAS), which include: PIAS1, PIAS3, PIASxα, PIASxβ and PIASy. Protein inhibitor of activated STAT3 (PIAS3) was the first family member to be identified by its PIAS3 association with tyrosine-phosphorylated STAT3 and thus prevention of STAT3 DNA binding (Chung et al., 1997a). PIAS1 was later identified using a yeast two-hybrid screen with STAT1β as the bait. It was also described as a novel regulator of STAT1 that blocks DNA binding and consequently inhibits STAT1 mediated IFN-induced transcriptional activity (Liu et al., 1998). In addition to inhibiting STATs, PIAS proteins have been shown to impact on the function of many different proteins, but a major process on which all these proteins act is in the controlling gene expression (Schmidt and Muller, 2003, Shuai and Liu, 2005). Thus, PIAS proteins can be thought of as transcriptional co regulators.

1.2.6.3 Protein phosphatases

Dephosphorylation is an important way of inhibiting the STAT-signaling pathway. It can occur at the cell membrane, where the receptors, JAKs and STATs are targets, as well as in the nucleus where dephosphorylation of STATs take place. The best-characterised protein tyrosine phosphatase is SHP-1. SHP-1 contains two SH2 domains and

can bind to phosphorylated JAKs and receptors. Expression of SHP-1 is restricted to haematopoietic cells (Neel et al., 2003). SHP-1 down-regulates erythropoietin (EPO)-induced proliferation signals by binding to the EPO-receptor and dephosphorylating the associated JAK2 (Klingmuller et al., 1995). SHP-2 shares a similar overall structure and high homology with SHP-1 but is ubiquitously expressed. SHP-1 negatively regulates the IFN-induced JAK1/STAT1 pathway (Shuai and Liu, 2003) and has also been shown to negatively regulate the activity of STAT3 (Chan et al., 2003a). Studies have identified that $SHP^{\Delta/\Delta}$ mutated murine ES cells showed defective differentiation and more efficient renewal in the presence of leukemia inhibitory factor (LIF), which was due in part to increased STAT3 activity (Chan et al., 2003a).

Protein tyrosine phosphatases also regulate STATs in the nucleus. STAT1 protein tyrosine phosphatase activity was identified in HeLa nuclear extracts, known as TC45. TC45 can dephosphorylate STAT1 both *in vitro* and *in vivo* and nuclear extracts lacking TC45 failed to dephosphorylate STAT1 (ten Hoeve et al., 2002). More recently receptor-type tyrosine phosphatase, PTPRT has been shown to dephosphorylate STAT3 at Y705. Overexpression of PTPRT leads to the reduction in STAT3 target gene expression (Zhang et al., 2007). Studies have shown that there in an inter-relationship between DNA-binding and nuclear phosphatase activity. Meyer and colleagues demonstrated that inactivation of STAT1 is controlled by its exchange with DNA, whereby DNA binding protects STAT1 from

dephosphorylation in a sequence specific manner (Meyer et al., 2003). This was also observed with a constitutively active form of STAT3 known as STAT-C (Li and Shaw, 2006). This STAT3 mutant displayed a higher DNA binding affinity than $STAT3^{Wt}$ and its slower DNA off rates delayed dephosphorylation by nuclear phosphatases (Li and Shaw, 2006).

1.2.7 Biological roles of STATs

Although STAT proteins are structurally very similar, studies with genetically manipulated mice suggest a high degree of specificity for each STAT protein. The biological functions of STAT proteins have been extensively investigated through the generation of gene-targeted mice. All STAT family members have been successfully knocked-out and their phenotypes described with the exception of STAT3 (discussed in more detail in section 1.2.7.1).

1.2.7.1 Biological roles of STAT3

STAT3 is ubiquitously expressed in many tissues including the kidney, liver, lungs and the heart (GeneCards ID: GC17M040465). However, unlike other STAT family members, functional analysis of STAT3 *in vivo* has been more complex. Takeda and colleagues generated STAT3-deficient mice to examine the biological function of STAT3. Homozygous null ($STAT3^{-/-}$) mice were not generated, indicating embryonic lethality. STAT3 null embryos were able to implant and

develop until E6.0, however rapidly degenerated with no obvious mesoderm formation between E6.5-E7.5 (Takeda et al., 1997).

Therefore, to investigate the biological roles of STAT3 in adult mice, the gene has been conditionally knocked out in a tissue- or cell-specific manner using the Cre-LoxP recombination system (Rajewsky et al., 1996).

The role of STAT3 has been investigated in the skin. Using the Cre-LoxP system, STAT3 was specifically disrupted in keratinocytes. Despite functional ablation of STAT3 in kerationcytes, the development of the epidermis and hair follicles appeared normal. However these mice had sparse hair; wound-healing processes were severely compromised and they spontaneously developed ulcers of the skin with age (Sano et al., 1999). This analysis provided the first *in vivo* data showing STAT3 has a function in cell migration and that STAT3 is necessary for skin remodeling, including hair cycle and wound healing (Sano et al., 1999). STAT3 has also been implicated in the initiation and progression of skin cancer (Chan et al., 2004). Epidermis STAT3-deficient mice showed a significant reduction in the proliferative response following treatment with the tumor-promoter agent 12-O-tetradecanoylphorbol-13-acetate (TPA) due to a defect in G1-S phase cell cycle progression (Chan et al., 2004).

STAT3 also appears to play a regulatory role in the immune system. Mice generated with STAT3-deficient macrophages and neutrophils were highly susceptible to endotoxin shock with increased production of inflammatory cytokines such as TNF alpha (Takeda et al., 1999).

STAT3 has also been implicated in the immune system in an anti-apoptotic role. Studies show that STAT3-deficient T-cells exhibited loss of a proliferative response to IL-6 due to a defect in IL-6-mediated suppression of apoptosis. (Takeda et al., 1998). More recently, STAT3 has also been shown to play an essential role in the pathogenesis of the IgG immune complex in acute lung injury by mediating the acute inflammatory responses in lung and alveolar macrophages (Tang et al., 2011). Specific siRNA knockdown of STAT3 in alveolar macrophages showed a significant reduction in the production of pro-inflammatory mediators of IgG immune complex stimulation (Tang et al., 2011).

STAT3 is also expressed in mammary glands where it displays a pro-apoptotic role in post-lactational regression. STAT3 phosphorylation occurs at the onset of mammary gland involution. STAT3-deficient mammary glands showed a decrease in apoptosis and exhibited a dramatic delay in mammary gland involution, a stage of mammary gland post-lactational regression that is characterised by extensive apoptosis of epithelial cells due to impaired epithelial cell apoptosis (Chapman et al., 1999). This study identified for the first time that STAT3 plays an important role in apoptosis *in vivo*. However recently, morphological analysis of mammary gland involution in mice revealed features that were atypical for classical apoptosis, such as hypercondensed nuclei, swelling of cells and a complete lack of membrane blebbing. Studies show that STAT3 controls involution of the mammary gland by epithelial cells undergoing a lysosomal-

dependent programmed cell death, which is independent of executioner caspases (Kreuzaler et al., 2011).

The role of STAT3 in cardiomyocytes has also been extensively studied through the cardiomyocyte-specific disruption of STAT3 and is discussed in more detail in section 1.2.7.2.

Further information regarding the biological functions of STAT3 has emerged from overexpression studies utilising dominant negative versions of STAT3. Nakajima and colleagues described a role of STAT3 in differentiation. They used STAT3 mutants lacking the tyrosine phosphorylation site (Y705F), which were shown to block IL-6 and LIF-induced macrophage differentiation of myeloid leukaemia (ML) cells (Nakajima et al., 1996).

The self-renewal of embryonic stem (ES) cells has also been associated with STAT3. Self-renewal allows the continuously propagation of cells in an undifferentiated, pluripotent state. The pluripotency of mouse stem cells depends on LIF-activated STAT3, since mutations of either gp130 receptor or STAT3 abrogated the self-renewal of ES cells and led to the onset of differentiation (Humphrey et al., 2004). The importance of the LIF/STAT3 pathway in self-renewal has also been documented in chicken and rat ES cells (Horiuchi et al., 2004, Buehr et al., 2008). ChIP-on-chip and ChIP-seq analyses has revealed that STAT3 binds to the regulatory regions of several self-renewal genes in ES cells suggesting that LIF signaling in ES cells promotes expression of self-renewal genes and simultaneously suppresses induction of differentiation-associated genes (Chen et al., 2008, Kidder et al., 2008).

1.2.7.2. STAT3 and the heart

STAT3 elicits diverse functions in various cell types and has also been showed to play extensive roles in the heart. Cardiomyocyte-STAT3 activity is required for controlling cardiac growth, function, tissue architecture and protection against cardiovascular stress.

It has been suggested that STAT3 plays a role in the early phase of postnatal angiogenesis of the heart – a process involving the growth of new blood vessels from pre-existing vessels. During postnatal growth of the heart there is rapid vascular development, providing nutrient-rich, oxygenated blood to the heart which is required for optimum function of cardiac tissue (Hudlicka and Brown, 1996). Vascular endothelial growth factor (VEGF) is one of the most important known inducers of angiogenesis. Funamoto and colleagues have demonstrated that VEGF induction in cardiomyocytes by glycoprotein (gp) 130, a subunit of the IL-6 receptor requires STAT3 signaling (Funamoto et al., 2000). More recently the siRNA knockdown of STAT3 lead to a down-regulation of mRNA expression of VEGF, thus reducing angiogenesis in lung cancer cells (Zhao et al., 2011)

Studies have shown that mice containing the $STAT3^{S727A}$ gene mutation show a failure to thrive as well as increased lethality during the first week of birth (Shen et al., 2004). The STAT3 serine deletion was associated with a reduction in the transcriptional activity of STAT3 alongside a reduction in the serum levels of insulin-like growth factor (IGF-1) - a known proangiogenic factor, which is involved the upregulation of pro-angiogenic VEGF (Dunn, 2000). Cardiomyocyte-

specific deletion of STAT3 has also been implicated in mechanisms that control cardiac vasculature and extra-cellular matrix (ECM) composition. Cardiomyocyte specific overexpression of STAT3 increased myocardial capillary density and enhanced expression of VEGF – a STAT3 target gene (Hilfiker-Kleiner et al., 2004). Conversely, cardiomyocyte STAT3 knockout mice display a progressive decrease in capillary density together with alterations in the ECM composition, which led to subsequent heart failure in older age (Jacoby et al., 2003).

Earlier studies showed that STAT3 plays a key role in cardiac-hypertrophy (Yasukawa et al., 2001). Cardiomyocyte-specific over-expression of STAT3 in mice caused spontaneous cardiac hypertrophy (Kunisada et al., 2000). Activation of gp130 receptor signaling via LIF, induced hypertrophic growth in cardiomyocytes, a feature that was abolished by over expression of the negative regulator of gp130/JAK/STAT signaling, SOCS3 (Yasukawa et al., 2001). Recently it has been shown that he angiotensin II type 1 receptor induces unregulated expression of STAT3, leading to nuclear accumulation of STAT3 that significantly correlated with the progression of cardiac hypertrophy (Yue et al., 2010). Yan and colleagues also suggests that the α_1-Adrenergic receptor (α_1-AR) induces the activation of STAT3, mainly through transactivation of EGFR, which plays an important role in α_1-AR-induced cardiac hypertrophy (Li et al., 2011).

Changes in the regulation of STAT3 have been observed in failing hearts. Powedski and colleagues analysed samples obtained from patients undergoing heart transplantation due to dilated cardiomyopathy (DCM), which represents a common end-stage disease state of the myocardium that leads to cardiac dilation and heart failure (Hunter and Chien, 1999). In these samples they observed that the expression and tyrosine phosphorylation of STAT3 was severely reduced (Podewski et al., 2003). This raised the possibility that decreased activation of STAT3 may contribute to the development of heart failure in patients. This hypothesis was later supported by the observation that mice with cardiomyocyte-specific disruption of STAT3 developed DCM, heart failure and succumbs to early death (Jacoby et al., 2003, Hilfiker-Kleiner et al., 2004).

STAT3 also seems to modulate inflammation in the heart in response to environmental factors. Treatment of cardiomyocytes with bacterial endotoxin lipopolysacharide (LPS) induced the activation of STAT3 (Cowan et al., 2000). In support of this, cardiomyocyte-restricted knockout of STAT3 in mice led to enhanced apoptosis upon LPS treatment, indicating that STAT3 knock-out mice may have a hyperactive response to inflammatory stimuli induced by bacterial toxins (Jacoby et al., 2003).

Studies have also demonstrated that STAT3 plays an integrated role in ischaemic preconditioning (IPC) (Smith et al., 2004) (Boengler et al., 2008b). In 2004 Smith and colleagues demonstrated that STAT3 is necessary for IPC; genetic depletion of cardiomyocyte-specific STAT3

completely abolished the cardio-protective effects observed with classical IPC. These findings were confirmed in isolated cardiomyocytes from STAT3 knockout mice, which did not display an increase in cell viability by IPC after 26h ischaemia (Smith et al., 2004). Consistent with this, later studies in mouse hearts identified an increase in the tyrosine phosphorylation of JAK proteins (JAK1 and JAK2), STAT1 and STAT3, as well as enhanced STAT3 DNA binding in response to IPC (Boengler et al., 2008b). In addition to IPC, STAT3 has also been associated with the cardioprotective roles of ischaemic post conditioning (postC) – a process in which transient periods of ischaemia/reperfusion occur at the onset a reperfusion assault. Boengler and colleagues demonstrated that during postC there was an increase in phosphorylated STAT3, which accompanied a reduction in infarct size. The cardioprotection observed with postC was also abolished in cardiomyocyte-specific STAT3 deficient mice (Boengler et al., 2008a).

Cardioprotective effects by STAT3 have been linked to direct transcriptional up-regulation of antioxidant enzymes such as manganese dismutase (MnSOD) (discussed in section 1.3.3), as well as the induction of anti-apoptotic and cytoprotective proteins including Bcl_{XL} and Hsp70 (Hilfiker-Kleiner et al., 2004, Stephanou and Latchman, 1999). In addition, studies on transgenic hearts expressing constitutively active STAT3 have shown resistance to I/R injury through the upregulation of reactive oxygen species (ROS) scavengers Metallothionein1 (MT1) and metallothionein2 (MT2), which are

associated with reduction in ROS generation and apoptosis (Oshima et al., 2005).

STAT3 also offers protection against age-related cardiac dysfunction (Jacoby et al., 2003). Cardiomyocyte-specific STAT3 knock-out mice develop normally into adulthood without any obvious cardiac abnormalities. However, slight morphological changes such as a marginal increase in interstitial fibrosis and decrease in myocardial capillary density became apparent in young adult STAT3-KO mice (3 months). Beyond 8 months STAT3-KO mice developed dilated cardiomyopathy with severe heart failure and premature death (Jacoby et al., 2003).

1.3 Reactive Oxygen Species

1.3.1 What are Reactive Oxygen Species?

Reactive oxygen species (ROS) include free radicals, which typically have oxygen or nitrogen based unpaired electron. Examples of free radicals include O_2^- (superoxide anion), $OH^\bullet$ (hydroxyl radical) and $ONOO^-$ (peroxynitrite). Other species such as hydrogen peroxide (H_2O_2) can also act as oxidants (reviewed in (D'Autreaux and Toledano, 2007)).

The physiological generation of ROS can occur as a by-product of other biochemical processes including within mitochondria, peroxisomes, xanthine oxidase and other cellular elements (Balaban et al., 2005, Schrader and Fahimi, 2004, Tsutsui, 2001). The phagocyte NADPH

Oxidase (NOX) was the first identified by Rossi and colleagues in 1964 as example of a system that generates ROS not as a by-product, but rather as a primary function (Rossi and Zatti, 1964). NADPH oxidases generate superoxide by transferring electrons to NADPH inside the cell, across the membrane and coupling these to molecular oxygen to produce superoxide, thus providing host defense against bacterial and fungal pathogens (Geiszt and Leto, 2004).

1.3.2 Consequences of ROS

Accumulation of ROS promotes the onset of cell death, resulting in characteristic cellular changes including lipid peroxidation, protein oxidation and double-stranded DNA breaks (Kukreja and Hess, 1992).

Oxygen radicals catalyse the oxidation of lipids (figure 1.10) (Gardner, 1989). For example, cell membranes, which are structurally composed of polyunsaturated fatty acids, which are highly susceptible to oxidative attack leading to changes in membrane fluidity and permeability. Indeed a study has shown that cell membrane damage and lipid peroxidation occurs during hypoxia-reoxygenation (Yajima et al., 2009).

Excess ROS can also cause damage to nuclear and mitochondrial DNA (figure 1.10) The nature of the damage includes base modifications, strand breakage and DNA-protein cross-links, which can lead to DNA mutations. For example, ROS have been shown to induce mutations in the p53 tumour-suppressor gene (Hussain et al., 1994).

Proteins are major targets for ROS because of their abundance in biological systems. Oxidative damage to proteins is induced directly by ROS or indirectly by reactions of secondary by-products of oxidative stress, and can lead to peptide-backbone cleavage, cross-linking, and/or modifications to amino acid side chains (Dalle-Donne et al., 2003). The susceptibility to oxidation varies from one amino acid to another (Stadtman, 1995). The most sensitive amino acids are those containing sulfhydryl groups, which include methionine and cysteine. Sulphydryl groups interact with ROS producing sulphoxides, sulphenic acids and disulphide bridges (Sohal, 2002).

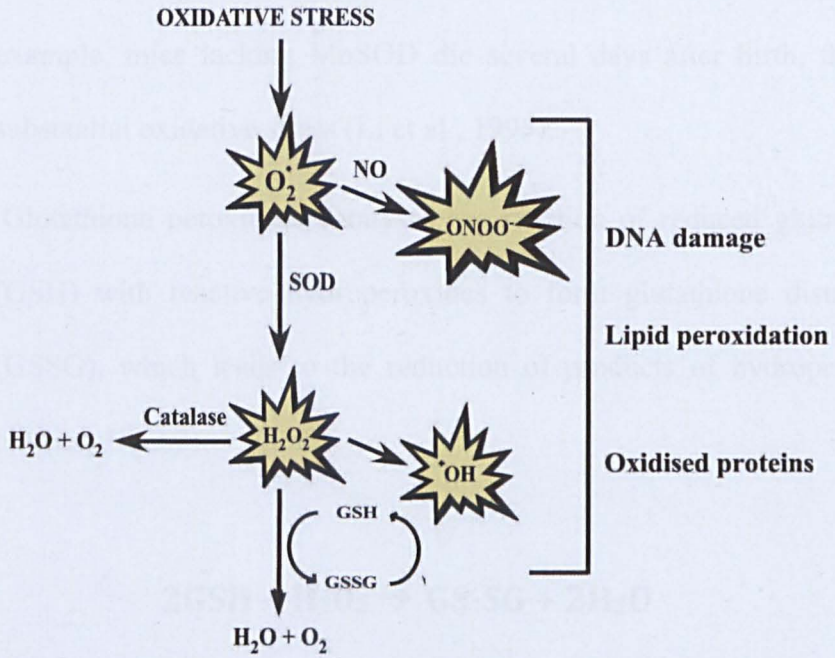

Figure 1.10. Reactive Oxygen Species production and cellular defense mechanisms. Antioxidant enzymes; Catalase, Superoxide Dismutase (SOD) and Glutathione (GSH) remove reactive oxygen species $O_2^{\bullet}$ (superoxide) and hydrogen peroxide (H_2O_2) from the cell. Modified from (Dennis V. Cokkinos, 2006).

1.3.3 Defenses against ROS

Cells have well adapted mechanisms that control the formation of excess free radicals, which utilise antioxidant enzymes and free radical scavengers. The antioxidant superoxide dismutase (SOD) (Fridovich, 1983, Fridovich, 1986) catalyses the conversion of superoxide into hydrogen peroxide. The copper-zinc SOD metalloprotein is located in the cytosol, while the manganese SOD (mnSOD) is located in the mitochondria. The biosynthesis of SOD is mainly controlled by its substrate, superoxide anion O_2^-. Increased expression of SOD is observed with intracellular fluxes of O_2^- (Rister and Baehner, 1976). The physiological importance of SODs is illustrated by the severe pathologies demonstrated through studies on SOD knock-out mice. For example, mice lacking MnSOD die several days after birth, through substantial oxidative stress (Li et al., 1995).

Glutathione peroxidase catalyses the reaction of reduced glutathione (GSH) with reactive hydroperoxides to form glutathione disulphide (GSSG), which leads to the reduction of products of hydroperoxide (section 1.3.2.2).

$$\mathbf{2GSH + H_2O_2 \rightarrow GS\text{-}SG + 2H_2O}$$

Glutathione peroxidase is a saleno-enzyme that is present in the cytosol and mitochondria (Freeman and Crapo, 1982).

Catalase is present in all mammalian cells and is localised to the peroxisomes. Catalase aids in the rapid decomposition of hydrogen

peroxide into less reactive gaseous oxygen and water molecules (Deisseroth and Dounce, 1970)

In addition to the primary defense against ROS by antioxidant enzymes, a secondary defense is offered by small molecules that can act as direct redox regulators to protein thiols. Thioredoxins are small thiol-oxidoreducatases that act as antioxidants by facilitating the reduction of other proteins by cysteine-thiol-disulphide exchange. Thioredoxins contain two vicinal cysteines in a CxxC motif that participates in protein thiol reduction. Another antioxidant that can protect against ROS is a cysteine-containing tri-peptide called glutathione. Glutathione exists both in a reduced (GSH) and oxidised glutathione disulphide (GSSG). The reduced glutathione acts as an antioxidant by serving as an electron donor. In the process, glutathione is converted to its oxidised form, GSSG. Glutathione is found almost exclusively in its reduced form, since the enzyme that reverts it from its oxidised form, glutathione reductase (GR) is constitutively active and inducible upon oxidative stress. In fact, the ratio of GSH:GSSG within cells is often used as a measure of cellular oxidative stress (Pastore et al., 2001).

1.3.4 ROS during cellular signaling

High levels of ROS production can be detrimental leading to cell death, however ROS production at lower concentrations can modulate intracellular signaling pathways (Redox signaling).

The best understood pathway by which ROS achieves regulation through cell function occurs through regulating tyrosine phosphatases (PTPs). PTPs control the phosphorylation status of many signal-transducing proteins and are therefore involved in many processes including proliferation, differentiation and survival (Hunter, 2000). The catalytic region of PTPs contains cysteines (Barford, 2004), which are susceptible to oxidation inactivation (Denu and Tanner, 1998). Consistent with this mechanism, NOX-derived ROS has shown to regulate protein tyrosine phosphorylation (Goldstein et al., 2005).

ROS is also a regulator in the SUMOlyation/deSUMOlyation equilibrium. Studies have shown that low levels of ROS cause a rapid disappearance of most SUMO-conjugates. Inhibition was achieved through the formation of disulphide bonds involving the catalytic cysteines of the SUMO E1 subunit Uba2 and the conjugating enzyme Ubc9 (Bossis and Melchior, 2006).

Studies have shown that ROS can also offer cardioprotection - Yue and colleagues demonstrated that the mitochondrial ROS generator menadione can cause cardioprotection through a pathway involving p38-mitogen activated protein kinase (MAPK) activation (Yue et al., 2002). Antimycin has also been shown to generate mitochondrially-derived ROS, which activates PKCε that has been shown to be crucial for cardioprotection (Kabir et al., 2006).

ROS had also been shown to stimulate cardiac hypertrophy – Kwon and colleagues demonstrated that hydrogen peroxide caused concentration dependant effects on adult rat ventricular myocytes (ARVM)

phonotype. Hypertrophy was observed at low concentrations (10-30μM) whereas high concentration (100 μM) leads to apoptosis (Kwon et al., 2003).

ROS has also been implicated in redox signaling in cardiomyocytes. A variety of cardiac proteins are susceptible to redox modification including PKG 1α and the sacroplasmic reticulum calcium pump (SERCA) (Burgoyne et al., 2007, Adachi et al., 2004). In addition ROS can modulate signaling pathways including the activation of ERK1/2, p38 MAPK, Akt, PKCs and NF-κB that are involved in cardiac hypertrophy (reviewed in (Sugden and Clerk, 2006).

1.3.4.1 Regulation of JAK/STAT pathway by ROS

Reactive oxygen species have also been implicated in the regulation of the JAK/STAT pathway. Studies have shown that tyrosine phosphorylation and DNA binding activities of STAT3 were activated in response to oxidative stress (Simon et al., 1998, Carballo et al., 1999). Rat-1 fibroblast cells exposed hydrogen peroxide (1mM H_2O_2) showed an induction STAT3 activity and this activity could be abolished by the addition of antioxidants (Simon et al., 1998). Enhanced tyrosine phosphorylated of STAT3 was later observed in human lymphocytes exposed to oxidative stress (Carballo et al., 1999).

STAT3 has also been associated with protection against oxidative stress. Studies show that STAT3 deficient mouse embryonic fibroblasts (MEFs) were more sensitive to death when treated with H_2O_2 in a dose

dependent manner, indicating that STAT3-deficiency renders cells more susceptible to oxidative stress (Barry et al., 2009).

STAT3 is also modified directly in response to oxidative stress. STAT3 becomes s-glutathionylated upon mild oxidative stress (section 1.2.5.4) leading to marked reduction in IL-6-dependent STAT3 signaling (Xie et al., 2009). More recently, Li and colleagues have demonstrated that STAT3 is capable of forming high molecular weight (~180kDa, ~270kDa and ~360kDa) complexes in various cell types that are exposed to peroxide. As mass spectrometry analyses did not detect other proteins within these complexes it suggests the formation of STAT3 redox multimers. The formation of these STAT3 redox multimers also correlated with the loss of STAT3 DNA binding during peroxide treatment (Li et al., 2010).

1.3.5 ROS and cardiovascular disease

ROS generated during I/R injury has been implicated as primary cause of oxidative stress and tissue damage in ischaemic heart disease (Turrens and Boveris, 1980, Blake et al., 1987).

The concept that oxidative stress is important in the pathogenesis of cardiovascular disease was conceived from studies that noted the cytotoxic and atherogenic properties of oxidized LDL (oxLDL). Free radicals oxidise LDL causing macrophages to devour them and become "foam cells" which clog up arterial walls and contribute to the development of atherosclerosis. Steinberg and colleagues revealed that macrophages engulf oxLDL at a faster rate than un-oxidised LDL,

accelerating the process of atherosclerosis (Steinberg et al., 1989, Witztum and Steinberg, 1991).

The superoxide anion $O_2^{\bullet-}$ is capable of reacting with nitric oxide (NO), a blood vessel dilator and anti-thrombotic agent generated in the lining of the blood vessel. This reaction inactivates nitric oxide and its diminished bioactivity causes constriction of coronary arteries, which contributes to myocardial ischaemia in patients with coronary artery disease (Cannon, 1998). The reaction between NO and $O_2^{\bullet-}$ also leads to the formation of peroxynitrite ($ONOO^-$), which is implicated in DNA damage (Ballinger et al., 2000), enzyme inactivation (MacMillan-Crow et al., 1998) and lipid peroxidation.

1.4 Mitochondrial dysfunction

1.4.1 The role of mitochondria

Mitochondria are membrane-enclosed organelles found in most eukaryotic cells (Henze and Martin, 2003). Mitochondria are generally considered "cellular power plants" due to the fact they generate the majority of the cell's supply of adenosine triphosphate (ATP) in a process called oxidative phosphorylation. In this process, electrons are transported between complexes I to IV of the mitochondrial electron transport chain (ETC) (figure 1.11) (McBride et al., 2006). Electron transport is coupled with the movement of protons from complexes I, III and IV into the intermembrane space, creating an electrochemical gradient ($\Delta\psi$) across the inner mitochondrial membrane. Protons then

flow through complex V (ATP synthase), which utilises the energy to generate ATP. In addition to cellular energy, mitochondria are involved in various other cellular processes including signaling, cell death, control of the cell cycle and growth (McBride et al., 2006).

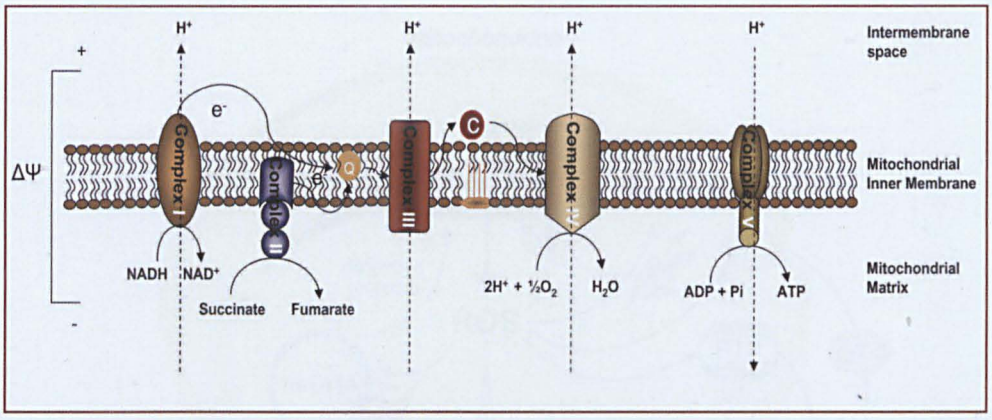

Figure 1.11. Electron Transport Chain. The diagram shows the five complexes that are involved in the mitochondrial electron-transport chain. Complexes I–IV are the electron-transport complexes, whereas complex V synthesizes adenosine triphosphate (ATP). Electrons are passed down the four complexes (black arrows) to molecular oxygen and then complex V generates one ATP molecule from ADP and inorganic phosphate (P_i). The dotted arrows show where the protons are pumped into the inter-membrane space to generate an electrochemical gradient ($\Delta\psi$) and where proton movement back across complex V (the ATP synthase) is used to drive ATP synthesis. Adapted from (Bayir and Kagan, 2008).

1.4.2 Mitochondria and ROS production

Mitochondria are considered the primary source of endogenous oxidants within the cell (figure 1.12). Chance and colleagues demonstrated that isolated mitochondria produce H_2O_2 (Loschen et al., 1971, Chance et al., 1979). It was later confirmed that this H_2O_2 in fact, arose from the dismutation of superoxide generated within mitochondria (Loschen et al., 1974). The majority of oxygen is consumed by the mitochondrion and converted into water in the

electron transport chain (ETC) at complex IV (cytochrome c oxidase). However oxygen is able to acquire electrons directly from the ubiquinone site at complex III and from flavin mononucleotide (FMN) group at complex I to generate $O_2^{\bullet -}$ (Zhang et al., 1990, Turrens, 2003).

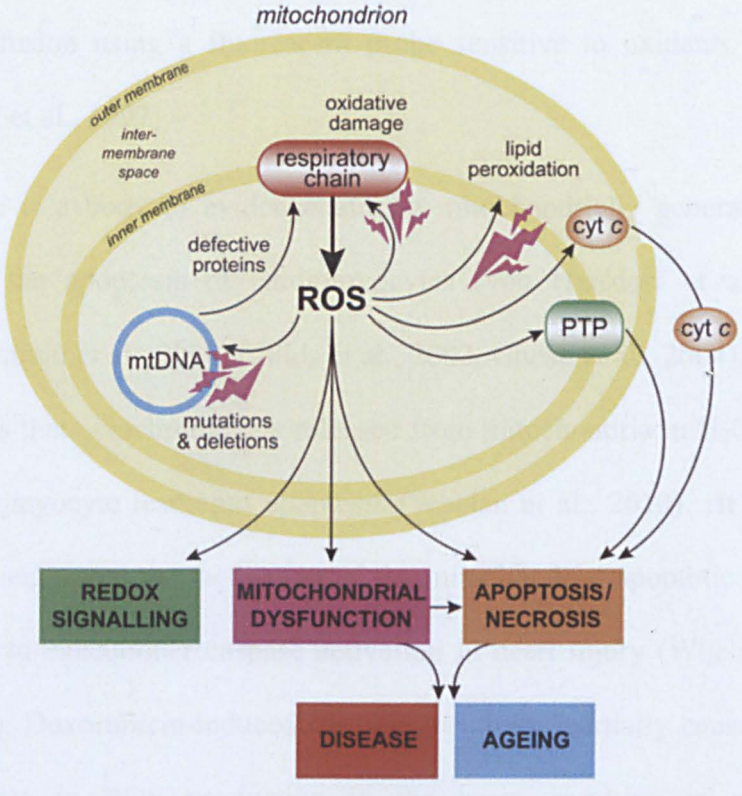

Figure 1.12. Mitochondrial ROS production. Schematic diagram representing ROS production by mitochondria. ROS leads to oxidative damage of mitochondrial proteins, membrane and DNA, which impairs the ability of mitochondria to synthesize ATP. PTP; Permeability Transition Pore, cyt c; cytochrome c.Taken from (Murphy, 2009).

Mitochondrial ROS production has also been observed to increase under conditions of low oxygen (hypoxia) (Semenza, 2004). Increased ROS production during hypoxia was revealed from investigations initially carried out on HIF-1, which plays a central role in the response of cells to hypoxia (Semenza, 2004). Hypoxia has been shown to

significantly increases the generation of ROS in adipose-derived stem cells (ASCs) and this increase is reversed by the treatment with the antioxidants N-acetyl-cysteine and diphenyleneiodonium (Kim et al., 2011). Evidence also suggests that ischaemia/reperfusion injury causes a "burst" in mitochondrial ROS production. This burst was demonstrated clearly in cardiomyocytes in the first several minutes of reperfusion using a fluorescent probe sensitive to oxidants (Vanden Hoek et al., 1997).

There is a body of evidence linking mitochondrially generated ROS with the apoptosis of cardiomyocytes (von Harsdorf et al., 1999, Kotamraju et al., 2000, Childs et al., 2002, Ghosh et al., 2004). A study shows that cytochrome c is released from mitochondria in H_20_2 treated cardiomyocyte leadingto apoptosis (Whelan et al., 2010). It has also been suggested that activation of the mitochondrial apoptotic pathway leads to executioner caspase activation in heart injury (Whelan et al., 2010). Doxorubicin-induced cardiomyopathy is partially caused by an increase in ROS production in the heart, resulting in apoptosis (Kotamraju et al., 2000) and Childs and colleagues demonstrated that doxorubicin induced radical production and oxidative stress that triggers the release of cytochrome c from the mitochondria, resulting in the activation of caspase-3 and apoptosis (Childs et al., 2002). In addition, a study has shown that rats treated with streptozotocin to simulate acute diabetes displayed depletion in the antioxidant glutathione, leading to increased ROS levels and cardiac apoptosis

(Ghosh et al., 2004). Later work demonstrated that the ROS generated in this scenario was due to mitochondria (Ghosh et al., 2005).

1.4.3. Cardiovascular disease and mitochondria

The function of the heart is highly dependent on oxidative energy, which is generated in mitochondria. Defects in mitochondrial structure and function can be found in association with cardiovascular diseases. Abnormalities in mitochondrial structure and function have been associated with numerous myocardial injury and disease states (Marin-Garcia and Goldenthal, 2002). Morphological studies using transmission electron microscopy revealed that the number, size and structural integrity of mitochondria were compromised in the myocardium of dogs suffering from chronic heart failure (CHF) (Sabbah et al., 1992).

Mitochondrial function was also reduced in failing hearts.(Sharov et al., 1998). The capacity of the mitochondria for oxygen consumption and oxidative phosphorylation was significantly reduced compared to normal hearts. The results indicate abnormal mitochondrial respiratory activity in myocardium of dogs with CHF (Sharov et al., 1998). In addition, patients suffering from DCM and heart failure with a history of ischeamic heart disease showed a reduction in the activity of complex III, a component of the ETC (Jarreta et al., 2000). A study hast also reported that prolonged ischaemia significantly impairs the mitochondrial respiratory chain at the level of complexes I/II and IPC

(cardioprotective mechanism) protected against such impairments (Thaveau et al., 2007).

1.4.4. Mitochondria and STAT3

Recently it has emerged that STAT3 plays a role in mitochondrial respiration. Wegrzyn and colleagues identified a population of STAT3 present in the mitochondria that regulated oxidative phosphorylation through association with complexes I and II of the ETC (Wegrzyn et al., 2009). Later studies confirmed the mitochondrial localisation of STAT3 and its role in respiration (Boengler et al., 2010). This group also demonstrated that STAT3 co-immunoprecipitated with cyclophilin D, a mitochondrial matrix protein that facilitates membrane permeability transition pore (MPTP) opening when bound to the mitochondrial membrane. Interaction of cyclophilin D with STAT3 caused a delay in MPTP opening and a reduction in infarct size in response to I/R injury (Boengler et al., Boengler et al., 2010).

1.5 Research aims and objectives

Cardiovascular disease represents a significant threat to the health of an aging society and the development of effective treatments for this disease will require an understanding of the aging and ischaemic heart. STAT3 is important for the phenotypic stability and survival of cardiac tissue; it plays a crucial role in hypoxic preconditioning (Smith et al., 2004) and is susceptible to regulation by oxidative stress (Barry et al., 2009, Xie et al., 2009, Li et al., 2010). These data indicate that STAT3 may be subject to direct control by oxygen levels in cardiac cells, which warrants further investigation. This study aims to identify the effects of hypoxia and reoxygenation (oxidative stress) on STAT3 activity in two cardiomyocyte-like cell lines (P19CL6 and H9c2) and primary rat cardiomyocytes (RCMs). This will be achieved by assessing the phosphorylation status of STAT3 and its ability to bind to DNA from cardiomyocyte cells exposed to hypoxic/oxidative stress. The contribution of STAT3 towards cardiomyocyte survival following hypoxic/oxidative stress will also be addressed through the exogenous expression of STAT3 and various STAT3 mutants ($STAT3^{C3S}$ and $STAT3^{S727A}$) and measuring levels of apoptosis. Understanding the mechanism and consequences of STAT3 regulation by hypoxia and oxidative stress in cardiomyocytes will be important for developing new therapeutic approaches to progressive ischaemic heart disease.

Chapter 2. Materials and methods

2.1 Materials

2.1.1. Antibodies

Table 1. Antibodies used throughout this study.

Antibody	Manufacturer	Dilution
α-Actin (A-2066)	Sigma Aldrich	1:1000
α-Bid (FL-195)	Santa Cruz Biotechnology	1:500
α-Flag (F3165)	Sigma Aldrich	1:1000
α-Mcl-1 (s-19)	Santa Cruz Biotechnology	1:500
α-PKCδ (2058)	Cell signaling	1:1000
α-phospho-PKCδ/θ (Ser 643/676) (9376)	Cell Signaling	1:1000
α-TBP (N-12)	Santa Cruz Biotechnology	1:1000
α-Tubulin (H-300)	Santa Cruz Biotechnology	1:500
α-STAT3 (S21320)	Transduction Laboratories	1:1000
α-phospho-STAT3 (Y705)	Upstate	1:500
α-phospho-STAT3 (S727)	Cell Signaling	1:500
α-VDAC (D73012)	Cell Signaling	1:500
α-mouse HRP-conjugated (A6782)	Sigma Aldrich	1:5,000
α-Rabbit HRP-conjugated (A0545)	Sigma Aldrich	1:10,000

2.1.2. Commercial chemicals and Kits

- Annexin V-FITC apoptosis kit (Autogen Bioclear)
- ATP monitoring reagent (BioTherma)
- BioRad protein assay kit (BioRad)
- Complete protease inhibitor cocktail tablets (Roche)
- ECL detection reagent (Millipore)

- ECL advance detection reagent (Amersham UK)
- JetSorb gel extraction kit (Genomed)
- Leukemia Inhibitory Factor (L5158) (Sigma Aldrich)
- Nucleobond AX maxi-prep kit (Machery Nagal Germany)
- Phos-Stop phosphatase inhibitor tablets (Roche)
- Protein-G-sepharose™ beads (GE Healthcare)
- Qiagen QIAprep spin mini-prep kit (Qiagen)
- Qiagen Nucleotide removal kit (Qiagen)
- Trypan blue solution - 0.4% (Sigma Aldrich)
- Strep-Tactin® sepharose (IBA BIOTAGnology)

2.1.3. Bacterial strains

All cloning was achieved using the bacterial strains NM522 and XL-2 blue ultra-competent cells. Bacmid DNA for baculovirus expression was generated using max efficiency® DH10 Bac ™ chemically competent cells.

2.1.4. Plasmid constructs

Table 2. Plasmids used throughout this study

Plamid	Description	Constructed by
pFastBac mSTAT3 wt	Mouse wild-type STAT3 cDNA expression cassette	Emma Evans
pFastBac mSTAT3 C3S	Mouse $STAT3^{C3S}$ cDNA expression cassette. C418S, C426S and C468S. Residues changed to serine render the molecule as redox-insenstive	Emma Evans
pRc/CMV Flag STAT3 wt	Mouse Wild-type STAT3 cDNA expression vector	(Horvath et al., 1995)
pRc/CMV Flag STAT3 C3S	Mouse $STAT3^{C3S}$ cDNA expression vector. C418S, C426S and C468S. Residues changed to serine render the molecule as redox-insenstive	(Li et al.)
pRc/CMV Flag STAT3C	Mouse STAT3-C cDNA expression vector. A662C and N664C. Residues changed to Cys renders the molecule constitutively active	(Li and Shaw, 2006)
pRc/CMV Flag STAT3 S272A	Mouse $STAT3^{S727A}$ cDNA expression vector. Residue changed to Ala prevents serine phosphorylation of this molecule	(Wen and Darnell, 1997)
pRc/CMV Flag STAT3 S727D	Mouse $STAT3^{S272D}$ cDNA expression vector. Residue changed to Asp renders the molecule as serine phospho-mimetic	Emma Evans
pRc/CMV Flag STAT3 S727E	Mouse $STAT3^{S272E}$ cDNA expression vector. Residue changed to Glu renders the molecule as serine phospho-mimetic	Emma Evans

2.1.5. Oligonucleotides

Table 3. Cloning oligonucleotides used to PCR clone Strep tagged STAT3 cDNA

Oligo name	Sequence	Constructed by
Rev STAT3 +Strep	5'GCTTGCGCATGCTATTCT CGAAC3'	Emma Evans
For STAT3	5'AAGACACTGACTGATGAA GAGC3'	Emma Evans

Table 4. Mutagenic oligonucleotides used to generate serine phospho-mimetic STAT3 cDNA

Oligo name	Sequence	Constructed by
S727E For	5'GACCTGCCGATGGAACCCCGC ATTTAG3'	Emma Evans
S272E Rev	5'CTAAAGTGCGGGGTTCCATCG GCAGGTC3'	Emma Evans
S727D For	GACCTGCCGATGGACCCCCGCA CTTTAG3'	Emma Evans
S272 Rev	5'CTAAAGTGCGGGGGTCCATCG GCAGGTC3'	Emma Evans

Table 5. Oligonucleotides used for synthesis of ^{32}P labeled oligonucleotide probes used in electrophoretic mobility shift assays

Oligo name	Sequence	Constructed by
SIEU	5'CTAGCATTTCCCGTAAAAT3'	Li Li
SIEL	5'CTAATTTACGGGAAATG3'	Li Li

2.2. Methods

2.2.1. Nucleic Acid Techniques

2.2.1.1. Amplification of DNA

Small scale DNA Preparation

Five mls of Luria-Bertani (LB) broth supplemented with appropriate antibiotics, were inoculated with a bacterial strain of interest (from a colony or glycerol stock) and incubated over night at 37°C on a rotating wheel (New Brunswick Scientific). Cells from 1-2ml of the over night culture were collected by centrifugation at 8,000rpm for 3 minutes at room temperature. The supernatant was discarded and the bacterial cell pellet resuspended in 250 µl Buffer P1 and then lysed using 250 µl Buffer P2. The denatured lysate was neutralised by the addition of 350 µl Buffer N3 causing the formation of a precipitate containing chromosomal DNA and other cellular compounds. The precipitate was cleared by centrifugation at 13,000rpm for 10 minutes. The cleared lysate was applied to the QIAprep column where plasmid DNA bound to the unique silica membrane, while RNA, cellular proteins, and metabolites were not retained on the membrane and removed by centrifugation at 13,000rpm for 30 seconds. Salts were efficiently removed by a brief wash step with 750µl of buffer PE buffer followed by centrifugation at 13,000rpm for 30 seconds. High-quality plasmid DNA was then eluted from the QIAprep column with 50–100µl of

buffer EB and collected by centrifugation at 13,000rpm for 30 seconds and purified DNA was stored at -20°C. Small scale DNA was prepared using the QIAprep Spin Miniprep Kit.

Large Scale DNA preparation

One hundred and fifty mls of LB broth supplemented with appropriate antibiotics, were inoculated with a bacterial strain of interest (from a colony or glycerol stock) and incubated over night at 37°C in a shaking incubator (New Brunswick Scientific). Cells from the overnight cultures were collected by centrifugation at 6,000rpm for 30 minutes at 4°C and the supernatant discarded. The bacterial pellet was resuspended in 12ml of resuspension buffer (50 mM Tris-HCl, 10 mM EDTA, 100 µg/mL RNase A, pH 8.0) and then lysed using 12ml lysis buffer (200 mM NaOH, 1 % SDS). The denatured lysate was neutralised by the addition of 12ml of neutralisation buffer (2.8 M KAc, pH 5.1) causing the formation of a precipitate containing chromosomal DNA and other cellular compounds. The precipitate was cleared by centrifugation at 12,000g for 45 minutes at 4°C. The cleared lysate was applied to the equilibrated NucleoBond® AX column and plasmid DNA is bound to the anion-exchange resin. The column was washed with 32ml of wash buffer (100 mM Tris, 15 % ethanol, 1.15 M KCl, pH 6.3) and DNA eluted from the column using 15ml of elution buffer (100 mM Tris, 15 % ethanol, 1 M KCl, pH 8.5). Eluted DNA was precipitated with 11ml of isopropanol and collected by centrifugation at 15,000g for 30 minutes at 4°C. The DNA pellet was subsequently

washed with 7ml ethanol (70%) and finally reconstituted in 1ml TE buffer (10mM Tris/HCl, 1mM EDTA, pH8.0).

Large scale DNA was extracted using the Nucleobond AX PC500 kit (Machery Nagal Germany).

Small Scale bacmid DNA preparation

Bacmid DNA was utilised in the generation of recombinant proteins using the baculovirus expression system (Section 3.7)

Two mls of LB broth supplemented with with 50µl/ml kanamycin, 7µg/ml gentamicin and 10µg/ml tetracycline were inoculated with DH10Bac (Invitrogen) cells containing pFastBac plasmid of interest overnight at 37°C on a rotating wheel. Cells from the overnight cultures were collected by centrifugation at 14,000g for 1 minute at 4°C. Cells were resuspended in 300µl of solution I (15mM Tris, 10mM EDTA, 100µg/ml RNase A pH 8.0) before lysing the cells in solution II (200mM NaOH, 1% SDS) at room temperature for 5 minutes. To precipitate proteins and chromosomal DNA, 300µl 3M potassium acetate pH 5.5 was added to the samples and incubated on ice for 10 minutes. Lysates were cleared by centrifugation at 14,000g for 10 minutes at 4°C and the supernatants were transferred to a fresh Eppendorf tube containing 800µl of isopropanol. Samples were mixed gently by inversion and incubated on ice for 10 minutes. Bacmid DNA was collected by centrifugation at 14,000g for 15 minutes at room temperature. DNA pellets were washed in 500µl 70% ethanol before drying in air for 10 minutes. Bacmid DNA was dissolved in 40µl 1xTE

(10mM Tris, 1mM EDTA) pH8.0 with gentle rocking at room temperature for 3 minutes before storing at 4°C.

2.2.1.2. Restriction digestion of DNA

Restriction digests of DNA were carried out in a standard 15µl reaction volume. DNA was digested using 5U of appropriate restriction enzyme supplemented with restriction buffer supplied by the manufacturer. Digests were incubated for 1 hour 30 minutes at 37°C in a water bath.

2.2.1.3. Alkaline phosphatase treatment of DNA

Subsequent to restriction digest, 5' phosphate groups were removed from DNA vectors with calf intestinal alkaline phosphatase (CIAP) to prevent self-ligation. To the 15µl restriction digest, 1.5µl of 1M Tris-HCl pH 9.5 and 1U of CIAP (MBI Fermentas) were added to the reaction. After incubation for 20 minutes at 37°C, CIAP was by heat inactivated at 65°C for 5 minutes.

2.2.1.4. Ligation of DNA

The ligation of DNA fragments was performed in a 10µl reaction volume using 1U of DNA ligase (Fermentas Life Sciences) with a 1:2 ratio of vector to insert. Ligations were incubated at 16°C in a water bath overnight.

2.2.1.5. Oligonucleotide ^{32}P-ATP 5' end-labelling

Routinely 400ng of ^{32}P-ATP labeled oligonucleotide duplex was prepared using a modified protocol from Wagner and colleagues (Wagner et al., 1990). Water was added to 200ng of "upper" oligonucleotide strand to give a final volume of 6µl. To remove secondary structure (from the DNA) the sample was incubated at 95°C for 5 minutes and then immediately placed on ice for two minutes. After brief centrifugation, 1µl of 10X polynucleotide (PNK) buffer A (Promega UK), 2µl of ^{32}Pγ-ATP (3000 Ci/mmol, Amersham Pharmacia Biotech) and 1µl T4 polynucleotide kinase (PNK, 10U) (Promega UK) was added. The reaction was incubated at 37°C for 30 minutes before enzyme inactivation at 65°C for 10 minutes. Water was added to 400ng of lower oligonucleotide strand to a final volume of 4µl. The sample was heated to 95°C for 5minutes, cooled on ice for 2 minutes and after brief centrifugation added to the ^{32}P ATP- labeled lower oligonucleotide strand. The two oligonucleotide strands were denatured by immersing the tube in a 1L beaker of boiling water and allowed to cool slowly to room temperature (approx. 4 hours), creating an oligonucleotide duplex.

Unincorporated ^{32}P-ATP was removed from the oligonucleotide duplex using the Qiagen nucleotide removal kit following manufacturer's instructions. The ^{32}P-labelled oligonucleotide duplex was eluted from the Qiagen column in 100µl of Qiagen EB buffer and stored at -20°C until required.

2.2.1.6.DNA Cloning

Polymerase chain reaction

During this study the polymerase chain reaction PCR was used to modify and amplify target DNA sequences for subsequent cloning. A proof reading DNA polymerase pfu (New England Biolabs) was utilised to ensure that errors were not introduced into the sequence during amplification. The following thermal profile was used for PCR with extension times calculated based on amplicon length and polymerase synthesis rate. Annealing temperatures were dependent on the melting temperature (Tm) of the primers.

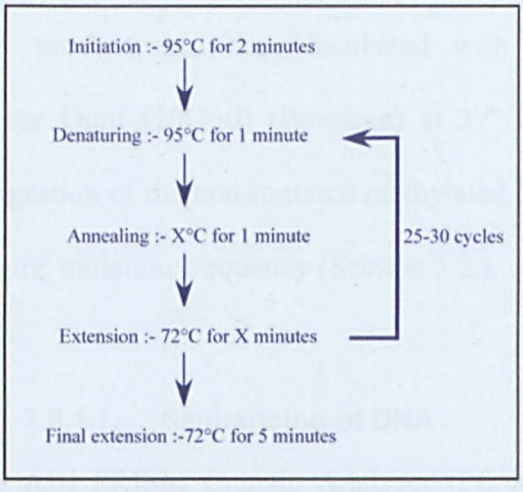

Site-directed mutagenesis

Mutation of a single amino acid was achieved by PCR-based QuickChange® Site- Directed Mutagenesis (Stratagene). The reaction mixture consisted of :- 25ng template plasmid DNA, 5µl 10x reaction buffer (Stratagene), 125ng forward and reverse primer, 200µM dNTPs,

0.5µl pfu (1.24 units) in a final volume of 50µl. The thermal profile below was used.

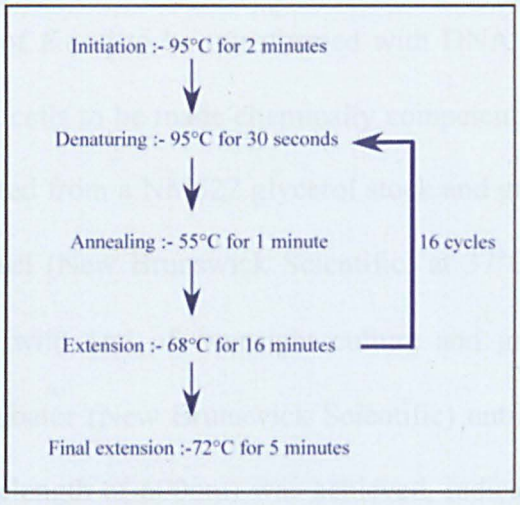

The PCR product was then incubated with 0.5µl of restriction endonuclease DpnI (10U/µl) (Promega) at 37°C for 1.5 hours. This allowed digestion of the non-mutated methylated template plasmid thus increasing the mutation frequency (Section 3.2.).

2.2.1.7. Sequencing of DNA

The 3130 ABI PRISM Genetic Analyser (PE Applised Biosystems) was used for sequencing reactions. Approximately 100ng purified plasmid DNA was used for each reaction. Analyses were performed in the Biopolymer Synthesis and Analysis Unit of the School of Biomedical Sciences, University of Nottingham.

2.2.2. Bacterial Techniques

2.2.2.1. Production of chemically competent cells

The ability of *E.coli* to be transformed with DNA (by heat shocking) required the cells to be made chemically competent. A 5ml LB culture was inoculated from a NM522 glycerol stock and grown overnight in a rotating wheel (New Brunswick Scientific) at 37°C. A 100ml culture was seeded with 1ml of overnight culture and grown at 37°C in a shaking incubator (New Brunswick Scientific) until an optical density of 0.4 (wavelength of 600nm) was achieved, indicating mid-log phase The bacterial cells were collected by centrifugation at 4300rpm for 10 minutes at 4°C and the LB discarded. Cells were resuspended in 30ml of sterile (ice cold) transformation buffer I (TFBI) (10mM MOPS pH7.0, 10mM RbCl) before incubating them on ice for 10 min. Cells were collected by centrifugation at 4300rpm for 10 minutes at 4°C and the TFBI discarded. The bacterial cell pellet was resuspended in 4ml of sterile (ice cold) transformation buffer III (TFBIII) (100mM MOPS pH6.5, 50mM $CaCl_2$, 10mM KCl, 15% glycerol) before aliquoting into 200µl aliquots and snap freezing in liquid nitrogen. The competent cells were stored at -80°C until use.

2.2.2.2.Transformation of competent NM522 cells

Plasmid DNA or ligation reactions were gently added to 50µl of thawed NM522 competent cells and incubated on ice for 20 minutes. Cells

were heat shocked at 42°C in a waterbath for 2 minutes before immediately returning to ice for 2 minutes. Cells were allowed to recover by the addition of 1ml LB for 1 hour at 37°C in a bench top shaker at 400rpm (Thermomixer compact, Eppendorf). Cells were collected by centrifugation at 5,500rpm for 2 minutes at room temperature and 1ml of LB discarded. The bacterial cell pellet was resuspended in residual LB and spread evenly across pre-warmed LB/Agar plates containing appropriate antibiotics under sterile conditions. Plates were inverted and incubated at 37°C over night.

2.2.2.3.Transformation of ultracompetent XL2-Blue cells

Ultracompetent XL-2 blue cells (Stratagene) were thawed on ice before adding 2µl β-mercaptoethanol to each aliquot of cells (100µl) and incubating on ice for 10 minutes. Plasmid DNA or ligation reactions were gently added to 50µl of ultracompetent cells and allowed to incubate on ice for a further 30 minutes. After incubation, cells were heat shocked in a 42°C waterbath for 30 seconds before immediately returning to ice for 2 minutes. Cells were allowed to recover by the addition of 900µl of preheated NZY+ broth (GIBCO) and incubated at 37°C with gentle shaking (225-250rpm) for 1 hour. Bacterial cells were collected by centrifugation at 8,000rpm for 3 minutes at room temperature and 900µl of NZY+ broth discarded. The bacterial cell pellet was resuspended in residual NZY+ broth and spread evenly over pre-warmed LB/agar plates containing appropriate antibiotics under sterile conditions and incubated at 37°C over night.

2.2.2.4. Transformation of Max efficiency® DH10Bac™ chemically competent cells

An aliquot (100µl) of Max efficiency® DH10Bac™ chemically competent cells (Invitrogen) was thawed on ice before the addition of 1ng of pFastBac plasmid DNA and allowed to incubate on ice for 30 minutes. After incubation, cells were heat shocked in a 42°C waterbath for 45 seconds before immediately being returned to ice for 2 minutes. Cells were allowed to recover by the addition of 900µl of S.O.C medium (2% tryptone, 0.5% yeast extract, 10 mM sodium chloride, 2.5 mM potassium chloride, 10 mM magnesium chloride, 10 mM magnesium sulfate and 20 mM glucose) (Invitrogen) and incubated at 37°C with gentle shaking (225rpm) for 4 hours. The bacterial suspension was diluted 10-fold in pre-warmed S.O.C medium and 100µl spread evenly over pre-warmed LB/agar plates supplemented with appropriate antibiotics (50µl/ml kanamycin, 7µg/ml gentamicin and 10µg/ml tetracycline, 100µg/ml X-gal and 40µg IPTG) under sterile conditions and incubated at 37°C for 48 hours.

2.2.3. Gel Electrophoresis

2.2.3.1. Agarose gel electrophoresis

DNA agarose electrophoresis

DNA was separated by electrophoresis in 0.8-3% (w/v) agarose (Biorad Laboratories) depending on DNA fragment size. Agarose was suspended in 1xTAE (40mM Tris-acetate pH8.0, 1mM EDTA) and solubilised by heating in a microwave oven. The agarose mixture was cooled to approximately 60°C and then poured into a casting tray. Once the agarose had set, the electrophoresis tank (Biorad Laboratories) was filled with cold 1xTAE until the gel was completely immersed. DNA mixed with 1xDNA loading dye (0.25% (w/v) bromophenol blue, 0.25% (w/v) xylene cyanol FF, and 15% (v/v) ficoll) was then loaded into the wells. Gels were run at 70-90V for 40-60 minutes (dependent on DNA fragment size and gel percentage). DNA was visualised by staining the agarose gel in ethidium bromide (0.5μg/ml in 1xTAE) for 20 minutes. The gel was briefly washed with water to remove excess ethidium bromide before the stained DNA was visualised using a UV gel documentation system (Syngene).

Extraction of DNA from agarose gels

The desired DNA band was excised from the agarose gel with a scalpel. DNA was extracted from the agarose gel slice using the Jetsorb gel extraction kit (Genomed) according to the manufacturer's protocol. The

gel slice was melted in A1 buffer (100µl per 100mg gel slice) containing 10µl of Jetsorb resin at 50°C for 15 minutes with brief mixing every 3 minutes. Jetsorb resin was collected by centrifugation at 14,000rpm for 1 minute at room temperature and the supernatant discarded. The Jetsorb resin was subsequently washed twice with 300µl of A2 buffer. The A2 buffer was removed and the Jetsorb resin dried by incubating at 50°C for 10 minutes with the eppendorf tube lid left open. DNA was eluted from the Jetsorb resin by incubation in 20µl of TE buffer (10mM Tris/HCl, 1mM EDTA, pH8.0) and incubated at 50°C for 5 minutes. The DNA eluate was cleared by centrifugation at 14,000rpm for 1 minute.

2.2.3.2. Polyacrylamide gels

Non-denaturing polyacrylamide gel electrophoresis

DNA/protein complexes were resolved on non-denaturing 5% polyacrylamide gels (9.4ml 40% acrylamide:bis-acrylamide 37.5:1 ratio) (Sigma Aldrich), 7.5ml 5xTBE (445mM Tris, 445mM boric acid, 10mM EDTA), 1.8ml (2.4% v/v) glycerol, 65µl TEMED, 700µl ammonium persulphate (10% w/v) made to 75ml with water). The gels were pre-electrophoresed in 0.5xTBE at 18mA for 30 minutes. After loading DNA/protein complexes into the wells, gels were electrophoresed at 18-20mA until the lower dye band had migrated ⅔ the total length of the gel, taking approximately 4-5 hours. Gels were fixed in 10% glacial acetic acid, 40% methanol for 2 minutes before

being placed on filter paper and dried at 85°C for 60 minutes using a vacuum gel drier.

SDS polyacrylamide gel electrophoresis

Proteins were separated according to size using SDS polyacrylamide gel electrophoresis (SDS-PAGE) using the Biorad mini protean II system.

Resolving gels (7.5-10% acrylamide (29:1 acrylamide:bis-acrylamide), 500mM Tris-HCl pH6.8, 0.4%SDS, 0.25% TEMED, 0.038% APS) were poured first and 1ml of water saturated iso-butanol was layered on top during gel polymerization to ensure the top edge of the gel was level. A stacking gel (4% acrylamide (29:1 acrylamide:bis-acrylamide), 1.5mM Tris-HCl pH 8.8, 0.4%SDS, 0.2% TEMED, 0.025% APS) was poured onto the set resolving gel to allow concentration of proteins before entering the resolving gel.

SDS loading buffer (50mM Tris-HCl pH 8.0. 2% SDS, 10% glycerol, 144mM 2-mercaptoethanol, 0.05% bromophenol blue, 2mM EDTA) was added to protein samples before heating to 100°C for 5 minutes. After brief centrifugation, samples were loaded into the gel and subjected to electrophoresis (80-160V) using the Biorad mini protean II system in 1X SDS running buffer (25mM Tris-HCl, 192mM glycine, 1% SDS) until the dye front reached the end of the gel.

2.2.4. Protein Techniques

2.2.4.1 Protein Extraction

Production of whole cell protein extracts

Medium was removed and adherent cells were detached from plates in 1ml of cold phosphate-buffered saline (PBS) with a rubber cell scraper. Cells were collected by centrifugation at 14,000rpm for 1 minute at 4°C. Supernatants were discarded and cell pellets resuspended in 1ml cold PBS. Cells were collected by centrifugation at 14,000rpm for 1 minute at 4°C. Cells were lysed in 100-200µl of RIPA buffer (150mM NaCl, 50mM Tris-HCl pH8.0, 0.1% SDS, 0.1% NP-40, 1mM DTT and complete protease inhibitor cocktail tablets (Roche)). Lysates were sonicated with two 5-second pulses (Jencons Vibracell, amplitude 50), before incubation on ice for 30 minutes. Cellular debris was removed by centrifugation at 14,000rpm for 1 minute at 4°C and the cleared whole cell lysates were transferred to fresh 1.5ml eppendorf tubes, snap frozen in liquid N_2 and stored at -80°C.

Production of nuclear protein extracts

Medium was removed and adherent cells were washed once with 1ml cold PBS+V+F (1X PBS, 1mM Na_3VO_4, 5mM NaF) and once with 1ml of hypotonic buffer (20mM HEPES pH 7.9, 20mM NaF, 1mM Na_3VO_4, 1mM $Na_4P_2O_7$, 1mM EDTA, 1mM DTT, complete protease inhibitor cocktail tablets (Roche)). Cells were lysed by the addition of 0.5ml cold hypotonic buffer + 0.1% NP-40. Nuclei were collected by

centrifugation at 14,000rpm for 30 seconds at 4°C. Supernatants were transferred to fresh eppendorf tubes, supplemented with NaCl to 120mM and 10% (v/v) glycerol to generate the cytoplasmic fractions. Nuclear pellets were resuspended in 100µl of high salt buffer (Hypotonic buffer supplemented with 420mM NaCl, 0.2% (v/v) NP-40, 20% (v/v) glycerol, 1mM DTT, complete protease inhibitor cocktail tablets (Roche)). The nuclei were lysed by incubation at 4°C for 60 minutes with gentle rocking. Nuclear lysates were cleared by centrifugation at 14,000rpm for 20 minutes at 4°C, cleared nuclear extracts were transferred to fresh Eppendorf tubes, snap frozen in liquid N_2 and stored at -80°C.

Production of mitochondrial protein extracts

Medium was removed and adherent cells were detached from plates in 1ml of cold 1X PBS using a rubber scraper. Cells were collected by centrifugation at 300g for 3 minutes at 4°C, supernatants were discarded and the cell pellets washed in 1ml of cold 1X PBS. Cells were collected by centrifugation at 300g for 3 minutes at 4°C. Cell pellets were resuspended in 0.5ml of extraction buffer (10mM HEPES pH 7.5, 200mM mannitol, 1mM EGTA, 70nM sucrose, protease inhibitor cocktail tablets (Roche), Phos-Stop phosphatase inhibitor cocktail tablets (Roche) before lysing with 20 gentle strokes using a 2ml teflon/glass homogeniser. Nuclei were collected by centrifugation at 1,000g for 5 minutes at 4°C and supernatants transferred to fresh 1.5ml Eppendorf tubes (labeled mitochondrial fraction). Nuclei were washed in 200µl extraction buffer followed by centrifugation at 1,000g

for 10 minutes at 4°C and supernatants pooled together (mitochondrial fraction). Mitochondria were collected from pooled cytoplasmic supernatants by centrifugation at 10,000g for 15 minutes at 4°C. Supernatants were transferred to fresh 1.5ml Eppendorf tubes (labeled cytoplasmic fraction). The brownish mitochondrial pellets were washed with 200µl of extraction buffer before being subjected to centrifugation at 10,000g for 10 minutes at 4°C. The supernatants were again pooled together with the cytoplasmic extracts and the nuclear and mitochondrial pellets were resuspended in 200µl and 100µl of extraction buffer respectively. All samples were snap frozen in liquid N_2 and stored at -80°C.

2.2.4.2. Immunoprecipitation of proteins

This procedure was utilised to concentrate STAT3 from protein extracts. Approximately 90% of the protein extract was made up to a final volume of 500µl using an appropriate buffer (RIPA and extraction buffer for whole cell and mitochondrial extracts respectively) before the addition of 2µg flag antibody (Sigma) and incubated on a wheel (Stuart Scientific) at 4°C over night. In parallel 25µl of protein-G-sepharose™ bead slurry (GE Healthcare) was added to 1ml of cold 1XPBS and centrifuged at 4000g for 2 minutes at room temperature. This step was repeated before pre-blocking the beads in 1ml of 1% BSA (Sigma) in PBS on a wheel at 4°C over night. The next day, beads were collected by centrifugation at 4000g for 2 minutes at room temperature and washed in the appropriate buffer (RIPA or extraction buffer). The

centrifugation step was repeated before resuspending the beads in the protein extract (+ flag antibody) and incubating on the wheel at 4°C for a further 2 hours. Beads were collected by centrifugation at 4000g at room temperature for 2 minutes. The beads were subsequently washed 3 times in an appropriate buffer (same buffer as protein extract) before the addition of 30µl 1xSDS loading buffer. Samples were boiled for 5 minutes before centrifugation at 13,000g for 1 minute at room temperature. Supernatants were loaded onto polyacrylamide gels (Section 3.3.2.2.) and immunoprecipitated STAT3 detected by western blot analysis (Section 3.4.4.).

2.2.4.3. Protein quantification

Nanodrop spectrophotometer

To ensure equal loading of proteins between lanes on a polyacrylamide gel the Nanodrop OD280 program was used to determine relative protein concentrations. Protein concentrations were measured in duplicate and mean value calculated.

Bradford protein assay

Protein concentration was also determined using the Biorad protein assay kit. The assay was performed according to the manufacturer's protocol and a standard curve prepared using BSA. Samples under investigation were diluted 1:500 and 1:1000; however these dilutions were adjusted accordingly if the protein concentrations were outside the

range of the standard curve. Diluted sample or BSA standard (800µl) was added to a 1ml path length spectrophotometer cuvette, followed by 200µl of diluted dye reagent. The solutions were mixed by inversion and incubated at room temperature for 10 minutes before reading the optical density at 595nm using a spectrophotometer (Pharmacia Biotech). Standards and samples were analysed in duplicate and mean values calculated.

2.2.4.4. Western Blot analysis

Transfer of protein to polyvinylidene fluoride membrane

Proteins resolved by SDS-PAGE (Section 3.3.2.2.) were transferred to a polyvinylidene fluoride (PVDF) 0.2µM membrane (Schleicher and Schuell) using a semi-dry transfer system (Biorad). Prior to transfer the membrane was immersed in methanol for 10 seconds before equilibrating in transfer buffer (24mM Tris, 192mM glycine, 20% (v/v) methanol). Filter paper and the polyacrylamide gel were soaked in transfer buffer for 5 minutes. Three layers of wet filter paper were laid on the bottom of the transfer apparatus followed by the PVDF membrane, polyacrylamide gel and finally three more wet filter papers. Proteins were transferred to the PVDF membrane at 12V, 100mA per gel for 1 hour 45 minutes.

Immuno-detection of desired protein

After transfer, PVDF membranes were blocked for 1 hour at room temperature in 5% milk in 1xTBST (50mM Tris, 150mM NaCl, 0.05% (v/v) tween) with gentle shaking. Primary antibodies (section 2.1.1, table 1) were added at dilutions indicated by manufacturers protocol and incubated at 4°C over night on the roller. Membranes were washed 3 times in 1xTBST for 10 minutes. HRPO-coupled secondary antibodies were applied at a dilution between 1:10,000 and 1:5,000 in 5% milk in 1xTBST and incubated at room temperature for 1 hour. Membranes were then washed a further 3 times in 1xTBST before ECL reagent (Millipore) was added and an image captured using a LAS-3000 mini chemiluminescence camera (Fuji-film). Images were analysed using the AIDA v4.20 software package.

2.2.4.5. Electrophoretic mobility shift assay

This assay was utilised to identify DNA-bound protein complexes using a ^{32}P-labeled oligonucleotide duplex (Fried and Crothers, 1981, Garner and Revzin, 1981).

A complex formation reaction containing 100µg nuclear protein and 15µl 2xDNA binding buffer (26mM HEPES pH7.9, 130mM NaCl, 2mM DTT, 0.3mM EDTA, 100ng/ml poly dI/dC, 8% (v/v) glycerol) made up to a final volume of 30µl was left to incubate on ice for 20 minutes. For supershift analysis of SIE/STAT3 complexes, nuclear extracts were pre-incubated with 1µl α-STAT3 antibody in 2xbinding buffer supplemented with 0.05% (v/v) NP-40 at room temperature for

30 minutes. DNA/protein complexes were formed by the addition of ^{32}P-labeled oligonucleotide duplex (Section 3.1.5.) and incubated at room temperature for 15 minutes. After the addition of 2µl DNA loading buffer (0.25% bromophenol blue, 0.25% xylene cyanol FF and 15% ficoll) complexes were loaded onto a 5% non-denaturing polyacrylamide gel. Complexes were resolved by electrophoresis (section 3.3.2.2.). Dried gels were placed into a Fuji film phosphoimager cassette and exposed for between 16 hours and 14 days before reading the plate using an FLA-2000 phosphoimager (Fuji-film). Images were analysed using the AIDA v4.20 software package.

2.2.5. Eukaryotic cell techniques

2.2.5.1. Determination of cell number

A haemocytometer (Hawksley) was used to determine the density of cells in suspension using a light microscope.

2.2.5.2. Trypan blue exclusion assay

Cell viability was assessed using a Trypan blue exclusion assay. To a cell suspension, a 1:1 ratio of 0.4% trypan blue solution (Sigma) was added and incubated at room temperature for 5 minutes. The density of stained and unstained cells was determined using a haemocytometer (Section 3.5.1.) and the percentage viability was determined using the following equation: -

$$\frac{\text{(Total Cells - Stained Cells)}}{\text{Total Cell}} \times 100 = \%\ \text{Cell Viability}$$

2.2.5.3. Isolation of neonatal rat cardiomyocytes

Neonatal rat cardiomyocytes (RCMs) were obtained from 20-60 Wistar rat pups between 2-5 days old. The rats were culled through cervical dislocation and the torso sterilised with 70% ethanol. Hearts were extracted using sterile fine forceps and any visible connective tissue removed using a pair of sterile micro dissection scissors. The hearts were then washed three times in ice cold saline A solution (137mM NaCl, 5.4mM KCl, 4.2mM $NaHCO_3$, 5.5mM D-glucose) to remove any excess blood and then diced into pieces approximately $0.5cm^3$. Diced hearts were subjected to two initial digests in 10ml of pre-warmed 0.1% trypsin (0.1% Trypsin/EDTA in saline A solution) for 10 minutes at 37°C with gentle stirring at 60 rpm with a magnetic flea. The trypsin solution from the first two digests was discarded. Subsequently, 9-15 cycles of 10 minute, 0.1% trypsin digests were carried out with the trypsin solution collected each time. The trypsin solution containing released cells was added to 10ml of ice cold plating medium (22mM glucose DMEM (D5796 Sigma Aldrich), 10% foetal calf serum (Autogen Bioclear UK), 100U/ml penicillin and 100µg/ml streptomycin) per digest to inactivate the trypsin. The cells were collected from the suspension by centrifugation at 1,200rpm for 5 minutes at room temperature and resuspended in 5ml of ice cold plating medium and stored on ice. After all digest steps, resuspended cells were

pooled together. Cells were plated onto 10cm cell culture dishes (BD Bioscience) and incubated at 37°C, 5% CO_2 for 1-1.5 hours. This step reduced fibroblast contamination as fibroblasts adhere to plates faster than cardiomyocytes. The enriched cardiomyocyte suspension was removed from the cell culture dishes and subjected to a trypan blue exclusion assay (Section 3.5.2.). Cells were replated at a density of $1x10^7$ viable cells per 10cm cell culture dish and incubated at 37°C, 5% CO_2. After 4-6 hours post-plating, the culture medium was replenished with 10ml of exchanging medium (5.5mM glucose DMEM, 10% foetal calf serum, 100U/ml penicillin and 100µg/ml streptomycin) and returned to a humidified 5% CO_2 incubator at 37°C (Shelton, 2009).

2.2.5.4. Maintenance of eukaryotic cells

Maintenance of isolated rat cardiomyocytes

Isolated RCMs (Section 3.5.3) began to beat 24 hours after initial plating. Cells were analysed within 3 days of isolation to ensure limited fibroblast contamination.

Maintenance of HEK293 cells

The human embryonic kidney cell line (HEK293) was used in this study to confirm whether STAT3 expression plasmids expressed STAT3 protein. HEK293 cells were cultured on 10cm Falcon tissue culture dishes (BD Biosciences) using Full DMEM culture medium (5.5mM glucose, DMEM (Sigma D6046), 10% foetal calf serum, 100U/ml penicillin and 100µg/ml streptomycin). Cells were cultured at

37°C in a humidified 7.5% CO_2 incubator. Cells were passaged between 1:8 and 1:10 every 3-4 days.

Maintenance of H9c2 cells

H9c2 is a cell line derived from rat ventricular tissue and was obtained from American Type Culture Collection (ATCC number: CRL 1446). Cells were cultured in 75cm^2 easy flask (Nunc) in maintenance medium (22mM glucose DMEM, 10% foetal calf serum, 100U/ml penicillin and 100µg/ml streptomycin) at 37°C in a humidified 5% CO_2 incubator. Cells were passaged between 1:3 and 1:5 every 2-3 days.

Maintance of P19CL6 cells

P19Cl6 is a subclone (Clone 6) of the P19 cell line that was initially derived from mouse embryonic carcinoma cells. The cells were obtained from Dr Alison Brewer, Kings College London.

Cells were cultured on 10cm falcon tissue culture dishes (BD Biosciences) in full α-MEM medium (Alpha MEM (12-169F) (Lonza), 10% foetal calf serum (Lonza), 2mM L-glutamine, 100U/ml penicillin and 100µg/ml streptomycin) at 37°C in a humidified 5% CO_2 incubator (Revco). Cells were passaged 1:15 every two days.

Maintance of sf9 cells

Spodoptera frugiperda (sf9) cells are insect cells that grow in suspension and are used for recombinant protein expression using insect-specific viruses called baculoviruses.

Sf9 cells were cultured at a density of 1-2x10^6 cells/ml in serum free medium (Insect-xpress medium (Lonza), 100U/ml penicillin, 10% pluronic F-68 (Sigma) and 10% partricin (Biochrom AG) in 50ml round bottom shaker flask and incubated at 27°C, 120rpm (Kuhnershaker). Cells were passaged every 2-3 days.

2.2.5.5. Cell recovery from liquid nitrogen stock

For consistency between experiments a fresh vial of cells under investigation (from the same master batch) were thawed for each experiment. This ensured each experiment used cells with a similar passage number and reduced the possibility of the cells changing over time.

Recovery of H9c2 cells

A cell vial was removed from liquid N_2 tank and immediately thawed in a water bath at 37°C. Cells were diluted into 10ml of pre-warmed full (22mM glucose) DMEM medium to remove dimethyl sulfoxide (DMSO) and collected by centrifugation at 1,000rpm for 5 minutes at room temperature. The supernatant was discarded and the cell pellet resuspended in 1ml of pre-warmed full DMEM medium before adding to a pre-incubated tissue culture dish containing 10ml full (22mM

glucose) DMEM medium. Cells were left to recover overnight at 37°C in a humidified 5% CO_2 incubator before replenishing with 10ml of fresh full (22mM glucose) DMEM medium.

Recovery of P19CL6 cells

A cell vial was removed from liquid N_2 tank and immediately thawed in a water bath at 37°C. Cells were diluted into 10ml of pre-warmed full α-MEM medium to remove DMSO and collected by centrifugation at 1,000rpm for 5 minutes at room temperature. As P19CL6 cells differentiate in the presence of DMSO it was important to ensure that all residual DMSO was removed, therefore the cells were resuspended in a further 10ml pre-warmed α-MEM medium and the centrifugation step repeated. The supernatant was discarded and the cell pellet resuspended in 4ml of pre-warmed α-MEM media before adding to a pre-incubated tissue culture dish containing 16ml full α-MEM. Cells were left to recover overnight at 37°C in a humidified 5% CO_2 incubator before replenishing with 10ml of fresh full α-MEM media.

2.2.5.6. Cardiac differentiation of eukaryotic cells

Throughout this study a number of cell lines required differentiation towards a cardiac phenotype. The differentiation procedure varied between cell lines, but involved regulation of growth and differentiation signals by varying the foetal calf serum level and culturing cells in the presence of compounds such as DMSO.

Cardiac differentiation of H9c2 cells

When cultured in low-serum containing medium, H9c2 cells exit the cell cycle and differentiate into myocytes (Kimes and Brandt, 1976). The cell density was adjusted to $5x10^5$ cells per 10cm plate in full (22mM glucose) DMEM medium and cultured overnight at 37°C in a humidified 5% CO_2 incubator. The following day the medium was exchanged for low glucose starvation DMEM medium (DMEM 5.5mM glucose, 100U/ml penicillin and 100μg/ml streptomycin) and cultured for 24 hours at 37°C in a humidified 5% CO_2 incubator. The cells were allowed to recover for 5 days in full low glucose DMEM media (DMEM 5.5mM glucose, 10% foetal calf serum, 100U/ml penicillin and 100μg/ml streptomycin). As H9c2 cells fail to beat, cardiac differentiation was characterized by an increase in the expression of cardiac markers Nkx2.5 and Gata-4 (Shelton, 2009).

Cardiac differentiation of P19CL6 cells

P19CL6 cells have been partially differentiated towards a cardiac phenotype. This was achieved by culturing the P19 cell line in the presence of 1nM retinoic acid for 6 months and selecting a single clone (clone 6). The resulting P19CL6 cell line shows a greatly enhanced ability to form beating cardiomyocytes when cultured in the presence of DMSO (Habara-Ohkubo, 1996).

The cell density was adjusted to $1.75x10^5$ cells per 6cm plate (Corning). Cells were cultured in differentiation medium (α-MEM, 10 % foetal

calf serum, 2mM L-glutamine, 100U/ml penicillin and 100µg/ml streptomycin supplemented with 0.5% (v/v) DMSO) for 16 days at 37°C in a humidified 5% CO_2 incubator. Differentiation medium was replenished every two days.

2.2.5.7. Transfection of eukaryotic cells

Calcium phosphate

During this study HEK293 cells were transfected using DNA calcium phosphate coprecipitation (to confirm whether newly generated STAT3 expression plasmids express STAT3 protein). Cells were passaged 1:5 to 1:7 depending on cell density the day before transfection. Four hours prior transfection, the culture medium was exchanged for fresh full DMEM medium. A total of 10µg of plasmid DNA was diluted to a final volume of 50µl in sterile water. To the DNA mixture, 500µl of ice cold 300mM $CaCl_2$ was mixed under vortex before incubation on ice for 10 minutes. After incubation, 550µl of 2xHEPES buffered saline (HBS) (280mM NaCl, 50mM HEPES pH 7.1) was added dropwise to the DNA/CaCl2 while mixing slowly using a vortex mixer. The mixture was incubated for a further 20 minutes on ice before adding to the cells dropwise. The medium was gently mixed to ensure equal distribution of the calcium phosphate-DNA precipitate. The cells were returned to a 37°C humidified 7.5% CO_2 incubator.

Lipofectamine plus

In this study differentiated P19CL6 cells were transfected using Lipofectamine (Invitrogen) and Plus™ reagent (Invitrogen). Day 12 differentiated P19CL6 cells were passaged 1:4 the day before transfection. A total of 10μg of plasmid DNA was diluted to a final volume of 125μl in opti-MEM (GIBCO) before the addition of 15μl plus™ reagent and the DNA mixture incubated at room temperature for 20 minutes. During this time, 21μl lipofectamine was diluted to a final volume of 146μl in opti-MEM. After incubation the lipofectamine was added to the DNA mixture dropwise and incubated for a further 30 minutes at room temperature. During this time, medium was removed from the differentiated P19CL6 cells and exchanged for 2ml of pre-warmed opti-MEM. After 30 minutes incubation the DNA-lipofectamine mixture was added dropwise to the medium and mixed gently to ensure equal distribution. The cells were returned to a 37°C humidified 5% CO_2 incubator for 4-6 hours before exchanging the medium to α-MEM differentiating medium.

Monitoring transfection efficiency

To monitor the transfection efficiency, 1μg of plasmid expressing green fluorescence protein (GFP) was transfected to cells under the same condition. Transfected cells were allowed to recover overnight under normal growth conditions and monitored under Leica DMIRE inverted fluorescence microscope 16 hours post-transfection. Three areas of the

plate were assessed first by counting the total number of cells followed by counting the GFP-positive cells by turning on the green emission. Transfection efficiency was calculated based on the number of GFP-positive cells among the total cell population.

2.2.5.8. Cytokine stimulation of eukaryotic cells

LIF treatment of eukaryotic cells

Cells were treated with 10ng/ml of LIF (Sigma) for 20 minutes or immediately prior to exposure to hypoxia (Section 3.5.9.1.).

2.2.5.9. Exposure of eukaryotic cells to hypoxia and oxidative stress.

Hypoxia treatment of eukaryotic cells

Cells were exposed to hypoxia (defined by an atmospheric oxygen level of 1%) using a Biospherix ProOx chamber. Cells were cultured under hypoxia in the chamber at 37°C in a humidified incubator. After hypoxia treatment for the indicated times, cells were removed from the chamber and placed on ice prior to analysis.

Reoxygenation treatment of eukaryotic cells

Following exposure to hypoxia (Section 3.5.9.1.), cells were reoxygenated for 1 hour by returning to a 37°C humidified 5% CO_2. Cells were then removed from the incubator and placed on ice prior to analysis.

2.2.5.10. Annexin V staining assay

Following exposure to hypoxia (section 3.5.9.1.) an annexin V staining assay was performed to determine the level of apoptosis induced. This assay takes advantage of the redistribution of phosphatidylserine (PS) in the cell membrane during apoptosis. In non-apoptotic cells, the majority of PS molecules are localised to the inner layer of the plasma membrane, however soon after inducing apoptosis PS redistributes to the outer layer of the plasma membrane and becomes exposed to the extracellular environment. Annexin V FITC has a very strong affinity for PS therefore apoptotic cells can be easily distinguished.

For Annexin V binding the Annexin V-FITC apoptosis kit (ABE 2227) (Autogen Bioclear) was used according to the manufacturer's instructions. Treated cells were washed in 5ml ice-cold PBS, adherent cells were removed from the plate with 0.25% trypsin (Sigma-Aldrich) and the cell density determined (Section 3.5.1.). $5x10^5$ cells were collected by centrifugation at 1000g for 5 minutes at room temperature before being resuspended in 500µl of 1xbinding buffer (provided by the kit). A volume of 5µl of both annexin V-FITC and propidium iodide (PI) solution (provided by the kit) were added to the cellular suspension and allowed to incubate at room temperature for 5 minutes in the dark. Unstained, Annexin V-FITC only and PI only stained cells were used as controls for background staining. The stained cells were analysed immediately using a Coulter Altra Flow Sorter and the data

subsequently analysed using WinMDI v2.9 software. Three biological repeats were performed for each experiment.

2.2.5.11. DNA Laddering assay

Following exposure to hypoxia (section 3.5.9.1.), cells were washed in 5ml ice-cold PBS, adherent cells were removed from the plate with 0.25% trypsin (Sigma-Aldrich) and the cell density was determined. $2x10^6$ cells were collected by centrifugation at 200g for 5 minutes at room temperature. Cells were resuspended in 1ml of ice cold Hank's Buffered Salt Solution (HBS) (Sigma) and added dropwise to 10ml of ice cold 70% ethanol before storing at -20°C for at least 24 hours. Fixed cells were collected by centrifugation at 800g for 5 minutes at 4°C. Cells were resuspended in 40µl of phosphate-citrate buffer (192 parts 0.2M Na_2HPO_4 and 8 parts 0.1M citric acid pH 7.8) and incubated at room temperature for 30 minutes. Lysates were cleared by centrifugation at 1000g for 5 minutes at room temperature and the supernatant transferred to a fresh eppendorf tube and concentrated in a vacuum concentrator (BACHOFER) for 10 minutes. Next, 3µl of 0.25% (v/v) NP-40 AND 3µl of RNase A (Sigma) were added to the concentrated samples before incubating at 37°C for 30 minutes. After RNA digestion, 3µl of proteinase K (1mg/ml) (Sigma) was added to the samples and allowed to incubate for a further 30 minutes at 37°C. Before loading the samples onto a 1.5% agarose gel, 12µl of loading buffer (0.25% bromophenol blue, 30% glycerol) was added. The gel

was run at 28V for 4 hours at 4°C before ethidium bromide staining and DNA detection using the UV documentation system (Syngene).

2.2.5.12. Functional mitochondrial ATP assay

Isolation of functional mitochondria

Medium was removed and adherent cells were detached from the plate in 1ml of cold PBS with a rubber scraper. Cells were collected by centrifugation at 300g for 3 minutes at 4°C, supernatants were discarded and cell pellets resuspended in 1ml of cold PBS. Cells were collected by centrifugation at 300g for 3 minutes at 4°C. Cell pellets were resuspended in 0.5ml of extraction buffer before lysing with 20 gentle using a 2ml teflon/glass homogeniser. Lysates were cleared by centrifugation at 650g at 4°C for 3 minutes. Supernatants were transferred to a fresh Eppendorf tube and mitochondria collected by centrifugation at 15,000g at 4°C for 3 minutes. Supernatants were removed and the small brownish mitochondrial pellets washed in 200µl of extraction buffer and collected by centrifugation at 15,000g at 4°C for 3 minutes. Mitochondrial pellets were resuspended gently in 100µl of resuspension buffer (human serum albumin (0.5mg/ml) pH 7.2, 240mM sucrose, 15mM KH_2PO_4, 2mM magnesium acetate tetrahydrate, 0.5mM EDTA) and used immediately in the mitochondrial ATP production rate assay (Section 3.5.12.2).

Mitochondrial ATP production rate (MAPR) analysis

This procedure allows the analysis of mitochondrial ability to utilise different substrates for the production of ATP.

Having isolated mitochondria from treated cells the following 1cm cuvette compositions were made up. To each cuvette; 800µl ATP monitoring reagent (BioTherma) (Lyophilized ATP monitoring reagent (containing firefly luciferase, D-luciferine 0.1g/L, L-luciferine 4mg/L, bovine serum albumin 1g/L, and 1µM $Na_2P_2O_7$) dissolved in reagent buffer (0.19M sucrose, 19mM KH_2PO_4, 2.5mM magnesium acetate tetrahydrate, 0.7mM EDTA, pH 7), 140µl of chosen substrate (16.4mM glutamate/ 15mM succinate, 5µM palmitoyl-L-carnitine/1.5mM malate, 50mM pyruvate/ 22mM malate, 2.5mM succinate and 32.75mM glutamate/ 22mM malate.) and 50µl of 50mM ADP. The mitochondrial suspension (Section 3.5.12.1.) was diluted 300x in resuspension buffer before adding 10µl of this to each cuvette. The cuvettes were read immediately using the BioOrbit luminometer. After a 10 minute monitoring period 10µl 50µM ATP was added to each cuvette as an internal calibrator. All samples were measured in duplicate (technical repeats) and normalised to total mitochondrial protein concentration (Section 3.4.3.2.). Three biological repeats were performed for each experiment.

2.2.6. Viral techniques

2.2.6.1. Production of recombinant baculovirus

Transfection of Sf9 cells

In this study sf9 cells were transfected using lipofectamine and Plus™ reagent in order to generate baculovirus containing the gene of interest. Sf9 cells were plated at a cell density of $9x10^5$ cells per 35mm well (of a 6-well plate) and allowed to adhere for at least 1 hour. A total of 1.5μg of bacmid DNA (prepared as in section 3.1.1.3.) was diluted to a final volume of 90μl in serum free medium (SFM) (Insect-xpress, no antibiotics) before the addition of 10μl of Plus™ reagent. The DNA mixture was incubated at room temperature for 30 minutes. During this time, 5μl of lipofectamine was diluted to a final volume of 100μl in SFM (no antibiotics). After incubation, the two mixtures were combined and allowed to incubate for a further 30 minutes at room temperature. During this time, medium was removed from the sf9 cells and exchanged with 800μl of SFM (no antibiotics). After the 30 minute incubation the DNA-lipofectamine mixture was added dropwise to the cells and mixed gently to ensure equal distribution. Cells were incubated at 27°C for 4-6 hours before exchanging the medium for SFM supplemented with antibiotics (100U/ml penicillin, 10% pluronic F-68 and 10% partricin).

Isolation of P1 viral stock

Once transfected s9f cells (Section 3.6.1.1) demonstrated signs of infection (e.g. 72 hours post infection) the medium containing baculovirus was cleared by centrifugation at 500xg for 5 minutes at room temperature. To concentrate the viral stock, the supernatant was filtered through a 0.2μM, low protein binding filter followed by the addition of 2% foetal calf serum to act as substrates for proteases. The viral P1 stock was protected from light and stored at 4°C.

Amplification of viral stock

To amplify the P1 viral stock sf9 cells were infected at a multiplicity of infection (MOI) of 0.1 with the assumption that the P1 viral stock had a titer of $5x10^6$ pfu/ml. To calculate the inoculum required, the equation below was utilised.

$$\text{Inoculum required (ml)} = \frac{\text{MOI (pfu/cell) X number of cells}}{\text{Titer of viral stock (pfu/ml)}}$$

On the day of infection $2x10^6$ cells were cultured in 10ml of SFM in a 50ml round bottom shaker flask and incubated at room temperature, 120rpm for 1 hour. After incubation, 0.4ml of P1 viral stock was added to the cells and allowed to incubate at 120rpm for 48 hours in a 27°C humidified incubator. Post-infection (48 hours) medium was removed from the cells and cleared by centrifugation at 500xg at room temperature for 5 minutes. The supernatant was filtered through a 0.2μM, low protein binding filter followed by the addition of 2% foetal

bovine serum. The viral stock was protected from light and stored at 4°C.

Expression and extraction of recombinant protein

Sf9 cells were seeded at the cell density of $4x10^5$cells/ml and incubated at 120rpm in a 27°C humidified incubator until they reached mid-logarithmic phase of growth at a density of ~$2x10^6$ cells/ml. At this time 10% (total final volume) of amplified viral stock was added to the cells and incubated at 120rpm in a 27°C humidified incubator. Sf9 cells were infected with baculovirus for 72 hours and collected by centrifugation at 4,000rpm for 15 minutes at 4°C. Cell pellets were resuspended in (10ml per gram of pellet) extraction buffer (10mM HEPES, 150mM NaCl. 0.5% (v/v) Triton x-100, 10% (v/v) glycerol, 1mM Na_3VO_4, complete protease inhibitor cocktail tablets (Roche)) and lysed using a dounce homogeniser, 5 gentle strokes. Lysates were cleared by centrifugation at 14,000prm for 45 minutes at 4°C. To precipitate DNA, 0.1% (v/v) polyethylenimine (Sigma Aldrich) was added to the supernatant before centrifugation at 14,000rpm at 4°C for 30 minutes. Proteins were precipitated by the addition of 50% (v/v) saturated ammonium sulphate (Sigma) drop-wise before incubating overnight at 4°C on the roller. The next day the protein precipitate was collected by centrifugation at 4,000rpm for 30 minutes at 4°C. The protein pellet was then resuspended in 10ml of buffer W (100mM Tris-HCl, 150mM NaCl, 1mM EDTA pH 8.0) ready for purification using the Strep-Tactin® purification system (Section 3.6.1.5).

Purification of recombinant protein using a Strep-Tactin® column

Three column bed volumes (CV) of a 50% suspension of Strep-Tactin sepharose (IBA BIOTAGnology) were added gently to a column (Brand) before equilibrating with 2CV of buffer W under gravity flow. Protein extracts (Section 3.6.1.4.) were loaded onto the column and the flow-through collected for SDS-PAGE analysis. The column was subsequently washed 5 times with 1CV of buffer W and the first wash step collected for SDS-PAGE analysis. The recombinant protein was eluted from the column using 6 times 0.5CV of buffer E (100mM Tris-HCl, 150mM NaCl, 1mM EDTA, 2.5mM desthiobiotin pH 8.0). A 20µl sample was taken from each fraction for SDS-PAGE analysis (Section 3.3.2.2) and the rest of the sample aliquoted, snap frozen in liquid N_2 and stored at -80°C. For regeneration, the column was washed with three times 5CV of buffer R (100mM Tris-HCl, 150mM NaCl, 1mM EDTA, 1mM hydroxy-azophenyl-benzoic acid (HABA), pH 8.0) in which a colour change from yellow to red is observed. The column was stored at 4°C overlaid with 2ml of buffer R.

2.2.7. Data presentation and statistics

Data are expressed as means with error bars representing standard error of the mean. The Student t-test was employed to evaluate if differences between two data points were statistically significant. Generally p-values smaller than 0.05 were considered significant. The t-test was performed using Prism 4 for Macintosh version 4.0.

Chapter 3. Results

3.1. STAT3 regulation in an ischaemic heart disease model.

This study set out to develop a model system relevant to ischaemic heart disease whereby the regulation of STAT3 in response to hypoxia/reoxygenation could be studied. The model system employed cardiomyocytes (primary and cell lines) exposed to hypoxia (1% O_2) with or without reoxygenation for 1h to mimic the conditions experienced by cardiomyocytes in hypoxia heart (Jiang et al., 1996).

4.1.1 STAT3 activity remains constant during with long exposures to hypoxia

To establish the overall picture of the effects of hypoxia on STAT3 activity on cardiomyocytes, isolated primary rat cardiomyocytes (RCMs) were subjected to hypoxia (1% O_2, 5% CO_2) over increasing time periods in a Biospherix ProOx chamber. Reoxygenation following hypoxia has been shown to increase levels of cardiomyocyte apoptosis over hypoxia treatment alone (Yang et al., 1999a), therefore cells were harvested immediately or returned to aerobic conditions for 1 hour (reoxygenation) prior to harvest. To determine the phosphorylation status of STAT3 during hypoxia/reoxygenation, nuclear extracts were analysed by western blotting using phospho-specific antibodies.

(a)

(b)

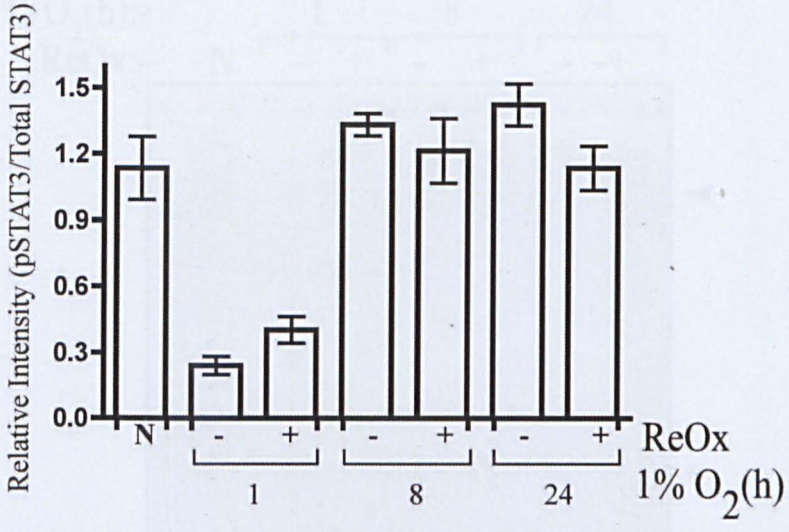

Figure 3.1. (a) Tyrosine phosphorylation status of STAT3 in isolated RCMs cells following hypoxia/reoxygenation. RCMs were exposed to normoxia (N) or hypoxia for indicated times (+) or (-) reoxygenation for 1 hour and nuclear extracts prepared. 50μg of protein for each sample was resolved by denaturing polyacrylamide gel electrophoresis. The resolved proteins were transferred to a PVDF membrane and subjected to western blotting with the antibodies indicated. **(b) Tyrosine phosphorylation status of STAT3 in RCM cells following hypoxia/reoxygenation.** Densitometry was performed using AIDA and expressed as a ratio of pSTAT3 (Y705) against total STAT3. n=3.

STAT3 protein levels were stable under hypoxia/reoxygenation (figure 3.1a, middle panel), however STAT3 tyrosine phosphorylation levels decreased approximately 4 fold after 1 hour of hypoxia (figure 3.1b) but recovered by 8h and remained stable thereafter (figure 3.1a, top

panel). TATA-Binding Protein (TBP) was used as a nuclear loading control (figure 3.1a, lower panel).

The DNA binding activity of STAT3 in nuclear extracts prepared from hypoxia/reoxygenated treated RCM cells was demonstrated by EMSA using the *vSis*-inducible element (SIE) (Wagner et al., 1990) .

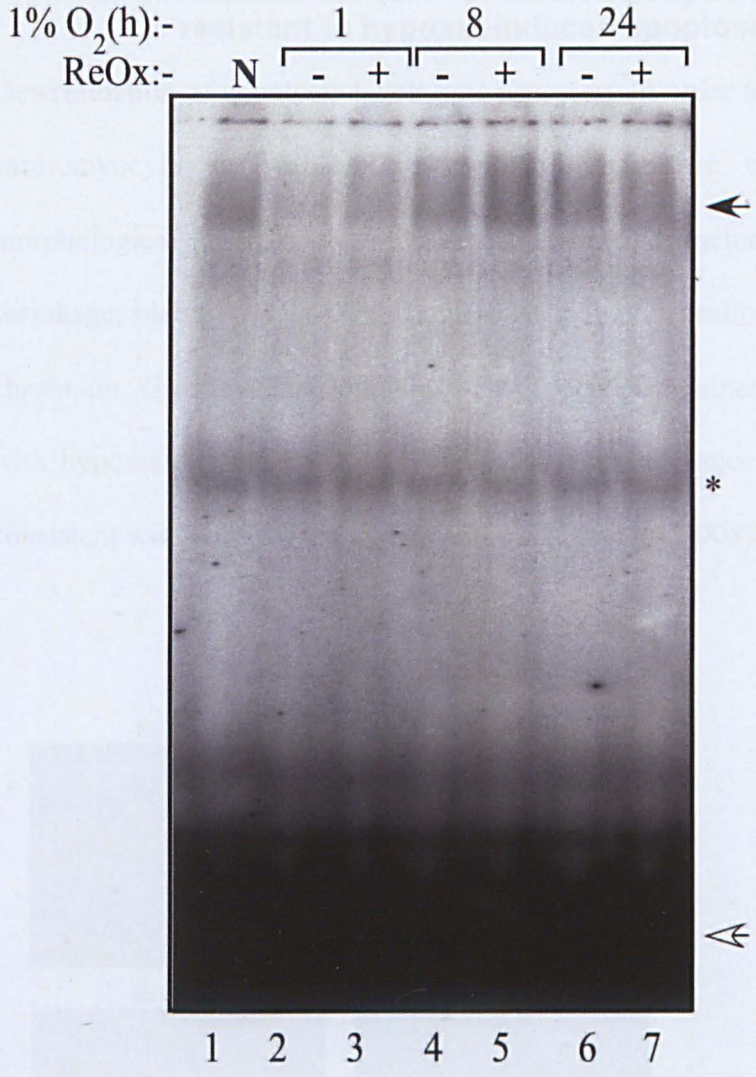

Figure 3.2. *In vitro* DNA binding of endogenous STAT3 from isolated RCM cells exposed to hypoxia/reoxygenation. Nuclear extracts prepared from RCM cells exposed to normoxia (N) or hypoxia for indicated times (+) or (-) reoxygenation for 1 hour and subjected to EMSA on the M67 SIE probe. Black arrow indicates STAT3 homodimer/DNA complex. White Arrow indicates free probe. * Indicates unidentified complex n=1.

STAT3 binding to the SIE also decreased temporarily after 1h hypoxia (figure 3.2, lane 2) showing a correlation between STAT3 tyrosine phosphorylation (figure 3.1a) and its DNA activity. Reoxygenation following hypoxia had little effect of STAT3 tyrosine phosphorylation and ultimately DNA binding in RCM cells.

4.1.2 Isolated neonatal rat cardiomyocytes are resistant to hypoxia-induced apoptosis.

Determination of apoptosis levels was necessary in order to investigate cardiomyocyte survival during hypoxia. There are characteristic morphological changes observed during apoptosis, including cellular shrinkage, blebbing, DNA fragmentation, and condensation of nuclear chromatin. Gross cell morphology of RCM cells remained unchanged with hypoxia (figure 3.3.) indicating a level of resistance to hypoxia, consistent with work by Lu and colleagues (Lu et al., 2008).

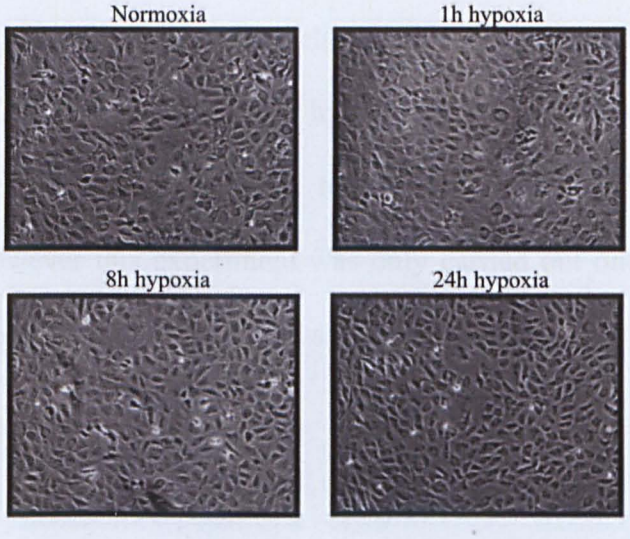

Figure 3.3. Phase images of isolated RCMs exposed to hypoxia. Phase images of RCMs exposed to hypoxia for times indicated.

Apoptosis involves the activation of executioner caspases, including caspase-3. Cleavage of the caspase-3 substrate Poly-ADP Ribose Polymerase (PARP) was assessed by western blot analysis to give an indication of apoptosis induced by hypoxia.

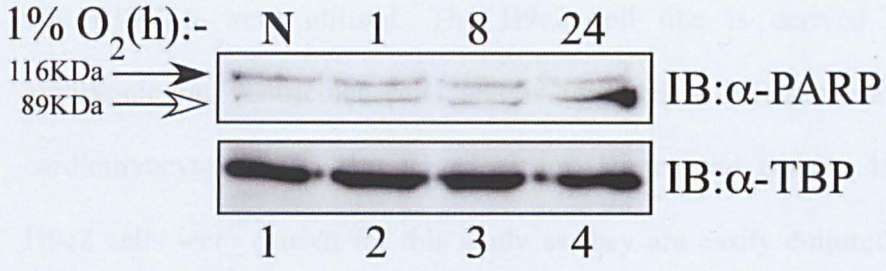

Figure 3.4. Caspase- cleavage of poly ADP-Ribose polymerase (PARP) in isolated RCM cells exposed to hypoxia. RCM cells were exposed to normoxia (N) or hypoxia for indicated times and nuclear extracts prepared. 50μg of protein for each sample was resolved by denaturing polyacrylamide gel electrophoresis. The resolved proteins were transferred to a PVDF membrane and subjected to western blotting with antibodies indicated. Black arrow 1 indicates full-length 116KDa PARP and the white arrow 2 indicates the 89KDa caspase generated fragment. n=1.

Nuclear extracts prepared from RMCs treated with hypoxia were subjected to western blot analysis using an antibody capable of detecting full-length and cleaved fragments of PARP. There was a slight increase in the levels of cleaved PARP with 1h hypoxia when RCMs were treated with hypoxia (figure 3.4, lane 2) and this signal increased with exposure to hypoxia for 24h (figure 3.4, lane 4). However this experiment was only carried out once, thus needs to be repeated in order to obtain significant results.

3.2. Validation of STAT3 regulation using alternative cell models.

3.2.1 Hypoxia differentially affects STAT3 activity in H9c2 and P19CL6 cells

To broaden the picture of STAT3 regulation, cardiac cell lines H9c2 and P19CL6 were utilised. The H9c2 cell line is derived from embryonic rat ventricular cells and is reported to differentiate into cardiomyocytes in the absence of serum (Kimes and Brandt, 1976). H9c2 cells were chosen for this study as they are easily cultured and have been used as a cardiomyocyte model previously (Hescheler et al., 1991, Hescheler et al., 1999). H9c2 cells were incubated in starvation medium for 24 hours before recovery in full medium for 5 days. This 5-day recovery allowed expression of cardiac markers including Nkx2.5 and Gata-4, indicating a cardiac phenotype (Shelton, 2009).

(a)

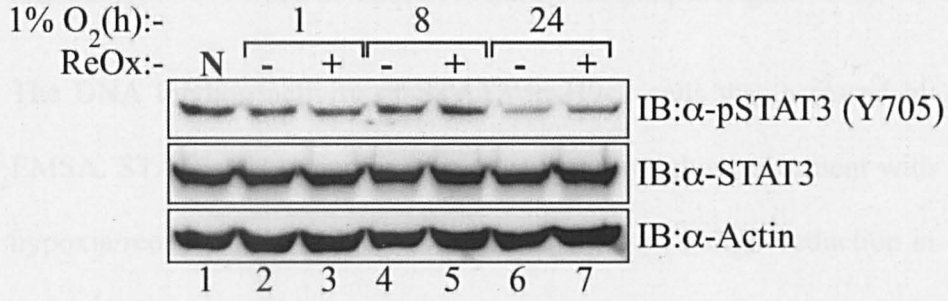

(b)

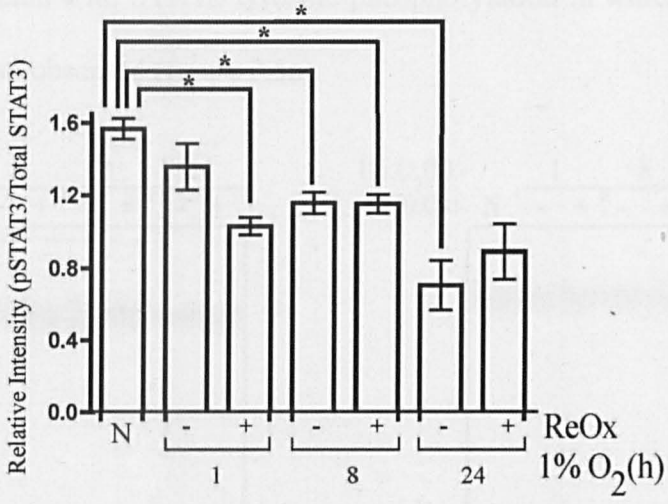

Figure 3.5. (a) Tyrosine phosphorylation status of STAT3 in H9c2 cells following hypoxia/reoxygenation. H9c2 cells were exposed to normoxia (N) or hypoxia for indicated times (+) or (-) reoxygenation for 1 hour and nuclear extracts prepared. 100µg of protein for each sample was resolved by denaturing polyacrylamide gel electrophoresis. The resolved proteins were transferred to PVDF membrane and subjected to western blotting with the antibodies indicated. (b) **Tyrosine phosphorylation status of STAT3 in H9c2 cells following hypoxia/reoxygenation**. Densitometry was performed using AIDA and expressed as a ratio of pSTAT3 (Y705) against total STAT3. Results are means ± SEM, n=3 *P<0.05.vs normoxia.

In H9c2 cells there is a slight but significant time-dependant decrease in the levels of tyrosine phosphorylated STAT3 under hypoxia/reoxygenation (figure 3.5a, top panel), whereas total STAT3 levels remained unchanged (figure 3.5a, bottom panel). A maximum reduction (0.70±0.13 relative intensity) in tyrosine phosphorylated

STAT3 was observed at 24h hypoxia, demonstrating an approximate reduction of 50% when compared to normoxia sample (figure 3.5b).

The DNA binding activity of STAT3 in H9c2 cells was assessed by EMSA. STAT3 DNA binding was observed throughout treatment with hypoxia/reoxygenation (figure 3.6, lanes 1-5), with a slight reduction in DNA binding at 24h hypoxia (figure 3.6, lane 6), displaying a positive correlation with STAT3 tyrosine phosphorylation in which a reduction was also observed (figure 3.5a).

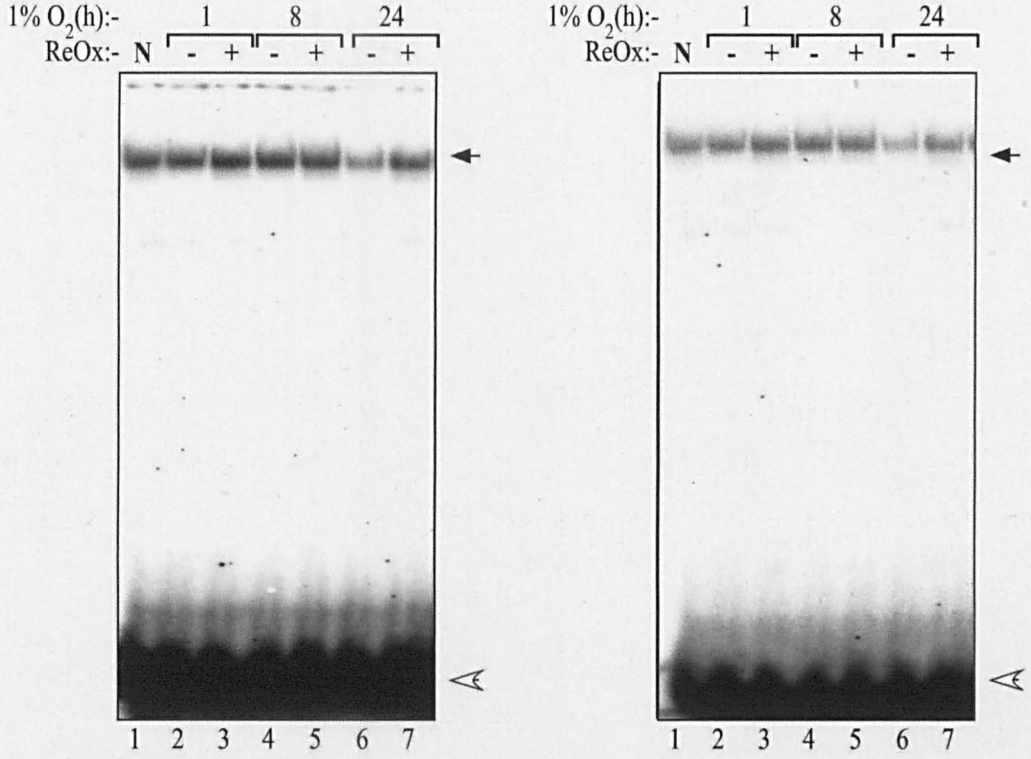

Figure 3.6. In Vitro DNA binding of endogenous STAT3 from H9c2 cells exposed to hypoxia/reoxygenation. Nuclear extracts prepared from H9c2 cells exposed to normoxia (N) or hypoxia for indicated times (+) or (-) reoxygenation for 1 hour and subjected to EMSA on the M67 SIE probe. Black arrow indicates STAT3 homodimer/DNA complex. White Arrow indicates free probe. n=2.

P19Cl6 is a subclone of the P19 cell line that was initially derived from mouse embryonic carcinoma cells. P19CL6 cells have been reported to

differentiate efficiently into beating cardiomyocytes in the presence of 0.5-1% DMSO (Habara-Ohkubo, 1996). Differentiated P19CL6 cells have been reported to retain the ability to spontaneously contract and express cardiac transcripts, suggestive of a cardiac phenotype (Skerjanc, 1999, Wobus et al., 1994). P19CL6 cells have also been extensively used to study cardiac cell physiology (van der Heyden and Defize, 2003, Anisimov et al., 2002, Rudnicki et al., 1990).

(a)

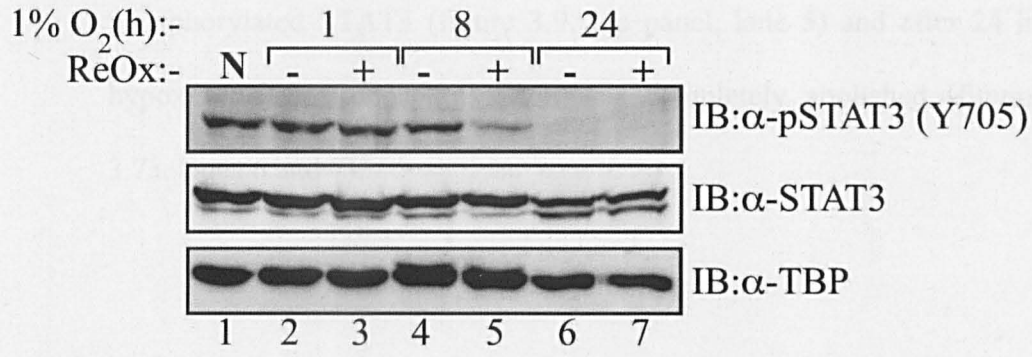

(b)

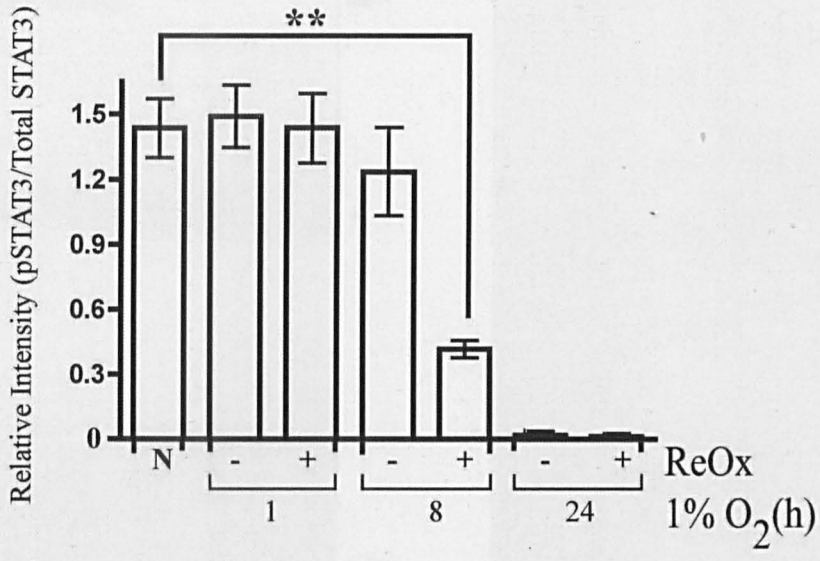

Figure 3.7. (a) Tyrosine phosphorylation status of STAT3 in P19CL6 cells following hypoxia/reoxygenation. P19CL6 cells were exposed to normoxia (N) or hypoxia for indicated times (+) or (-) reoxygenation for 1 hour and nuclear extracts prepared. 100μg of protein for each sample was resolved by denaturing polyacrylamide gel electrophoresis. The resolved proteins were transferred to a PVDF membrane and subjected to western blotting with antibodies indicated. **(b) Tyrosine phosphorylation status of STAT3 in P19CL6 cells following hypoxia/reoxygenation.** Densitometry was performed using AIDA and expressed as a ratio of pSTAT3 (Y705) against total STAT3. Results are means ± SEM, n=3 **P<0.005.

Similar to RCMs and H9c2 cells, STAT3 protein levels remained unchanged in P19CL6 exposed to hypoxia/reoxygenation (figure 3.7a, middle panel). In contrast, reoxygenation of P19CL6 cells after 8h

hypoxia caused a substantial 3.5 fold reduction (figure 3.7b) in tyrosine phosphorylated STAT3 (figure 3.9, top panel, lane 5) and after 24 h hypoxia tyrosine phosphorylation was completely abolished (figure 3.7a, lanes 6 and 7).

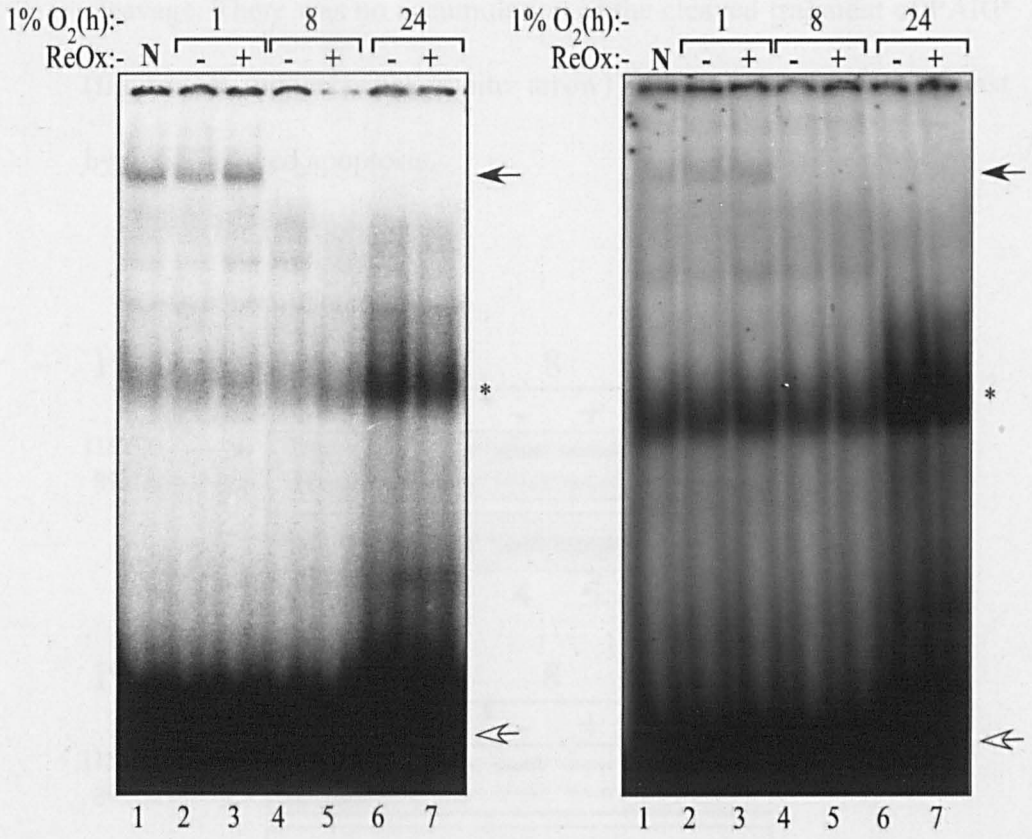

Figure 3.8. In vitro DNA binding of endogenous STAT3 from P19CL6 cells exposed to hypoxia/reoxygenation. Nuclear extracts prepared from P19CL6 cells exposed to normoxia (N) or hypoxia for indicated times (+) or (-) reoxygenation for 1 hour and subjected to EMSA on the M67 SIE probe. Black arrow indicates STAT3 homodimer/DNA complex. White Arrow indicates free probe. * Indicates an unidentified complex. n=2.

STAT3 was detected binding to the SIE in P19CL6 cells under normoxic conditions and when exposed to 1h hypoxia (+/- reoxygenation) (figure 3.8, lanes 1-3). Interestingly, a complete loss of STAT3 DNA binding was observed in P19CL6 cells after 8h hypoxia

(figure 3.8, lane 4) even though tyrosine phosphorylation was still detectable at the time point (figure 3.7a, top panel, lane 4).

3.2.2 P19L6 but not H9c2 cells are sensitive to hypoxia-induced apoptosis

Apoptosis was determined in H9c2 cells with reference to PARP cleavage. There was no accumulation of the cleaved fragment of PARP (figure 3.9, upper panel, white arrow) indicating resistance against hypoxia-induced apoptosis.

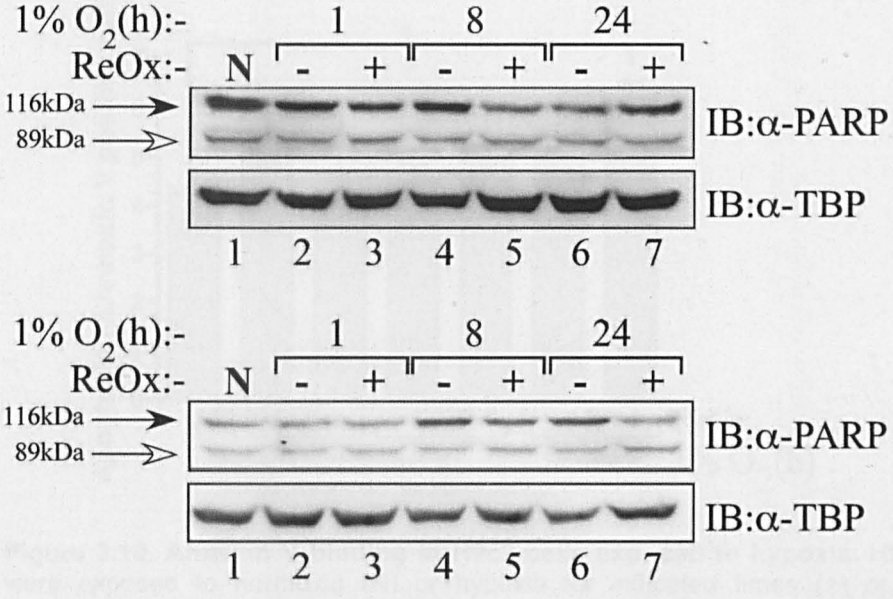

Figure 3.9. Caspase-cleavage of poly ADP-Ribose polymerase (PARP) in H9c2 cells exposed to hypoxia/reoxygenation. H9c2 cells were exposed to normoxia (N) or hypoxia for indicated times (+) or (-) reoxygenation for 1 hour and nuclear extracts prepared. 100μg of protein for each sample was resolved by denaturing polyacrylamide gel electrophoresis. The resolved proteins were transferred to a PVDF membrane and subjected to western blotting with antibodies indicated. Black arrow 1 indicates full-length 116KDa PARP and the white arrow 2 indicates the 89KDa caspase generated fragment. n=2.

Apoptosis was also determined experimentally by annexin V binding followed by fluorescence activated cell sorting (FACS). Levels of apoptosis were very low in H9c2 cells exposed to hypoxia/reoxygenation with approximately a 1.3-fold increase with reoxygenation after 24h hypoxia (figure 3.10). This indicates that H9c2 cells are resistant to hypoxia-induced apoptosis for long periods of time, which is consistent with studies carried out by Bonavita and colleagues (Bonavita et al., 2003).

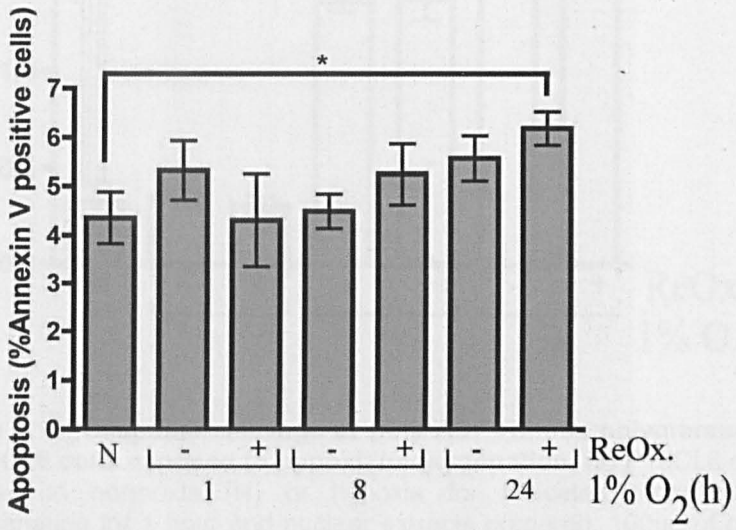

Figure 3.10. Annexin V binding in H9c2 cells exposed to hypoxia. H9c2 were exposed to normoxia (N) or hypoxia for indicated times (+) or (-) reoxygenation for 1 hour and then subjected to Annexin V binding assay. The stained cells were then sorted using a Coulter Altra Flow Cytometer, set to count 20000 events. Results are means ± SEM, n=3, *P < 0.05.

Hypoxia-induced apoptosis was also determined using the P19CL6 cell line model. In contrast to RCMs and H9c2 cells, P19CL6 cells were extremely sensitive to hypoxia-induced apoptosis.

(a)

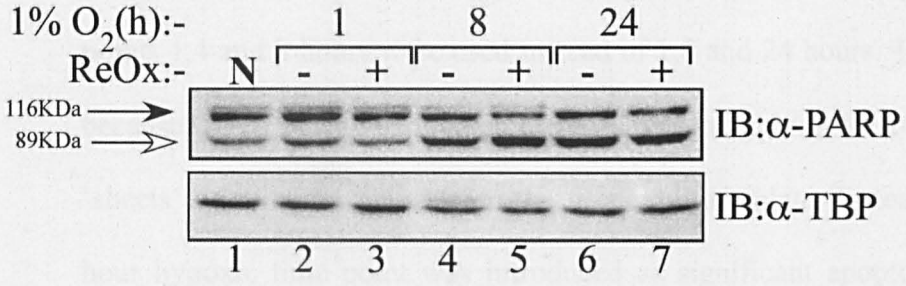

(b)

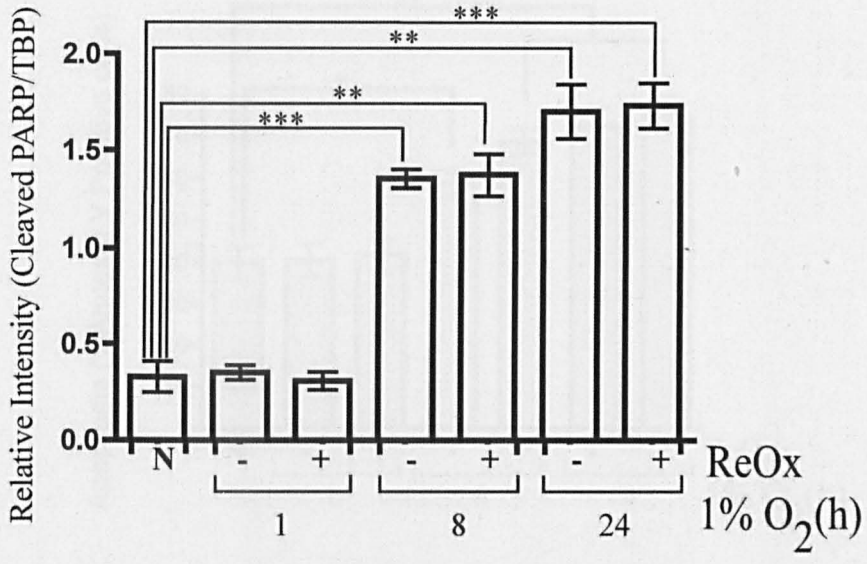

Figure 3.11. Caspase- cleavage of poly ADP-Ribose polymerase (PARP) in P19CL6 cells exposed to hypoxia/reoxygenation. (a) P19CL6 cells were exposed to normoxia (N) or hypoxia for indicated times (+) or (-) reoxygenation for 1 hour and nuclear extracts prepared. 100μg of protein for each sample was resolved by denaturing polyacrylamide gel electrophoresis. The resolved proteins were transferred to a PVDF membrane and subjected to western blotting with antibodies indicated Black arrow 1 indicates full-length 116KDa PARP and the white arrow 2 indicates the 89KDa caspase generated fragment. **(b)** Densitometry was performed using AIDA and expressed as a ratio of pSTAT3 (Y705) against total STAT3. Results are means ± SEM, n=3, *P < 0.05, **P<0.005, ***P<0.001.

P19CL6 cells displayed an increase in cleaved PARP following exposure to hypoxia for 8 or longer (+/- reoxygenation) (figure 3.11, upper panel, white arrow, lanes 4-7), Cleaved PARP increased by

approximately 3-fold (figure 3.11b), indicative of apoptosis. Levels of apoptosis was also measured in P19CL6 cells however hypoxic time points 1,4 and 8 hours were used instead of 1,8 and 24 hours. This was because the P19CL6 were extremely sensitive to hypoxia for 24h, with 'sheets' of cells detaching from the tissue culture plate. Instead the 4 hour hypoxic time point was introduced as significant apoptosis had already been observed in P19CL6 cells with 8h hypoxia (Figure 3.11).

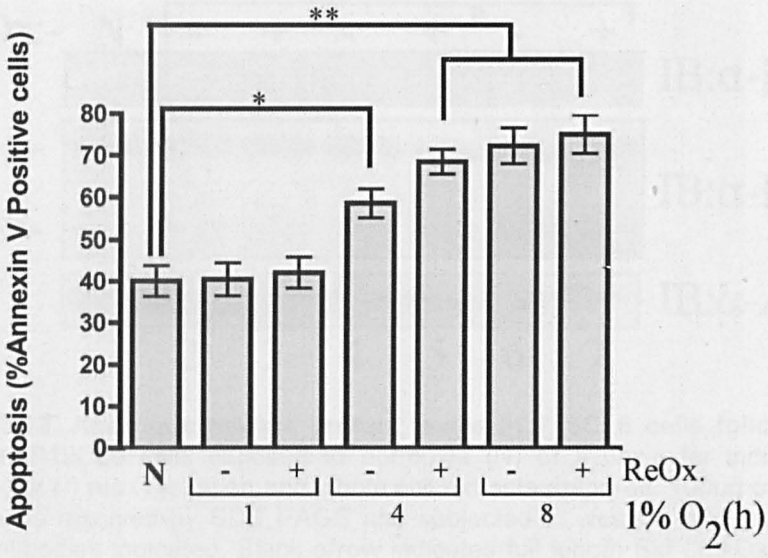

Figure 3.12. Annexin V binding in P19CL6 cells exposed to hypoxia. P19CL6 were exposed to normoxia (N) or hypoxia for indicated times (+) or (-) reoxygenation for 1 hour and then subjected to Annexin V binding assay. The stained cells were then sorted using a Coulter Altra Flow Cytometer, set to count 20000 events. Results are means ± SEM, n=3, *P < 0.05, **P<0.001

P19CL6 cells displayed a high basal level of apoptosis with around 40% of cells staining positive for annexin V under normoxic conditions (figure 3.12) when compared to 4.5% annexin V-stained H9c2 cells (figure 3.10). Exposure to hypoxia for 4 and 8 hours caused a significant 1.5-fold and 1.75-fold increase in apoptosis respectively (figure 3.12).

In addition to PARP-cleavage and annexin V staining, hypoxia-induced apoptosis was also assessed in P19CL6 cells by apoptotic marker expression. Whole cell extracts were subjected to western blotting with antibodies raised against the anti-apoptotic factor Mcl-1 and the pro-apoptotic factor Bid.

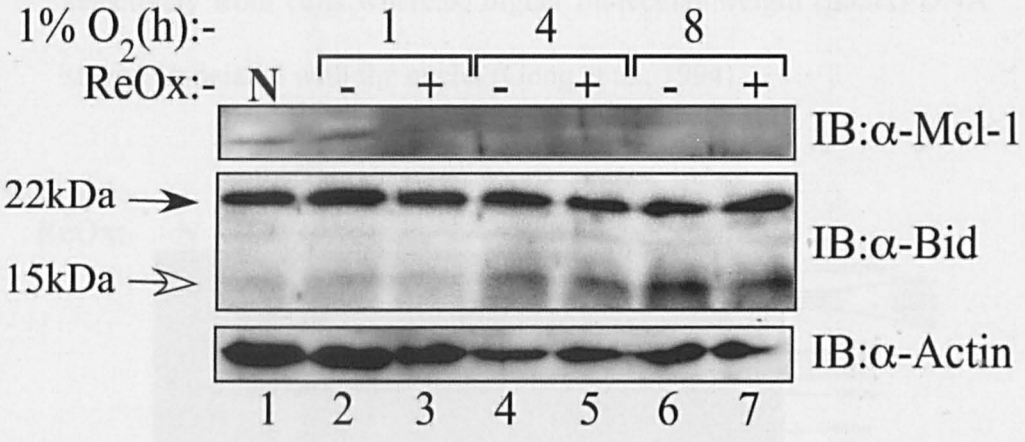

Figure 3.13. Apoptotic marker protein levels in P19CL6 cells following hypoxia. P19CL6 cells exposed to normoxia (N) or hypoxia for indicated times (+) or (-) reoxygenation and whole cell extracts prepared. 100μg of total protein was resolved by SDS PAGE and subjected to western blot analysis using antibodies indicated. Black arrow indicates full length Bid (22kDa) and the white arrow indicates caspase-cleaved Bid (15kDa). n=1.

Mcl-1 protein was detected in P19CL6 cells under normoxia but detection was abolished with reoxygenation after 1h hypoxia and remained undetectable thereafter (figure 3.13, upper panel, lanes 3-7). Conversely, accumulation of the caspase-cleaved pro-apoptotic factor Bid was detected in P19CL6 cells treated with 4 and 8h hypoxia/reoxygenation (figure 3.13, lower panel, lanes 4-7, white arrow). The cleavage of Bid is a process, indicative of apoptosis as this

cleaved product translocates to mitochondria triggers the permeability transition and release of pro-apoptotic factors (Li et al., 1998).

Finally hypoxia-induced apoptosis was also identified in P19CL6 cells using a DNA fragmentation assay. DNA fragmentation is a morphological characteristic of apoptotic cells. The protocol used allowed partially degraded oligonucleosomal DNA to be extracted quite selectively from cells whereas, higher molecular weight (intact) DNA stayed associated with the nuclei (Gong et al., 1994).

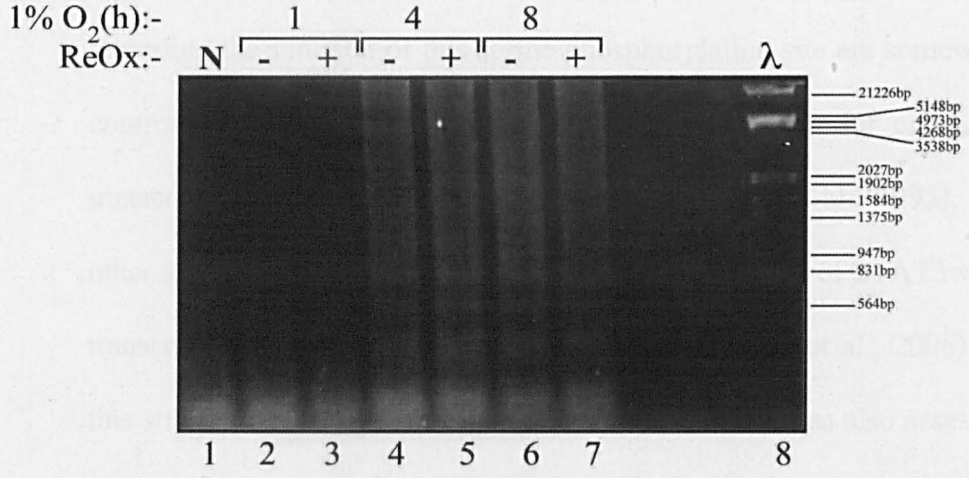

Figure 3.14. DNA fragmentation in P19CL6 cells following hypoxia. P19CL6 cells exposed to normoxia (N) or hypoxia for indicated times (+) or (-) and DNA extracts prepared. Samples were resolved on a 1.5% Agarose gel; stained with ethidium bromide and DNA detected using an UV documentation system. n=1

Partially degraded DNA was observed from P19CL6 cells exposed to hypoxia for 4 hours or more (+/-reoxygenation) (figure 3.14, lanes 4-7), correlating with data collected from the annexin V binding assay and western blot analysis. These results show that differentiated P19CL6 cells exhibit a higher sensitivity to hypoxia compared to RCMs and

H9c2 cells. The increased sensitivity observed in P19CL6 cells makes them a more responsive model to study changes induced by hypoxia.

3.3. The role of PKCδ in cardiomyocytes during hypoxia.

3.3.1 Hypoxia differentially affects STAT3 serine phosphorylation in H9c2 and P19CL6 cells

In addition to tyrosine phosphorylation, STAT3 is also phosphorylated on a serine residue (S727) in its carboxyl-terminal domain. Studies regarding the function of this serine phosphorylation site are somewhat controversial. Initially it was thought to be important for enhanced transcriptional activation (Wen et al., 1995, Zhang et al., 1995), but other studies have associated the serine phosphorylation of STAT3 with transcriptional repression (Jain et al., 1999, Gartsbein et al., 2006). In this study the serine phosphorylated status of STAT3 was also assessed in response to hypoxia/reoxygenation. In H9c2 cells, STAT3 S727 phosphorylation was observed under normoxia and levels decreased approximately 3-fold with 8 and 24h hypoxia (figure 3.15b) and recovered upon reoxygenation (figure 3.15a, upper panel, lanes 5 and 7).

(a)

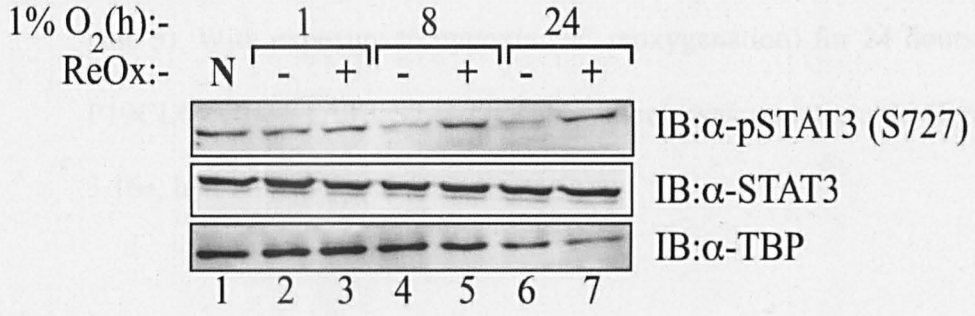

(b)

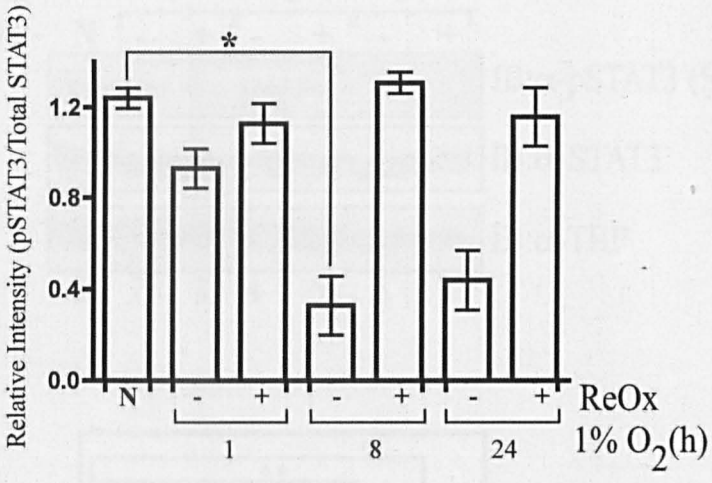

Figure 3.15. (a) Serine phosphorylation status of STAT3 in H9c2 cells following hypoxia/reoxygenation. H9C2 cells were exposed to normoxia (n) or hypoxia for indicated times (+) or (-) reoxygenation for 1 hour and nuclear extracts prepared. 100µg of protein for each sample was resolved by denaturing polyacrylamide gel electrophoresis. The resolved proteins were transferred to a PVDF membrane and subjected to western blotting with antibodies indicated. **(b) Serine phosphorylation status of STAT3 in H9c2 cells following hypoxia/reoxygenation.** Densitometry was performed using AIDA and expressed as a ratio of pSTAT3 (S727) against total STAT3. Results are means ± SEM, n=3, *P<0.05.

In contrast, P19CL6 cells displayed lower levels of STAT3 S727 phosphorylation under normoxic conditions, with no change after 1-hour hypoxia/reoxygenation (figure, 3.17a, upper panel. lanes 1-3). However, after 8 hours hypoxia STAT3 S727 phosphorylation was

significantly elevated approximately 2.5-fold (figure 3.16b) and decreased only marginally (2-fold) upon reoxygenation (figure 3.16a, lane 5). With exposure to hypoxia (+/- reoxygenation) for 24 hours in P19CL6 cells, STAT3 S727 phosphorylation was undetectable (figure 3.16a, lanes 6-7).

(a)

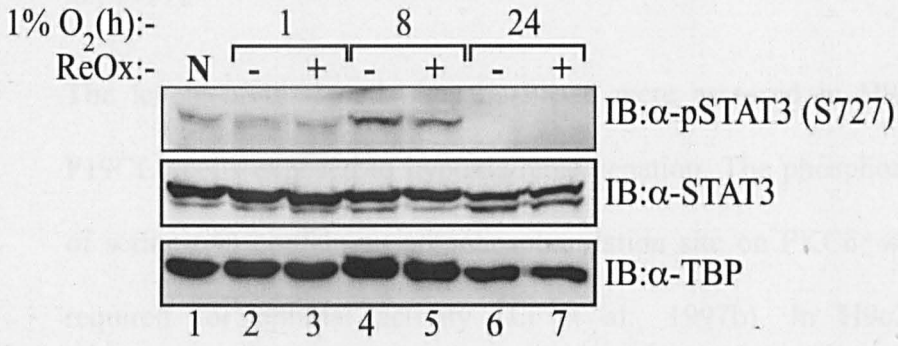

(b)

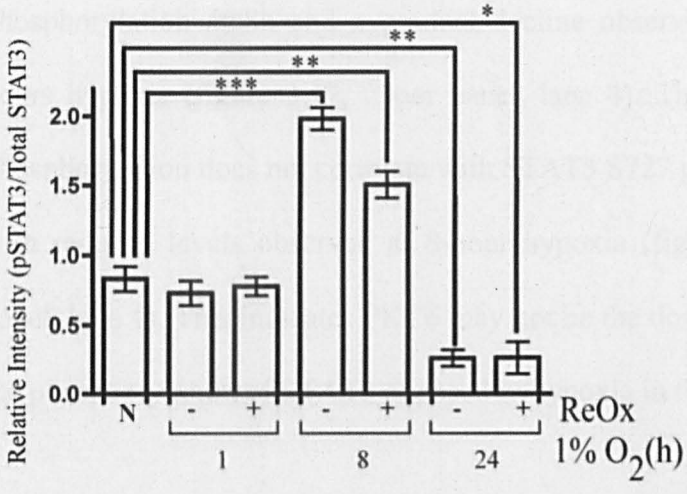

Figure 3.16. (a) Serine phosphorylation status of STAT3 in P19CL6 cells following hypoxia/reoxygenation. P19CL6 cells were exposed to normoxia (N) or hypoxia for indicated times (+) or (-) reoxygenation for 1 hour and nuclear extracts prepared. 100μg of protein for each sample was resolved by denaturing polyacrylamide gel electrophoresis. The resolved proteins were transferred to a PVDF membrane and subjected to western blotting with antibodies indicated. **(b) Serine phosphorylation status of STAT3 in P19CL6 cells following hypoxia/reoxygenation.** Densitometry was performed using AIDA and expressed as a ratio of pSTAT3 (S727) against total STAT3. Results are means ± SEM, n=3 ***P<0.001, **P<0.005, *P<0.05.

3.3.2 PKCδ activity differs in H9c2 and P19CL6 cells during hypoxia

Novel PKC isoforms have been implicated in the phosphorylation of STAT3 on serine 727 and in the context of PKCδ linked to STAT3 inhibition. For example, IL-6 inducible association of PKCδ with STAT3 caused an increase in the S727 phosphorylation and the down-regulation of STAT3 DNA binding and transcriptional activity (Jain et al., 1999).

The levels of total and phospho-PKCδ were assessed in H9c2 and P19CL6 cells exposed to hypoxia/reoxygenation. The phosphorylation of serine 643 confers an autophosphorylation site on PKCδ, which is required for optimal activity (Li et al., 1997b). In H9c2 cells phosphorylation of PKCδ increased with hypoxia, with peak phosphorylation at 8h and a gradual decline observed at 16 and 24 hours hypoxia (figure 3.17, upper panel, lane 4). The peak in PKCδ phosphorylation does not correlate with STAT3 S727 phosphorylation - with reduced levels observed at 8-hour hypoxia (figure 3.15a, upper panel, lane 4). This indicates PKCδ may not be the dominant kinase for the phosphorylation of STAT3 exposed to hypoxia in these cells.

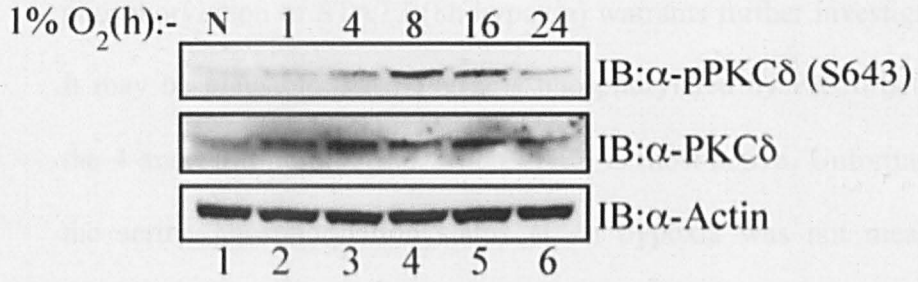

Figure 3.17.Levels of PKCδ in H9c2 cells exposed to hypoxia. H9c2 cells were exposed to normoxia (N) hypoxia for indicated times and whole cell extracts prepared. 100µg of protein for each sample was resolved by denaturing polyacrylamide gel electrophoresis. The resolved proteins were transferred to a PVDF membrane and subjected to western blotting with antibodies indicated. n=1.

The peak in PKCδ autophosphorylation was observed earlier in P19CL6 cells, with maximal PCKδ phosphorylation observed at 4h hypoxia and then a subsequent reduction at 8h hypoxia (figure 3.18, upper panel lanes 3-4).

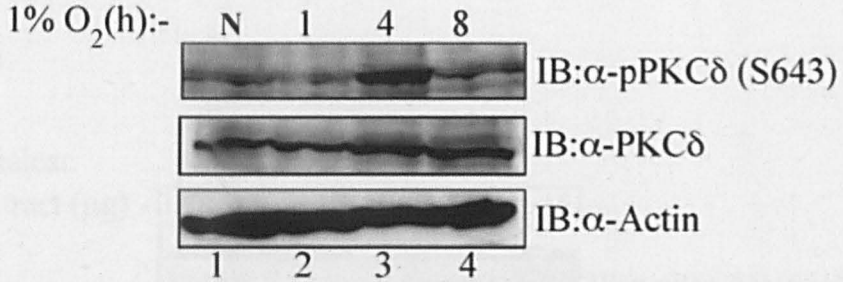

Figure 3.18. Levels of PKCδ in P19CL6 cells exposed to hypoxia. P19CL6 cells were exposed to normoxia (N) or hypoxia for indicated times and whole cell extracts prepared. 100µg of protein for each sample was resolved by denaturing polyacrylamide gel electrophoresis. The resolved proteins were transferred to a PVDF membrane and subjected to western blotting with antibodies indicated. n=1

These data shows that in P19CL6 cells, phosphorylation and activation of PKCδ in response to hypoxia is present before (4 hours earlier) the phosphorylation of STAT3 on serine 727 (figure 3.16a). PKCδ may still be the kinase that phosphorylates S727 on STAT3, however the 4h time difference between the activation of PKCδ (4h hypoxia) and the serine

phosphorylation of STAT3 (8h hypoxia) warrants further investigation. It may be plausible that STAT3 is phosphorylated by PKCδ between the 4 and 8h time point i.e. when PKCδ is most active. Unfortunately the serine phosphorylation status at 4h hypoxia was not measured therefore further investigation is required before interpretations can be made.

The overall basal levels PKCδ also varied between H9c2 and P19CL6 cell lines. A titration (120μg-15μg) of nuclear extracts from normoxic H9c2 and P19CL6 cells was subjected to western blot analysis. The level of phospho-PKCδ in H9c2 was significantly lower when compared to equal total protein amounts from P19CL6 cells (figure 3.19, upper panel).

(a)

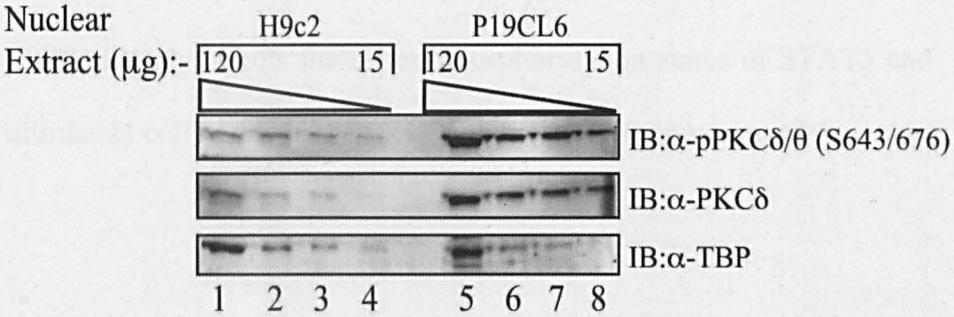

(b)

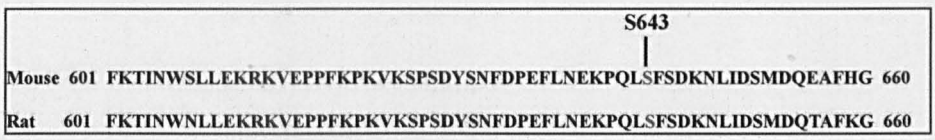

Figure 3.19. (a) Comparison of PKCδ activity in H9c2 and P19CL6 cells. Normoxic nuclear extracts from H9C2 and P19CL6 cells were prepared. Total protein concentration was determined by Bradford assay and a 2-fold dilution series from 120μg to 15μg prepared. Sample were resolved by denaturing polyacrylamide gel electrophoresis, transferred to a PVDF

membrane and subjected to western blotting with antibodies indicated. **(b)** Mouse and rat PKCδ protein sequence alignment.

However, H9c2 and P19CL6 cells are from different species (rat and mouse respectively). Therefore it could be possible that the antibody has different specificities for different species of PKCδ. However this is unlikely due to high level of protein sequence homology between the two species (figure 3.19b).

3.3.3 Rottlerin enhances apoptosis in P19CL6 cells

In this study the data shows that in P19CL6 cells, there is a correlation between the activation of PKCδ at 4h hypoxia (figure 3.18) followed by the serine phosphorylation of STAT3 at 8h hypoxia (figure 3.16). Enhancement of serine phosphorylation accompanies loss of STAT3 DNA binding and increased levels of apoptosis. To identify whether PKCδ directly affects the serine phosphorylation status of STAT3 and ultimately cell survival, the PKCδ inhibitor, rottlerin was used.

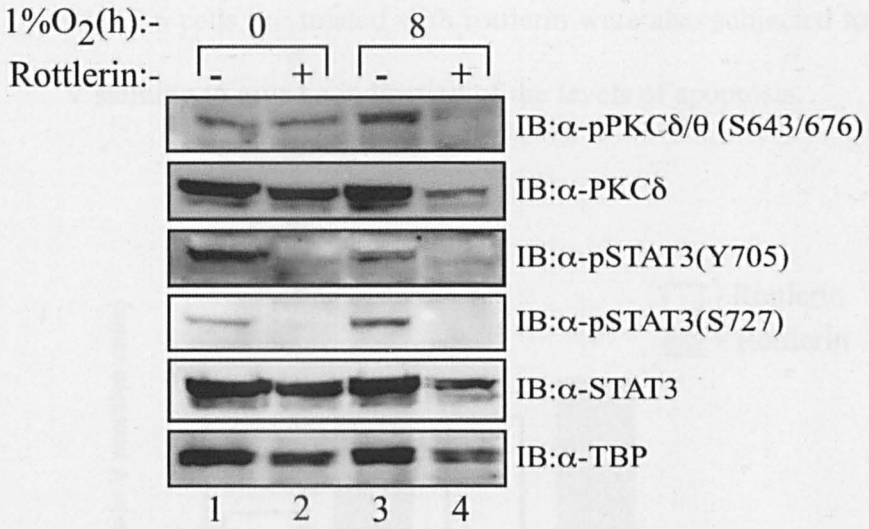

Figure 3.20. Effect of rottlerin on P19CL6 cells exposed to hypoxia. P19CL6 cells were pre-treated with (+) or (-) PCKδ inhibitor rottlerin (3μM) before exposure to hypoxia and nuclear extracts prepared. 100μg of protein for each sample was resolved by denaturing polyacrylamide gel electrophoresis. The resolved proteins were transferred to a PVDF membrane and subjected to western blotting with antibodies indicated. N=2.

P19CL6 cells were pre-treated with rottlerin immediately before exposure to 8h hypoxia. Maximal PKCδ phosphorylation was observed with 8h hypoxia and this was completely abolished with rottlerin treatment (figure 3.20, upper panel, lanes 3-4).

The increase in STAT3 S727 phosphorylation previously observed with 8h hypoxia (figure 3.20, lane 4) was also abolished upon treatment with rottlerin (figure 3.20, lanes 3-4, panel 4). However unexpectedly STAT3 Y705 phosphorylation was also lost with rottlerin treatment, even under normoxic conditions (figure 3.20, 3rd panel lanes 1-2.). There were also lots of accompanying changes associated with rottlerin treatment, including reductions in total STAT3 (figure 3.20, 5th panel) and PKCδ (figure 3.20 2nd panel) protein levels and even levels of the loading control TBP (figure 3.2 6th panel). Therefore it was very difficult to interpret these results.

P19CL6 cells pre-treated with rottlerin were also subjected to Annexin V staining to give an indication of the levels of apoptosis.

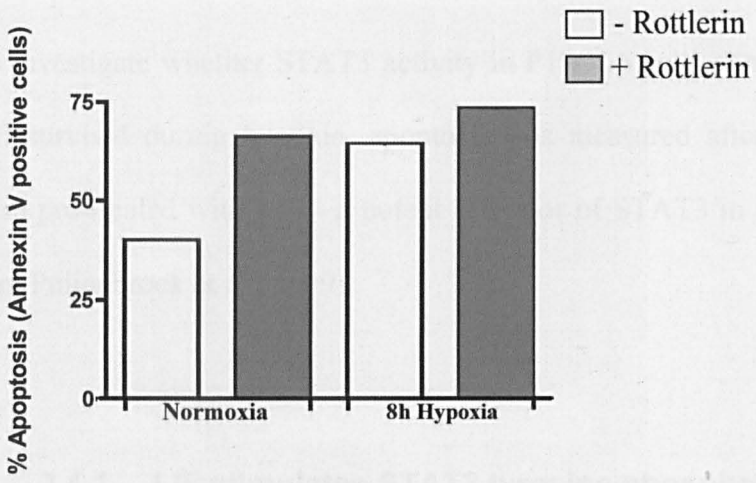

Figure 3.21 Annexin V binding in P19CL6 cells pre-treated with Rottlerin before exposure to hypoxia. P19CL6 were pre-treated with (+) or (-) Rottlerin (3μM) before exposure to normoxia or hypoxia for 8 hours and then subjected to Annexin V binding assay. The stained cells were then sorted using a Coulter Altra Flow Cytometer, set to count 20000 events. n=2.

P19CL6 cells were highly sensitive to rottlerin. There is an approximate 1.75-fold increase in the number of annexin V-stained cells treated with rottlerin under normoxic conditions (figure 3.21). Although it continues to be used, rottlerin has been discredited as a selective and specific inhibitor of PKCδ due to its potent mitochondrial uncoupling and K^+ channel activating properties (Soltoff, 2007).

3.4. Elevated STAT3 activity protects P19CL6 from hypoxia-induced apoptosis.

To investigate whether STAT3 activity in P19CL6 cells contributes to cell survival during hypoxia, apoptosis was measured after the cells were pre-treated with LIF - a potent activator of STAT3 in these cells (van Puijenbroek et al., 1999).

3.4.1 LIF stimulates STAT3 tyrosine phosphorylation in P19CL6 cells

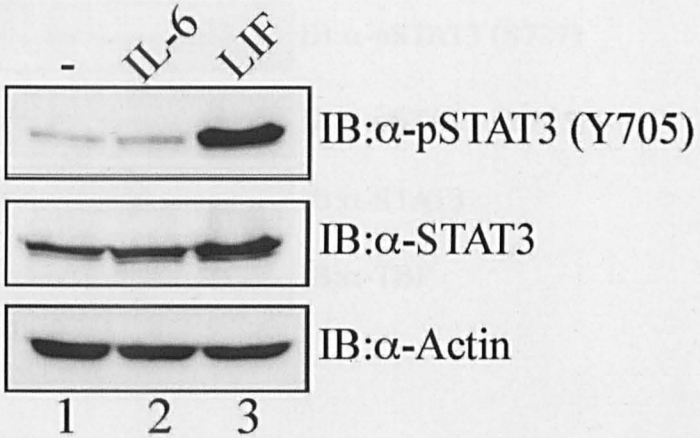

Figure 3.22. STAT3 tyrosine phosphorylation in P19CL6 cells upon LIF treatment. P19CL6 cells were treated with 10ng/ml LIF or 10ng/ml IL-6 for 20 minutes and whole cell extracts prepared. 100μg of protein for each sample was resolved by denaturing polyacrylamide gel electrophoresis. The resolved proteins were transferred to a PVDF membrane and subjected to western blotting with antibodies indicated.

Pre-treating P19CL6 cells with 10ng/ml of LIF for 20 minutes caused tyrosine phosphorylation of STAT3 (figure 3.22, upper panel, lane 3),

whereas another type I cytokine IL-6, had no effect (figure 3.22, upper panel, lane 2).

3.4.2 LIF maintains STAT3 phosphorylation but not DNA binding activity in P19CL6 cells during hypoxia

3.4.2

Stimulation of STAT3 with LIF increased STAT3 tyrosine phosphorylation levels by approximately 2-fold in both normoxic and 1h hypoxia treated cells (figure 3.23, 2nd panel and figure 3.31).

(a)

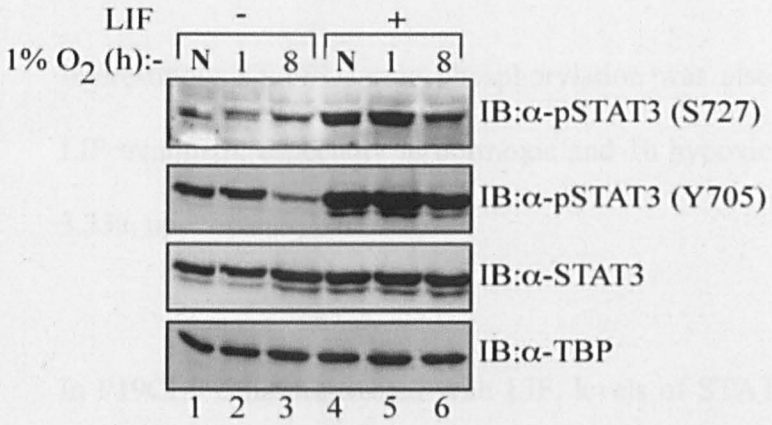

(b)

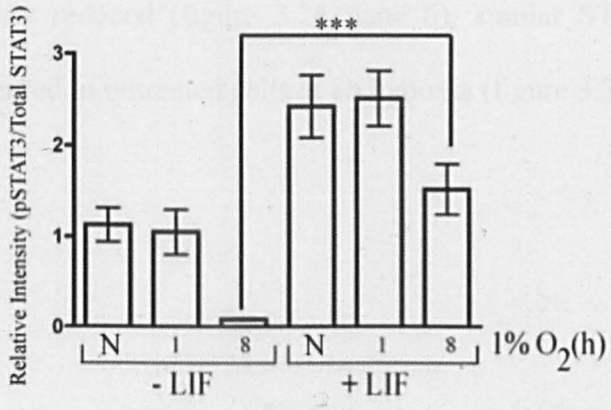

Figure 3.23. (a) Phosphorylation status of STAT3 in P19CL6 pre-treated with LIF prior to exposure to hypoxia. P19CL6 were pre-treated with (+) or (-) LIF (10ng/ml) before exposure to normoxia (N) or hypoxia for indicated times and nuclear extracts prepared. 100µg of protein for each sample was resolved by denaturing polyacrylamide gel electrophoresis. The resolved proteins were transferred to a PVDF membrane and subjected to western blotting with antibodies indicated. **(b) Tyrosine phosphorylation status of STAT3 in P19CL6 cells pre-treated with LIF following hypoxia.** Densitometry was performed using AIDA and expressed as a ratio of pSTAT3 (Y705) against total STAT3. Results are means ± SEM, n=3 ***P<0.001.

There was also a significant level of STAT3 tyrosine phosphorylation still remaining after 8h hypoxia (figure 3.23a, 2nd panel, lane 6) with only ~1.3 fold reduction after 8h hypoxia (normoxia vs. 8h hypoxia) in LIF treated cells compared to ~12 fold reduction after 8h hypoxia (normoxia vs. 8h hypoxia) in untreated cells (figure 3.23b).

Interestingly STAT3 serine phosphorylation was also enhanced upon LIF treatment, especially in normoxic and 1h hypoxic samples (figure 3.23a, upper panel, lane 4-6).

In P19CL6 cells pre-treated with LIF, levels of STAT3 DNA binding substantially increased under normoxia and after 1h hypoxia (figure 3.24, lanes 4-5). However, after 8h hypoxia STAT3 DNA binding was greatly reduced (figure 3.24, lane 6), similar STAT3 DNA binding observed in untreated cells at 8h hypoxia (figure 3.24, lane 3).

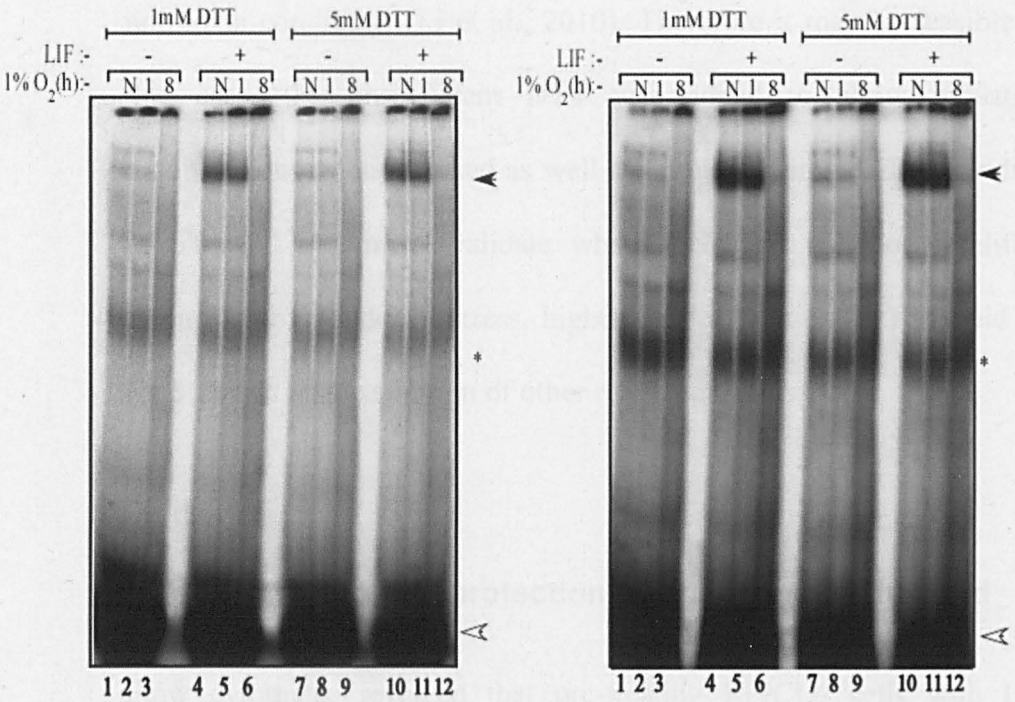

Figure 3.24. In Vitro DNA binding of endogenous STAT3 from P19CL6 cells pre-treated with LIF prior to exposure to hypoxia. P19CL6 were pre-treated with (+) or (-) LIF (10ng/ml) before exposure to normoxia (N) or hypoxia for indicated times. Nuclear extracts were prepared and subjected to EMSA on the M67 SIE probe using DTT concentrations indicated. Black arrow indicates STAT3 homodimer/DNA complex and the white Arrow indicates free probe. * Indicates unidentified complex. n=2.

During hypoxia excessive levels of ROS are generated, which could lead to oxidative modification of proteins, including STAT3. Such modifications may impair STAT3 ability to bind to DNA. Studies have shown that STAT3 DNA binding is sensitive to peroxide treatment (Li et al., 2010). The DNA binding assay was also carried out under high levels (5mM) of DTT (a reducing agent) in order to reverse any such oxidative modifications that lead to the inhibition of DNA binding. The addition of DTT had no effect, with loss of STAT3 DNA binding still apparent with 8h hypoxia (figure 3.24, lane 12). Studies have shown that the addition of DTT is required for *in vitro* DNA binding under

normoxia conditions (Li et al., 2010). Therefore it may be feasible in this case, that insufficient DTT was added to allow oxidative modifications to be reversed as well as ensuring optimal DNA binding of STAT3. To further validate whether STAT3 is redox modified during hypoxia-induced stress, higher concentration of DTT could be used as well as the addition of other reducing agents.

3.4.3 LIF offers protection against hypoxia-induced apoptosis

Flow cytometry revealed that pre-treating P19CL6 cells with LIF offered a degree of protection against hypoxia-induced apoptosis. P19CL6 cells displayed approximately 65% positive staining for annexin V at 8h hypoxia in untreated cells which, significantly reduced to 55% positively stained annexin V cells when pre-treated with LIF (figure 3.25).

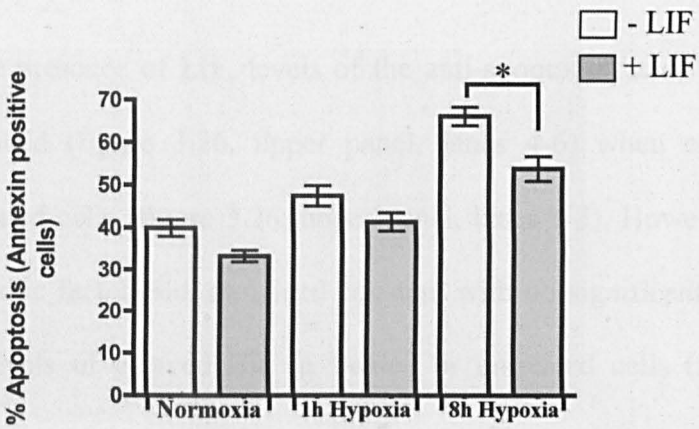

Figure 3.25. Annexin V binding in P19CL6 cells pre-treated with LIF before exposure to hypoxia. P19CL6 were pre-treated with (+) or (-) LIF (10ng/ml) before exposure to hypoxia for indicated times and then subjected to an annexin V binding assay. The stained cells were then sorted using a Coulter Altra Flow Cytometer, set to count 20000 events. n=3, *P < 0.05.

The effects of LIF on hypoxia-induced apoptosis were also assessed by apoptotic marker expression. Whole cell extracts were subjected to western blotting with antibodies raised against the anti-apoptotic factor Mcl-1 and the pro-apoptotic factor Bid.

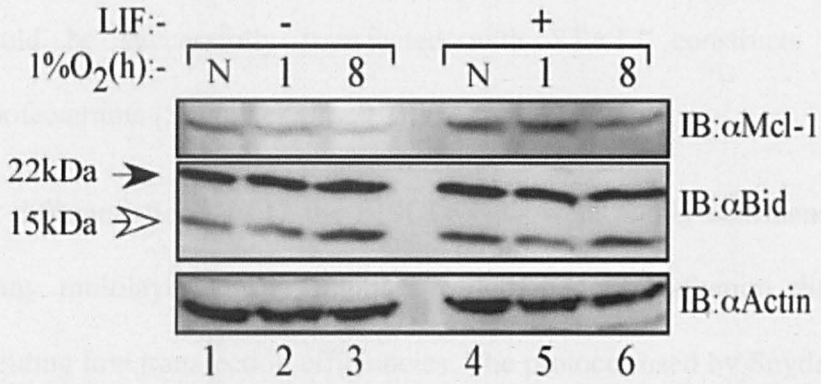

Figure 3.26. Apoptotic marker protein levels in P19CL6 cells pre-treated with LIF prior to exposure to hypoxia. P19CL6 cells were treated with (+) or (-) LIF (10ng/ml) prior to exposure to normoxia (N) or hypoxia for indicated times and whole cell extracts prepared. 100µg of total protein was resolved by SDS PAGE and subjected to western blot analysis using antibodies indicated. Black arrow indicates full length Bid and the white arrow indicates caspase-cleaved Bid. n=1.

In the presence of LIF, levels of the anti-apoptotic factor Mcl-1 were enhanced (figure 3.26, upper panel, lanes 4-6) when compared to untreated cells (figure 3.26, upper panel, lanes 1-3). However the pro-apoptotic factor Bid, remained constant with no significant changes in the levels of cleaved Bid in treated or untreated cells (figure 3.26, middle panel, lanes 1-6).

3.5. Exogenous expression of STAT3 offers protection against hypoxia-induced apoptosis in P19CL6 Cells

3.5.1 Passaging differentiated P19CL6 prior to transfection enhances transfection efficiency

Snyder and colleagues demonstrated that differentiated P19CL6 cells could be successfully transfected with STAT3 constructs using lipofectamine (Snyder et al., 2010).

At differentiation day 12 the P19CL6 cells were highly confluent with many multilayer cluster regions, which made transfection difficult yielding low transfection efficiencies. The protocol used by Snyder and colleagues (Snyder et al., 2010) was modified slightly to give improved transfection efficiencies. Modifications included passaging the cells (1-4 dilution) the day before transfection (figure 3.27, bottom panels) and also using the lipofectamine enhancer, Plus™ reagent. These modifications greatly enhanced the transfection efficiency.

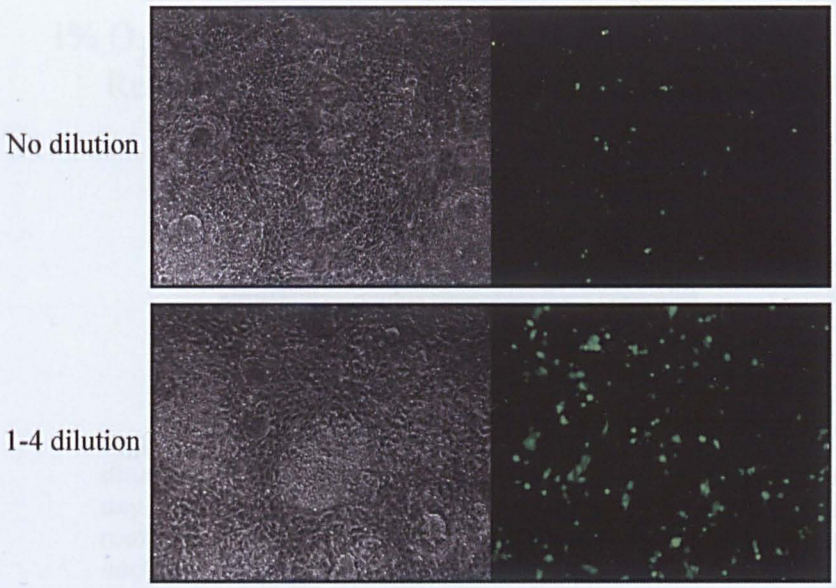

Figure 3.27. GFP expression in P19CL6 cells. GFP and phase images of P19CL6 cells transfected (lipofectamine in the presence of Plus™ reagent) with a vector containing GFP and cultured for 48h.

Preliminary experiments were carried out to ensure that the additional passage to P19CL6 cells did not affect the phosphorylation status of STAT3 that was observed previously (figures 3.7a and 3.16a). Differentiated P19CL6 cells were passaged (1-4 dilution) and the next day exposed to hypoxia for varying time lengths before the generation of nuclear extracts. Tyrosine phosphorylation began to reduce at 8h hypoxia with only very low levels visible with reoxygenation (figure 3.28, 2nd panel, lanes 6-7). Serine phosphorylation remained low until 4h hypoxia with reoxygenation and remained stable with 8h hypoxia (+/- reoxygenation) (figure 3.28, upper panel, lanes 5-7).

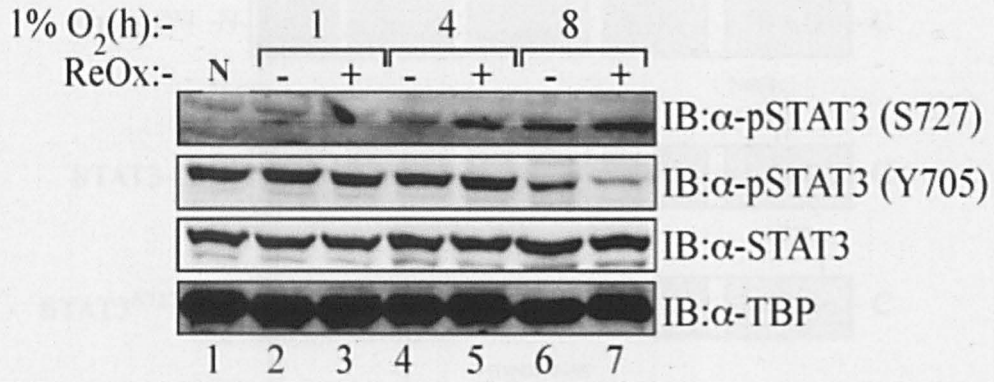

Figure 3.28. Phosphorylation status of STAT3 in P19CL6 passaged 1-4 dilution prior to exposure to hypoxia. P19CL6 were passaged 1-4 one day before exposed to normoxia (N) or hypoxia for indicated times (+) or (-) reoxygenation for 1 hour and nuclear extracts prepared. 100μg of protein for each sample was resolved by denaturing polyacrylamide gel electrophoresis. The resolved proteins were transferred to a PVDF membrane and subjected to western blotting with antibodies indicated. n=1.

The phosphorylation status of STAT3 at Y705 and S727 remained unchanged by the additional passage step.

3.5.2 Exogenous expression of STAT3 protects P19CL6 cells from hypoxia-induced apoptosis

Differentiated P19CL6 cells were transfected with equal amounts (figure 3.29) of $STAT3^{Wt}$ and several STAT3 mutants including STAT3C (hyperactive mutant) (Li and Shaw, 2006), $STAT3^{C3S}$ (a redox-insensitive mutant) (Li et al., 2010) and $STAT3^{S727A}$ (a mutant lacking the serine phosphorylation site) (Wen and Darnell, 1997).

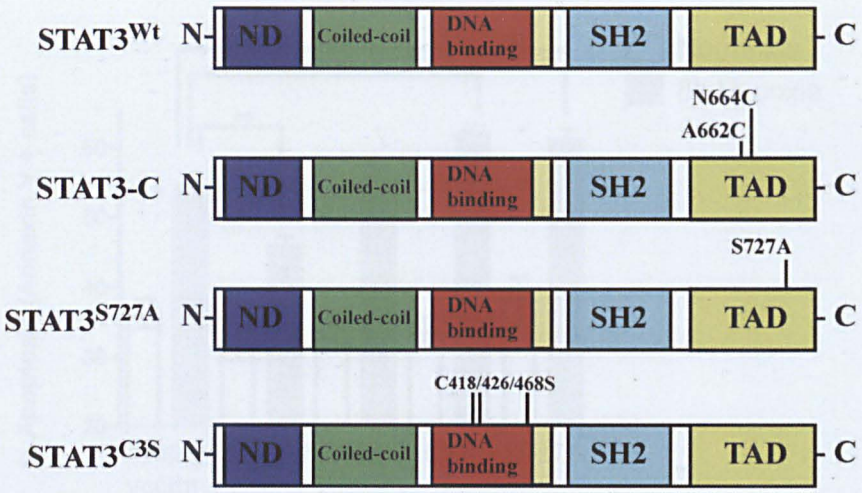

Figure 3.29. Schematic representation of STAT proteins used throughout this study. Mutational changes represented above the appropriate function domains.

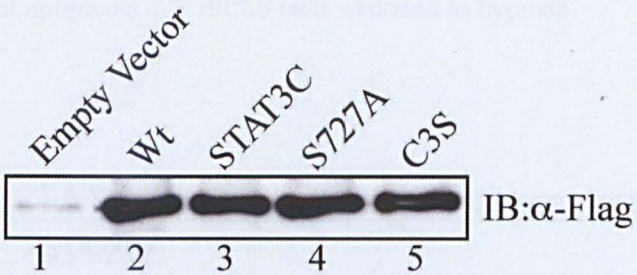

Figure 3.30. Expression of exogenous STAT3 and various mutants. Anti-Flag immuno-precipitates were collected from whole cell extracts prepared from P19Cl6 cells transfected with the indicated STAT3 expression plasmids.

STAT3 expression in P19CL6 cells (figure 3.30) significantly reduced apoptosis induced by hypoxia by approximately by half (figure 3.31), whereas STAT3C a hyperactive mutant of STAT3 had no effect on cell survival during hypoxia. In contrast, expression of $STAT3^{C3S}$ or $STAT3^{S727A}$ increased levels of apoptosis by approximately 20% when compared to mock (figure 3.31). These data indicate that serine phosphorylation and the redox status of STAT3 may be important for cell survival during hypoxia.

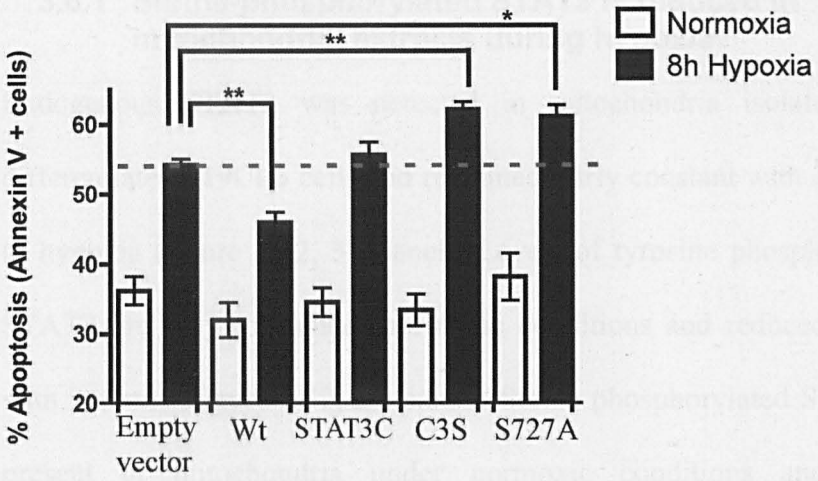

Figure 3.31. Annexin V binding in P19CL6 cells over expressing STAT3 forms before exposure to hypoxia. P19CL6 were transfected with indicated STAT3 expression plasmids before exposure to normoxia or hypoxia for 8h and then subjected to Annexin V binding assay. The stained cells were then sorted using a Coulter Altra Flow Cytometer, set to count 20000 events. n=3, *P < 0.05, **P<0.005. The dotted line indicates general level of apoptosis in P19CL6 cells exposed to hypoxia.

3.6. STAT3 protects mitochondrial respiration during hypoxia

There has been extensive work recently indicating a functional role for STAT3 in the mitochondria. A population of STAT3 is found in the mitochondria and mitochondria from cells lacking STAT3 display defects in oxidative phosphorylation, which can be rescued by exogenous expression of mitochondrial-targeted STAT3 (Wegrzyn et al., 2009).

3.6.1 Serine-phosphorylated STAT3 is reduced in mitochondrial extracts during hypoxia

Endogenous STAT3 was detected in mitochondria isolated from differentiated P19CL6 cells and remained fairly constant with exposure to hypoxia (figure 3.32, 3rd panel). Levels of tyrosine phosphorylated STAT3 are very low under normoxic conditions and reduced further with hypoxia (figure 3.32, 2nd panel). Serine phosphorylated STAT3 is present in mitochondria under normoxic conditions and levels decreased gradually during hypoxia in a time-dependant manner (figure 3.32, 1st panel).

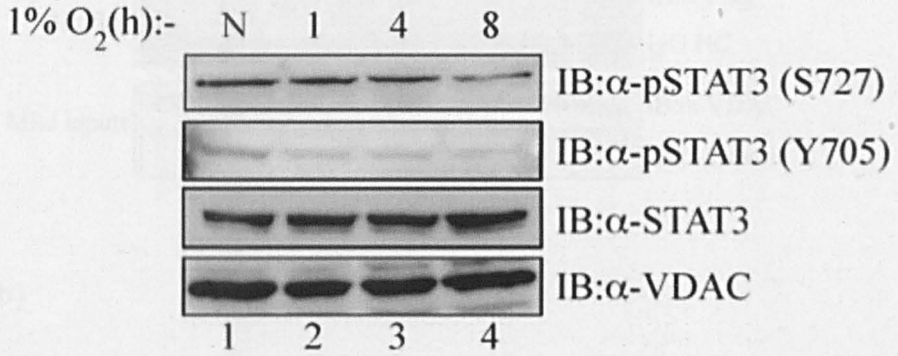

Figure 1.32. Phosphorylation status of STAT3 in mitochondrial extracts following hypoxia. P19CL6 cells were exposed to normoxia (N) or hypoxia for indicated times and mitochondrial extracts prepared. 100µg of protein for each sample was resolved by denaturing polyacrylamide gel electrophoresis, transferred to a PVDF membrane and subjected to western blotting with antibodies indicated. n=2.

3.6.2 Exogenous STAT3 and redox-insensitive mutant are present in mitochondria whereas S727A mutant is not.

$STAT3^{Wt}$, $STAT3^{C3S}$ and $STAT3^{S272A}$ were also exogenously expressed in differentiated P19CL6 cells and their association with mitochondria assessed. Immunoprecipitation assays from isolated mitochondrial

lysates revealed that $STAT3^{Wt}$ associated with mitochondria and levels increased slightly when exposed to hypoxia for 8h (figure 3.33, upper panel, lanes 3 and 4). The redox insensitive $STAT3^{C3S}$ mutant was similarly associated with mitochondria from both normoxic and hypoxic cell lysates (figure 3.33, upper panel, lanes 5 and 6), whereas the serine phosphorylation mutant $STAT3^{S272A}$ was absent in both conditions (figure 3.33, upper panel, lanes 7 and 8).

(a)

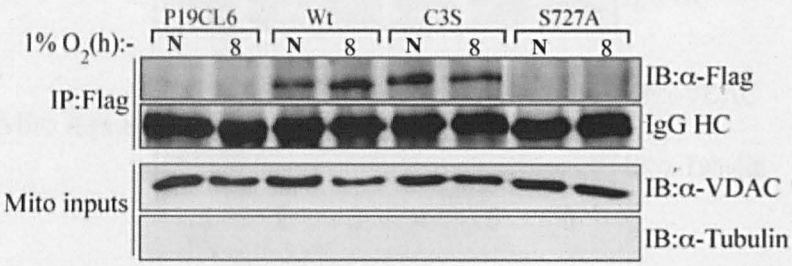

(b)

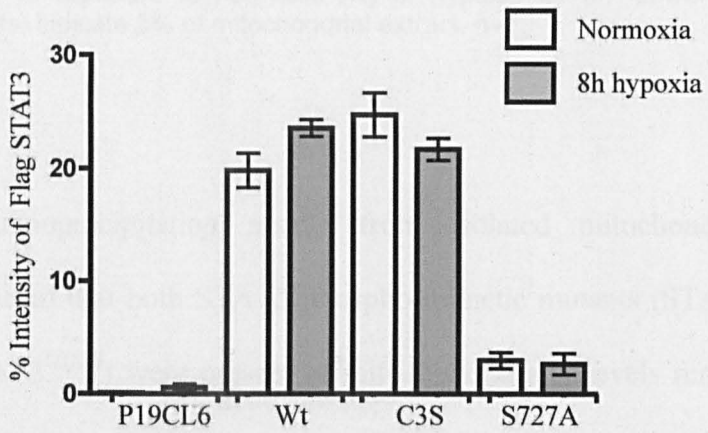

Figure 3.33. Mitochondrial localisation of exogenous STAT3 and mutants during hypoxia. (a) Protein expression was analysed by anti-FLAG immunoprecipitation from mitochondrial extracts (Flag IP – top panels) from P19CL6 cells transfected with STAT3 and various mutants prior to exposure to normoxia (N) or hypoxia for 8h. Middle panels (Mito inputs) indicate 5% of mitochondrial extract. **(b)** Densitometry was performed using AIDA and percentage intensity STAT3. n=3.

The lack of $STAT3^{S272A}$ present in mitochondrial extracts indicates that serine phosphorylation of STAT3 may be required for STAT3 mitochondrial localisation. In order to investigate this further serine phospho-mimetic mutants of STAT3 ($STAT3^{S272D}$ and $STAT3^{S727E}$) were generated using site-directed mutagenesis and their presence in mitochondria assessed by immunoprecipitation assays.

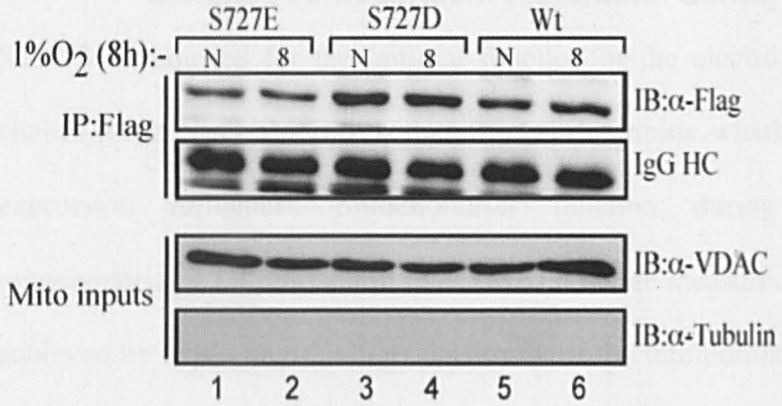

Figure 3.34. Mitochondrial localisation of exogenous STAT3 and phosoho-mimetic during hypoxia. Protein expression was analysed by anti-FLAG immunoprecipitation from mitochondrial extracts (Flag IP – top panels) from P19CL6 cells transfected with STAT3 and phospho-mimetic mutants) prior to exposure to normoxia (N) or hypoxia for 8h. Lower panels (Mito inputs) indicate 5% of mitochondrial extract. n=1.

Immunoprecipitation assays from isolated mitochondrial lysates revealed that both STAT3 phospho-mimetic mutants ($STAT3^{S272D}$ and $SRAT3^{S272E}$) were present in mitochondria and levels remained when exposed to hypoxia for 8h (figure 3.34, upper panel, lanes 1-4). $STAT3^{S727D}$ levels in the mitochondria were higher when compared to $STAT3^{Wt}$ (figure 3.42, upper panel, lanes 3-6). These results indicate that STAT3 serine phosphorylation is important for mitochondrial import. Wegrzyn and colleagues demonstrated that the phospho-

mimetic mutant MLS Stat3 Y705F/S727D reconstituted of complex I/II activities (Wegrzyn et al., 2009). Further investigation is required to see if these serine phospho-mimetic STAT3 mutants offer any protection against hypoxia-induced apoptosis in P19CL6 cells.

3.6.3 Exogenous STAT3 protects mitochondrial complex I/II-dependent respiration during hypoxia

STAT3 is required for the optimal function of the electron transport chain (Wegrzyn et al., 2009); therefore to determine whether STAT3 expression influences mitochondrial function during hypoxia, mitochondrial ATP production rates (MAPR) were measured. This was achieved by exploiting the high sensitivity of the luminometric method based on firefly luciferase. This method measures the rate of ATP production in isolated mitochondria with different respiratory substrate combinations (Wibom et al., 2002).

The activity of complex I (NADH dehydrogenase) was monitored by the addition of glutamate/malate substrate combination. Glutamate and malate are oxidised by mitochondrial enzymes, which in turn feeds NADH into the respiratory chain via complex I.

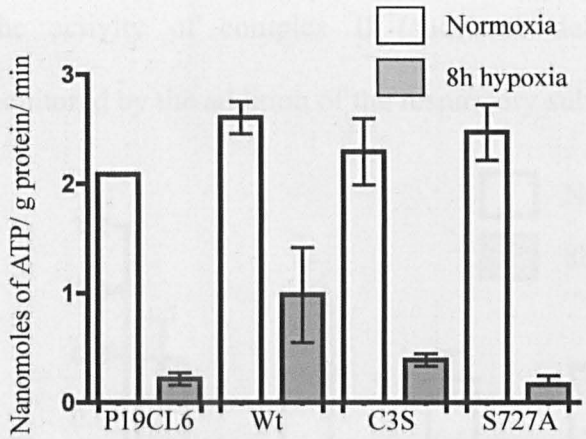

Figure 3.35. Expression of STAT3 may protect glutamate + malate-dependent respiration during hypoxia in P19CL6 cell mitochondria. P19CL6 cells transfected with STAT3 and various mutants (C3S; STAT3C418/426/486S, S727A; STAT3S727A) were exposed to normoxia/hypoxia for 8h and mitochondrial extracts prepared. ATP production was measured for glutamate + malate-dependent respiration. Results normalised to total mitochondrial protein concentration. N=3.

In mitochondria isolated from differentiated, mock-transfected P19CL6 cells, complex I-dependant (glutamate/malate) ATP production was reduced by approximately 85% after 8h hypoxia (figure 3.35). Exogenous expression of STAT3 proteins caused an increase in the overall rate of ATP production under normoxic conditions $STAT3^{Wt}$ and offered slight but insignificant protection against the loss of mitochondrial function from cells after 8h hypoxia (figure 3.35). Additional biological repeats need to be preformed in order to draw any statically significant results from this experiment. The serine phosphorylation mutant $STAT3^{S727}$ and the redox insensitive mutant $STAT3^{C3S}$ failed to protect complex I-dependant respiration against hypoxia (figure 3.35).

The activity of complex II (succinate dehydrogenase) was also monitored by the addition of the respiratory substrate succinate.

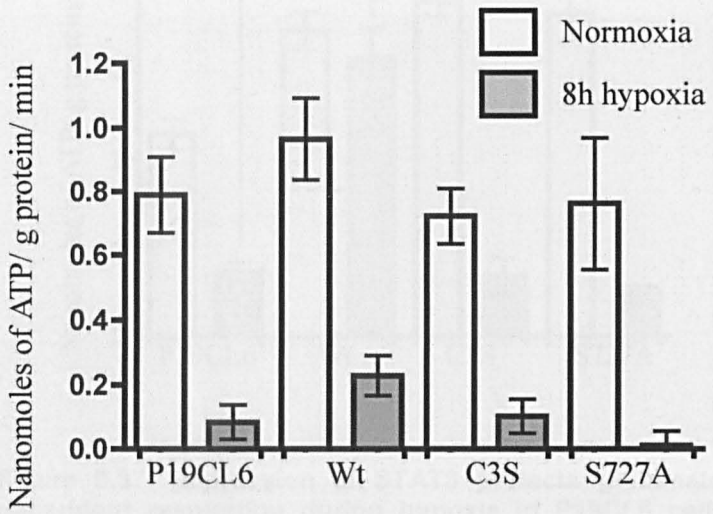

Figure 3.36. Expression of STAT3 may protect succinate-dependent respiration during hypoxia in P19CL6 cell mitochondria. P19CL6 cells transfected with STAT3 and various mutants were exposed to hypoxia for 8h and mitochondrial extracts prepared. ATP production was measured for succinate-dependent respiration. Results normalised to total mitochondrial protein concentration. N=3.

In mock-transfected P19CL6 cells, complex II-dependant (succinate) activity was reduced by approximately 87% after 8h hypoxia (figure 3.36). Exogenous expression of $STAT3^{Wt}$ again offered marginal protection for respiration observed after 8h hypoxia (figure, 3.36). However $STAT3^{S727}$ and $STAT3^{C3S}$ failed to protect respiration during hypoxia (figure 3.36).

In addition, complex I/II activities were measured simultaneously by via the glutamate/succinate respiratory substrate combination.

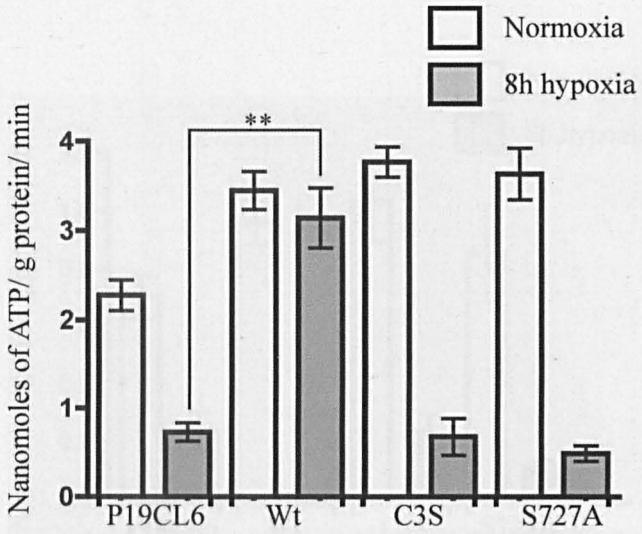

Figure 3.37. Expression of STAT3 protects glutamate + succinate-dependent respiration during hypoxia in P19CL6 cell mitochondria. P19CL6 cells transfected with STAT3 and various mutants were exposed to hypoxia for 8h and mitochondrial extracts prepared. ATP production was measured for glutamate + succinate-dependent respiration. Results normalised to total mitochondrial protein concentration. N=3, **P<0.005.

In mitochondria isolated from differentiated, mock-transfected P19CL6 cells, complex I/II-dependent (glutamate/succinate) ATP production was reduced by approximately 70% after 8h hypoxia (figure 3.37). Exogenous expression of STAT3 caused an increase in the overall rate of ATP production under normoxic conditions and $STAT3^{Wt}$ offered protection against the loss of mitochondrial function from cells after 8h hypoxia with a significant 4-fold increase in ATP production when compared to mock 8h hypoxia sample (figure, 4.37). The $STAT3^{S727}$ and $STAT3^{C3S}$ mutants also failed to rescue complex I/II-dependent ATP production.

As a control the respiratory substrate palmitoyl-L-carnitine/malate combination was used that monitors ATP production via beta-oxidation.

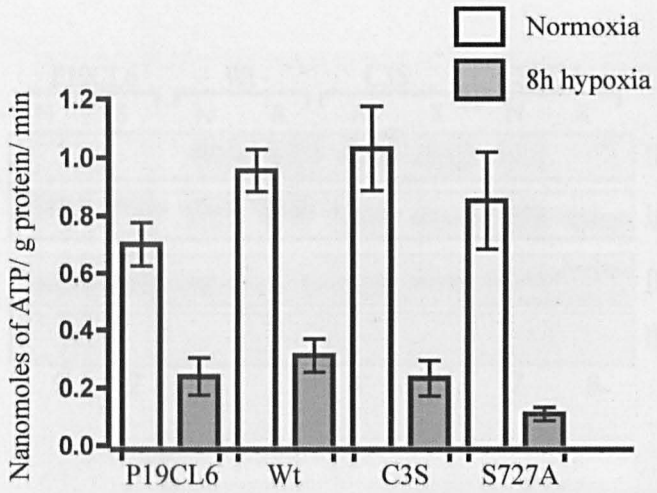

Figure 3.38. Expression of STAT3 does not protect palmitoyl-L-carnitine + malate-dependent respiration during hypoxia in P19CL6 cell mitochondria. P19CL6 cells transfected with STAT3 and various mutants were exposed to hypoxia for 8h and mitochondrial extracts prepared. ATP production was measured for palmitoyl-L-carnitine + malate -dependent respiration. Results normalised to total mitochondrial protein concentration. N=3.

No significant differences were observed mitochondrial ATP production fuelled by palmitoyl-L-carnitine in cells exogenously expressing STAT3 and various mutants (figure 3.38).

Parallel analysis of mitochondrial protein confirmed the presence of $STAT3^{Wt}$ and $STAT3^{C3S}$ in the MAPR assay samples (figure 3.39, upper panel, lane 3-6).

(a)

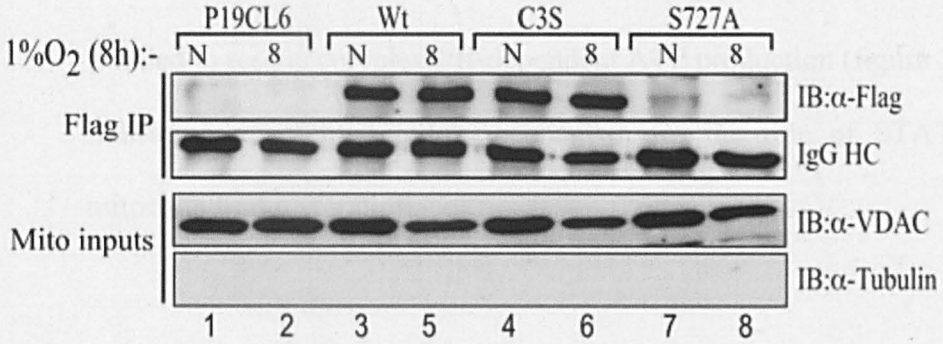

(b)

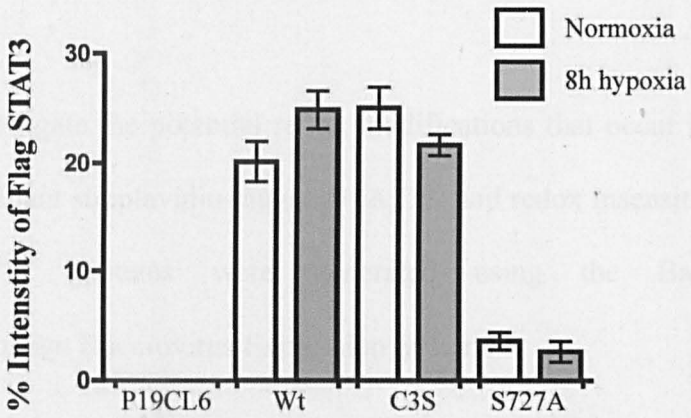

Figure 3.39. Flag-immunoprecipitation of exogenous STAT3 and mutants during hypoxia from ATP assay mitochondrial samples. (a) Protein expression was analysed by anti-FLAG immunoprecipitation from mitochondrial extracts (Flag IP – top panels) generated in the ATP formation assay prior exposure to normoxia (N) or hypoxia for 8h. Lower panels (Mito inputs) indicate 5% of mitochondrial extracts. **(b)** Densitometry was performed using AIDA and percentage intensity of STAT3 determined. n=3.

The serine phosphorylation mutant $STAT3^{S727}$ failed to accumulate in mitochondria (3.39, upper panel, lanes 7-8) under normoxic or hypoxic conditions as anticipated, did not sustain complex I/II-dependent ATP production (figure 3.37), indicating that serine phosphorylation is required for localisation/import into mitochondria in addition to mitochondrial function as previously reported (Wegrzyn et al., 2009).

Even though the redox insensitive mutant $STAT3^{C3S}$ accumulated in the mitochondria as effectively as $STAT3^{Wt}$ (3.39, upper panel, lanes 7-8), it failed to rescue complex I/II-dependent ATP production (figure 3.37), indicating a potential redox mechanism for the role of STAT3 in mitochondrial respiration.

4.7. Generation of recombinant Flag-tagged STAT3 using the baculovirus expression system

To investigate the potential redox modifications that occur in STAT3, recombinant streptavidin-tagged $STAT3^{wt}$ and redox insensitive mutant $STAT3^{C3S}$ proteins were generated using the Bac-to-Bac® Recombinant Baculovirus Expression System.

pFastBac $STAT3^{Wt}$ and $STAT3^{C3S}$ vectors were generated by amplifying a region of STAT3 cDNA sequence (765-2378) from the pRc/cmv $STAT3^{Wt}$/$STAT3^{C3S}$ vectors using the PCR. STAT3 amplified PCR fragments and pFastBac hSTAT3 (kindly provided by Vinkemeier group) were digested with Sph1 before ligating together to generate pFastBac $STAT3^{Wt}$ and pFastBac $STAT3^{C3S}$ vectors. Vectors were subsequently sequenced for verification (section 2.17).

Dh10Bac™ E.Coli competent cells were transformed with the expression cassette pFastBac $STAT3^{Wt}$/$STAT3^{C3S}$, which allowed recombination with the parent bacmid in DH10Bac cells to form an

expression bacmid. The bacmid was then transfected into sf9 insect cells for the production of recombinant baculovirus particles.

3.7.1 Sf9 phenotypic change and reduced cell number indicates viral infection

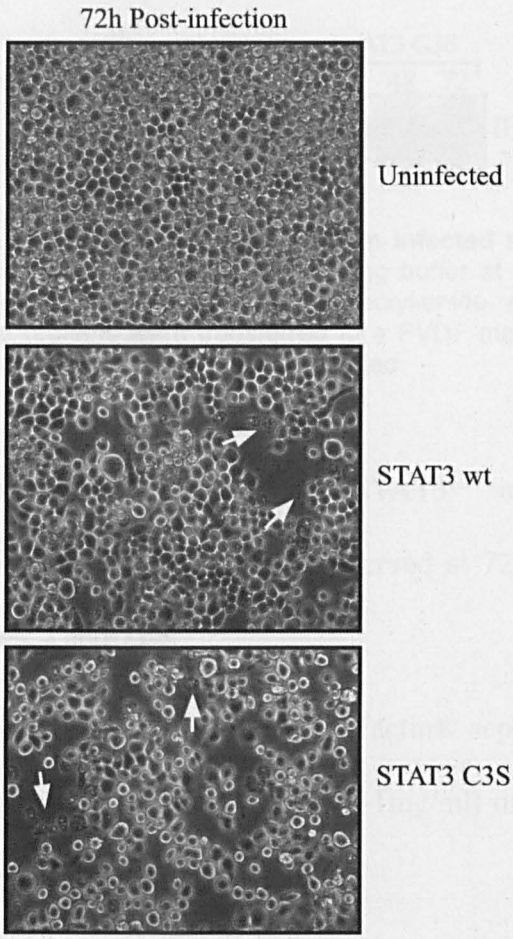

Figure 3.40. Sf9 cell images 72h post-baculovirus infection. Phase images of sf9 cells 72 hours after initial baculovirus infection.

Positive signs of recombinant baculovirus expression are evident by a reduction in cell number and increased areas of cellular debris when compared to uninfected cells 27h post transfection (figure 3.40).

3.7.2 Expression and purification of recombinant STAT3 proteins

In order to verify expression of recombinant STAT3 proteins, sf9 whole cell lysates were prepared after 24, 48 and 72h post infection and subjected to western blot analysis.

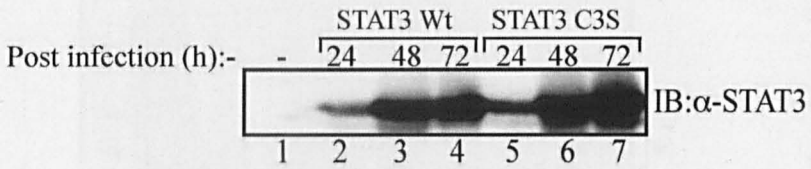

Figure 3.41. STAT3 expression from infected sf9 cells. 10µl of infected sf9 cells were lysed in 1XSDS loading buffer at indicated times. Samples were resolved by denaturing polyacrylamide gel electrophoresis. The resolved proteins were transferred to a PVDF membrane and subjected to western blotting with antibodies indicated.

The expression of $STAT3^{Wt}$ and $STAT3^{C3S}$ increased with infection time, with maximal expression observed at 72h post-infection (figure 3.41, lanes 4 and 7).

Large scale expression and Strep-Tactin® sepharose purification was performed to yield large amounts (~1mg/ml) of recombinant $STAT3^{wt}$ and $STAT^{C3S}$ proteins (figure 3.42).

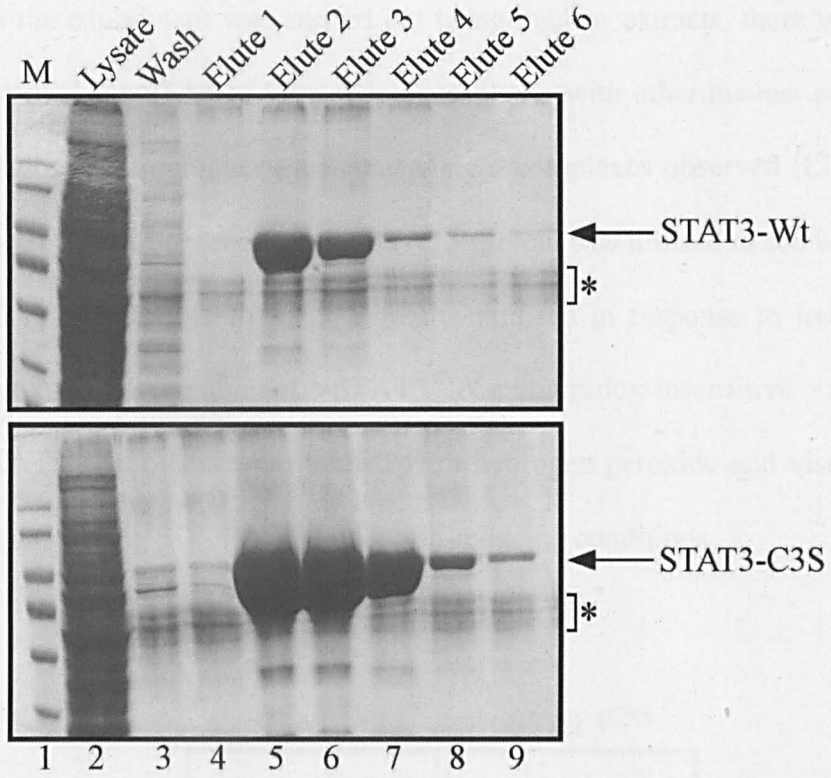

Figure 3.42. Purification of recombinant STAT3 using a strep-Tactin® column. Infected sf9 cells were lysed using a dounce homogeniser. Lysates were loaded onto a Strep-Tactin® column and washed with buffer w before eluting the protein in buffer E (6x 0.5ml fractions). 20µl of each sample was resolved by denaturing polyacrylamide gel electrophoresis and visualised using coomassie blue stain. Black arrow indicates purified STAT3 protein. * Indicates contaminating band present in SDS loading buffer.

3.7.3 Oxidation of recombinant STAT3 proteins

Previous studies relieved that STAT3 is capable of forming higher molecular weight complexes when treated with hydrogen peroxide (Li et al., 2010). Cell extracts treated with hydrogen peroxide were resolved on a polyacrylamide gel under non-reducing conditions and subjected to western blot analysis using a STAT3 antibody. The experiment revealed that STAT3 dimers, trimers and tetramers were formed upon exposure to hydrogen peroxide (Li et al., 2010).

As the experiment was carried out using nuclear extracts, there was the potential for STA3 to form redox complexes with other nuclear proteins resulting in the higher molecular weight complexes observed (Li et al., 2010). Therefore recombinant STAT3 protein was utilised to see whether STAT3 is capable of being directly oxidised in response to hydrogen peroxide. Recombinant $STAT3^{Wt}$ and redox-insensitive mutant $STAT3^{C3S}$ proteins were treated with hydrogen peroxide and visualised by denaturing SDS PAGE under non-reducing conditions.

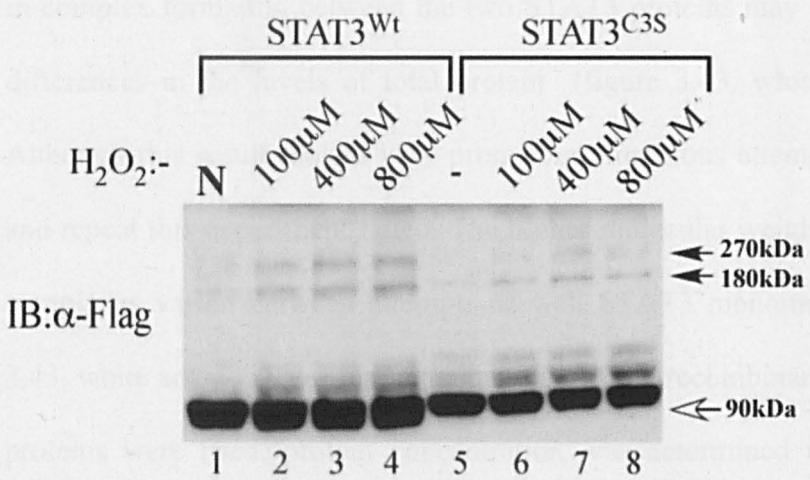

Figure 3.43. Oxidation of recombinant STAT3. Recombinant $STAT3^{Wt}$ and $STAT3^{C3S}$ proteins were exposed normoxia (N) or varying concentrations H_2O_2 for 2 minutes at 37°C. 20μl of each sample was resolved by denaturing polyacrylamide gel electrophoresis under non-denaturing conditions (no β-mercaptoethanol or DTT) The resolved proteins were transferred to a PVDF membrane and subjected to western blotting with antibodies indicated. White arrow indicates STAT3 monomer and the black arrows indicate possible dimers and trimers of STAT3. n=1.

Western blotting analysis revealed that STAT3 is capable of forming higher molecular weight complexes. STAT3 containing species are visible at approximately 180KDa and 270KDa, levels increased with the addition of hydrogen peroxide in a concentration dependent manner

(figure 3.43, black arrows). The recombinant proteins were resolved under denaturing, non-reducing conditions suggesting that these complexes are stablised through disulphide-bridge covalent interactions, consistent with previous findings (Li et al., 2010).

Increased complex formation was observed with $STAT3^{Wt}$ when compared to the redox insensitive STAT3 mutant $STAT3^{C3S}$ exposed to peroxide, indicating the cysteine residues C418, C426 and C468 are sensitive to oxidation and required for the formation of the higher molecular weight STAT3 complexes. However, the difference observed in complex formation between the two STAT3 proteins may be due to differences in the levels of total protein (figure 3.43, white arrow). Although this result looked very promising, numerous attempts to try and repeat this experiment failed. The higher molecular weight STAT3 complexes varied between attempts as well STAT3 monomer (figure 3.43, white arrow). To ensure equal amount of the recombinant STAT3 proteins were used, protein concentration was determined using the Bradford protein assay. Equal protein loading still varied between the two STAT3 recombinant proteins suggesting potential aggregation/precipitation of the proteins. This in turn could affect the proportions of higher molecular complexes observed due to varying amounts of protein being exposed to hydrogen peroxide. Due to time restraints, the direct oxidation of recombinant STAT3 and the redox insensitive mutant still warrants further investigation.

Chapter 4. Discussion

STAT3 participates in a wide variety of seemingly contradictory processes, such as proliferation and apoptosis. Accumulating evidence links STAT3 with normal heart development and numerous studies have shown that STAT3 activation promotes cardiomyocyte survival, suggesting STAT3 is beneficial for the heart. Loss of STAT3 in cardiac tissue has been linked to fibrosis and heart failure in aging mice (Jacoby et al., 2003) and down regulation of STAT3 was observed in myocardial tissue from patients suffering from dilated cardiomyopathy (Podewski et al., 2003). The mechanism underlying the role of STAT3 in cardiac protection has yet to be fully defined and this thesis aimed to investigate this role further. By exploring various cardiomyocyte models this thesis addressed clear differences between cell models for hypoxia-induced apoptosis thus, providing insight into which model is most representative of the diseased heart.

The main aim of this study was to explore the protective role of STAT3 in cardiomyocytes during hypoxia/oxidative stress; this was achieved by stimulating STAT3 activity with LIF and exogenously expressing wt and mutant versions of STAT3 in cardiomyocytes and looking for differences in levels of apoptosis.

There is also accumulating evidence pointing to a protective role for STAT3 in the mitochondria, including cellular respiration (Boengler et al., 2010, Wegrzyn et al., 2009). Therefore to shed further insight on

this work, this study investigated the mitochondrial role of STAT3 during hypoxia/oxidative stress.

4.1 Characterisation of STAT3 activity during hypoxia/reoxygenation

Altered regulation of STAT3 has been reported in human failing hearts. Podewski and colleagues reported that STAT3 expression and phosphorylation were severely reduced in failing hearts (Podewski et al., 2003). This was later supported by the observation that mice with cardiomyocyte-specific disruption of STAT3 developed DCM, heart failure and early death (Jacoby et al., 2003, Hilfiker-Kleiner et al., 2004).

STAT3 is activated by phosphorylation at tyrosine 705. Phospho-tyrosine STATs dimerise and translocate to the nucleus, where they bind to DNA and activate transcription of various genes (Akira et al., 1994, Zhong et al., 1994). Thus, to monitor STAT3 activity during hypoxia/reoxygenation, STAT3 tyrosine phosphorylation and STAT3 DNA binding were measured throughout this study by immunoblotting and EMSA respectively.

In RCMs and H9c2 cells, tyrosine phosphorylation of STAT3 remained detectable when exposed to hypoxia. A slight but reproducible reduction in STAT3 tyrosine phosphorylation was observed at 1h and 24h hypoxia for RCMs (figure 3.1) and 24h for H9c2 (figure 3.5a). Similarly, the DNA binding profile of STAT3 showed a direct

correlation with levels of phospho-tyrosine STAT3 for both RCMs (figure 3.2) and H9c2 cell lines (figure 3.6).

In contrast, reoxygenation of P19CL6 cells after 8h hypoxia displayed a substantial reduction in tyrosine phosphorylation of STAT3, which was completely abolished with exposure to hypoxia for 24h (figure 3.7a). The DNA binding activity of STAT3 was also more sensitive to hypoxia when compared to RCM and H9c2 cell lines, with complete loss of STAT3 DNA binding with 8h hypoxia, even though tyrosine phosphorylation was still detectable (figure 3.8).

The ratio between activated kinases and inactivated phosphatases could explain why STAT3 tyrosine phosphorylation and ultimately STAT3 DNA binding is maintained during long periods of hypoxia-induced oxidative stress in RCM and H9c2 cell lines. STAT3 activity is required by a variety of processes during of mild hypoxia including tumourigenesis and angiogenesis (Kang et al., 2010). Studies have shown that hypoxia markedly augmented phosphorylation and activation of JAKS (JAK1, JAK2 and JAK3) and their substrates, STATs (STAT3 and STAT5) in lung microvascular endothelial cells (Wang et al., 2008). In addition, ROS has been implicated in the activation of the JAK/STAT pathway, in which H_2O_2 treatment was shown to stimulate the activity of JAK2 and TYK2 (Simon et al., 1998).

The inactivation of protein tyrosine phosphatases (PTPs) is also associated with oxidative stress. PTPs contain cysteine residues in their catalytic site and ROS-mediated oxidation of these cysteine residues

results in their inactivation. Meng and colleagues demonstrated that multiple PTPs were reversibly oxidised and inactivated in Rat-1 cells following treatment with H_2O_2 (Meng et al., 2002). More recently, the catalytic pan-PTP and SHP-2 activities were dramatically reduced from samples taken from *ex vivo* langendorff-model of rat heart ischaemia/reperfusion (Sandin et al., 2011).

Therefore a balance between kinase activation and PTP inactivation would allow levels of tyrosine-phosphorylated STAT3 and ultimately STAT3 DNA binding activities to be effectively maintained during prolonged exposures to hypoxia in RCM and H9c2 cells. To validate this hypothesis further investigation is required. Kinase inhibitors such as AG490, (a potent inhibitor for JAK2 and JAK3) could be utilised to determine whether STAT3 tyrosine phosphorylation and DNA binding would be disrupted during hypoxia-induced oxidative stress. However, the balance between active kinases and inactivation of phosphatases does not explain the loss of STAT3 DNA-binding 8h hypoxia in P19CL6 cells, even though STAT3 tyrosine phosphorylation is still detectable – another mechanism must be in operation.

In theory, one reason for the dissonance between tyrosine phosphorylation and DNA binding could be direct oxidation of STAT3 by ROS. It is important for proteins to maintain a proper structure to perform their biological functions. This 'proper' structure may be altered if proteins become oxidised during oxidative stress. Oxidation of redox elements (mainly cysteine residues) will generate sulphoxides, sulphenic acids and disulphide bridges within the protein, this will

result in changes in secondary and tertiary structure, which may affect the stability of DNA binding.

Redox sensitive cysteine residues have been reported in the DNA binding domain of many transcription factors. For example, cysteine residues are found in the basic region of c-myb (Guehmann et al., 1992), the leucine zipper of AP-1 (Abate et al., 1990) and the zinc-finger motif of the glucocorticoid receptor (Hutchison et al., 1991). Tolendano and colleagues demonstrated that *in vitro* DNA binding of NF-κB could be inhibited by oxidative stress (Toledano and Leonard, 1991). The transcription factor GA-binding protein (GABP) has also been implicated in redox regulation. *In vitro* and *in vivo* studies have show that oxidative conditions result in inhibition of DNA binding through COOH-terminal cysteine residues in the GABPα subunit (Martin et al., 1996).

DNA binding of STAT3 also appears to be regulated by oxidative stress. Studies have shown that *in vivo* DNA binding of STAT3 to the hepcidin promoter is diminished by hypoxia-induced oxidative stress and such a DNA binding decrease can be rescued with the addition of antioxidants (Choi et al., 2007). More recently, we have demonstrated that the DNA binding properties of STAT3 are sensitive to treatment with hydrogen peroxide (Li et al., 2010). Also in this study, mutational analysis revealed three redox-sensitive cysteine residues (Cys418, Cys426 and Cys468) present in the DNA binding domain of STAT3. Substituting these cysteines for serine residues protected DNA binding during oxidative stress (Li et al., 2010).

Studies have shown that DNA-binding STAT protects proteins from dephosphorylation by phosphatases. DNA-bound STAT1 has been shown to be protected from dephosphorylation by phosphatases (Meyer et al., 2003) and also the STAT3 constitutively active mutant STAT3C, displays higher affinities for DNA with delayed dephosphorylation rates by nuclear phosphatases (Li and Shaw, 2006).

During hypoxia-induced oxidative stress, it is feasible that redox modifications occur to cysteine residues within the DNA binding domain of STAT3. Modifications may alter the tertiary structure of STAT3 and in turn reduce its affinity for DNA, resulting in loss of STAT3 DNA binding. Once STAT3 possesses a weaker affinity for DNA, it may become more susceptible to dephosphorylation via phosphatases – explaining the loss of DNA binding before the subsequent reduction in tyrosine phosphorylation. The protein phosphatase SHP-2 (Src-homolgy-2 domain-containing protein 2) has been shown to dephosphorylate STAT3. In rat astrocytes, SHP-2 has been shown to form a complex with STAT3 and reduce the steady state STAT3 tyrosine phosphorylation when exposed to oxidative stress (Park et al., 2009). However, a redox modification of STAT3 many be questioned as the reducing agent DTT (5mM) did not rescue STAT3 DNA binding at 8h hypoxia (figure 3.24). The addition of DTT has been shown to be required for optimal STAT3 *in vitro* DNA binding (Li et al., 2010), therefore it may be possible that P19CL6 cells have different buffer capacities and higher concentrations of reducing agents are required.

In addition, this study also revealed that serine-phosphorylated STAT3 is significantly increased in P19Cl6 cells with 8h hypoxia (figure 3.16). Studies have shown that STAT3 is serine-phosphorylated by ERK2. Serine phosphorylation is also associated with a reduction in DNA binding activity and lower tyrosine-phosphorylated STAT3 levels (Jain et al., 1998). Therefore the loss of STAT3 DNA binding could be associated with the elevated levels of serine-phosphorylated STAT3 observed at 8h hypoxia in P19CL6 cells (discussed later).

4.2 Hypoxia-induced apoptosis of cardiomyocytes

The severity of hypoxia determines whether cells become apoptotic or adapt to hypoxia and survive. RCM and H9c2 cells are resistant to hypoxia-induced oxidative stress and only a slight but significant increase in levels of apoptosis were observed in H9c2 cells exposed to reoxygenation after 24h hypoxia (figure 3.10). However, on the other hand, P19CL6 cells were extremely sensitive to hypoxia-induced oxidative stress, showing ~50% increase over normoxia level of apoptosis when exposed to hypoxia for only 8h (figure 3.12). This clearly demonstrated differences in apoptotic-sensitivity during hypoxia in the different cell models.

A wealth of evidence documents that STAT3 is involved in cell survival. One mechanism is its ability to drive expression of anti-apoptotic factors, including Mcl-1 (Epling-Burnette et al., 2001). The rapid loss of STAT3 activity in P19CL6 cells following hypoxia could

be responsible for the observed reduction in Mcl-1 protein levels (figure 3.13). Down regulation of *Mcl-1* is thought to be required for Bax translocation to mitochondria and cytochrome c release - events indicative of apoptosis (Nijhawan et al., 2003).

There are substantial differences in the sensitively to hypoxia-induced apoptosis between RCM and H9c2 cells compared to P19CL6 cells. One possible reason for this could be due to species differences (Houweling et al., 2005). RCM and H9c2 cells are both of rat origin, whereas P19CL6 cells are mouse. Phenotypic variations between species may account for the differences observed in hypoxia sensitivity throughout this study. This is unlikely to be the sole reason as it has been reported that cardiac function is highly conserved between species and both rat and mouse models are highly comparable with human development and pathology (Houweling et al., 2005).

The differences in sensitivity to hypoxia between cell lines could be due to the relative age of the cells. Increased incidence of apoptosis had been reported in several tissues during aging. For example, the aging-associated atrophy of muscle – sarcopenia. Studies on sarcopenia in rodents have identified an apoptotic-like mechanism characterised by mitochondrial changes and caspase-independence (Marzetti et al., 2009). More recent studies have shown that aging increases myocardial ischaemia/reperfusion-induced apoptosis(Liu et al., 2011). Young (2 months) and old (24 months) rats were subjected to I/R injury followed by TUNEL staining and caspase activity measurements. The results revealed a higher myocardial apoptotic ratio in the older rat group. This

study was validated in humans as elderly patients manifested decreased cardiac function and increased plasma apoptotic markers (soluble form of Fas and TNF-α) when compared to adult patients (Liu et al., 2011).

Pl9CL6 cells were isolated from the P19 mouse embryonal carcinoma cell line through an extensive 6 months selection process (Habara-Ohkubo, 1996), followed by a 16-day differentiation step. Therefore, P19CL6 cells were cultured significantly longer than RCMs or H9c2 cells. RCMs were isolated directly from neonatal rat hearts and not passaged while, H9c2 cells were obtained from ATCC at passage 12 and were not passaged more than 10 times during this study.

Throughout this study RCM and H9c2 cells have been resistant to hypoxia-induced apoptosis. Consistent with this observation, studies have also shown that neonatal rat ventricular myocytes (NRVMs) possess an apoptotic-resistance that acts as a cytoprotective mechanism against stress-induced injury (Lu et al., 2008). In addition, Bonavita and colleagues demonstrated that hypoxia alone did not induce apoptosis in H9c2 cells for at least 48h (Bonavita et al., 2003).

Expression profiles in aged hearts indicate decreased cellular adaptation and protection against stress-induced injury together with the development of contractile dysfunction (Bodyak et al., 2002). Aging expression profiles for the cardiac cell line models would reveal whether or not the age of the cells contributes to the differences observed in hypoxia-induced apoptosis. Recently, Ding and colleagues set out to identify novel biomarkers of normal aging in male mice from 2-19 months of age (Ding and Kopchick, 2011). They identified several

proteins that were significantly increased (transthyretin and haptoglobin) and a number of proteins that were significantly decreased (peroxiredoxin-2 and serum amyloid protein A-1) during aging (Ding and Kopchick, 2011).

Regulated ROS production can modulate intracellular signaling pathways, which have been associated with growth of cardiac myocytes (Siwik et al., 1999) and ischaemic preconditioning (Vanden Hoek et al., 1998), both of which increase the ability of cardiac myocytes to survive oxidative stress. It could be feasible that RCMs and H9c2 cells have different tolerations to ROS during times of oxidative stress when compared to P19CL6 cells. Differences in the concentrations of ROS generated could be due to variations in levels of antioxidant enzymes and free radical scavengers between the different cell lines. Indeed, studies on other cell lines have shown that HepG2 cells are extremely resistant to hydrogen peroxide treatment when compared to BR293 and MCF-7 cells (Chua et al., 2009, Sekiya et al., 2008). The level of ROS production during hypoxia was not measured in this study however, warrants further investigation. Chemiluminescence-based techniques could be utilised to measure ROS production in the different cardiac cell lines exposed to hypoxia. On exposure to ROS a chemiluminescent probe releases a photon, which in turn can be detected and measured by a luminometer.

Given that IHD is typically a disease of old age, as it takes many years for fat deposition to restrict the coronary arteries, it may have been more appropriate to use an adult rat cardiomyocytes model to study the

pathological stresses associated with IHD. However, adult RCMs are difficult to isolate and have sensitive culture conditions when compared to neonatal RCMs. In particular, studies have shown that adult RCMs are extremely sensitive to $Ca2^{+}$ levels and an increase in $Ca2^{+}$ is associated with a reduction in membrane permeability and myocardial damage (Zimmerman and Hulsmann, 1966). P19CL6 may reflect a phenotype representative on an aging cardiomyocyte, which have a reduced ability to adapt to hypoxic stress and hence enhanced levels of ROS and ultimately apoptosis. This would agree with studies that demonstrate that aging cardiomyocytes have a reduced ability to adapt to pathological conditions such as myocardial ischaemia, which is displayed in an aging diseased heart (Takahashi et al., 1992, Liu et al., 2011).

P19CL6 cells are able to differentiate into a beating phenotype that is reminiscent of cardiomyocytes upon exposure to DMSO (Habara-Ohkubo, 1996). Khodadadi and colleagues demonstrated that differentiated P19CL6 cells exhibit some markers of a cardiac phenotype (a-MHC, b-MHC) and the beating phenotype is positively responsive to adrenaline (Khodadadi, 2010). However, closer examination revealed a mixed, cardiac/skeletal muscle phenotype questioning the role of P19CL6 cells as a cardiac cell model (Khodadadi, 2010).

Embryonic and neonatal rat cardiomyocytes have been extensively used models to study cardiac biology (Hescheler et al., 1999, van der Heyden and Defize, 2003, Chlopcikova et al., 2001), however their use

may be limited due to the lack of some adult cardiomyocyte characteristics (Khodadadi, 2010). In addition, isolated primary cardiomyocytes become overgrown by non-moyoctyes after a few days in culture, they cease to divide after the neonatal period and genetic manipulation is extremely difficult (Claycomb, 1985). Another potential cell line that could be considered in this study is the HL-1 cell line, which is derived from atrial cardiomyocyte AT-1 cells. HL-1 cells can be serially passaged while maintaining a differentiated phenotype (Claycomb et al., 1998). HL-1 cardiomyocytes have been characterised and show highly organised sarcomeres (necessary for mediating contraction) and gene expression analysis reveals HL-1 cells exhibit an adult cardiomyocyte-like phenotype expression profile (Claycomb et al., 1998). In addition, the angiotensin/STAT3 pathway has been shown to be important the atrial myocardium (Tsai et al., 2008) implicating further potential roles of STAT3 in this cardiac cell line.

Further investigation is required for determining the appropriate cardiac cell model for studying the role of STAT3 in cardiomyocytes during hypoxia-induced apoptosis. H9c2 and RCMs have been shown to be relatively resistant to hypoxia-induced apoptosis in this study and previous work (Lu et al., 2008)((Bonavita et al., 2003) therefore not effective cardiac cell models for investigation STAT3 and its role during hypoxia-induced apoptosis. P19CL6 are indeed extremely sensitive to hypoxia-induced apoptosis, therefore providing an excellent cell model for the investigation the mechanisms of apoptosis. However there are doubts to whether these cells represent a true adult-

cardiomyocyte cell model (Khodadadi, 2010). Future studies looking at the role of STAT3 during hypoxia-induced apoptosis should be considered in a more appropriate cardiac cell model, potentially the HL-1 cell line.

4.3 The role of PKC in cardiomyocytes during hypoxia

In addition to tyrosine phosphorylation, several STATs are phosphorylated on a serine residue (S727 in STAT3) in their carboxyl-terminal domain, which was initially reported to be important for transcriptional activation (Wen et al., 1995, Zhang et al., 1995). Unlike tyrosine phosphorylation, the functional significance of serine phosphorylation of STAT3 remains controversial. Depending on the cell type and the extracellular stimulus, serine phosphorylation can either enhance or suppress the transcriptional activity of phosphorylated STAT3 (Chung et al., 1997b, Jain et al., 1998, Yokogami et al., 2000).

This study shows that serine phosphorylation of STAT3 increases in P19CL6 cells exposed to 8h hypoxia (figure 3.16a, lane 4). An increase in serine phosphorylation is due to a shift in balance between inactive protein phosphatases and active protein kinases.

Protein phosphatase 2A (PP2A) has been shown to have a direct effect the regulation of STAT3. Woetmann and colleagues demonstrated that PP2A inhibitors cause the serine phosphorylation of STAT3, inhibition

of tyrosine phosphorylation, loss of DNA binding activity and translocation of STAT3 from the nucleus to the cytoplasm (Woetmann et al., 1999). This supports observations in this thesis by which an increase in STAT3 serine phosphorylation (figure 3.16a, lane 4) is accompanied by a loss in STAT3 DNA binding (figure 3.8, lane 4) and subsequent reduction in tyrosine phosphorylation (figure 3.7a, lane 4). This suggests that PP2A inactivation may be responsible for the accumulation of serine-phosphorylated STAT3 observed. Indeed, studies have shown that PP2A is susceptible to reversible inhibitory modification by thiol-disulphide exchange, indicating that PP2A is a redox-sensitive protein phosphatase (Foley and Kintner, 2005). Further investigation is required to determine whether PP2A is inactivated in P19CL6 cells during hypoxia-induced oxidative stress and is responsible for the increase in serine-phosphorylated STAT3.

Another possible explanation for the increase in serine phosphorylation of STAT3 observed in P19CL6 cells exposed to hypoxia could be due to the activation of STAT3 serine kinases. Serine phosphorylation of STAT3 is mediated by several kinases. However, this study focused on the serine/threonine kinase PKCδ due to the accumulating evidence associating this protein with apoptosis (Hahn et al., 2002, Inagaki et al., 2003, Clavijo et al., 2007). PKCδ activation has been documented to be crucial in cardiac pathology such as hypertrophy, heart failure and I/R injury (Hahn et al., 2002, Inagaki et al., 2003). A study has shown that prolonged exposure to hypoxia causes the proteolytic and feed-forward activation of PKCδ and caspase-3, resulting in the irreversible

commitment to apoptosis (Clavijo et al., 2007). In addition, PKCδ is described as a proapoptotic kinase due to the fact it is activated by oxidative stress and promotes apoptosis (Kanthasamy et al., 2003).

There is a potential positive correlation between PKCδ activity and serine-phosphorylated STAT3 during hypoxia in P19CL6 cells. The phosphorylation of PKCδ peaked at 4h hypoxia (figure 3.18) with an elevation in STAT3 serine phosphorylation with 8h hypoxia (figure 3.16), which, accompanied the loss of DNA binding (figure 3.8) and increased levels of apoptosis (4h hypoxia) (figure 3.12). However further experiments will need to be carried out to include the serine phosphorylation status of STAT3 and it's DNA binding abilities at 4h hypoxia in order to effectively correlate with PKCδ activation. A study in HepG2 cells and other cell lines stimulated with IL-6, where PKCδ was shown to physically interact with STAT3 resulting in elevated levels of serine-phosphorylated STAT3, which in turn suppressed STAT3 DNA binding to the SIE (Jain et al., 1999). However the data presented in this study shows only circumstantial evidence linking increased PKCδ activity to the elevation of serine-phosphorylated STAT3 in P19CL6 cells during hypoxia. To try and establish whether PKCδ is the kinase responsible for phosphorylating STAT3 during hypoxia-induced oxidative stress, the PKCδ inhibitor, and rottlerin was utilised in this study. The addition of rottlerin did in fact abolish the levels of STAT3 serine phosphorylation previously observed with 8h hypoxia (figure 3.20), but levels of apoptosis were significantly enhanced, even under normoxic conditions (figure 3.21). Studies have

shown that using rottlerin is not be suitable as a selective inhibitor of PKCδ due to its potent mitochondrial uncoupling and K^+ channel activating properties (Soltoff, 2007). Due to these findings the data generated (figure 3.20 and figure 3.21) in this thesis that uses the inhibitor rottlerin cannot be interpreted efficiently due to its wide spread application with other cellular targets (Soltoff, 2007). However research articles using rottlerin as a specific PKCδ inhibitor are currently still being published (Wallerstedt et al., 2010, Matta et al., 2011).

The use of inhibitors to identify targets of specific PKC isoforms is fraught with difficulty. A number of PKC inhibitors exist however some have broad specificity and additional cellular targets. For example, Gö 6983 (bisindolylmaleimide) is a fast acting, lipid soluble, broad-spectrum protein kinase C inhibitor (α, β, γ, δ, ζ). A study has shown that when the inhibitor is administered at the beginning of reperfusion, it can restore cardiac function within 5 min and attenuate the deleterious effects associated with acute ischemia/reperfusion (Young et al., 2005). Chelerythrine has also been used as a PKC inhibitor and a study demonstrated that chelerythrine suppressed the translocation of PKCδ and PKCε to the membrane and blocked the improvement of cardiac function and ATP generation (Xu et al., 2004). However chelerythrine is known to inhibit an additional cellular target - Bcl_{XL}. Chan and colleagues suggested that chelerythrine triggers apoptosis through a mechanism that involves direct inhibition of Bcl-2 family proteins (Chan et al., 2003b).

Additional experiments will be required to validate the correlation observed between PKCδ and STAT3. Investigating the biochemical interactions between STAT3 and PKCδ and generating PKCδ knockdown experiments would give a clearer insight to whether PKCδ is responsible for STAT3 serine phosphorylation and contributes to cell death during hypoxia. Preliminary immunoprecipitation experiments have revealed that STAT3 and PKCδ do interact in P19CL6 cells and this interaction is marginally increased during hypoxia (unpublished data). These data so far implicates PKCδ as a kinase that is capable of serine--phosphorylating STAT3 in P19CL6 cells during hypoxia however; phosphorylation by other kinases has not been ruled out.

4.4 Elevated STAT3 activity protects P19CL6 against hypoxia-induced apoptosis

Persistent activation of STAT3 is frequently associated with malignant transformation and it is established that constitutively active STAT3 is one of the molecular abnormalities in oncogenesis (Turkson, 2004). In contrast to its negative effects in malignant transformation, studies have shown that continual activation of STAT3 offers cardioprotection. For example, the over expression of STAT3 in the heart protects from doxorubicin-induced cardiomyopathy – an adverse side effect of the chemotherapy drug doxorubicin (Kunisada et al., 2000).

To establish whether promoting STAT3 activity could contribute to P19CL6 cell survival during prolonged hypoxia, apoptosis was

monitored after pre-treatment with LIF – a cytokine that stimulates STAT3 activity in these cells (van Puijenbroek et al., 1999). Stimulation of P19CL6 cells with LIF increased tyrosine phosphorylation of STAT3 in both normoxic and hypoxic cells (figure 3.23a). In addition, STAT3 DNA binding was substantially enhanced in LIF treated cells and residual binding was still detectable after 8h hypoxia (figure 3.24). Importantly, stimulation of STAT3 activity with LIF was associated with reduced levels of apoptosis in P19CL6 cells after 8h hypoxia (figure 3.25). This data is consistent with studies suggesting that LIF may promote survival of cardiomyocytes and regeneration of the myocardium. Zou and colleagues demonstrated that LIF protected cardiomyocytes from death and enhanced neovascularisation after myocardial infarction (Zou et al., 2003).

The protective effects of LIF observed in P19CL6 cells during hypoxia could be due to enhanced expression of STAT3 target genes, as residual DNA binding was still detectable after 8h hypoxia (figure 3.24). Indeed, expression of Mcl-1 was still apparent in P19CL6 pre-treated with LIF even after 8h hypoxia (figure 3.26). Equally, LIF stimulation may offer protection via a non-transcriptional route. It was noted in this study that not only did LIF treatment stimulate tyrosine phosphorylation of STAT3 but also the phosphorylation of serine 727 (figure 3.23a). In addition to accumulating evidence suggesting that serine phosphorylation of STAT3 is associated with transcriptional suppression (Jain et al., 1998, Jain et al., 1999) it is also required for functional mitochondrial respiration (Wegrzyn et al., 2009). Therefore

under hypoxic conditions, LIF stimulation may in fact direct STAT3 from the nucleus to the mitochondria where it is able to maintain mitochondrial function during hypoxia-induced oxidative stress.

4.5 Exogenous expression of STAT3 in cardiomyocytes

The role of STAT3 in cardiomyocyte survival following hypoxia was addressed through exogenous expression of STAT3 and several mutants. STAT3 over-expression significantly reduced apoptosis, whereas STAT3C a constitutively active mutant of STAT3 had no significant effect on cell survival under hypoxia. As discussed earlier, STAT3C possesses higher DNA binding affinity when compared to $STAT3^{Wt}$ (Li and Shaw, 2006). If the protective role of STAT3 during hypoxia is indeed associated with mitochondrial respiration, then increased DNA binding affinities would reduce the latent pool of STAT3 available for the mitochondria, causing a reduction in mitochondrial function and in turn increased levels of apoptosis. In addition, exogenous expression of the serine phosphorylation mutant $STAT3^{S727}$ and the redox-insensitive mutant $STAT3^{C3S}$ also increased levels of apoptosis in P19CL6 cells. This indicates that serine phosphorylation and redox modification of STAT3 may both contribute to the protective roles of STAT3 in cardiomyocytes during hypoxia through mechanisms involving mitochondrial function, which is discussed later.

4.6 STAT3 protects mitochondrial respiration during hypoxia

Loss of mitochondrial integrity is central to the initiation of apoptosis. Although STAT3 has not been directly implicated in this process, defects in mitochondrial respiration have been reported. Mitochondria isolated from STAT3-deficient cells show impaired respiratory function of complexes I/II of the ETC and exogenously expressing STAT3 targeted to the mitochondria was shown to rescue respiration (Wegrzyn et al., 2009). In this thesis, the role of STAT3 in mitochondrial ATP production during hypoxia was accessed by exogenously expressing STAT3 and various mutants. Measuring mitochondrial ATP production would give an insight to the functional activities of the ETC during hypoxia and depending on the substrate used, focus on a particular complex of the ETC. In mock-transfected P19CL6 cells, mitochondrial ATP production was abolished during hypoxia. However, expressing $STAT3^{Wt}$ maintained the mitochondria's ability to produce complex I/II dependant ATP post hypoxia (figure 3.37), which in turn accompanied reduced levels of apoptosis (figure 3.31). Interestingly the redox-insensitive $STAT3^{C3S}$ mutant, although imported into the mitochondria, failed to rescue ATP production (figure 3.37) or offer protection to P19CL6 cells under hypoxia (figure 3.31). This indicates that redox modulation of STAT3 is involved in this protective mechanism. This supports a previous publication that demonstrated that breast carcinoma cells expressing $STAT3^{C3S}$ were more sensitive to oxidative stress when compared to $STAT3^{Wt}$ counterparts (Li et al., 2010). The serine

phosphorylation mutant $STAT3^{S727A}$ also failed to rescue ATP production during hypoxia, consistent with previous findings (Wegrzyn et al., 2009). However, unlike Wegrzyn and colleagues who used a mitochondrial-targeted $STAT3^{S727}$ mutant, this study revealed that serine phosphorylation of STAT3 may be required for mitochondrial import/retention in addition to an intra-mitochondrial function. Phospho-mimetic versions of STAT3 ($STAT3^{S727D}$ and $STAT3^{S272E}$) have also been over expressed in P19CL6 cells. $STAT3^{S727D}$ and to a lesser extent $STAT3^{S272E}$ are detected in mitochondrial extracts under both normoxic and hypoxic conditions (figure 3.34), further validating that the serine phosphorylation of STAT3 is required for import into the mitochondrial. Experiments investigating levels of apoptosis and mitochondrial ATP production in response to these phospho-mimetic mutants have yet to be completed.

It still remains unclear how STAT3, which lacks a putative mitochondrial import signal, can be translocated into mitochondria. It may be possible that STAT3 is able to interact and bind to other mitochondrial proteins to aid its translocation. Recent studies have shown that serine phosphorylated STAT3 highly co-localises with GRIM-19, a known STAT3 binding partner and component of the mitochondrial electron transport complex I (Zhou and Too, 2011). In addition, studies have also shown that the serine phosphorylation status of a protein may enhance its translocation to the mitochondria. Robin and colleagues demonstrated using *in vivo* and *in vitro* systems, that the mitochondrial targeting of GSTA4-4, an isoform of glutathione S-

transferase (GST) is highly dependent on the phosphorylation status of the protein. They suggest that phosphorylation increases the affinity of the protein for binding to cytoplasmic chaperone Hsp70 as a possible basis for its enhanced mitochondrial targeting (Robin et al., 2003).

Another chaperone, Hsp90 has also been implicated in cellular protection during oxidative stress. Hsp90 has a mitochondrially-localised paralogue, TRAP1 that offers protection against oxidative stress (Pridgeon et al., 2007). Kang and colleagues reported that mitochondria isolated from a panel of tumour cell lines express markedly higher levels of TRAP1 and Hsp90 when compared to normal tissues and that mitochondrial specific inhibitors of TRAP1 (Hsp90 ATPase antagonists) caused a sudden collapse in mitochondrial integrity and apoptosis in selective tumours (Kang et al., 2007). Sano and colleagues have reported a direct interaction between STAT3 and Hsp90. Immunoprecipitation assays demonstrated that Hsp90 directly binds to STAT3 via its N-terminal region (Sato et al., 2003). Interestingly, recent studies have shown that STAT3 and Hsp90 interact upon stimulation with LIF in cultured mouse embryonic stem (mES) (Setati et al., 2010), yielding a possible explanation to the cardioprotective effects observed in this study when P19CL6 cells pre-treated with LIF were exposed to hypoxia. The mitochondrial function of STAT3 has also been linked to another heat shock protein, H11 kinase/Hsp22 (Hsp22). Qiu and colleagues demonstrated that mitochondrial STAT3 translocation and respiration were significantly impaired in Hps22 knockout mice and these mice experienced

accelerated heart failure in response to pressure overload (Qiu et al., 2011). The potential interaction of STAT3 with various chaperones and their roles in mitochondrial function during oxidative stress warrants further investigation.

Results from this study and previous publications have led to a proposed mechanism on how STAT3 may regulate mitochondrial respiration to aid cardiac survival during hypoxia/oxidative stress. During cellular stress STAT3 is an anti-apoptotic factor that works both as a signaling molecule involved in the regulation of genes (Levy and Lee, 2002, Negoro et al., 2001, Oshima et al., 2005) and by modulating function of the electron transport chain (Wegrzyn et al., 2009). Over expression of STAT3 in P19CL6 cells during 8h hypoxia leads to the rescue of complex I/II activities of the ETC. STAT3 is unlikely to influence oxidative phosphorylation directly as it has been reported by proteomic analysis that mitochondrial STAT3 is not present in stoichiometric amounts when compared to complex I/II of the ETC (Phillips et al., 2010). Instead, STAT3 is more likely to act by modulating activities of the ETC through non-stoichiometric mechanisms. STAT3 has been shown to influence opening of the mitochondrial permeability transition pore (mPTP) in response to calcium uptake through protein-protein interactions with cyclophilin D (Boengler et al., 2010). Redox modification of STAT3 may play a part in modulating complex I/II activity during hypoxia. During this study a redox-insensitive form of STAT3, $STAT3^{C3S}$ was able to translocate to mitochondria but failed to rescue respiration like exogenous $STAT3^{wt}$.

Ischaemia-reperfusion injury induces oxidative stress via the production of reactive oxygen species (Zweier et al., 1987). Increased levels of ROS are capable of modulating intracellular redox pathways. In the context of STAT3, this can be achieved by the inactivation of protein phosphatases by oxidation (Meng et al., 2002, Woetmann et al., 1999) or the upregulation of STAT3 protein kinases including PKCδ leading to increased levels of serine phosphorylated STAT3. In addition STAT3 can be directly modified by ROS to form redox dimers and trimers (figure 3.43) (Li et al., 2010), or through interactions with other proteins (Xie et al., 2009, Qiu et al., 2011, Setati et al., 2010).

In a post-ischaemic heart oxygen delivery to the myocardium is not sufficient to meet the needs of mitochondrial respiration during the physiological conditions of hypoxia, leaving the mitochondrial ETC in a mono-reduced state. This results in leakage of electrons from the ETC that in turn reacts with molecular oxygen to give superoxide (Ambrosio et al., 1993). Over production of ROS in mitochondria also initiates inactivation of the ETC (Zhao et al., 2005). Dysfunction of mitochondrial respiration and increased ROS production will lead to impaired mitochondrial integrity and enhanced levels of apoptosis.

Data from this study suggest that redox modified, serine phosphorylated STAT3 is required for mitochondrial function and it rescues mitochondrial respiration by modulating the activities of complex I/II of the ETC during hypoxia. As oxidative phosphorylation is maintained through mechanisms involving STAT3, levels of electron leakage from the ETC are reduced resulting in less mitochondrial ROS

being generated. Recently, Zhou and colleagues demonstrated that inactivation of STAT3 leads to suppression of load driven mitochondrial activity and ultimately an elevated level of ROS in cultured primary osteoblasts (Zhou et al., 2011). This supports the idea that mitochondrial STAT3 maintains respiration to prevent the further production of ROS that would ultimately lead to apoptosis.

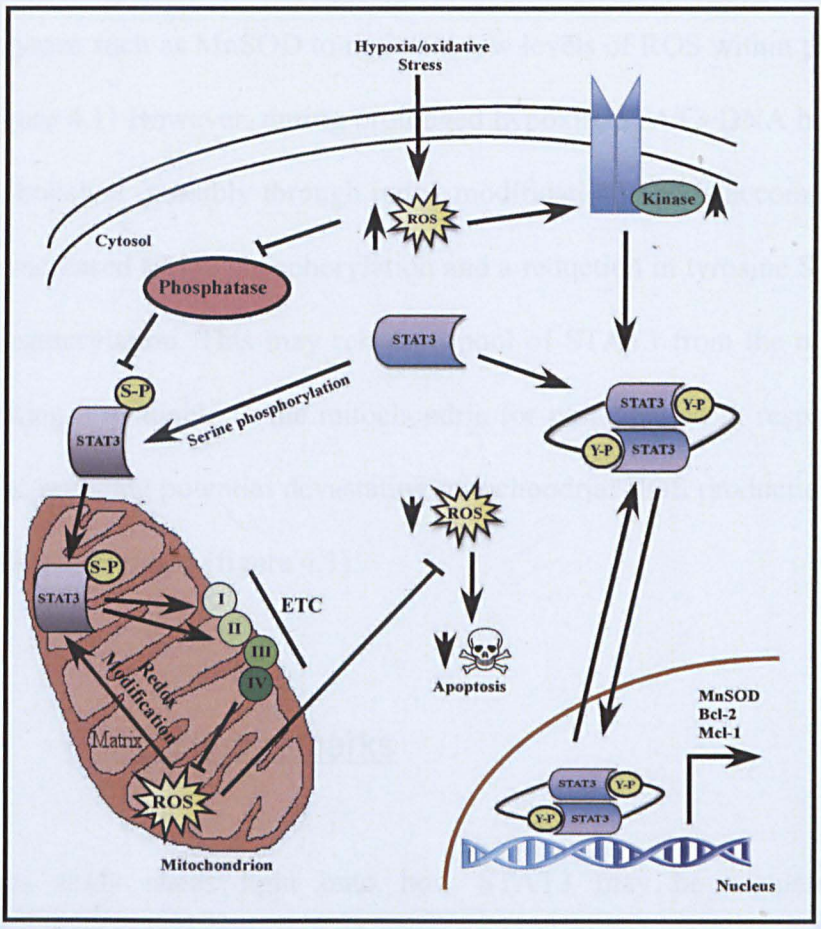

Figure 4.1 Proposed model for the role of STAT3 during hypoxia-induced stress. Hypoxia induced stress causes accumulation of reactive oxygen species (ROS) within the cells. Signaling levels of ROS can active kinases and inactive phosphatases resulting in the accumulation of serine phosphorylated STAT3, which can translocate the mitochondria. Further ROS production in the mitochondria leads to the redox modification of STAT3 and restoration of the electron transport chain (ETC) via complex I/II- dependant

respiration. This results in a reduction in cellular ROS production and apoptotic cell death.

The results from this study have also suggested there may be a switch between nuclear and mitochondrial functions of STAT3. During brief hypoxia (1h) STAT3 tyrosine phosphorylation and DNA binding are apparent which could lead to the transcriptional upregulation of antiapoptotic proteins such as Bcl-2 and Mcl-1 and antioxidant enzymes such as MnSOD to maintain low levels of ROS within the cell (figure 4.1) However, during prolonged hypoxia, STAT3 DNA binding is abolished (possibly through redox modification) and is accompanied by increased serine phosphorylation and a reduction in tyrosine STAT3 phosphorylation. This may release a pool of STAT3 from the nucleus making it available to the mitochondria for participation in respiration thus, reducing potential devastating mitochondrial ROS production that leads to apoptosis (figure 4.1)

4.7. Concluding remarks

Thus study sheds light onto how STAT3 may be regulated in cardiomyocytes during hypoxia. By exploring cardiac cell models this study indentified clear differences in the susceptibility to hypoxia-induced apoptosis between the different cell models. RCMs and H9c2 cells had a high resilience to hypoxic insult, whereas P19CL6 cells were extremely sensitive to hypoxia-induced apoptosis. Due to the fact

that apoptotic loss of cardiomyocytes is associated with ischaemic heart disease, this study suggests that P19CL6 cells may offer a useful model for investigating mechanisms involving apoptosis in the future. However the use of P19CL6 cells as a cardiac cell model has been questioned and warrants further investigation. This study has also identified a redox-dependant contribution of mitochondrial STAT3 to the survival of cardiomyocytes during hypoxia with the use of the redox-insensitive STAT3 mutant $STAT3^{C3S}$. In addition, preliminary data has shed light on one of the potential kinases (PKCδ) responsible for serine phosphorylation STAT3 in response to hypoxia. Having shown is importance STAT3 to the survival of cardiomyocytes during hypoxia; the next step will be to investigate its significance in the heart.

References

ABATE, C., PATEL, L., RAUSCHER, F. J., 3RD & CURRAN, T. (1990) Redox regulation of fos and jun DNA-binding activity in vitro. *Science,* 249, 1157-61.

ADACHI, T., WEISBROD, R. M., PIMENTEL, D. R., YING, J., SHAROV, V. S., SCHONEICH, C. & COHEN, R. A. (2004) S-Glutathiolation by peroxynitrite activates SERCA during arterial relaxation by nitric oxide. *Nat Med,* 10, 1200-7.

AKIRA, S., NISHIO, Y., INOUE, M., WANG, X. J., WEI, S., MATSUSAKA, T., YOSHIDA, K., SUDO, T., NARUTO, M. & KISHIMOTO, T. (1994) Molecular cloning of APRF, a novel IFN-stimulated gene factor 3 p91-related transcription factor involved in the gp130-mediated signaling pathway. *Cell,* 77, 63-71.

ALEXANDER, W. S. (2002) Suppressors of cytokine signalling (SOCS) in the immune system. *Nat Rev Immunol,* 2, 410-6.

AMBROSIO, G., ZWEIER, J. L., DUILIO, C., KUPPUSAMY, P., SANTORO, G., ELIA, P. P., TRITTO, I., CIRILLO, P., CONDORELLI, M., CHIARIELLO, M. & ET AL. (1993) Evidence that mitochondrial respiration is a source of potentially toxic oxygen free radicals in intact rabbit hearts subjected to ischemia and reflow. *J Biol Chem,* 268, 18532-41.

ANISIMOV, S. V., TARASOV, K. V., RIORDON, D., WOBUS, A. M. & BOHELER, K. R. (2002) SAGE identification of differentiation responsive genes in P19 embryonic cells induced to form cardiomyocytes in vitro. *Mech Dev,* 117, 25-74.

ANTUNES, F., MARG, A. & VINKEMEIER, U. (2011) STAT1 signaling is not regulated by a phosphorylation-acetylation switch. *Mol Cell Biol,* 31, 3029-37.

ASHKENAZI, A. & DIXIT, V. M. (1998) Death receptors: signaling and modulation. *Science,* 281, 1305-8.

AUERNHAMMER, C. J. & MELMED, S. (2001) The central role of SOCS-3 in integrating the neuro-immunoendocrine interface. *J Clin Invest,* 108, 1735-40.

AZAM, M., ERDJUMENT-BROMAGE, H., KREIDER, B. L., XIA, M., QUELLE, F., BASU, R., SARIS, C., TEMPST, P., IHLE, J. N. & SCHINDLER, C. (1995) Interleukin-3 signals through multiple isoforms of Stat5. *EMBO J,* 14, 1402-11.

AZIZ, M. H., MANOHARAN, H. T., CHURCH, D. R., DRECKSCHMIDT, N. E., ZHONG, W., OBERLEY, T. D., WILDING, G. & VERMA, A. K. (2007) Protein kinase Cepsilon interacts with signal transducers and activators of transcription 3 (Stat3), phosphorylates Stat3Ser727, and regulates its constitutive activation in prostate cancer. *Cancer Res,* 67, 8828-38.

BALABAN, R. S., NEMOTO, S. & FINKEL, T. (2005) Mitochondria, oxidants, and aging. *Cell,* 120, 483-95.

BALLINGER, S. W., PATTERSON, C., YAN, C. N., DOAN, R., BUROW, D. L., YOUNG, C. G., YAKES, F. M., VAN HOUTEN, B., BALLINGER, C. A., FREEMAN, B. A. & RUNGE, M. S. (2000) Hydrogen peroxide- and peroxynitrite-induced mitochondrial DNA damage and dysfunction in vascular endothelial and smooth muscle cells. *Circ Res,* 86, 960-6.

BANAI, S., SHWEIKI, D., PINSON, A., CHANDRA, M., LAZAROVICI, G. & KESHET, E. (1994) Upregulation of vascular endothelial growth factor expression induced by myocardial ischaemia: implications for coronary angiogenesis. *Cardiovasc Res,* 28, 1176-9.

BARFORD, D. (2004) The role of cysteine residues as redox-sensitive regulatory switches. *Curr Opin Struct Biol,* 14, 679-86.

BARRY, S. P., TOWNSEND, P. A., MCCORMICK, J., KNIGHT, R. A., SCARABELLI, T. M., LATCHMAN, D. S. & STEPHANOU, A. (2009) STAT3 deletion sensitizes cells to oxidative stress. *Biochem Biophys Res Commun,* 385, 324-9.

BAYIR, H. & KAGAN, V. E. (2008) Bench-to-bedside review: Mitochondrial injury, oxidative stress and apoptosis--there is nothing more practical than a good theory. *Crit Care,* 12, 206.

BELTRAMI, C. A., FINATO, N., ROCCO, M., FERUGLIO, G. A., PURICELLI, C., CIGOLA, E., QUAINI, F., SONNENBLICK, E. H., OLIVETTI, G. & ANVERSA, P. (1994) Structural basis of end-stage failure in ischemic cardiomyopathy in humans. *Circulation,* 89, 151-63.

BLAKE, D. R., ALLEN, R. E. & LUNEC, J. (1987) Free radicals in biological systems--a review orientated to inflammatory processes. *Br Med Bull,* 43, 371-85.

BOATRIGHT, K. M., RENATUS, M., SCOTT, F. L., SPERANDIO, S., SHIN, H., PEDERSEN, I. M., RICCI, J. E., EDRIS, W. A., SUTHERLIN, D. P., GREEN, D. R. & SALVESEN, G. S. (2003) A unified model for apical caspase activation. *Mol Cell,* 11, 529-41.

BODYAK, N., KANG, P. M., HIROMURA, M., SULIJOADIKUSUMO, I., HORIKOSHI, N., KHRAPKO, K. & USHEVA, A. (2002) Gene expression profiling of the aging mouse cardiac myocytes. *Nucleic Acids Res,* 30, 3788-94.

BOENGLER, K., BUECHERT, A., HEINEN, Y., ROESKES, C., HILFIKER-KLEINER, D., HEUSCH, G. & SCHULZ, R. (2008a) Cardioprotection by ischemic postconditioning is lost in aged and STAT3-deficient mice. *Circ Res,* 102, 131-5.

BOENGLER, K., HILFIKER-KLEINER, D., DREXLER, H., HEUSCH, G. & SCHULZ, R. (2008b) The myocardial JAK/STAT pathway: from protection to failure. *Pharmacol Ther,* 120, 172-85.

BOENGLER, K., HILFIKER-KLEINER, D., HEUSCH, G. & SCHULZ, R. Inhibition of permeability transition pore opening by mitochondrial STAT3 and its role in myocardial ischemia/reperfusion. *Basic Res Cardiol,* 105, 771-85.

BOENGLER, K., HILFIKER-KLEINER, D., HEUSCH, G. & SCHULZ, R. (2010) Inhibition of permeability transition pore opening by mitochondrial STAT3 and its role in myocardial ischemia/reperfusion. *Basic Res Cardiol,* 105, 771-85.

BONAVITA, F., STEFANELLI, C., GIORDANO, E., COLUMBARO, M., FACCHINI, A., BONAFE, F., CALDARERA, C. M. & GUARNIERI, C. (2003) H9c2 cardiac myoblasts undergo apoptosis in a model of ischemia consisting of serum deprivation and hypoxia: inhibition by PMA. *FEBS Lett,* 536, 85-91.

BOSSIS, G. & MELCHIOR, F. (2006) Regulation of SUMOylation by reversible oxidation of SUMO conjugating enzymes. *Mol Cell,* 21, 349-57.

BRILL, A., TORCHINSKY, A., CARP, H. & TODER, V. (1999) The role of apoptosis in normal and abnormal embryonic development. *J Assist Reprod Genet,* 16, 512-9.

BROMBERG, J. & DARNELL, J. E., JR. (2000) The role of STATs in transcriptional control and their impact on cellular function. *Oncogene,* 19, 2468-73.

BROMBERG, J. F., WRZESZCZYNSKA, M. H., DEVGAN, G., ZHAO, Y., PESTELL, R. G., ALBANESE, C. & DARNELL, J. E., JR. (1999) Stat3 as an oncogene. *Cell,* 98, 295-303.

BUEHR, M., MEEK, S., BLAIR, K., YANG, J., URE, J., SILVA, J., MCLAY, R., HALL, J., YING, Q. L. & SMITH, A. (2008) Capture of authentic embryonic stem cells from rat blastocysts. *Cell,* 135, 1287-98.

BURGOYNE, J. R., MADHANI, M., CUELLO, F., CHARLES, R. L., BRENNAN, J. P., SCHRODER, E., BROWNING, D. D. & EATON, P. (2007) Cysteine redox sensor in PKGIa enables oxidant-induced activation. *Science,* 317, 1393-7.

CALDENHOVEN, E., VAN DIJK, T. B., SOLARI, R., ARMSTRONG, J., RAAIJMAKERS, J. A., LAMMERS, J. W., KOENDERMAN, L. & DE GROOT, R. P. (1996) STAT3beta, a splice variant of transcription factor STAT3, is a dominant negative regulator of transcription. *J Biol Chem,* 271, 13221-7.

CANNON, R. O., 3RD (1998) Role of nitric oxide in cardiovascular disease: focus on the endothelium. *Clin Chem,* 44, 1809-19.

CAO, X., TAY, A., GUY, G. R. & TAN, Y. H. (1996) Activation and association of Stat3 with Src in v-Src-transformed cell lines. *Mol Cell Biol,* 16, 1595-603.

CARBALLO, M., CONDE, M., EL BEKAY, R., MARTIN-NIETO, J., CAMACHO, M. J., MONTESEIRIN, J., CONDE, J., BEDOYA, F. J. & SOBRINO, F. (1999) Oxidative stress triggers STAT3 tyrosine phosphorylation and nuclear translocation in human lymphocytes. *J Biol Chem,* 274, 17580-6.

CERESA, B. P., HORVATH, C. M. & PESSIN, J. E. (1997) Signal transducer and activator of transcription-3 serine phosphorylation by insulin is mediated by a Ras/Raf/MEK-dependent pathway. *Endocrinology,* 138, 4131-7.

CHAN, K. S., SANO, S., KIGUCHI, K., ANDERS, J., KOMAZAWA, N., TAKEDA, J. & DIGIOVANNI, J. (2004) Disruption of Stat3 reveals a

critical role in both the initiation and the promotion stages of epithelial carcinogenesis. *J Clin Invest,* 114, 720-8.

CHAN, R. J., JOHNSON, S. A., LI, Y., YODER, M. C. & FENG, G. S. (2003a) A definitive role of Shp-2 tyrosine phosphatase in mediating embryonic stem cell differentiation and hematopoiesis. *Blood,* 102, 2074-80.

CHAN, S. L., LEE, M. C., TAN, K. O., YANG, L. K., LEE, A. S., FLOTOW, H., FU, N. Y., BUTLER, M. S., SOEJARTO, D. D., BUSS, A. D. & YU, V. C. (2003b) Identification of chelerythrine as an inhibitor of BclXL function. *J Biol Chem,* 278, 20453-6.

CHANCE, B., SIES, H. & BOVERIS, A. (1979) Hydroperoxide metabolism in mammalian organs. *Physiol Rev,* 59, 527-605.

CHANG, L. & KARIN, M. (2001) Mammalian MAP kinase signalling cascades. *Nature,* 410, 37-40.

CHAPMAN, R. S., LOURENCO, P. C., TONNER, E., FLINT, D. J., SELBERT, S., TAKEDA, K., AKIRA, S., CLARKE, A. R. & WATSON, C. J. (1999) Suppression of epithelial apoptosis and delayed mammary gland involution in mice with a conditional knockout of Stat3. *Genes Dev,* 13, 2604-16.

CHEN, X., XU, H., YUAN, P., FANG, F., HUSS, M., VEGA, V. B., WONG, E., ORLOV, Y. L., ZHANG, W., JIANG, J., LOH, Y. H., YEO, H. C., YEO, Z. X., NARANG, V., GOVINDARAJAN, K. R., LEONG, B., SHAHAB, A., RUAN, Y., BOURQUE, G., SUNG, W. K., CLARKE, N. D., WEI, C. L. & NG, H. H. (2008) Integration of external signaling pathways with the core transcriptional network in embryonic stem cells. *Cell,* 133, 1106-17.

CHILDS, A. C., PHANEUF, S. L., DIRKS, A. J., PHILLIPS, T. & LEEUWENBURGH, C. (2002) Doxorubicin treatment in vivo causes cytochrome C release and cardiomyocyte apoptosis, as well as increased mitochondrial efficiency, superoxide dismutase activity, and Bcl-2:Bax ratio. *Cancer Res,* 62, 4592-8.

CHINNAIYAN, A. M., O'ROURKE, K., TEWARI, M. & DIXIT, V. M. (1995) FADD, a novel death domain-containing protein, interacts with the death domain of Fas and initiates apoptosis. *Cell,* 81, 505-12.

CHLOPCIKOVA, S., PSOTOVA, J. & MIKETOVA, P. (2001) Neonatal rat cardiomyocytes--a model for the study of morphological, biochemical and electrophysiological characteristics of the heart. *Biomed Pap Med Fac Univ Palacky Olomouc Czech Repub,* 145, 49-55.

CHOI, S. O., CHO, Y. S., KIM, H. L. & PARK, J. W. (2007) ROS mediate the hypoxic repression of the hepcidin gene by inhibiting C/EBPalpha and STAT-3. *Biochem Biophys Res Commun,* 356, 312-7.

CHUA, P. J., YIP, G. W. & BAY, B. H. (2009) Cell cycle arrest induced by hydrogen peroxide is associated with modulation of oxidative stress related genes in breast cancer cells. *Exp Biol Med (Maywood),* 234, 1086-94.

CHUNG, C. D., LIAO, J., LIU, B., RAO, X., JAY, P., BERTA, P. & SHUAI, K. (1997a) Specific inhibition of Stat3 signal transduction by PIAS3. *Science,* 278, 1803-5.

CHUNG, J., UCHIDA, E., GRAMMER, T. C. & BLENIS, J. (1997b) STAT3 serine phosphorylation by ERK-dependent and -independent pathways negatively modulates its tyrosine phosphorylation. *Mol Cell Biol,* 17, 6508-16.

CLAVIJO, C., CHEN, J. L., KIM, K. J., REYLAND, M. E. & ANN, D. K. (2007) Protein kinase Cdelta-dependent and -independent signaling in genotoxic response to treatment of desferroxamine, a hypoxia-mimetic agent. *Am J Physiol Cell Physiol,* 292, C2150-60.

CLAYCOMB, W. C. (1985) Long-term culture and characterization of the adult ventricular and atrial cardiac muscle cell. *Basic Res Cardiol,* 80 Suppl 2, 171-4.

CLAYCOMB, W. C., LANSON, N. A., JR., STALLWORTH, B. S., EGELAND, D. B., DELCARPIO, J. B., BAHINSKI, A. & IZZO, N. J., JR. (1998) HL-1 cells: a cardiac muscle cell line that contracts and retains phenotypic characteristics of the adult cardiomyocyte. *Proc Natl Acad Sci U S A,* 95, 2979-84.

CORY, S. & ADAMS, J. M. (2002) The Bcl2 family: regulators of the cellular life-or-death switch. *Nat Rev Cancer,* 2, 647-56.

COWAN, D. B., POUTIAS, D. N., DEL NIDO, P. J. & MCGOWAN, F. X., JR. (2000) CD14-independent activation of cardiomyocyte signal transduction by bacterial endotoxin. *Am J Physiol Heart Circ Physiol,* 279, H619-29.

D'AUTREAUX, B. & TOLEDANO, M. B. (2007) ROS as signalling molecules: mechanisms that generate specificity in ROS homeostasis. *Nat Rev Mol Cell Biol,* 8, 813-24.

DALLE-DONNE, I., GIUSTARINI, D., COLOMBO, R., ROSSI, R. & MILZANI, A. (2003) Protein carbonylation in human diseases. *Trends Mol Med,* 9, 169-76.

DANIAL, N. N. & KORSMEYER, S. J. (2004) Cell death: critical control points. *Cell,* 116, 205-19.

DANIAL, N. N. & ROTHMAN, P. (2000) JAK-STAT signaling activated by Abl oncogenes. *Oncogene,* 19, 2523-31.

DARNELL, J. E., JR. (1997) STATs and gene regulation. *Science,* 277, 1630-5.

DECKER, T. & KOVARIK, P. (2000) Serine phosphorylation of STATs. *Oncogene,* 19, 2628-37.

DEISSEROTH, A. & DOUNCE, A. L. (1970) Catalase: Physical and chemical properties, mechanism of catalysis, and physiological role. *Physiol Rev,* 50, 319-75.

DENNIS V. COKKINOS, C. P., GERD HEUSCH (2006) *Myocardial Ischemia: From Mechanisms to Therapeutic Potential.*

DENU, J. M. & TANNER, K. G. (1998) Specific and reversible inactivation of protein tyrosine phosphatases by hydrogen peroxide: evidence for a sulfenic acid intermediate and implications for redox regulation. *Biochemistry,* 37, 5633-42.

DING, J. & KOPCHICK, J. J. (2011) Plasma biomarkers of mouse aging. *Age (Dordr),* 33, 291-307.

DODD, R. (2005) ubiquitylation system. IN UBIQUITYLATION (Ed.

DROESCHER, M., BEGITT, A., MARG, A., ZACHARIAS, M. & VINKEMEIER, U. (2010) Cytokine-induced paracrystals prolong the activity of signal transducers and activators of transcription (STAT) and provide a model for the regulation of protein solubility by small ubiquitin-like modifier (SUMO). *J Biol Chem,* 286, 18731-46.

DUILIO, C., AMBROSIO, G., KUPPUSAMY, P., DIPAULA, A., BECKER, L. C. & ZWEIER, J. L. (2001) Neutrophils are primary source of O2 radicals during reperfusion after prolonged myocardial ischemia. *Am J Physiol Heart Circ Physiol,* 280, H2649-57.

DUNN, S. E. (2000) Insulin-like growth factor I stimulates angiogenesis and the production of vascular endothelial growth factor. *Growth Horm IGF Res,* 10 Suppl A, S41-2.

EEFTING, F., RENSING, B., WIGMAN, J., PANNEKOEK, W. J., LIU, W. M., CRAMER, M. J., LIPS, D. J. & DOEVENDANS, P. A. (2004) Role of apoptosis in reperfusion injury. *Cardiovasc Res,* 61, 414-26.

EHRET, G. B., REICHENBACH, P., SCHINDLER, U,, HORVATH, C. M., FRITZ, S., NABHOLZ, M. & BUCHER, P. (2001) DNA binding specificity of different STAT proteins. Comparison of in vitro specificity with natural target sites. *J Biol Chem,* 276, 6675-88.

EILERS, A., GEORGELLIS, D., KLOSE, B., SCHINDLER, C., ZIEMIECKI, A., HARPUR, A. G., WILKS, A. F. & DECKER, T. (1995) Differentiation-regulated serine phosphorylation of STAT1 promotes GAF activation in macrophages. *Mol Cell Biol,* 15, 3579-86.

EPLING-BURNETTE, P. K., LIU, J. H., CATLETT-FALCONE, R., TURKSON, J., OSHIRO, M., KOTHAPALLI, R., LI, Y., WANG, J. M., YANG-YEN, H. F., KARRAS, J., JOVE, R. & LOUGHRAN, T. P., JR. (2001) Inhibition of STAT3 signaling leads to apoptosis of leukemic large granular lymphocytes and decreased Mcl-1 expression. *J Clin Invest,* 107, 351-62.

FESTJENS, N., VANDEN BERGHE, T., CORNELIS, S. & VANDENABEELE, P. (2007) RIP1, a kinase on the crossroads of a cell's decision to live or die. *Cell Death Differ,* 14, 400-10.

FISCHER, U., JANICKE, R. U. & SCHULZE-OSTHOFF, K. (2003) Many cuts to ruin: a comprehensive update of caspase substrates. *Cell Death Differ,* 10, 76-100.

FOLEY, T. D. & KINTNER, M. E. (2005) Brain PP2A is modified by thiol-disulfide exchange and intermolecular disulfide formation. *Biochem Biophys Res Commun,* 330, 1224-9.

FREEMAN, B. A. & CRAPO, J. D. (1982) Biology of disease: free radicals and tissue injury. *Lab Invest,* 47, 412-26.

FRIDOVICH, I. (1983) Superoxide radical: an endogenous toxicant. *Annu Rev Pharmacol Toxicol,* 23, 239-57.

FRIDOVICH, I. (1986) Biological effects of the superoxide radical. *Arch Biochem Biophys,* 247, 1-11.

FRIED, M. & CROTHERS, D. M. (1981) Equilibria and kinetics of lac repressor-operator interactions by polyacrylamide gel electrophoresis. *Nucleic Acids Res,* 9, 6505-25.

FRYER, R. M., WANG, Y., HSU, A. K. & GROSS, G. J. (2001) Essential activation of PKC-delta in opioid-initiated cardioprotection. *Am J Physiol Heart Circ Physiol,* 280, H1346-53.

FUNAMOTO, M., FUJIO, Y., KUNISADA, K., NEGORO, S., TONE, E., OSUGI, T., HIROTA, H., IZUMI, M., YOSHIZAKI, K., WALSH, K., KISHIMOTO, T. & YAMAUCHI-TAKIHARA, K. (2000) Signal transducer and activator of transcription 3 is required for glycoprotein 130-mediated induction of vascular endothelial growth factor in cardiac myocytes. *J Biol Chem,* 275, 10561-6.

GARDNER, H. W. (1989) Oxygen radical chemistry of polyunsaturated fatty acids. *Free Radic Biol Med,* 7, 65-86.

GARIMORTH, K., WELTE, T. & DOPPLER, W. (1999) Generation of carboxy-terminally deleted forms of STAT5 during preparation of cell extracts. *Exp Cell Res,* 246, 148-51.

GARNER, M. M. & REVZIN, A. (1981) A gel electrophoresis method for quantifying the binding of proteins to specific DNA regions:

application to components of the Escherichia coli lactose operon regulatory system. *Nucleic Acids Res,* 9, 3047-60.

GARTSBEIN, M., ALT, A., HASHIMOTO, K., NAKAJIMA, K., KUROKI, T. & TENNENBAUM, T. (2006) The role of protein kinase C delta activation and STAT3 Ser727 phosphorylation in insulin-induced keratinocyte proliferation. *J Cell Sci,* 119, 470-81.

GEISZT, M. & LETO, T. L. (2004) The Nox family of NAD(P)H oxidases: host defense and beyond. *J Biol Chem,* 279, 51715-8.

GHOSH, S., PULINILKUNNIL, T., YUEN, G., KEWALRAMANI, G., AN, D., QI, D., ABRAHANI, A. & RODRIGUES, B. (2005) Cardiomyocyte apoptosis induced by short-term diabetes requires mitochondrial GSH depletion. *Am J Physiol Heart Circ Physiol,* 289, H768-76.

GHOSH, S., TING, S., LAU, H., PULINILKUNNIL, T., AN, D., QI, D., ABRAHANI, M. A. & RODRIGUES, B. (2004) Increased efflux of glutathione conjugate in acutely diabetic cardiomyocytes. *Can J Physiol Pharmacol,* 82, 879-87.

GIESE, B., RODERBURG, C., SOMMERAUER, M., WORTMANN, S. B., METZ, S., HEINRICH, P. C. & MULLER-NEWEN, G. (2005) Dimerization of the cytokine receptors gp130 and LIFR analysed in single cells. *J Cell Sci,* 118, 5129-40.

GOLDSTEIN, B. J., MAHADEV, K. & WU, X. (2005) Redox paradox: insulin action is facilitated by insulin-stimulated reactive oxygen species with multiple potential signaling targets. *Diabetes,* 54, 311-21.

GONG, J., TRAGANOS, F. & DARZYNKIEWICZ, Z. (1994) A selective procedure for DNA extraction from apoptotic cells applicable for gel electrophoresis and flow cytometry. *Anal Biochem,* 218, 314-9.

GONZALEZ, F. A., RADEN, D. L. & DAVIS, R. J. (1991) Identification of substrate recognition determinants for human ERK1 and ERK2 protein kinases. *J Biol Chem,* 266, 22159-63.

GOTTLIEB, R. A., BURLESON, K. O., KLONER, R. A., BABIOR, B. M. & ENGLER, R. L. (1994) Reperfusion injury induces apoptosis in rabbit cardiomyocytes. *J Clin Invest,* 94, 1621-8.

GREGORIO, C. C. & ANTIN, P. B. (2000) To the heart of myofibril assembly. *Trends Cell Biol,* 10, 355-62.

GRUNDY, S. M., BENJAMIN, I. J., BURKE, G. L., CHAIT, A., ECKEL, R. H., HOWARD, B. V., MITCH, W., SMITH, S. C., JR. & SOWERS, J. R. (1999) Diabetes and cardiovascular disease: a statement for healthcare professionals from the American Heart Association. *Circulation,* 100, 1134-46.

GUEHMANN, S., VORBRUEGGEN, G., KALKBRENNER, F. & MOELLING, K. (1992) Reduction of a conserved Cys is essential for Myb DNA-binding. *Nucleic Acids Res,* 20, 2279-86.

HAANEN, C. & VERMES, I. (1995) Apoptosis and inflammation. *Mediators Inflamm,* 4, 5-15.

HABARA-OHKUBO, A. (1996) Differentiation of beating cardiac muscle cells from a derivative of P19 embryonal carcinoma cells. *Cell Struct Funct,* 21, 101-10.

HAHN, H. S., YUSSMAN, M. G., TOYOKAWA, T., MARREEZ, Y., BARRETT, T. J., HILTY, K. C., OSINSKA, H., ROBBINS, J. & DORN, G. W., 2ND (2002) Ischemic protection and myofibrillar cardiomyopathy: dose-dependent effects of in vivo deltaPKC inhibition. *Circ Res,* 91, 741-8.

HENGARTNER, M. O. & HORVITZ, H. R. (1994) Programmed cell death in Caenorhabditis elegans. *Curr Opin Genet Dev,* 4, 581-6.

HENZE, K. & MARTIN, W. (2003) Evolutionary biology: essence of mitochondria. *Nature,* 426, 127-8.

HESCHELER, J., FLEISCHMANN, B. K., WARTENBERG, M., BLOCH, W., KOLOSSOV, E., JI, G., ADDICKS, K. & SAUER, H. (1999) Establishment of ionic channels and signalling cascades in the embryonic stem cell-derived primitive endoderm and cardiovascular system. *Cells Tissues Organs,* 165, 153-64.

HESCHELER, J., MEYER, R., PLANT, S., KRAUTWURST, D., ROSENTHAL, W. & SCHULTZ, G. (1991) Morphological, biochemical, and electrophysiological characterization of a clonal cell (H9c2) line from rat heart. *Circ Res,* 69, 1476-86.

HILFIKER-KLEINER, D., HILFIKER, A., FUCHS, M., KAMINSKI, K., SCHAEFER, A., SCHIEFFER, B., HILLMER, A., SCHMIEDL, A., DING, Z., PODEWSKI, E., POLI, V., SCHNEIDER, M. D., SCHULZ, R., PARK, J. K., WOLLERT, K. C. & DREXLER, H. (2004) Signal transducer and activator of transcription 3 is required for myocardial capillary growth, control of interstitial matrix deposition, and heart protection from ischemic injury. *Circ Res,* 95, 187-95.

HO, A. S., LIU, Y., KHAN, T. A., HSU, D. H., BAZAN, J. F. & MOORE, K. W. (1993) A receptor for interleukin 10 is related to interferon receptors. *Proc Natl Acad Sci U S A,* 90, 11267-71.

HOEY, T., ZHANG, S., SCHMIDT, N., YU, Q., RAMCHANDANI, S., XU, X., NAEGER, L. K., SUN, Y. L. & KAPLAN, M. H. (2003) Distinct requirements for the naturally occurring splice forms Stat4alpha and Stat4beta in IL-12 responses. *EMBO J,* 22, 4237-48.

HORIUCHI, H., TATEGAKI, A., YAMASHITA, Y., HISAMATSU, H., OGAWA, M., NOGUCHI, T., AOSASA, M., KAWASHIMA, T., AKITA, S., NISHIMICHI, N., MITSUI, N., FURUSAWA, S. & MATSUDA, H. (2004) Chicken leukemia inhibitory factor maintains chicken embryonic stem cells in the undifferentiated state. *J Biol Chem,* 279, 24514-20.

HORVATH, C. M., WEN, Z. & DARNELL, J. E., JR. (1995) A STAT protein domain that determines DNA sequence recognition suggests a novel DNA-binding domain. *Genes Dev,* 9, 984-94.

HOU, J., SCHINDLER, U., HENZEL, W. J., HO, T. C., BRASSEUR, M. & MCKNIGHT, S. L. (1994) An interleukin-4-induced transcription factor: IL-4 Stat. *Science,* 265, 1701-6.

HOUWELING, A. C., SOMI, S., MASSINK, M. P., GROENEN, M. A., MOORMAN, A. F. & CHRISTOFFELS, V. M. (2005) Comparative analysis of the natriuretic peptide precursor gene cluster in vertebrates reveals loss of ANF and retention of CNP-3 in chicken. *Dev Dyn,* 233, 1076-82.

HUDLICKA, O. & BROWN, M. D. (1996) Postnatal growth of the heart and its blood vessels. *J Vasc Res,* 33, 266-87.

HUMPHREY, R. K., BEATTIE, G. M., LOPEZ, A. D., BUCAY, N., KING, C. C., FIRPO, M. T., ROSE-JOHN, S. & HAYEK, A. (2004) Maintenance of pluripotency in human embryonic stem cells is STAT3 independent. *Stem Cells,* 22, 522-30.

HUNTER, J. J. & CHIEN, K. R. (1999) Signaling pathways for cardiac hypertrophy and failure. *N Engl J Med,* 341, 1276-83.

HUNTER, T. (2000) Signaling--2000 and beyond. *Cell,* 100, 113-27.

HUSSAIN, S. P., AGUILAR, F. & CERUTTI, P. (1994) Mutagenesis of codon 248 of the human p53 tumor suppressor gene by N-ethyl-N-nitrosourea. *Oncogene,* 9, 13-8.

HUTCHISON, K. A., MATIC, G., MESHINCHI, S., BRESNICK, E. H. & PRATT, W. B. (1991) Redox manipulation of DNA binding activity and BuGR epitope reactivity of the glucocorticoid receptor. *J Biol Chem,* 266, 10505-9.

IEMITSU, M., MIYAUCHI, T., MAEDA, S., SAKAI, S., KOBAYASHI, T., FUJII, N., MIYAZAKI, H., MATSUDA, M. & YAMAGUCHI, I. (2001) Physiological and pathological cardiac hypertrophy induce different molecular phenotypes in the rat. *Am J Physiol Regul Integr Comp Physiol,* 281, R2029-36.

INAGAKI, K., HAHN, H. S., DORN, G. W., 2ND & MOCHLY-ROSEN, D. (2003) Additive protection of the ischemic heart ex vivo by combined

treatment with delta-protein kinase C inhibitor and epsilon-protein kinase C activator. *Circulation,* 108, 869-75.

ITOH, G., TAMURA, J., SUZUKI, M., SUZUKI, Y., IKEDA, H., KOIKE, M., NOMURA, M., JIE, T. & ITO, K. (1995) DNA fragmentation of human infarcted myocardial cells demonstrated by the nick end labeling method and DNA agarose gel electrophoresis. *Am J Pathol,* 146, 1325-31.

IVAN, M., KONDO, K., YANG, H., KIM, W., VALIANDO, J., OHH, M., SALIC, A., ASARA, J. M., LANE, W. S. & KAELIN, W. G., JR. (2001) HIFalpha targeted for VHL-mediated destruction by proline hydroxylation: implications for O2 sensing. *Science,* 292, 464-8.

JACOBY, J. J., KALINOWSKI, A., LIU, M. G., ZHANG, S. S., GAO, Q., CHAI, G. X., JI, L., IWAMOTO, Y., LI, E., SCHNEIDER, M., RUSSELL, K. S. & FU, X. Y. (2003) Cardiomyocyte-restricted knockout of STAT3 results in higher sensitivity to inflammation, cardiac fibrosis, and heart failure with advanced age. *Proc Natl Acad Sci U S A,* 100, 12929-34.

JAIN, N., ZHANG, T., FONG, S. L., LIM, C. P. & CAO, X. (1998) Repression of Stat3 activity by activation of mitogen-activated protein kinase (MAPK). *Oncogene,* 17, 3157-67.

JAIN, N., ZHANG, T., KEE, W. H., LI, W. & CAO, X. (1999) Protein kinase C delta associates with and phosphorylates Stat3 in an interleukin-6-dependent manner. *J Biol Chem,* 274, 24392-400.

JARRETA, D., ORUS, J., BARRIENTOS, A., MIRO, O., ROIG, E., HERAS, M., MORAES, C. T., CARDELLACH, F. & CASADEMONT, J. (2000) Mitochondrial function in heart muscle from patients with idiopathic dilated cardiomyopathy. *Cardiovasc Res,* 45, 860-5.

JEREMIAS, I., KUPATT, C., MARTIN-VILLALBA, A., HABAZETTL, H., SCHENKEL, J., BOEKSTEGERS, P. & DEBATIN, K. M. (2000) Involvement of CD95/Apo1/Fas in cell death after myocardial ischemia. *Circulation,* 102, 915-20.

JIANG, B. H., SEMENZA, G. L., BAUER, C. & MARTI, H. H. (1996) Hypoxia-inducible factor 1 levels vary exponentially over a physiologically relevant range of O2 tension. *Am J Physiol,* 271, C1172-80.

JOHN, S., VINKEMEIER, U., SOLDAINI, E., DARNELL, J. E., JR. & LEONARD, W. J. (1999) The significance of tetramerization in promoter recruitment by Stat5. *Mol Cell Biol,* 19, 1910-8.

KABIR, A. M., CLARK, J. E., TANNO, M., CAO, X., HOTHERSALL, J. S., DASHNYAM, S., GOROG, D. A., BELLAHCENE, M., SHATTOCK, M. J. & MARBER, M. S. (2006) Cardioprotection initiated by reactive

oxygen species is dependent on activation of PKCepsilon. *Am J Physiol Heart Circ Physiol,* 291, H1893-9.

KANG, B. H., PLESCIA, J., DOHI, T., ROSA, J., DOXSEY, S. J. & ALTIERI, D. C. (2007) Regulation of tumor cell mitochondrial homeostasis by an organelle-specific Hsp90 chaperone network. *Cell,* 131, 257-70.

KANG, S. H., YU, M. O., PARK, K. J., CHI, S. G., PARK, D. H. & CHUNG, Y. G. (2010) Activated STAT3 regulates hypoxia-induced angiogenesis and cell migration in human glioblastoma. *Neurosurgery,* 67, 1386-95; discussion 1395.

KANTHASAMY, A. G., KITAZAWA, M., KANTHASAMY, A. & ANANTHARAM, V. (2003) Role of proteolytic activation of protein kinase Cdelta in oxidative stress-induced apoptosis. *Antioxid Redox Signal,* 5, 609-20.

KATZ (2006) *Physiology of the heart. 4th Edition*, Lippincott Williams and Wilkins.

KERR, J. F. (1965) A histochemical study of hypertrophy and ischaemic injury of rat liver with special reference to changes in lysosomes. *J Pathol Bacteriol,* 90, 419-35.

KERR, J. F., WYLLIE, A. H. & CURRIE, A. R. (1972) Apoptosis: a basic biological phenomenon with wide-ranging implications in tissue kinetics. *Br J Cancer,* 26, 239-57.

KHODADADI, P., MERSINIAS, THUMSER (2010) Applicability of the P19CL6 cells as a model of cardiomyocytes – a transcriptome analysis. *Health,* 2, 24-32.

KIDDER, B. L., YANG, J. & PALMER, S. (2008) Stat3 and c-Myc genome-wide promoter occupancy in embryonic stem cells. *PLoS One,* 3, e3932.

KIM, H. J., KIM, J. H., SHIN, Y. K., LEE, S. I. & AHN, K. M. (2009) A novel mutation in the linker domain of the signal transducer and activator of transcription 3 gene, p.Lys531Glu, in hyper-IgE syndrome. *J Allergy Clin Immunol,* 123, 956-8.

KIM, J. H., PARK, S. H., PARK, S. G., CHOI, J. S., XIA, Y. & SUNG, J. H. (2011) The Pivotal Role of Reactive Oxygen Species Generation in the Hypoxia-Induced Stimulation of Adipose-Derived Stem Cells. *Stem Cells Dev.*

KIM, T. K. & MANIATIS, T. (1996) Regulation of interferon-gamma-activated STAT1 by the ubiquitin-proteasome pathway. *Science,* 273, 1717-9.

KIMES, B. W. & BRANDT, B. L. (1976) Properties of a clonal muscle cell line from rat heart. *Exp Cell Res,* 98, 367-81.

KISCHKEL, F. C., HELLBARDT, S., BEHRMANN, I., GERMER, M., PAWLITA, M., KRAMMER, P. H. & PETER, M. E. (1995) Cytotoxicity-dependent APO-1 (Fas/CD95)-associated proteins form a death-inducing signaling complex (DISC) with the receptor. *EMBO J,* 14, 5579-88.

KLATT, P. & LAMAS, S. (2000) Regulation of protein function by S-glutathiolation in response to oxidative and nitrosative stress. *Eur J Biochem,* 267, 4928-44.

KLINGMULLER, U., LORENZ, U., CANTLEY, L. C., NEEL, B. G. & LODISH, H. F. (1995) Specific recruitment of SH-PTP1 to the erythropoietin receptor causes inactivation of JAK2 and termination of proliferative signals. *Cell,* 80, 729-38.

KORZUS, E., TORCHIA, J., ROSE, D. W., XU, L., KUROKAWA, R., MCINERNEY, E. M., MULLEN, T. M., GLASS, C. K. & ROSENFELD, M. G. (1998) Transcription factor-specific requirements for coactivators and their acetyltransferase functions. *Science,* 279, 703-7.

KOTAMRAJU, S., KONOREV, E. A., JOSEPH, J. & KALYANARAMAN, B. (2000) Doxorubicin-induced apoptosis in endothelial cells and cardiomyocytes is ameliorated by nitrone spin traps and ebselen. Role of reactive oxygen and nitrogen species. *J Biol Chem,* 275, 33585-92.

KRAMER, O. H., BAUS, D., KNAUER, S. K., STEIN, S., JAGER, E., STAUBER, R. H., GREZ, M., PFITZNER, E. & HEINZEL, T. (2006) Acetylation of Stat1 modulates NF-kappaB activity. *Genes Dev,* 20, 473-85.

KRAMER, O. H., KNAUER, S. K., GREINER, G., JANDT, E., REICHARDT, S., GUHRS, K. H., STAUBER, R. H., BOHMER, F. D. & HEINZEL, T. (2009) A phosphorylation-acetylation switch regulates STAT1 signaling. *Genes Dev,* 23, 223-35.

KREBS, D. L. & HILTON, D. J. (2000) SOCS: physiological suppressors of cytokine signaling. *J Cell Sci,* 113 (Pt 16), 2813-9.

KREUZALER, P. A., STANISZEWSKA, A. D., LI, W., OMIDVAR, N., KEDJOUAR, B., TURKSON, J., POLI, V., FLAVELL, R. A., CLARKSON, R. W. & WATSON, C. J. (2011) Stat3 controls lysosomal-mediated cell death in vivo. *Nat Cell Biol,* 13, 303-9.

KROEMER, G., EL-DEIRY, W. S., GOLSTEIN, P., PETER, M. E., VAUX, D., VANDENABEELE, P., ZHIVOTOVSKY, B., BLAGOSKLONNY, M. V., MALORNI, W., KNIGHT, R. A., PIACENTINI, M., NAGATA, S. & MELINO, G. (2005) Classification

of cell death: recommendations of the Nomenclature Committee on Cell Death. *Cell Death Differ,* 12 Suppl 2, 1463-7.

KUKREJA, R. C. & HESS, M. L. (1992) The oxygen free radical system: from equations through membrane-protein interactions to cardiovascular injury and protection. *Cardiovasc Res,* 26, 641-55.

KUNISADA, K., NEGORO, S., TONE, E., FUNAMOTO, M., OSUGI, T., YAMADA, S., OKABE, M., KISHIMOTO, T. & YAMAUCHI-TAKIHARA, K. (2000) Signal transducer and activator of transcription 3 in the heart transduces not only a hypertrophic signal but a protective signal against doxorubicin-induced cardiomyopathy. *Proc Natl Acad Sci U S A,* 97, 315-9.

KWON, S. H., PIMENTEL, D. R., REMONDINO, A., SAWYER, D. B. & COLUCCI, W. S. (2003) H(2)O(2) regulates cardiac myocyte phenotype via concentration-dependent activation of distinct kinase pathways. *J Mol Cell Cardiol,* 35, 615-21.

LAHTEENVUO, J. E., LAHTEENVUO, M. T., KIVELA, A., ROSENLEW, C., FALKEVALL, A., KLAR, J., HEIKURA, T., RISSANEN, T. T., VAHAKANGAS, E., KORPISALO, P., ENHOLM, B., CARMELIET, P., ALITALO, K., ERIKSSON, U. & YLA-HERTTUALA, S. (2009) Vascular endothelial growth factor-B induces myocardium-specific angiogenesis and arteriogenesis via vascular endothelial growth factor receptor-1- and neuropilin receptor-1-dependent mechanisms. *Circulation,* 119, 845-56.

LAMB, P., SEIDEL, H. M., HASLAM, J., MILOCCO, L., KESSLER, L. V., STEIN, R. B. & ROSEN, J. (1995) STAT protein complexes activated by interferon-gamma and gp130 signaling molecules differ in their sequence preferences and transcriptional induction properties. *Nucleic Acids Res,* 23, 3283-9.

LAUGWITZ, K. L., MORETTI, A., WEIG, H. J., GILLITZER, A., PINKERNELL, K., OTT, T., PRAGST, I., STADELE, C., SEYFARTH, M., SCHOMIG, A. & UNGERER, M. (2001) Blocking caspase-activated apoptosis improves contractility in failing myocardium. *Hum Gene Ther,* 12, 2051-63.

LEE, C., PIAZZA, F., BRUTSAERT, S., VALENS, J., STREHLOW, I., JAROSINSKI, M., SARIS, C. & SCHINDLER, C. (1999) Characterization of the Stat5 protease. *J Biol Chem,* 274, 26767-75.

LEVY, D. E. & DARNELL, J. E., JR. (2002) Stats: transcriptional control and biological impact. *Nat Rev Mol Cell Biol,* 3, 651-62.

LEVY, D. E. & LEE, C. K. (2002) What does Stat3 do? *J Clin Invest,* 109, 1143-8.

LI, H., ZHU, H., XU, C. J. & YUAN, J. (1998) Cleavage of BID by caspase 8 mediates the mitochondrial damage in the Fas pathway of apoptosis. *Cell,* 94, 491-501.

LI, L., CHEUNG, S. H., EVANS, E. L. & SHAW, P. E. Modulation of gene expression and tumor cell growth by redox modification of STAT3. *Cancer Res,* 70, 8222-32.

LI, L., CHEUNG, S. H., EVANS, E. L. & SHAW, P. E. (2010) Modulation of gene expression and tumor cell growth by redox modification of STAT3. *Cancer Res,* 70, 8222-32.

LI, L. & SHAW, P. E. (2006) Elevated activity of STAT3C due to higher DNA binding affinity of phosphotyrosine dimer rather than covalent dimer formation. *J Biol Chem,* 281, 33172-81.

LI, P., NIJHAWAN, D., BUDIHARDJO, I., SRINIVASULA, S. M., AHMAD, M., ALNEMRI, E. S. & WANG, X. (1997a) Cytochrome c and dATP-dependent formation of Apaf-1/caspase-9 complex initiates an apoptotic protease cascade. *Cell,* 91, 479-89.

LI, W., ZHANG, J., BOTTARO, D. P. & PIERCE, J. H. (1997b) Identification of serine 643 of protein kinase C-delta as an important autophosphorylation site for its enzymatic activity. *J Biol Chem,* 272, 24550-5.

LI, Y., HUANG, T. T., CARLSON, E. J., MELOV, S., URSELL, P. C., OLSON, J. L., NOBLE, L. J., YOSHIMURA, M. P., BERGER, C., CHAN, P. H., WALLACE, D. C. & EPSTEIN, C. J. (1995) Dilated cardiomyopathy and neonatal lethality in mutant mice lacking manganese superoxide dismutase. *Nat Genet,* 11, 376-81.

LI, Y., ZHANG, H., LIAO, W., SONG, Y., MA, X., CHEN, C., LU, Z., LI, Z. & ZHANG, Y. (2011) Transactivated EGFR mediates alpha-AR-induced STAT3 activation and cardiac hypertrophy. *Am J Physiol Heart Circ Physiol,* 301, H1941-51.

LIM, C. P. & CAO, X. (1999) Serine phosphorylation and negative regulation of Stat3 by JNK. *J Biol Chem,* 274, 31055-61.

LIM, H., FALLAVOLLITA, J. A., HARD, R., KERR, C. W. & CANTY, J. M., JR. (1999) Profound apoptosis-mediated regional myocyte loss and compensatory hypertrophy in pigs with hibernating myocardium. *Circulation,* 100, 2380-6.

LIPPI, G., FRANCHINI, M. & TARGHER, G. (2011) Arterial thrombus formation in cardiovascular disease. *Nat Rev Cardiol,* 8, 502-12.

LIU, B., LIAO, J., RAO, X., KUSHNER, S. A., CHUNG, C. D., CHANG, D. D. & SHUAI, K. (1998) Inhibition of Stat1-mediated gene activation by PIAS1. *Proc Natl Acad Sci U S A,* 95, 10626-31.

LIU, G. S., THORNTON, J., VAN WINKLE, D. M., STANLEY, A. W., OLSSON, R. A. & DOWNEY, J. M. (1991) Protection against infarction afforded by preconditioning is mediated by A1 adenosine receptors in rabbit heart. *Circulation,* 84, 350-6.

LIU, M., ZHANG, P., CHEN, M., ZHANG, W., YU, L., YANG, X. C. & FAN, Q. (2011) Aging might increase myocardial ischemia / reperfusion-induced apoptosis in humans and rats. *Age (Dordr).*

LIU, X., KIM, C. N., YANG, J., JEMMERSON, R. & WANG, X. (1996) Induction of apoptotic program in cell-free extracts: requirement for dATP and cytochrome c. *Cell,* 86, 147-57.

LOSCHEN, G., AZZI, A., RICHTER, C. & FLOHE, L. (1974) Superoxide radicals as precursors of mitochondrial hydrogen peroxide. *FEBS Lett,* 42, 68-72.

LOSCHEN, G., FLOHE, L. & CHANCE, B. (1971) Respiratory chain linked H(2)O(2) production in pigeon heart mitochondria. *FEBS Lett,* 18, 261-264.

LU, Y., ZHOU, J., XU, C., LIN, H., XIAO, J., WANG, Z. & YANG, B. (2008) JAK/STAT and PI3K/AKT pathways form a mutual transactivation loop and afford resistance to oxidative stress-induced apoptosis in cardiomyocytes. *Cell Physiol Biochem,* 21, 305-14.

LUO, X., BUDIHARDJO, I., ZOU, H., SLAUGHTER, C. & WANG, X. (1998) Bid, a Bcl2 interacting protein, mediates cytochrome c release from mitochondria in response to activation of cell surface death receptors. *Cell,* 94, 481-90.

MACMILLAN-CROW, L. A., CROW, J. P. & THOMPSON, J. A. (1998) Peroxynitrite-mediated inactivation of manganese superoxide dismutase involves nitration and oxidation of critical tyrosine residues. *Biochemistry,* 37, 1613-22.

MAK, T. W. & YEH, W. C. (2002) Signaling for survival and apoptosis in the immune system. *Arthritis Res,* 4 Suppl 3, S243-52.

MARIN-GARCIA, J. & GOLDENTHAL, M. J. (2002) Understanding the impact of mitochondrial defects in cardiovascular disease: a review. *J Card Fail,* 8, 347-61.

MARRERO, M. B., SCHIEFFER, B., PAXTON, W. G., HEERDT, L., BERK, B. C., DELAFONTAINE, P. & BERNSTEIN, K. E. (1995) Direct stimulation of Jak/STAT pathway by the angiotensin II AT1 receptor. *Nature,* 375, 247-50.

MARTIN, M. E., CHINENOV, Y., YU, M., SCHMIDT, T. K. & YANG, X. Y. (1996) Redox regulation of GA-binding protein-alpha DNA binding activity. *J Biol Chem,* 271, 25617-23.

MARZETTI, E., HWANG, J. C., LEES, H. A., WOHLGEMUTH, S. E., DUPONT-VERSTEEGDEN, E. E., CARTER, C. S., BERNABEI, R. & LEEUWENBURGH, C. (2009) Mitochondrial death effectors: relevance to sarcopenia and disuse muscle atrophy. *Biochim Biophys Acta,* 1800, 235-44.

MATSUMOTO, A., MASUHARA, M., MITSUI, K., YOKOUCHI, M., OHTSUBO, M., MISAWA, H., MIYAJIMA, A. & YOSHIMURA, A. (1997) CIS, a cytokine inducible SH2 protein, is a target of the JAK-STAT5 pathway and modulates STAT5 activation. *Blood,* 89, 3148-54.

MATTA, C., JUHASZ, T., SZIJGYARTO, Z., KOLOZSVARI, B., SOMOGYI, C., NAGY, G., GERGELY, P. & ZAKANY, R. (2011) PKCdelta is a positive regulator of chondrogenesis in chicken high density micromass cell cultures. *Biochimie,* 93, 149-59.

MATTSON, M. P. (2000) Apoptosis in neurodegenerative disorders. *Nat Rev Mol Cell Biol,* 1, 120-9.

MAYR, M., METZLER, B., CHUNG, Y. L., MCGREGOR, E., MAYR, U., TROY, H., HU, Y., LEITGES, M., PACHINGER, O., GRIFFITHS, J. R., DUNN, M. J. & XU, Q. (2004) Ischemic preconditioning exaggerates cardiac damage in PKC-delta null mice. *Am J Physiol Heart Circ Physiol,* 287, H946-56.

MCBRIDE, H. M., NEUSPIEL, M. & WASIAK, S. (2006) Mitochondria: more than just a powerhouse. *Curr Biol,* 16, R551-60.

MCDONALD, C. & REICH, N. C. (1999) Cooperation of the transcriptional coactivators CBP and p300 with Stat6. *J Interferon Cytokine Res,* 19, 711-22.

MCGILL, H. C., JR., MCMAHAN, C. A., HERDERICK, E. E., ZIESKE, A. W., MALCOM, G. T., TRACY, R. E. & STRONG, J. P. (2002) Obesity accelerates the progression of coronary atherosclerosis in young men. *Circulation,* 105, 2712-8.

MCNEILL, L. A., HEWITSON, K. S., GLEADLE, J. M., HORSFALL, L. E., OLDHAM, N. J., MAXWELL, P. H., PUGH, C. W., RATCLIFFE, P. J. & SCHOFIELD, C. J. (2002) The use of dioxygen by HIF prolyl hydroxylase (PHD1). *Bioorg Med Chem Lett,* 12, 1547-50.

MCWHINNEY, C. D., HUNT, R. A., CONRAD, K. M., DOSTAL, D. E. & BAKER, K. M. (1997) The type I angiotensin II receptor couples to Stat1 and Stat3 activation through Jak2 kinase in neonatal rat cardiac myocytes. *J Mol Cell Cardiol,* 29, 2513-24.

MEDICALSYMPTOMSGUIDE (2009) Atherosclerosis symptoms.

MELLOR, H. & PARKER, P. J. (1998) The extended protein kinase C superfamily. *Biochem J,* 332 (Pt 2), 281-92.

MENG, T. C., FUKADA, T. & TONKS, N. K. (2002) Reversible oxidation and inactivation of protein tyrosine phosphatases in vivo. *Mol Cell,* 9, 387-99.

MEYER, T., MARG, A., LEMKE, P., WIESNER, B. & VINKEMEIER, U. (2003) DNA binding controls inactivation and nuclear accumulation of the transcription factor Stat1. *Genes Dev,* 17, 1992-2005.

MINEGISHI, Y., SAITO, M., TSUCHIYA, S., TSUGE, I., TAKADA, H., HARA, T., KAWAMURA, N., ARIGA, T., PASIC, S., STOJKOVIC, O., METIN, A. & KARASUYAMA, H. (2007) Dominant-negative mutations in the DNA-binding domain of STAT3 cause hyper-IgE syndrome. *Nature,* 448, 1058-62.

MOCANU, M. M., BELL, R. M. & YELLON, D. M. (2002) PI3 kinase and not p42/p44 appears to be implicated in the protection conferred by ischemic preconditioning. *J Mol Cell Cardiol,* 34, 661-8.

MOWEN, K. A., TANG, J., ZHU, W., SCHURTER, B. T., SHUAI, K., HERSCHMAN, H. R. & DAVID, M. (2001) Arginine methylation of STAT1 modulates IFNalpha/beta-induced transcription. *Cell,* 104, 731-41.

MUI, A. L., WAKAO, H., O'FARRELL, A. M., HARADA, N. & MIYAJIMA, A. (1995) Interleukin-3, granulocyte-macrophage colony stimulating factor and interleukin-5 transduce signals through two STAT5 homologs. *EMBO J,* 14, 1166-75.

MURPHY, M. P. (2009) How mitochondria produce reactive oxygen species. *Biochem J,* 417, 1-13.

MURRIEL, C. L., CHURCHILL, E., INAGAKI, K., SZWEDA, L. I. & MOCHLY-ROSEN, D. (2004) Protein kinase Cdelta activation induces apoptosis in response to cardiac ischemia and reperfusion damage: a mechanism involving BAD and the mitochondria. *J Biol Chem,* 279, 47985-91.

MURRY, C. E., JENNINGS, R. B. & REIMER, K. A. (1986) Preconditioning with ischemia: a delay of lethal cell injury in ischemic myocardium. *Circulation,* 74, 1124-36.

NAKA, T., NARAZAKI, M., HIRATA, M., MATSUMOTO, T., MINAMOTO, S., AONO, A., NISHIMOTO, N., KAJITA, T., TAGA, T., YOSHIZAKI, K., AKIRA, S. & KISHIMOTO, T. (1997) Structure and function of a new STAT-induced STAT inhibitor. *Nature,* 387, 924-9.

NAKAJIMA, K., YAMANAKA, Y., NAKAE, K., KOJIMA, H., ICHIBA, M., KIUCHI, N., KITAOKA, T., FUKADA, T., HIBI, M. & HIRANO, T. (1996) A central role for Stat3 in IL-6-induced regulation of growth and differentiation in M1 leukemia cells. *EMBO J,* 15, 3651-8.

NANDI, D., TAHILIANI, P., KUMAR, A. & CHANDU, D. (2006) The ubiquitin-proteasome system. *J Biosci,* 31, 137-55.

NEEL, B. G., GU, H. & PAO, L. (2003) The 'Shp'ing news: SH2 domain-containing tyrosine phosphatases in cell signaling. *Trends Biochem Sci,* 28, 284-93.

NEGORO, S., KUNISADA, K., FUJIO, Y., FUNAMOTO, M., DARVILLE, M. I., EIZIRIK, D. L., OSUGI, T., IZUMI, M., OSHIMA, Y., NAKAOKA, Y., HIROTA, H., KISHIMOTO, T. & YAMAUCHI-TAKIHARA, K. (2001) Activation of signal transducer and activator of transcription 3 protects cardiomyocytes from hypoxia/reoxygenation-induced oxidative stress through the upregulation of manganese superoxide dismutase. *Circulation,* 104, 979-81.

NICHOLSON, S. E., WILLSON, T. A., FARLEY, A., STARR, R., ZHANG, J. G., BACA, M., ALEXANDER, W. S., METCALF, D., HILTON, D. J. & NICOLA, N. A. (1999) Mutational analyses of the SOCS proteins suggest a dual domain requirement but distinct mechanisms for inhibition of LIF and IL-6 signal transduction. *EMBO J,* 18, 375-85.

NIJHAWAN, D., FANG, M., TRAER, E., ZHONG, Q., GAO, W., DU, F. & WANG, X. (2003) Elimination of Mcl-1 is required for the initiation of apoptosis following ultraviolet irradiation. *Genes Dev,* 17, 1475-86.

NOVICK, D., COHEN, B. & RUBINSTEIN, M. (1994) The human interferon alpha/beta receptor: characterization and molecular cloning. *Cell,* 77, 391-400.

OKAMURA, T., MIURA, T., TAKEMURA, G., FUJIWARA, H., IWAMOTO, H., KAWAMURA, S., KIMURA, M., IKEDA, Y., IWATATE, M. & MATSUZAKI, M. (2000) Effect of caspase inhibitors on myocardial infarct size and myocyte DNA fragmentation in the ischemia-reperfused rat heart. *Cardiovasc Res,* 45, 642-50.

OLAYIOYE, M. A., BEUVINK, I., HORSCH, K., DALY, J. M. & HYNES, N. E. (1999) ErbB receptor-induced activation of stat transcription factors is mediated by Src tyrosine kinases. *J Biol Chem,* 274, 17209-18.

OLIVETTI, G., ABBI, R., QUAINI, F., KAJSTURA, J., CHENG, W., NITAHARA, J. A., QUAINI, E., DI LORETO, C., BELTRAMI, C. A., KRAJEWSKI, S., REED, J. C. & ANVERSA, P. (1997) Apoptosis in the failing human heart. *N Engl J Med,* 336, 1131-41.

OLIVETTI, G., QUAINI, F., SALA, R., LAGRASTA, C., CORRADI, D., BONACINA, E., GAMBERT, S. R., CIGOLA, E. & ANVERSA, P. (1996) Acute myocardial infarction in humans is associated with activation of programmed myocyte cell death in the surviving portion of the heart. *J Mol Cell Cardiol,* 28, 2005-16.

OSHIMA, Y., FUJIO, Y., NAKANISHI, T., ITOH, N., YAMAMOTO, Y., NEGORO, S., TANAKA, K., KISHIMOTO, T., KAWASE, I. & AZUMA, J. (2005) STAT3 mediates cardioprotection against ischemia/reperfusion injury through metallothionein induction in the heart. *Cardiovasc Res,* 65, 428-35.

OTTAVIANI, G., LAVEZZI, A. M., ROSSI, L. & MATTURRI, L. (1999) Proliferating cell nuclear antigen (PCNA) and apoptosis in hyperacute and acute myocardial infarction. *Eur J Histochem,* 43, 7-14.

PARK, S. J., KIM, H. Y., KIM, H., PARK, S. M., JOE, E. H., JOU, I. & CHOI, Y. H. (2009) Oxidative stress induces lipid-raft-mediated activation of Src homology 2 domain-containing protein-tyrosine phosphatase 2 in astrocytes. *Free Radic Biol Med,* 46, 1694-702.

PASTORE, A., PIEMONTE, F., LOCATELLI, M., LO RUSSO, A., GAETA, L. M., TOZZI, G. & FEDERICI, G. (2001) Determination of blood total, reduced, and oxidized glutathione in pediatric subjects. *Clin Chem,* 47, 1467-9.

PAUKKU, K., VALGEIRSDOTTIR, S., SAHARINEN, P., BERGMAN, M., HELDIN, C. H. & SILVENNOINEN, O. (2000) Platelet-derived growth factor (PDGF)-induced activation of signal transducer and activator of transcription (Stat) 5 is mediated by PDGF beta-receptor and is not dependent on c-src, fyn, jak1 or jak2 kinases. *Biochem J,* 345 Pt 3, 759-66.

PAULSON, M., PISHARODY, S., PAN, L., GUADAGNO, S., MUI, A. L. & LEVY, D. E. (1999) Stat protein transactivation domains recruit p300/CBP through widely divergent sequences. *J Biol Chem,* 274, 25343-9.

PERLMAN, H., PAGLIARI, L. J., LIU, H., KOCH, A. E., HAINES, G. K., 3RD & POPE, R. M. (2001) Rheumatoid arthritis synovial macrophages express the Fas-associated death domain-like interleukin-1beta-converting enzyme-inhibitory protein and are refractory to Fas-mediated apoptosis. *Arthritis Rheum,* 44, 21-30.

PHILLIPS, D., REILLEY, M. J., APONTE, A. M., WANG, G., BOJA, E., GUCEK, M. & BALABAN, R. S. (2010) Stoichiometry of STAT3 and mitochondrial proteins: Implications for the regulation of oxidative phosphorylation by protein-protein interactions. *J Biol Chem,* 285, 23532-6.

PODEWSKI, E. K., HILFIKER-KLEINER, D., HILFIKER, A., MORAWIETZ, H., LICHTENBERG, A., WOLLERT, K. C. & DREXLER, H. (2003) Alterations in Janus kinase (JAK)-signal transducers and activators of transcription (STAT) signaling in patients with end-stage dilated cardiomyopathy. *Circulation,* 107, 798-802.

PRANADA, A. L., METZ, S., HERRMANN, A., HEINRICH, P. C. & MULLER-NEWEN, G. (2004) Real time analysis of STAT3 nucleocytoplasmic shuttling. *J Biol Chem,* 279, 15114-23.

PRIDGEON, J. W., OLZMANN, J. A., CHIN, L. S. & LI, L. (2007) PINK1 protects against oxidative stress by phosphorylating mitochondrial chaperone TRAP1. *PLoS Biol,* 5, e172.

PUGH, C. W., TAN, C. C., JONES, R. W. & RATCLIFFE, P. J. (1991) Functional analysis of an oxygen-regulated transcriptional enhancer lying 3' to the mouse erythropoietin gene. *Proc Natl Acad Sci U S A,* 88, 10553-7.

QIU, H., LIZANO, P., LAURE, L., SUI, X., RASHED, E., PARK, J. Y., HONG, C., GAO, S., HOLLE, E., MORIN, D., DHAR, S. K., WAGNER, T., BERDEAUX, A., TIAN, B., VATNER, S. F. & DEPRE, C. (2011) H11 kinase/heat shock protein 22 deletion impairs both nuclear and mitochondrial functions of STAT3 and accelerates the transition into heart failure on cardiac overload. *Circulation,* 124, 406-15.

RAJEWSKY, K., GU, H., KUHN, R., BETZ, U. A., MULLER, W., ROES, J. & SCHWENK, F. (1996) Conditional gene targeting. *J Clin Invest,* 98, 600-3.

RAY, S., BOLDOGH, I. & BRASIER, A. R. (2005) STAT3 NH2-terminal acetylation is activated by the hepatic acute-phase response and required for IL-6 induction of angiotensinogen. *Gastroenterology,* 129, 1616-32.

REDDY, E. P., KORAPATI, A., CHATURVEDI, P. & RANE, S. (2000) IL-3 signaling and the role of Src kinases, JAKs and STATs: a covert liaison unveiled. *Oncogene,* 19, 2532-47.

RISTER, M. & BAEHNER, R. L. (1976) The alteration of superoxide dismutase, catalase, glutathione peroxidase, and NAD(P)H cytochrome c reductase in guinea pig polymorphonuclear leukocytes and alveolar macrophages during hyperoxia. *J Clin Invest,* 58, 1174-84.

ROBIN, M. A., PRABU, S. K., RAZA, H., ANANDATHEERTHAVARADA, H. K. & AVADHANI, N. G. (2003) Phosphorylation enhances mitochondrial targeting of GSTA4-4 through increased affinity for binding to cytoplasmic Hsp70. *J Biol Chem,* 278, 18960-70.

ROSSE, C., LINCH, M., KERMORGANT, S., CAMERON, A. J., BOECKELER, K. & PARKER, P. J. (2010) PKC and the control of localized signal dynamics. *Nat Rev Mol Cell Biol,* 11, 103-12.

ROSSI, F. & ZATTI, M. (1964) Biochemical aspects of phagocytosis in polymorphonuclear leucocytes. NADH and NADPH oxidation by the granules of resting and phagocytizing cells. *Experientia,* 20, 21-3.

RUDNICKI, M. A., JACKOWSKI, G., SAGGIN, L. & MCBURNEY, M. W. (1990) Actin and myosin expression during development of cardiac muscle from cultured embryonal carcinoma cells. *Dev Biol,* 138, 348-58.

SABBAH, H. N., SHAROV, V., RIDDLE, J. M., KONO, T., LESCH, M. & GOLDSTEIN, S. (1992) Mitochondrial abnormalities in myocardium of dogs with chronic heart failure. *J Mol Cell Cardiol,* 24, 1333-47.

SABIA, P. J., POWERS, E. R., RAGOSTA, M., SAREMBOCK, I. J., BURWELL, L. R. & KAUL, S. (1992) An association between collateral blood flow and myocardial viability in patients with recent myocardial infarction. *N Engl J Med,* 327, 1825-31.

SAFRAN, M. & KAELIN, W. G., JR. (2003) HIF hydroxylation and the mammalian oxygen-sensing pathway. *J Clin Invest,* 111, 779-83.

SANDIN, A., DAGNELL, M., GONON, A., PERNOW, J., STANGL, V., ASPENSTROM, P., KAPPERT, K. & OSTMAN, A. (2011) Hypoxia followed by re-oxygenation induces oxidation of tyrosine phosphatases. *Cell Signal,* 23, 820-6.

SANO, S., ITAMI, S., TAKEDA, K., TARUTANI, M., YAMAGUCHI, Y., MIURA, H., YOSHIKAWA, K., AKIRA, S. & TAKEDA, J. (1999) Keratinocyte-specific ablation of Stat3 exhibits impaired skin remodeling, but does not affect skin morphogenesis. *EMBO J,* 18, 4657-68.

SARASTE, A., PULKKI, K., KALLAJOKI, M., HENRIKSEN, K., PARVINEN, M. & VOIPIO-PULKKI, L. M. (1997) Apoptosis in human acute myocardial infarction. *Circulation,* 95, 320-3.

SATO, N., YAMAMOTO, T., SEKINE, Y., YUMIOKA, T., JUNICHO, A., FUSE, H. & MATSUDA, T. (2003) Involvement of heat-shock protein 90 in the interleukin-6-mediated signaling pathway through STAT3. *Biochem Biophys Res Commun,* 300, 847-52.

SCARBOROUGH, P., BHATNAGAR, P., WICKRAMASINGHE, K., SMOLINA, K., MITCHELL, C., RAYNER, M. (2010) Coronary heart disease statistics 2010 edition. *British Heart Foundation: London.*

SCHAEFER, L. K., REN, Z., FULLER, G. N. & SCHAEFER, T. S. (2002) Constitutive activation of Stat3alpha in brain tumors: localization to tumor endothelial cells and activation by the endothelial tyrosine kinase receptor (VEGFR-2). *Oncogene,* 21, 2058-65.

SCHAEFER, T. S., SANDERS, L. K. & NATHANS, D. (1995) Cooperative transcriptional activity of Jun and Stat3 beta, a short form of Stat3. *Proc Natl Acad Sci U S A,* 92, 9097-101.

SCHINDLER, C. & DARNELL, J. E., JR. (1995) Transcriptional responses to polypeptide ligands: the JAK-STAT pathway. *Annu Rev Biochem,* 64, 621-51.

SCHINDLER, C., FU, X. Y., IMPROTA, T., AEBERSOLD, R. & DARNELL, J. E., JR. (1992a) Proteins of transcription factor ISGF-3: one gene encodes the 91-and 84-kDa ISGF-3 proteins that are activated by interferon alpha. *Proc Natl Acad Sci U S A,* 89, 7836-9.

SCHINDLER, C., SHUAI, K., PREZIOSO, V. R. & DARNELL, J. E., JR. (1992b) Interferon-dependent tyrosine phosphorylation of a latent cytoplasmic transcription factor. *Science,* 257, 809-13.

SCHMIDT, D. & MULLER, S. (2003) PIAS/SUMO: new partners in transcriptional regulation. *Cell Mol Life Sci,* 60, 2561-74.

SCHRADER, M. & FAHIMI, H. D. (2004) Mammalian peroxisomes and reactive oxygen species. *Histochem Cell Biol,* 122, 383-93.

SEARLE, J., KERR, J. F. & BISHOP, C. J. (1982) Necrosis and apoptosis: distinct modes of cell death with fundamentally different significance. *Pathol Annu,* 17 Pt 2, 229-59.

SEKIYA, M., HIRAISHI, A., TOUYAMA, M. & SAKAMOTO, K. (2008) Oxidative stress induced lipid accumulation via SREBP1c activation in HepG2 cells. *Biochem Biophys Res Commun,* 375, 602-7.

SELZER, A. (1992) *Understanding heart disease,* Berkeley and Los Angeles, California.

SEMENZA, G. L. (2004) O2-regulated gene expression: transcriptional control of cardiorespiratory physiology by HIF-1. *J Appl Physiol,* 96, 1173-7; discussion 1170-2.

SETATI, M. M., PRINSLOO, E., LONGSHAW, V. M., MURRAY, P. A., EDGAR, D. H. & BLATCH, G. L. (2010) Leukemia inhibitory factor promotes Hsp90 association with STAT3 in mouse embryonic stem cells. *IUBMB Life,* 62, 61-6.

SHANKARANARAYANAN, P., CHAITIDIS, P., KUHN, H. & NIGAM, S. (2001) Acetylation by histone acetyltransferase CREB-binding protein/p300 of STAT6 is required for transcriptional activation of the 15-lipoxygenase-1 gene. *J Biol Chem,* 276, 42753-60.

SHAROV, V. G., GOUSSEV, A., LESCH, M., GOLDSTEIN, S. & SABBAH, H. N. (1998) Abnormal mitochondrial function in myocardium of dogs with chronic heart failure. *J Mol Cell Cardiol,* 30, 1757-62.

SHELTON, S. J. (2009) A role for Serum Response Factor in the phenotypic maintenance and survival of cardiomyocytes following exposure to hypoxia. *Thesis submitted to the University of Nottingham.*

SHEN, Y., SCHLESSINGER, K., ZHU, X., MEFFRE, E., QUIMBY, F., LEVY, D. E. & DARNELL, J. E., JR. (2004) Essential role of STAT3 in postnatal survival and growth revealed by mice lacking STAT3 serine 727 phosphorylation. *Mol Cell Biol,* 24, 407-19.

SHERMAN, M. A., SECOR, V. H. & BROWN, M. A. (1999) IL-4 preferentially activates a novel STAT6 isoform in mast cells. *J Immunol,* 162, 2703-8.

SHUAI, K., HORVATH, C. M., HUANG, L. H., QURESHI, S. A., COWBURN, D. & DARNELL, J. E., JR. (1994) Interferon activation of the transcription factor Stat91 involves dimerization through SH2-phosphotyrosyl peptide interactions. *Cell,* 76, 821-8.

SHUAI, K. & LIU, B. (2003) Regulation of JAK-STAT signalling in the immune system. *Nat Rev Immunol,* 3, 900-11.

SHUAI, K. & LIU, B. (2005) Regulation of gene-activation pathways by PIAS proteins in the immune system. *Nat Rev Immunol,* 5, 593-605.

SHUAI, K., SCHINDLER, C., PREZIOSO, V. R. & DARNELL, J. E., JR. (1992) Activation of transcription by IFN-gamma: tyrosine phosphorylation of a 91-kD DNA binding protein. *Science,* 258, 1808-12.

SILVENNOINEN, O., SCHINDLER, C., SCHLESSINGER, J. & LEVY, D. E. (1993) Ras-independent growth factor signaling by transcription factor tyrosine phosphorylation. *Science,* 261, 1736-9.

SIMON, A. R., RAI, U., FANBURG, B. L. & COCHRAN, B. H. (1998) Activation of the JAK-STAT pathway by reactive oxygen species. *Am J Physiol,* 275, C1640-52.

SIWIK, D. A., TZORTZIS, J. D., PIMENTAL, D. R., CHANG, D. L., PAGANO, P. J., SINGH, K., SAWYER, D. B. & COLUCCI, W. S. (1999) Inhibition of copper-zinc superoxide dismutase induces cell growth, hypertrophic phenotype, and apoptosis in neonatal rat cardiac myocytes in vitro. *Circ Res,* 85, 147-53.

SKERJANC, I. S. (1999) Cardiac and skeletal muscle development in P19 embryonal carcinoma cells. *Trends Cardiovasc Med,* 9, 139-43.

SMITH, R. M., SULEMAN, N., LACERDA, L., OPIE, L. H., AKIRA, S., CHIEN, K. R. & SACK, M. N. (2004) Genetic depletion of cardiac myocyte STAT-3 abolishes classical preconditioning. *Cardiovasc Res,* 63, 611-6.

SNYDER, M., HUANG, X. Y. & ZHANG, J. J. (2010) Stat3 directly controls the expression of Tbx5, Nkx2.5, and GATA4 and is essential for cardiomyocyte differentiation of P19CL6 cells. *J Biol Chem,* 285, 23639-46.

SOHAL, R. S. (2002) Role of oxidative stress and protein oxidation in the aging process. *Free Radic Biol Med,* 33, 37-44.

SOLTOFF, S. P. (2007) Rottlerin: an inappropriate and ineffective inhibitor of PKCdelta. *Trends Pharmacol Sci,* 28, 453-8.

SONNENBLICK, STROBECK J.E., CAPASSO J.M. & S.M., F. (1983) Ventricular hypertrophy: models and methods. *Perspectives in cardiovascular research,* 8, 13–20.

STADTMAN, E. R. (1995) Role of oxidized amino acids in protein breakdown and stability. *Methods Enzymol,* 258, 379-93.

STAMLER, J., NEATON, J. D. & WENTWORTH, D. N. (1989) Blood pressure (systolic and diastolic) and risk of fatal coronary heart disease. *Hypertension,* 13, I2-12.

STEINBERG, D., PARTHASARATHY, S., CAREW, T. E., KHOO, J. C. & WITZTUM, J. L. (1989) Beyond cholesterol. Modifications of low-density lipoprotein that increase its atherogenicity. *N Engl J Med,* 320, 915-24.

STEINBERG, S. F. (2008) Structural basis of protein kinase C isoform function. *Physiol Rev,* 88, 1341-78.

STEPHANOU, A. & LATCHMAN, D. S. (1999) Transcriptional regulation of the heat shock protein genes by STAT family transcription factors. *Gene Expr,* 7, 311-9.

STOUT, R. W. (1987) Ageing and atherosclerosis. *Age Ageing,* 16, 65-72.

SUGDEN, P. H. & CLERK, A. (2006) Oxidative stress and growth-regulating intracellular signaling pathways in cardiac myocytes. *Antioxid Redox Signal,* 8, 2111-24.

TAKAHASHI, T., SCHUNKERT, H., ISOYAMA, S., WEI, J. Y., NADAL-GINARD, B., GROSSMAN, W. & IZUMO, S. (1992) Age-related differences in the expression of proto-oncogene and contractile protein genes in response to pressure overload in the rat myocardium. *J Clin Invest,* 89, 939-46.

TAKEDA, K., CLAUSEN, B. E., KAISHO, T., TSUJIMURA, T., TERADA, N., FORSTER, I. & AKIRA, S. (1999) Enhanced Th1 activity and development of chronic enterocolitis in mice devoid of Stat3 in macrophages and neutrophils. *Immunity,* 10, 39-49.

TAKEDA, K., KAISHO, T., YOSHIDA, N., TAKEDA, J., KISHIMOTO, T. & AKIRA, S. (1998) Stat3 activation is responsible for IL-6-dependent T cell proliferation through preventing apoptosis: generation and characterization of T cell-specific Stat3-deficient mice. *J Immunol,* 161, 4652-60.

TAKEDA, K., NOGUCHI, K., SHI, W., TANAKA, T., MATSUMOTO, M., YOSHIDA, N., KISHIMOTO, T. & AKIRA, S. (1997) Targeted disruption of the mouse Stat3 gene leads to early embryonic lethality. *Proc Natl Acad Sci U S A,* 94, 3801-4.

TANG, H., YAN, C., CAO, J., SARMA, J. V., HAURA, E. B., WU, M. & GAO, H. (2011) An essential role for Stat3 in regulating IgG immune complex-induced pulmonary inflammation. *FASEB J,* 25, 4292-300.

TEN HOEVE, J., DE JESUS IBARRA-SANCHEZ, M., FU, Y., ZHU, W., TREMBLAY, M., DAVID, M. & SHUAI, K. (2002) Identification of a nuclear Stat1 protein tyrosine phosphatase. *Mol Cell Biol,* 22, 5662-8.

THAVEAU, F., ZOLL, J., ROUYER, O., CHAFKE, N., KRETZ, J. G., PIQUARD, F. & GENY, B. (2007) Ischemic preconditioning specifically restores complexes I and II activities of the mitochondrial respiratory chain in ischemic skeletal muscle. *J Vasc Surg,* 46, 541-7; discussion 547.

THOMPSON, C. B. (1995) Apoptosis in the pathogenesis and treatment of disease. *Science,* 267, 1456-62.

THORPE, P. E., HUNTER, W. J., 3RD, ZHAN, X. X., DOVGAN, P. S. & AGRAWAL, D. K. (1996) A noninjury, diet-induced swine model of atherosclerosis for cardiovascular-interventional research. *Angiology,* 47, 849-57.

TOLEDANO, M. B. & LEONARD, W. J. (1991) Modulation of transcription factor NF-kappa B binding activity by oxidation-reduction in vitro. *Proc Natl Acad Sci U S A,* 88, 4328-32.

TONG, H., CHEN, W., STEENBERGEN, C. & MURPHY, E. (2000) Ischemic preconditioning activates phosphatidylinositol-3-kinase upstream of protein kinase C. *Circ Res,* 87, 309-15.

TSAI, C. T., LAI, L. P., KUO, K. T., HWANG, J. J., HSIEH, C. S., HSU, K. L., TSENG, C. D., TSENG, Y. Z., CHIANG, F. T. & LIN, J. L. (2008) Angiotensin II activates signal transducer and activators of transcription 3 via Rac1 in atrial myocytes and fibroblasts: implication for the therapeutic effect of statin in atrial structural remodeling. *Circulation,* 117, 344-55.

TSUTSUI, H. (2001) Oxidative stress in heart failure: the role of mitochondria. *Intern Med,* 40, 1177-82.

TURKSON, J. (2004) STAT proteins as novel targets for cancer drug discovery. *Expert Opin Ther Targets,* 8, 409-22.

TURKSON, J., BOWMAN, T., ADNANE, J., ZHANG, Y., DJEU, J. Y., SEKHARAM, M., FRANK, D. A., HOLZMAN, L. B., WU, J., SEBTI, S. & JOVE, R. (1999) Requirement for Ras/Rac1-mediated p38 and c-

Jun N-terminal kinase signaling in Stat3 transcriptional activity induced by the Src oncoprotein. *Mol Cell Biol,* 19, 7519-28.

TURRENS, J. F. (2003) Mitochondrial formation of reactive oxygen species. *J Physiol,* 552, 335-44.

TURRENS, J. F. & BOVERIS, A. (1980) Generation of superoxide anion by the NADH dehydrogenase of bovine heart mitochondria. *Biochem J,* 191, 421-7.

UNGUREANU, D., SAHARINEN, P., JUNTTILA, I., HILTON, D. J. & SILVENNOINEN, O. (2002) Regulation of Jak2 through the ubiquitin-proteasome pathway involves phosphorylation of Jak2 on Y1007 and interaction with SOCS-1. *Mol Cell Biol,* 22, 3316-26.

UNGUREANU, D., VANHATUPA, S., KOTAJA, N., YANG, J., AITTOMAKI, S., JANNE, O. A., PALVIMO, J. J. & SILVENNOINEN, O. (2003) PIAS proteins promote SUMO-1 conjugation to STAT1. *Blood,* 102, 3311-3.

VAN DER HEYDEN, M. A. & DEFIZE, L. H. (2003) Twenty one years of P19 cells: what an embryonal carcinoma cell line taught us about cardiomyocyte differentiation. *Cardiovasc Res,* 58, 292-302.

VAN PUIJENBROEK, A. A., VAN DER SAAG, P. T. & COFFER, P. J. (1999) Cytokine signal transduction in P19 embryonal carcinoma cells: regulation of Stat3-mediated transactivation occurs independently of p21ras-Erk signaling. *Exp Cell Res,* 251, 465-76.

VANDEN HOEK, T. L., BECKER, L. B., SHAO, Z., LI, C. & SCHUMACKER, P. T. (1998) Reactive oxygen species released from mitochondria during brief hypoxia induce preconditioning in cardiomyocytes. *J Biol Chem,* 273, 18092-8.

VANDEN HOEK, T. L., LI, C., SHAO, Z., SCHUMACKER, P. T. & BECKER, L. B. (1997) Significant levels of oxidants are generated by isolated cardiomyocytes during ischemia prior to reperfusion. *J Mol Cell Cardiol,* 29, 2571-83.

VEALS, S. A., SCHINDLER, C., LEONARD, D., FU, X. Y., AEBERSOLD, R., DARNELL, J. E., JR. & LEVY, D. E. (1992) Subunit of an alpha-interferon-responsive transcription factor is related to interferon regulatory factor and Myb families of DNA-binding proteins. *Mol Cell Biol,* 12, 3315-24.

VIGNAIS, M. L. & GILMAN, M. (1999) Distinct mechanisms of activation of Stat1 and Stat3 by platelet-derived growth factor receptor in a cell-free system. *Mol Cell Biol,* 19, 3727-35.

VINKEMEIER, U., MOAREFI, I., DARNELL, J. E., JR. & KURIYAN, J. (1998) Structure of the amino-terminal protein interaction domain of STAT-4. *Science,* 279, 1048-52.

VON HARSDORF, R., LI, P. F. & DIETZ, R. (1999) Signaling pathways in reactive oxygen species-induced cardiomyocyte apoptosis. *Circulation,* 99, 2934-41.

WAGNER, B. J., HAYES, T. E., HOBAN, C. J. & COCHRAN, B. H. (1990) The SIF binding element confers sis/PDGF inducibility onto the c-fos promoter. *EMBO J,* 9, 4477-84.

WAKAO, H., GOUILLEUX, F. & GRONER, B. (1994) Mammary gland factor (MGF) is a novel member of the cytokine regulated transcription factor gene family and confers the prolactin response. *EMBO J,* 13, 2182-91.

WALLERSTEDT, E., SMITH, U. & ANDERSSON, C. X. (2010) Protein kinase C-delta is involved in the inflammatory effect of IL-6 in mouse adipose cells. *Diabetologia,* 53, 946-54.

WANG, D., MORIGGL, R., STRAVOPODIS, D., CARPINO, N., MARINE, J. C., TEGLUND, S., FENG, J. & IHLE, J. N. (2000) A small amphipathic alpha-helical region is required for transcriptional activities and proteasome-dependent turnover of the tyrosine-phosphorylated Stat5. *EMBO J,* 19, 392-9.

WANG, D., STRAVOPODIS, D., TEGLUND, S., KITAZAWA, J. & IHLE, J. N. (1996) Naturally occurring dominant negative variants of Stat5. *Mol Cell Biol,* 16, 6141-8.

WANG, G., QIAN, P., JACKSON, F. R., QIAN, G. & WU, G. (2008) Sequential activation of JAKs, STATs and xanthine dehydrogenase/oxidase by hypoxia in lung microvascular endothelial cells. *Int J Biochem Cell Biol,* 40, 461-70.

WANG, Y. & ASHRAF, M. (1999) Role of protein kinase C in mitochondrial KATP channel-mediated protection against Ca2+ overload injury in rat myocardium. *Circ Res,* 84, 1156-65.

WEBER, J. R. (1991) Left Ventricular Hypertrophy: Its Prevalence, Etiology, and Significance. *Clin. Cardiol.,* 14, 13-17.

WEBER, K. T. & BRILLA, C. G. (1991) Pathological hypertrophy and cardiac interstitium. Fibrosis and renin-angiotensin-aldosterone system. *Circulation,* 83, 1849-65.

WEGENKA, U. M., BUSCHMANN, J., LUTTICKEN, C., HEINRICH, P. C. & HORN, F. (1993) Acute-phase response factor, a nuclear factor binding to acute-phase response elements, is rapidly activated by interleukin-6 at the posttranslational level. *Mol Cell Biol,* 13, 276-88.

WEGRZYN, J., POTLA, R., CHWAE, Y. J., SEPURI, N. B., ZHANG, Q., KOECK, T., DERECKA, M., SZCZEPANEK, K., SZELAG, M., GORNICKA, A., MOH, A., MOGHADDAS, S., CHEN, Q., BOBBILI, S., CICHY, J., DULAK, J., BAKER, D. P., WOLFMAN, A.,

STUEHR, D., HASSAN, M. O., FU, X. Y., AVADHANI, N., DRAKE, J. I., FAWCETT, P., LESNEFSKY, E. J. & LARNER, A. C. (2009) Function of mitochondrial Stat3 in cellular respiration. *Science,* 323, 793-7.

WEN, Z. & DARNELL, J. E., JR. (1997) Mapping of Stat3 serine phosphorylation to a single residue (727) and evidence that serine phosphorylation has no influence on DNA binding of Stat1 and Stat3. *Nucleic Acids Res,* 25, 2062-7.

WEN, Z., ZHONG, Z. & DARNELL, J. E., JR. (1995) Maximal activation of transcription by Stat1 and Stat3 requires both tyrosine and serine phosphorylation. *Cell,* 82, 241-50.

WHELAN, R. S., KAPLINSKIY, V. & KITSIS, R. N. (2010) Cell death in the pathogenesis of heart disease: mechanisms and significance. *Annu Rev Physiol,* 72, 19-44.

WHITE, F. C., CARROLL, S. M., MAGNET, A. & BLOOR, C. M. (1992) Coronary collateral development in swine after coronary artery occlusion. *Circ Res,* 71, 1490-500.

WHO (2008) *The global burden of sisease 2004 update.*

WIBOM, R., HAGENFELDT, L. & VON DOBELN, U. (2002) Measurement of ATP production and respiratory chain enzyme activities in mitochondria isolated from small muscle biopsy samples. *Anal Biochem,* 311, 139-51.

WITZTUM, J. L. & STEINBERG, D. (1991) Role of oxidized low density lipoprotein in atherogenesis. *J Clin Invest,* 88, 1785-92.

WOBUS, A. M., KLEPPISCH, T., MALTSEV, V. & HESCHELER, J. (1994) Cardiomyocyte-like cells differentiated in vitro from embryonic carcinoma cells P19 are characterized by functional expression of adrenoceptors and Ca2+ channels. *In Vitro Cell Dev Biol Anim,* 30A, 425-34.

WOETMANN, A., NIELSEN, M., CHRISTENSEN, S. T., BROCKDORFF, J., KALTOFT, K., ENGEL, A. M., SKOV, S., BRENDER, C., GEISLER, C., SVEJGAARD, A., RYGAARD, J., LEICK, V. & ODUM, N. (1999) Inhibition of protein phosphatase 2A induces serine/threonine phosphorylation, subcellular redistribution, and functional inhibition of STAT3. *Proc Natl Acad Sci U S A,* 96, 10620-5.

WYLLIE, A. H. (1997) Apoptosis and carcinogenesis. *Eur J Cell Biol,* 73, 189-97.

XIE, Y., KOLE, S., PRECHT, P., PAZIN, M. J. & BERNIER, M. (2009) S-glutathionylation impairs signal transducer and activator of transcription 3 activation and signaling. *Endocrinology,* 150, 1122-31.

XU, P., WANG, J., KODAVATIGANTI, R., ZENG, Y. & KASS, I. S. (2004) Activation of protein kinase C contributes to the isoflurane-induced improvement of functional and metabolic recovery in isolated ischemic rat hearts. *Anesth Analg,* 99, 993-1000, table of contents.

XU, X., SUN, Y. L. & HOEY, T. (1996) Cooperative DNA binding and sequence-selective recognition conferred by the STAT amino-terminal domain. *Science,* 273, 794-7.

XUAN, Y. T., GUO, Y., HAN, H., ZHU, Y. & BOLLI, R. (2001) An essential role of the JAK-STAT pathway in ischemic preconditioning. *Proc Natl Acad Sci U S A,* 98, 9050-5.

YAJIMA, D., MOTANI, H., HAYAKAWA, M., SATO, Y., SATO, K. & IWASE, H. (2009) The relationship between cell membrane damage and lipid peroxidation under the condition of hypoxia-reoxygenation: analysis of the mechanism using antioxidants and electron transport inhibitors. *Cell Biochem Funct,* 27, 338-43.

YAMAMOTO, K., QUELLE, F. W., THIERFELDER, W. E., KREIDER, B. L., GILBERT, D. J., JENKINS, N. A., COPELAND, N. G., SILVENNOINEN, O. & IHLE, J. N. (1994) Stat4, a novel gamma interferon activation site-binding protein expressed in early myeloid differentiation. *Mol Cell Biol,* 14, 4342-9.

YAMASHITA, H., XU, J., ERWIN, R. A., FARRAR, W. L., KIRKEN, R. A. & RUI, H. (1998) Differential control of the phosphorylation state of proline-juxtaposed serine residues Ser725 of Stat5a and Ser730 of Stat5b in prolactin-sensitive cells. *J Biol Chem,* 273, 30218-24.

YANG, B. C., ZANDER, D. S. & MEHTA, J. L. (1999a) Hypoxia-reoxygenation-induced apoptosis in cultured adult rat myocytes and the protective effect of platelets and transforming growth factor-beta(1). *J Pharmacol Exp Ther,* 291, 733-8.

YANG, E., WEN, Z., HASPEL, R. L., ZHANG, J. J. & DARNELL, J. E., JR. (1999b) The linker domain of Stat1 is required for gamma interferon-driven transcription. *Mol Cell Biol,* 19, 5106-12.

YANG, J., HUANG, J., DASGUPTA, M., SEARS, N., MIYAGI, M., WANG, B., CHANCE, M. R., CHEN, X., DU, Y., WANG, Y., AN, L., WANG, Q., LU, T., ZHANG, X., WANG, Z. & STARK; G. R. (2010) Reversible methylation of promoter-bound STAT3 by histone-modifying enzymes. *Proc Natl Acad Sci U S A,* 107, 21499-504.

YAOITA, H., OGAWA, K., MAEHARA, K. & MARUYAMA, Y. (1998) Attenuation of ischemia/reperfusion injury in rats by a caspase inhibitor. *Circulation,* 97, 276-81.

YASUKAWA, H., HOSHIJIMA, M., GU, Y., NAKAMURA, T., PRADERVAND, S., HANADA, T., HANAKAWA, Y., YOSHIMURA, A., ROSS, J., JR. & CHIEN, K. R. (2001) Suppressor

of cytokine signaling-3 is a biomechanical stress-inducible gene that suppresses gp130-mediated cardiac myocyte hypertrophy and survival pathways. *J Clin Invest,* 108, 1459-67.

YELLON, D. M. & DANA, A. (2000) The preconditioning phenomenon: A tool for the scientist or a clinical reality? *Circ Res,* 87, 543-50.

YOKOGAMI, K., WAKISAKA, S., AVRUCH, J. & REEVES, S. A. (2000) Serine phosphorylation and maximal activation of STAT3 during CNTF signaling is mediated by the rapamycin target mTOR. *Curr Biol,* 10, 47-50.

YOSHIDA, K. (2007) PKCdelta signaling: mechanisms of DNA damage response and apoptosis. *Cell Signal,* 19, 892-901.

YOUNG, L. H., BALIN, B. J. & WEIS, M. T. (2005) Go 6983: a fast acting protein kinase C inhibitor that attenuates myocardial ischemia/reperfusion injury. *Cardiovasc Drug Rev,* 23, 255-72.

YU, C. L. & BURAKOFF, S. J. (1997) Involvement of proteasomes in regulating Jak-STAT pathways upon interleukin-2 stimulation. *J Biol Chem,* 272, 14017-20.

YU, C. L., MEYER, D. J., CAMPBELL, G. S., LARNER, A. C., CARTER-SU, C., SCHWARTZ, J. & JOVE, R. (1995) Enhanced DNA-binding activity of a Stat3-related protein in cells transformed by the Src oncoprotein. *Science,* 269, 81-3.

YU, H. & JOVE, R. (2004) The STATs of cancer--new molecular targets come of age. *Nat Rev Cancer,* 4, 97-105.

YUE, H., LI, W., DESNOYER, R. & KARNIK, S. S. (2010) Role of nuclear unphosphorylated STAT3 in angiotensin II type 1 receptor-induced cardiac hypertrophy. *Cardiovasc Res,* 85, 90-9.

YUE, Y., QIN, Q., COHEN, M. V., DOWNEY, J. M. & CRITZ, S. D. (2002) The relative order of mK(ATP) channels, free radicals and p38 MAPK in preconditioning's protective pathway in rat heart. *Cardiovasc Res,* 55, 681-9.

ZHANG, J. J., VINKEMEIER, U., GU, W., CHAKRAVARTI, D., HORVATH, C. M. & DARNELL, J. E., JR. (1996) Two contact regions between Stat1 and CBP/p300 in interferon gamma signaling. *Proc Natl Acad Sci U S A,* 93, 15092-6.

ZHANG, J. J., ZHAO, Y., CHAIT, B. T., LATHEM, W. W., RITZI, M., KNIPPERS, R. & DARNELL, J. E., JR. (1998) Ser727-dependent recruitment of MCM5 by Stat1alpha in IFN-gamma-induced transcriptional activation. *EMBO J,* 17, 6963-71.

ZHANG, T., KEE, W. H., SEOW, K. T., FUNG, W. & CAO, X. (2000) The coiled-coil domain of Stat3 is essential for its SH2 domain-mediated

receptor binding and subsequent activation induced by epidermal growth factor and interleukin-6. *Mol Cell Biol,* 20, 7132-9.

ZHANG, X., BLENIS, J., LI, H. C., SCHINDLER, C. & CHEN-KIANG, S. (1995) Requirement of serine phosphorylation for formation of STAT-promoter complexes. *Science,* 267, 1990-4.

ZHANG, X., GUO, A., YU, J., POSSEMATO, A., CHEN, Y., ZHENG, W., POLAKIEWICZ, R. D., KINZLER, K. W., VOGELSTEIN, B., VELCULESCU, V. E. & WANG, Z. J. (2007) Identification of STAT3 as a substrate of receptor protein tyrosine phosphatase T. *Proc Natl Acad Sci U S A,* 104, 4060-4.

ZHANG, X., WRZESZCZYNSKA, M. H., HORVATH, C. M. & DARNELL, J. E., JR. (1999) Interacting regions in Stat3 and c-Jun that participate in cooperative transcriptional activation. *Mol Cell Biol,* 19, 7138-46.

ZHANG, Y., MARCILLAT, O., GIULIVI, C., ERNSTER, L. & DAVIES, K. J. (1990) The oxidative inactivation of mitochondrial electron transport chain components and ATPase. *J Biol Chem,* 265, 16330-6.

ZHAO, M., LIU, F., WANG, J. Y., ZHANG, W. Y., GAO, F. H. & JIANG, B. (2011) [Effects of JAK2/STAT3 signaling pathway on angiogenesis in non-small cell lung cancer]. *Zhonghua Yi Xue Za Zhi,* 91, 375-81.

ZHAO, X., HE, G., CHEN, Y. R., PANDIAN, R. P., KUPPUSAMY, P. & ZWEIER, J. L. (2005) Endothelium-derived nitric oxide regulates postischemic myocardial oxygenation and oxygen consumption by modulation of mitochondrial electron transport. *Circulation,* 111, 2966-72.

ZHONG, Z., WEN, Z. & DARNELL, J. E., JR. (1994) Stat3: a STAT family member activated by tyrosine phosphorylation in response to epidermal growth factor and interleukin-6. *Science,* 264, 95-8.

ZHOU, H., NEWNUM, A. B., MARTIN, J. R., LI, P., NELSON, M. T., MOH, A., FU, X. Y., YOKOTA, H. & LI, J. (2011) Osteoblast/osteocyte-specific inactivation of Stat3 decreases load-driven bone formation and accumulates reactive oxygen species. *Bone,* 49, 404-11.

ZHOU, L. & TOO, H. P. (2011) Mitochondrial localized STAT3 is involved in NGF induced neurite outgrowth. *PLoS One,* 6, e21680.

ZIMMERMAN, A. N. & HULSMANN, W. C. (1966) Paradoxical influence of calcium ions on the permeability of the cell membranes of the isolated rat heart. *Nature,* 211, 646-7.

ZOROV, D. B., JUHASZOVA, M. & SOLLOTT, S. J. (2006) Mitochondrial ROS-induced ROS release: an update and review. *Biochim Biophys Acta,* 1757, 509-17.

ZOU, Y., TAKANO, H., MIZUKAMI, M., AKAZAWA, H., QIN, Y., TOKO, H., SAKAMOTO, M., MINAMINO, T., NAGAI, T. & KOMURO, I. (2003) Leukemia inhibitory factor enhances survival of cardiomyocytes

and induces regeneration of myocardium after myocardial infarction. *Circulation,* 108, 748-53.

ZWEIER, J. L., FLAHERTY, J. T. & WEISFELDT, M. L. (1987) Direct measurement of free radical generation following reperfusion of ischemic myocardium. *Proc Natl Acad Sci U S A,* 84, 1404-7.

Appendices

Clone charts

Abbreviation: pRc/CMV STAT3^{Wt} Flag

Description: Mouse wild-type STAT3 cDNA expression vector. Diagnostic Restriction Digest with BamHI (3.2kb, 2.8kb, and 2.0kb)

Size: Vector: 5500bp

Insert: 2600bp

Resistances: Ampicillin

Bacterial Strain: NM522

Constructed by: (Horvath et al., 1995)

Method: Due to a stop codon error made when tagging the Stat3 clone with FLAG (DYKDDDDK) additional residues precede (SR) and follow the tag (GPYSIVSPKC STOP). The ApaI cloning site is GGG CCC, which encodes the G and P residues coming after the FLAG tag. Therefore, if the insert is removed with a NotI and ApaI digestion, it will not have a stop codon included.

Special Remarks: Diagnostic Restriction Digest with BamHI (3.2kb, 2.8kb, and 2.0kb).

Map:

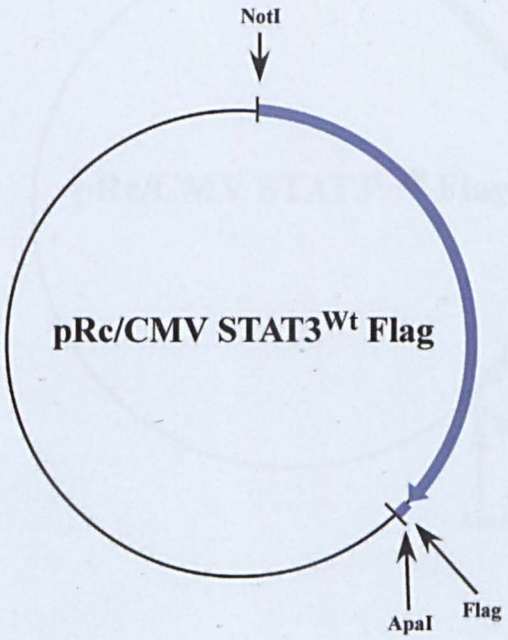

Abbreviation: pRc/CMV STAT3^{C3S} Flag

Description: Mouse STAT3 cDNA expression vector. C418S, C426S and C468S. Residues changed to serine render as redox-insenstive.

Size: Vector: 5500bp

Insert: 2600bp

Resistances: Ampicillin

Bacterial Strain: NM522

Constructed by: (Li et al., 2010)

Method: Due to a stop codon error made when tagging the Stat3 clone with FLAG (DYKDDDDK) additional residues precede (SR) and follow the tag (GPYSIVSPKC STOP). The ApaI cloning site is GGG CCC, which encodes the G and P residues coming after the FLAG tag. Therefore, if the insert is removed with a NotI and ApaI digestion, it will not have a stop codon included. C418S, C426S and C468S mutations were introduced into the pRc/CMV STAT3^{wt} Flag vector via site-directed mutagenesis.

Special Remarks: Diagnostic Restriction Digest with BamHI (3.2kb, 2.8kb, and 2.0kb).

Map:

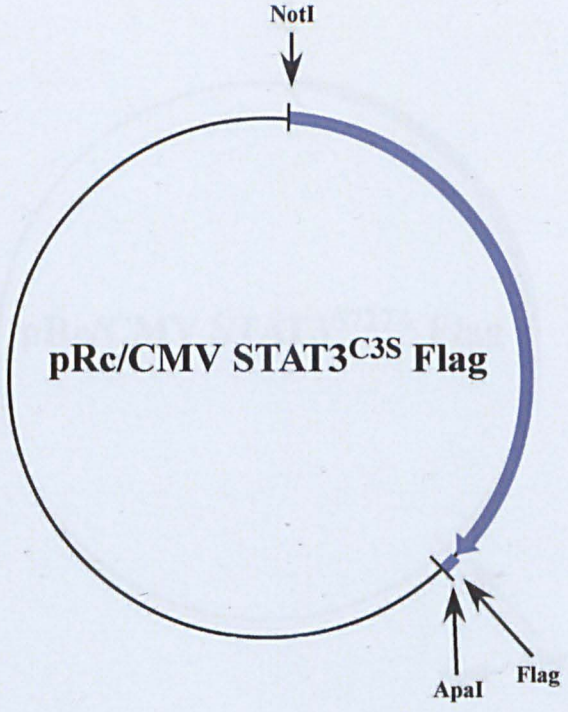

Abbreviation: pRc/CMV STAT3^{S727A} Flag

Description: Mouse STAT3 cDNA expression vector. Residues changed to Ala prevent serine phosphorylation of this molelcule.

Size: Vector: 5500bp

Insert: 2600bp

Resistances: Ampicillin

Bacterial Strain: NM522

Constructed by: (Wen and Darnell, 1997, Bromberg et al., 1999)

Method: Due to a stop codon error made when tagging the Stat3 clone with FLAG (DYKDDDDK) additional residues precede (SR) and follow the tag (GPYSIVSPKC STOP). The ApaI cloning site is GGG CCC, which encodes the G and P residues coming after the FLAG tag. Therefore, if the insert is removed with a NotI and ApaI digestion, it will not have a stop codon included

Special Remarks: Diagnostic Restriction Digest with BamHI (3.2kb, 2.8kb, and 2.0kb).

Map:

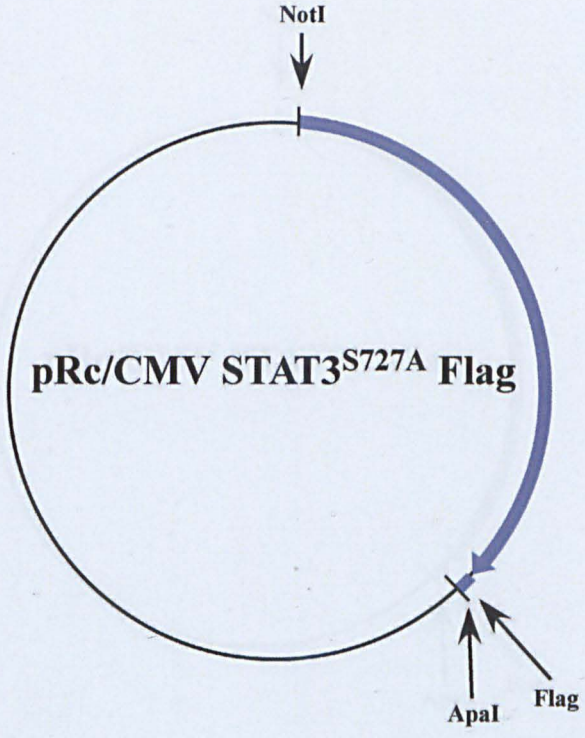

Abbreviation: pRc/CMV STAT3C Flag

Description: Mouse STAT3 cDNA expression vector. A662C and N664C mutants renders as constitutively active.

Size: Vector: 5500bp

Insert: 2600bp

Resistances: Ampicillin

Bacterial Strain: NM522

Constructed by: (Bromberg et al., 1999)

Method: Due to a stop codon error made when tagging the Stat3 clone with FLAG (DYKDDDDK) additional residues precede (SR) and follow the tag (GPYSIVSPKC STOP). The ApaI cloning site is GGG CCC, which encodes the G and P residues coming after the FLAG tag. Therefore, if the insert is removed with a NotI and ApaI digestion, it will not have a stop codon included

Special Remarks: Diagnostic Restriction Digest with BamHI (3.2kb, 2.8kb, and 2.0kb).

Map:

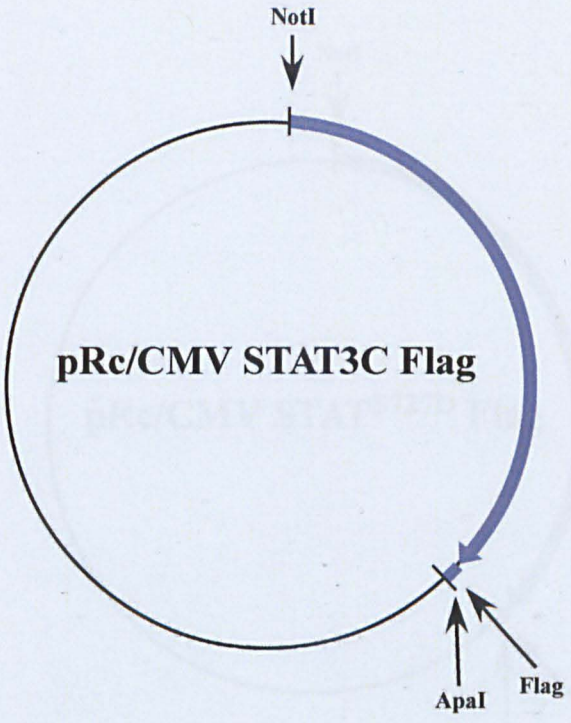

Abbreviation: pRc/CMV $STAT^{S727D}$ Flag

Description: Mouse STAT3 cDNA expression vector. Residues changed to Asp renders the molecule as phospho-mimetic.

Size: Vector: 5500bp

Insert: 2600bp

Resistances: Ampicillin

Bacterial Strain: NM522

Constructed by: Emma Evans

Method: Due to a stop codon error made when tagging the Stat3 clone with FLAG (DYKDDDDK) additional residues precede (SR) and follow the tag (GPYSIVSPKC STOP). The ApaI cloning site is GGG CCC, which encodes the G and P residues coming after the FLAG tag. Therefore, if the insert is removed with a NotI and ApaI digestion, it will not have a stop codon included. Serine to Aspartic acid mutation generated using site-directed mutagenesis.

Special Remarks: Diagnostic Restriction Digest with BamHI (3.2kb, 2.8kb, and 2.0kb).

Map:

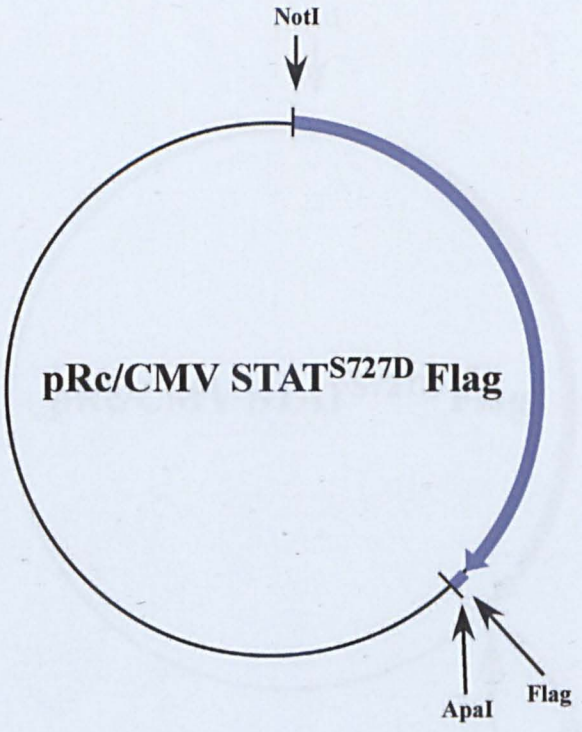

Abbreviation: pRc/CMV STAT^{S727E} Flag

Description: Mouse STAT3 cDNA expression vector. Residues changed to Glu renders the molecule as phospho-mimetic.

Size: Vector: 5500bp

Insert: 2600bp

Resistances: Ampicillin

Bacterial Strain: NM522

Constructed by: Emma Evans

Method: Due to a stop codon error made when tagging the Stat3 clone with FLAG (DYKDDDDK) additional residues precede (SR) and follow the tag (GPYSIVSPKC STOP). The ApaI cloning site is GGG CCC, which encodes the G and P residues coming after the FLAG tag. Therefore, if the insert is removed with a NotI and ApaI digestion, it will not have a stop codon included. Serine to glutamic acid mutation generated using site-directed mutagenesis.

Special Remarks: Diagnostic Restriction Digest with BamHI (3.2kb, 2.8kb, and 2.0kb).

Map: